DOE/FC/10619--2724

DE89 011690

Microbial Degradation of Polycyclic Aromatic Hydrocarbons Under Denitrification Conditions in Soil-Water Suspensions

Final Report

J.R. Mihelcic
R.G. Luthy

Work Performed Under Contract No.: DE-AC18-84FC10619

For
U.S. Department of Energy
Office of Fossil Energy
Morgantown Energy Technology Center
P.O. Box 880
Morgantown, West Virginia 26507-0880

By
Carnegie Mellon University
Department of Civil Engineering
Pittsburgh, Pennsylvania 15213

April 1988

Abstract

The microbial degradation of polycyclic aromatic hydrocarbons (PAH) under different redox conditions was examined for soil-water suspensions, with particular emphasis on microbial degradation under denitrification conditions. This was accomplished by experimental investigations using various batch tests, and theoretical considerations including a coupled solute desorption-degradation model.

Batch microbial degradation tests with 1 gram of soil per 50-ml aqueous phase showed that under aerobic conditions, naphthol, naphthalene, and acenaphthene degraded from initial aqueous-phase concentrations of several mg/liter to nondetectable levels (< 0.01 mg/liter) in 10 days or less. Under anaerobic conditions only naphthol degraded to nondetectable levels, whereas naphthalene and acenaphthene exhibited no significant degradation over time periods of 50 and 70 days, respectively. Under denitrification conditions naphthol, naphthalene, and acenaphthene were degraded to nondetectable levels in 16, 45, and 40 days, respectively. The results from the denitrification experiments were confirmed in additional batch microbial degradation tests with 2 grams of soil per 50 ml. Under nitrate-excess conditions both acenaphthene and naphthalene were degraded from initial aqueous-phase concentrations of about 1, and several mg/liter, respectively, to nondetectable levels following an initial lag period, whereas under nitrate-limiting conditions both compounds were stable for up to 83 days. These results provided the first evidence that low-molecular-weight, unsubstituted polycyclic aromatic hydrocarbons are amenable to microbial degradation in soil-water systems under denitrification conditions.

Acclimation periods of 2 to 36 days were observed prior to the onset of microbial degradation under denitrification conditions for soil not previously exposed to PAH. This was judged to be the result of the time necessary for a small population of microorganisms capable of PAH degradation to attain sufficient densities to exhibit detectable PAH reduction. About 0.9 percent of the naturally occurring soil organic carbon could be mineralized under denitrification conditions, and this accounted for the greater proportion of nitrate depletion in batch tests with 1 or 2 grams of soil.

Experimental studies confirmed that a linear partition coefficient could describe equilibrium partitioning of the three solutes between the aqueous and solid phases. It was shown experimentally, and supported by use of an intra-aggregate radial diffusion model, that the solute sorption reaction was reversible and that the kinetics of sorption and desorption were rapid compared to the rate of microbial degradation. This was a consequence of the relatively low solute hydrophobicity and of the small volumetric mean particle radius for the soil suspension used in the experiments. Modeling demonstrated that the particle radius would influence the PAH sorption and desorption kinetics in proportion to the second power of the particle radius. Solute hydrophobicity also affected the kinetics of the solute partitioning, as a more hydrophobic solute diffused at a much slower rate through the intraparticle pore fluids due to local partitioning.

A conceptual model was proposed to describe the aqueous-phase concentration of PAH solute under denitrification conditions for soil-water systems maintained under gentle suspension. The approach combined an intra-aggregate radial diffusion model to represent solute sorption and desorption with soil, with either Monod or first-order kinetics to describe the microbial degradation of solute from the bulk-aqueous phase. It was assumed that the rate of microbial degradation of these solutes was dependent primarily on aqueous-phase solute concentration, with the sorbed-phase solute being resistant to microbial degradation, and with the soil particles being modeled as spherical aggregates. The Monod biokinetic parameters for naphthalene degradation were obtained from an acclimated soil-water system for which the desorption kinetics were much faster than the rate of degradation. For the case of experiments which were conducted from large batches of acclimated soil similarly prepared, the half-saturation coefficient, K_s, was found to be approximately 2.9×10^{-6} M (0.37 mg/liter) and the maximum rate was shown to be proportional to the soil-to-water ratio and independent of the nitrate concentration. A comparison of the predicted model responses versus experimental data indicated that the coupled desorption-degradation model fit the data quite well. Nitrate reduction was modeled as independent of nitrate concentration and first-order with respect to the soil-to-water ratio and organic carbon substrate concentration.

The microbial degradation of naphthalene in soil-water suspensions under denitrification conditions was modeled by the coupled desorption-degradation approach in order to evaluate unexplored situations in which soil particle size may affect the rate of microbial degradation. For soil-water suspensions the particle radius would significantly affect the desorption kinetics and the degradation of naphthalene as soil particle radius approached 1 cm. Additional

modeling showed that the effect of soil particle radius on solute desorption and degradation would be especially significant for the more hydrophobic PAH compounds.

A preliminary assessment of the effect of solute hydrophobicity on microbial degradation was modeled for volumetric mean particle radii in the range of 0.01 to 0.1 cm. The coupled desorption-degradation model and first-order aerobic degradation kinetic information from the literature were used to predict the aqueous- and sorbed-phase concentrations for the solutes naphthalene, anthracene, and benzo(*a*)pyrene. These results demonstrated the persistence of the more hydrophobic PAH solutes in soil-water systems owing to the decreased availability of the solute to the microorganisms. This was a consequence of the assumption that sorbed-phase PAH solutes were resistant to microbial degradation, and the inherently slower rate of microbial degradation of the more hydrophobic PAH compounds.

The results of this study show that low-molecular-weight polycyclic aromatic hydrocarbons may be microbially degraded in soil-water systems in the absence of oxygen with nitrate as an electron acceptor, and that PAH sorption and desorption kinetics must be considered in conjunction with microbial kinetics to develop more complete understanding of the reactions and fate of hydrophobic compounds in soil-water environments.

Table of Contents

List of Figures

List of Tables

Chapter 1
Introduction

Concern for the nature and extent of groundwater and soil contamination by toxic and/or hazardous organic pollutants has increased significantly in the past decade. Remedial actions to alleviate problems with soil and groundwater contamination often entail treatment by extensive pumping or by removal of soil, both of which may be expensive and/or impractical measures. Thus, understanding of the manner in which an organic pollutant may either persist or degrade in a soil-water environment is essential for assessing strategies to prevent contaminant migration through the subsurface, and for assessing new procedures and alternatives for remediation of contaminated media.

Polycyclic aromatic hydrocarbons (PAH) are a generally hazardous class of organic compounds as characterized by their persistence and toxicity. They are neutral, non-polar, hydrophobic organic molecules which consist of two or more fused benzene rings in linear, angular, or cluster arrangements. Though natural processes such as forest and prairie fires contribute to the presence of PAH in the natural environment, anthropogenic sources constitute the largest contributions (Suess, 1976). The most significant anthropogenic sources have been identified with the utilization of fossil fuels, including chemical manufacturing, petroleum refining, and coke-producing processes. Coal, oil shale, and tar sand conversion facilities may also be important sources of PAH. Because of the hazardous nature of these substances, it is important to develop an understanding of the biological and chemical degradation mechanisms that may govern the persistence of these compounds in the environment.

The objective of this work was to evaluate the microbial degradation of selected PAH compounds in soil-water systems. This was accomplished by: (i) experimental studies which examined the microbial degradation of three PAH compounds under aerobic, anaerobic, and denitrification conditions, (ii) experimental studies which examined the microbial degradation

of two PAH compounds under nitrate-limiting and nitrate-excess conditions and the role assumed by naturally occurring soil organic carbon, (iii) experimental studies and modeling of nitrate reduction during the microbial degradation of two PAH, (iv) experimental studies and modeling of the reversibility and the rate of sorption and desorption of PAH with soil, and (v) development of a coupled solute desorption-degradation model to describe PAH sorption-desorption characteristics in a soil-water suspension along with microbial degradation of the soluble fraction of the PAH.

Chapter 2 provides a brief introduction to soil microbiology and the metabolic pathways associated with PAH degradation. Chapter 3 reports experimental results of the microbial degradation of naphthol, naphthalene, and acenaphthene under aerobic, anaerobic, and denitrification conditions in a soil-water system. The chemical degradation of naphthol and naphthalene in the presence of a manganese oxide was also reported. Chapter 4 reports on additional, confirmational studies of the microbial degradation of naphthalene and acenaphthene under denitrification conditions. This also includes a discussion of the role of naturally occurring soil organic carbon on the sorption and degradation of the PAH compounds, and the nitrate demand exerted by the labile fraction of soil organic carbon. The results presented in Chapters 3 and 4 provide the first known experimental evidence of microbial degradation of PAH compounds under denitrification conditions.

Chapter 5 examines the sorption and desorption properties of hydrophobic organic compounds onto soils and sediments by both experiment and modeling with emphasis on the partitioning of the solute naphthalene between aqueous and solid phases. An intra-aggregate radial diffusion model was utilized to explain the reversibility and rate of the sorption and desorption reactions which had been observed in the laboratory. The model was also used to assess the effect of intraparticle porosity, solute hydrophobicity, and particle size on the kinetics of sorption and desorption of PAH solutes with soils and sediments.

In Chapter 6 the processes which describe nitrate reduction due to microbial degradation of PAH are reviewed. A model is developed to describe aqueous-phase PAH concentration in soil-water suspensions by combining an intra-aggregate radial diffusion approach for solute sorption and desorption, with a model which describes the kinetics of microbial degradation of the PAH compounds. Modeling is performed to assess how particle radius and solute hydrophobicity may influence solute desorption, which in turn may affect the rate of microbial degradation of PAH from the bulk-aqueous phase in soil-water suspensions.

This portion of the study demonstrated the importance of coupling the rates of solute sorption, desorption, and degradation, and the role of soil particle size, on the processes affecting bio-remediation of a contaminated soil-water system. The report is concluded with a summary of the study.

Chapter 2

Metabolism of Polycyclic Aromatic Hydrocarbons by Soil Microorganisms

This chapter provides a brief review of soil microbiology and the biochemical processes which occur when aromatic compounds are microbially degraded. This includes a discussion of the degradation pathways and identification of specific microorganisms which degrade polycyclic aromatic hydrocarbons (PAH). Illustrative examples are presented to show the pathways of degradation. The majority of the studies performed on this subject have been conducted in aerobic systems, and thus the description emphasizes this environment. The pathways for microbial degradation of PAH compounds under denitrification, sulfate reducing, and methanogenic conditions have not been evaluated extensively since these types of compounds have been thought to be persistent in the absence of molecular oxygen. Evans (1977) has provided a review of the metabolism of some oxygen-containing aromatic compounds under anaerobic conditions. Included in this study were discussions of microbial degradation of phenol under denitrification conditions and benzoate and phenol under methanogenic conditions. This chapter will enable the reader to have a better understanding of a few of the many complex reactions which occur during the microbial degradation of PAH, especially in the diverse biological and chemical environment which soil provides.

2.1. Soil Microbiology and Microorganisms which Degrade PAH

Alexander (1977) has presented a detailed description of the ecology of soil microbiology. Though small organisms and microorganisms make up less than one percent of the total soil volume, their contribution to a soil's ability to support plant life is very essential. Five major groups of microorganisms exist in soil. These are bacteria, actinomycetes, fungi, algae and protozoa. Table 2-1 shows typical population densities and environmental influences affecting the distribution of these five groups in soil. From Table 2-1 it is seen that bacteria comprise a large portion of the total microbial population in soils, though fungi

comprise a larger portion of the biomass due to their large diameters and extensive filamentous networks.

Alexander (1977) has written that bacteria are the most dominant group of microorganisms which can degrade aromatic compounds, though fungi, streptomycetes, and filamentous microorganisms may contribute to aromatic substrate breakdown under proper conditions. Some of the bacterial species which are capable of degrading aromatic compounds include *Pseudomonas, Mycobacterium, Acinetobacter, Anthrobacter, Bacillus,* and *Nocarida*. Specific microorganisms which can degrade PAH compounds have been reported by many investigators and include bacteria, fungi, and algae (see references in Miheicic and Luthy, 1988a). Sims and Overcash (1983) and Cripps and Watkinson (1978) have provided a review of the various microorganisms which are capable of degrading particular PAH substrates, including naphthalene, anthracene, and phenanthrene. Ribbons and Eaton (1982) have provided a review of species which degrade naphthalene, methylnaphthalenes, phenanthrene, and anthracene.

2.2. Microbial Degradation of PAH

Microbial degradation of organic compounds is an essential component of nature's carbon cycle in which carbon compounds can be broken down into carbon dioxide, methane, and water. Microorganisms utilize enzymatic reactions in order to oxidize a substrate for energy, which is used for synthesis and growth, cell division and motion, and transport of chemicals into and out of the cell. The degradation of an aromatic compound to inorganic carbon may entail numerous steps, and some compounds may not be completely mineralized owing to the lack of suitable enzymatic pathways for certain intermediates, or because of chemical limitations of substrate molecules (i.e. molecule size and solubility).

2.2.1. Aerobic respiration

In the aerobic oxidation of a PAH compound, oxygenase enzymes are utilized to catalyze reactions in which one or both atoms of molecular oxygen are directly incorporated into a substrate molecule to functionalize it prior to further metabolism. This process adds hydroxyl groups onto the aromatic ring which results in changing a substrate from a biologically inert material to one that is biologically active. Known oxygenases are listed by Sims and Overcash (1983) and Hayaishi (1962). Oxygenases can be classified as

Table 2-1: Microbial ecology of soil.

Microbe Type	Counts per gram dry soil	Environmental Influences
Bacteria	10^5 - 2.0 x 10^8	moisture, aeration, temperature, organic matter, inorganic nutrient supply, acidity
Actinomycetes	10^5 - 10^6	organic matter, pH, moisture, temperature
Fungi	20,000 - 10^6	organic matter, pH, aeration, temperature, season of the year, vegetation composition, soil profile position, organic and inorganic fertilizers, moisture,
Algae	10^4 - 50,000	CO_2, sunlight, pH, moisture
Protozoa	10^4 - 10^5	moisture, food supply

After Alexander, 1977

monooxygenases and dioxygenases. Monooxygenases incorporate a single oxygen atom into the substrate and are characteristic of eucaryotes. Dioxygenases incorporate both atoms of oxygen into a substrate and are characteristic of procaryotes. Eucaryotes include fungi, protozoa, algae except blue green algae, and higher plant and animal organism cells. Procaryotes include bacteria and blue green algae.

The microbial degradation of aromatic compounds in the presence of molecular oxygen is described by Evans (1963) and Cripps and Watkinson (1978). The distinctive biochemical step is ring cleavage. This is accomplished by initially incorporating molecular oxygen into the ring. The source of molecular oxygen is thought to be gaseous oxygen rather than oxygen introduced from a compound such as water. If one atom of oxygen is incorporated into the aromatic molecule, an arene oxide is formed which is then available for further metabolism by hydration, conjugation, or isomerisation reactions. Arene oxides are very reactive and can react with various constituents, including cell DNA which can cause abnormal metabolism. If this pathway is taken, an arene oxide's carcinogenic potential can be realized (Cripps and Watkinson, 1978).

Microbial oxidation of aromatic hydrocarbons can also result in hydroxylation of the aromatic ring with two hydroxyl groups, either ortho to each other as in the formation of catechol, or para to each other as in the formation of gentisic and homogentisic acids (Gibson 1968). Ring fission occurs prior to metabolism of the hydroxylated product for the case of either mono or disubstituted compounds. Hopper (1978) has stated that ring fission follows two distinct pathways. Ortho fission is the process of ring cleavage between the two carbon atoms bearing hydroxyl groups, while meta fission occurs between the bond between a carbon with a hydroxyl group and a carbon without a hydroxyl group. The ortho pathway is used in catechol and benzene metabolism while the meta pathway is used in metabolism of toluene and other substituted intermediates.

The biological metabolism of PAH has been reviewed by Cripps and Watkinson (1978) and Sims and Overcash (1983) who have summarized descriptions of metabolic intermediates. Aerobic degradation pathways for naphthalene by prokaryotic microorganisms have been presented by many researchers, including Dean-Raymond and Bartha (1975) and Gibson (1976). Figure 2-1 shows the metabolism of naphthalene by *Pseudomonas* sp., a bacteria commonly found in soil. Degradation of naphthol by *Pseudomonas* sp. and *Mycobacterium* is shown in Figure 2-2. Figures 2-3 and 2-4 show the biodegradation of the trinuclear aromatic hydrocarbons phenanthrene and anthracene, respectively.

Figure 2-1: Metabolism of naphthalene by soil bacteria.

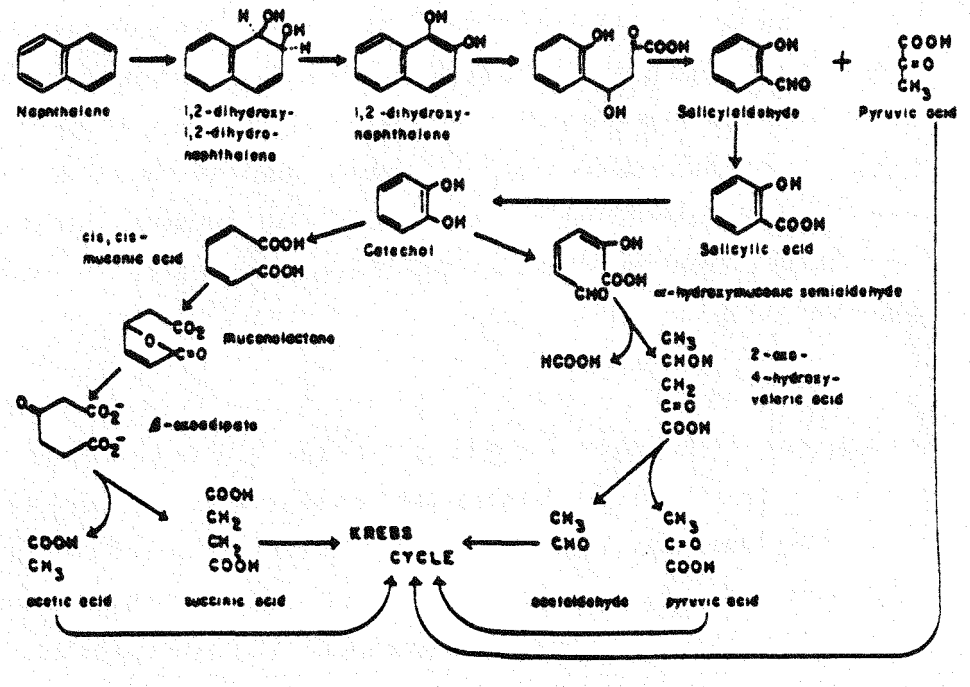

After Sims and Overcash, 1983

From these four figures it is demonstrated that the microbial metabolism of PAH compounds under aerobic conditions involves removing one cyclic unit at a time. Intermediates include catechol, protochatechuic acid, and gentisic acid. These three compounds then follow five pathways which can produce acetaldehyde and succinic, fumaric, pyruvic, and acetic acids. The aerobic metabolism of PAH compounds which consist of greater than three rings is reviewed by Cripps and Watkinson (1978). The authors report that although little detailed information is known about the specific details of metabolism of higher-ring PAH, soil microorganisms have been identified which have degraded compounds such as fluoranthene and benzo(*a*)pyrene. However, Sims and Overcash (1983) reported that no success has occurred in identifying microorganisms which can utilize higher-ring PAH compounds as a sole energy source.

2.2.2. Cometabolism

Some PAH compounds resistant to microbial degradation as the sole energy source can be degraded by a process known as cometabolism. Cometabolism is the process whereby an organic substrate is degraded in the presence of another substrate, though it itself is not utilized as a carbon and energy source. Since cometabolism of aromatics usually requires oxidation, the term cooxidation is often utilized to describe this phenomenon.

Sims and Overcash (1983) have provided a general review on studies of cometabolism of PAH compounds which supports the belief that cometabolism of one- and two-ring aromatics by soil microorganisms is very common. Horvath (1972) has summarized results of studies of cometabolism, including those with pure cultures of microorganisms as well as studies utilizing naturally occurring microbes. His review presented a wide range of microbial species which can cometabolize organic substrates and emphasized the possibility that this metabolic process may be used to degrade what were thought to be recalcitrant substrates. Perry (1979) has presented examples of cometabolism of alkyl- and methyl-substituted aromatic substrates including one- and two-ring cyclics. Also reported was a bacteria strain, *N. Corallina*, which was found to cometabolize such PAH as acenaphthylene and 3-methylphenanthrene. McKenna (1976) has demonstrated the ability of cometabolism to degrade multi-ring PAH such as pyrene and benzo(*a*)pyrene. The microorganisms used in these experiments were pure cultures of mixed bacteria commonly found in soil. Cripps and Watkinson (1978) have reviewed studies which identified microorganisms that could cometabolize PAH compounds such as fluorene, fluoranthene, and pyrene. The process of

Figure 2-2: Microbial metabolism of naphthol.

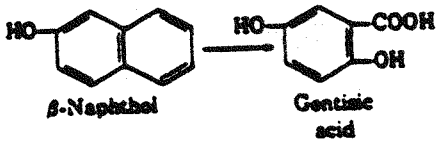

After Alexander, 1977

Figure 2-3: Microbial metabolism of phenanthrene.

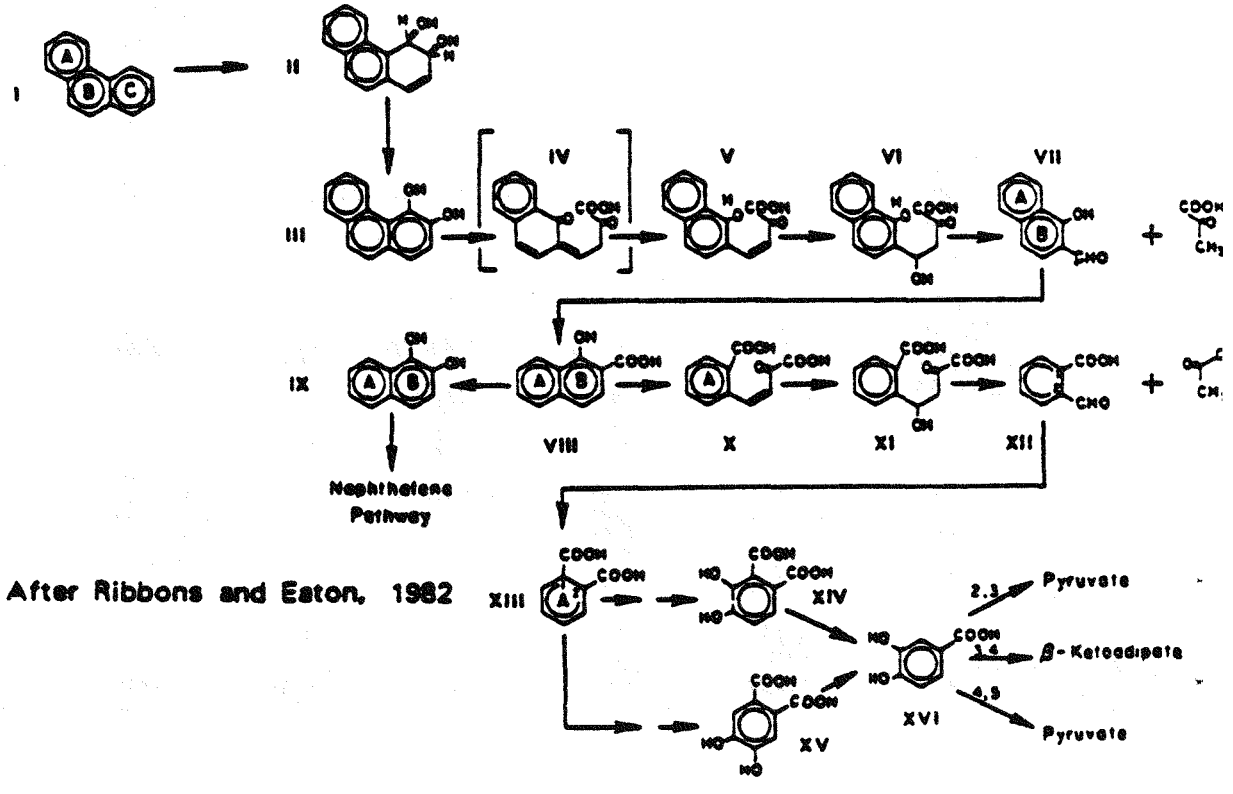

After Ribbons and Eaton, 1982

Figure 2-4: Microbial metabolism of anthracene

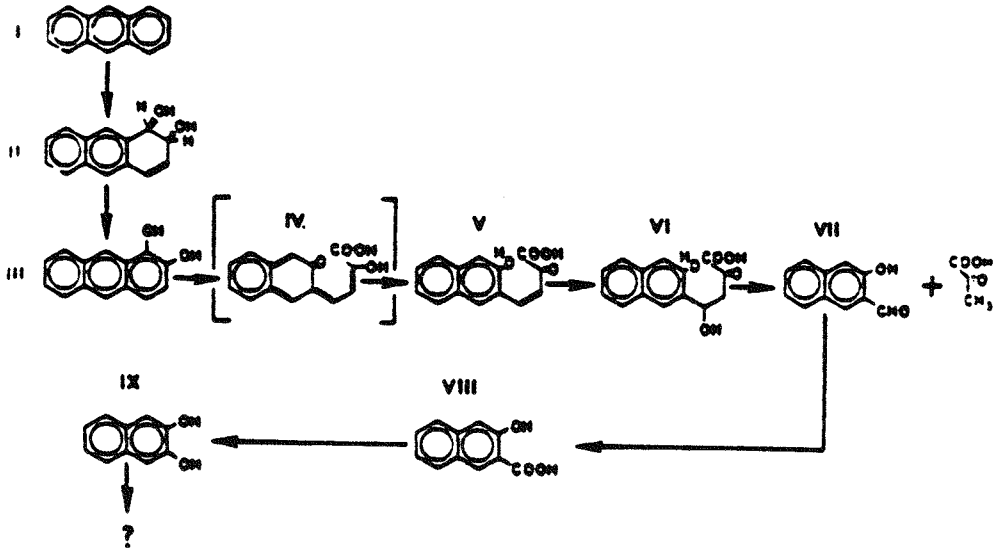

After Ribbons and Eaton, 1982

cometabolism appears to be an important naturally occurring process for degradation of PAH compounds, especially since many PAH contaminants found in the environment may not be in pure form, but in mixtures, often with other organic matter.

2.3. Summary

The microbial degradation of polycyclic aromatic hydrocarbons under aerobic conditions has been extensively studied, especially with regards to low-molecular-weight PAH. Specific PAH-degrading microorganisms have been identified, as well as the metabolic pathways. However, the understanding of the fate of these compounds in anaerobic environments is not understood well. It is believed that cometabolism may be an important process for microbial degradation of PAH, especially in the case of higher-molecular-weight PAH.

2.4. References

1. Alexander, M.A., *Introduction to Soil Microbiology,* John Wiley & Sons, New York, 1977.
2. Cripps, R.E., and R.J. Watkinson, "Polycyclic Aromatic Hydrocarbons: Metabolism and Environmental Aspects," in *Developments in Biodegradation of Hydrocarbons-1,* Ed. R.J. Watkinson, Applied Science Publishers, London, p. 113-134, 1978.
3. Dean-Raymond, D., and R. Bartha, "Biodegradation of Some Polynuclear Aromatic Petroleum Components of Marine Bacteria," in *Developments in Industrial Microbiology,* American Institute of Biological Sciences, Washington, D.C., p. 97-110, 1975.
4. Evans, W.C., "The Microbiological Degradation of Aromatic Compounds," *Journal of General Microbiology,* Vol. 32, p. 177-184, 1963.
5. Evans, W.C., "Biochemistry of the Bacterial Catabolism of Aromatic Compounds in Anaerobic Environments," *Nature,* Vol. 270, p. 17-22, 1977.
6. Gibson, D.T., "Microbial Degradation of Aromatic Compounds," *Science,* Vol. 161, p. 1093-1097, 1968.
7. Gibson, D.T., "Microbial Degradation of Carcinogenic Hydrocarbons and Related Compounds," *Proceedings of the Symposium on Sources, Effects, and Sinks of Hydrocarbons in the Aquatic Environment,* p. 225-237, American Institute of Biological Sciences, Washington, D.C. 1976.
8. Hayaishi, O., *Oxygenases,* Academic Press, New York, 1962.
9. Hopper, D.J., "Microbial Degradation of Aromatic Hydrocarbons," in *Developments in Biodegradation of Hydrocarbons-1,* Ed. R.J. Watkinson, Applied Science Publishers, London, p. 85-112, 1978.
10. Horvath, R.S., "Microbial Co-Metabolism and the Degradation of Organic Compounds in Nature," *Bacteriological Reviews,* Vol. 36, p. 146-155, 1972.
11. McKenna, E.J., and R.D. Heath, "Biodegradation of Polynuclear Aromatic Hydrocarbon Pollutants by Soil and Water Microorganisms," WRC Research Report No. 113, 25 pages, Department of Microbiology, University of Illinois, Urbana-Champaign, 1976.
12. Mihelcic, J.R., and R.G. Luthy, "Degradation of Polycyclic Aromatic Hydrocarbons under Various Redox Conditions in Soil-Water Systems," *Applied and Environmental Microbiology,* Vol. 54, 1988a.
13. Perry, J.J., "Microbial Cooxidations Involving Hydrocarbons," *Microbiological Review,"* Vol. 43, p. 485, 1979.
14. Ribbons, D.W., and R.W. Eaton, "Chemical Transformations of Aromatic Hydrocarbons that Support the Growth of Microorganisms," *In Biodegradation and Detoxification of Environmental Pollutants,* Ed. A.M. Chakrabarty, CRC Press, Boca Raton, Florida, p. 72 - 84, 1982.
15. Sims, R.C. and M.R. Overcash, "Fate of Polynuclear Aromatic Compounds (PNAs) in Soil-Plant Systems," *Residue Review,* Vol. 88, p. 1-88, 1983.
16. Suess, M.J., "Environmental Load and Cycle of Polycyclic Aromatic Hydrocarbons," *The Science of the Total Environment,* Vol. 6, p. 239, 1976.

Chapter 3

Degradation of Polycyclic Aromatic Hydrocarbon Compounds Under Various Redox Conditions in Soil-Water Systems

3.1. Abstract

This study evaluated the microbial degradation of naphthol, naphthalene, and acenaphthene under aerobic, anaerobic, and denitrification conditions in soil-water systems. Chemical degradation of naphthol and naphthalene in the presence of a manganese oxide was also studied. Naphthol, naphthalene, and acenaphthene were degraded microbially under aerobic conditions from initial aqueous-phase concentrations of 9, 7, and 1 mg/liter to nondetectable levels in 3, 10, and 10 days, respectively. Under anaerobic conditions naphthol degraded to nondetectable levels in 15 days, whereas naphthalene and acenaphthene showed no significant degradation over periods of 50 and 70 days, respectively. Under denitrification conditions naphthol, naphthalene, and acenaphthene were degraded from initial aqueous-phase concentrations of 8, 7, and 0.4 mg/liter to nondetectable levels in 16, 45, and 40 days, respectively. Acclimation periods of approximately 2 days under aerobic conditions and 2 weeks under denitrification conditions were observed for both naphthalene and acenaphthene. Abiotic degradation of naphthalene and naphthol were evaluated by reaction with manganese oxide, a minor soil constituent. In the presence of a manganese oxide, naphthalene showed no abiotic degradation over a period of 9 weeks, whereas the aqueous naphthol concentration decreased from 9 mg/liter to nondetectable levels in 9 days. The results of this study show that low-molecular-weight, unsubstituted, polycyclic aromatic hydrocarbons are amenable to microbial degradation in soil-water systems under denitrification conditions.

This chapter has been accepted for publication in *Applied and Environmental Microbiology*.

3.2. Introduction

Polycyclic aromatic hydrocarbon (PAH) compounds have been found to exhibit toxic and hazardous properties. As a consequence, the U.S. Environmental Protection Agency has listed 16 PAH compounds, including naphthalene and acenaphthene, as priority pollutants to be monitored in industrial effluents. For these reasons, there is interest in understanding the movement and fate of these compounds in subsurface aquatic environments, such as groundwaters and soil-water systems (11). Before the fate of PAH compounds in these environments can be evaluated, there must be an understanding of the various mechanisms which may degrade PAH compounds through biotic or abiotic processes. Currently there is little detailed information available on natural degradation reactions of PAH compounds, particularly in the context of soil-water systems and groundwater contamination. The purpose of this study was to provide initial observations on the microbial degradation of PAH compounds in soil-water systems under different redox conditions and to compare these pathways with abiotic degradation through reaction with manganese oxide.

Various studies have identified specific microorganisms which may degrade PAH compounds. These organisms include algae (6,7), fungi (5), and bacteria (12,18,19,25). Although much has been published on microbial metabolism of PAH compounds and on the reaction products of microbial degradation, this information is generally limited to aerobic pathways for two- and three-ring PAH compounds including naphthalene (8,9,14,24), acenaphthene (25), and phenanthrene (8,24). The literature on microbial degradation and stability of PAH compounds in soil-water systems has been summarized by Atlas (2) and Sims and Overcash (26). It is evident (26) that many of the previous data were obtained without considering the specific mechanisms responsible for the decrease of aqueous-phase PAH concentrations in soil-water systems, e.g., apparent reduction in the aqueous-phase PAH concentration owing to the physical processes of organic solute sorption and volatilization versus depletion of PAH compounds via microbial processes.

Microbial degradation of PAH compounds in soil-water systems is influenced strongly by the redox environment and the nature of any substituent groups on the PAH compound. Microbial degradation of unsubstituted PAH compounds in aerobic soil-water systems has been reported (3,10,16,17,25). In contrast, unsubstituted PAH compounds are thought to be refractory in anaerobic soil-water systems. This has been documented in a study showing the stability of naphthalene and anthracene in anaerobic sediment-water systems for periods up to

16 weeks (3) and in a study in which naphthalene showed minimal degradation over 96 days in an anaerobic soil-water system (10), as well as in other work (15,29). Naphthalene stability under denitrification conditions has been reported previously (4), and no significant degradation of naphthalene was evident over a time span of 11 weeks. It is recognized that the experimental conditions in that study were different from those reported here; particularly the initial naphthalene concentrations were approximately 41 to 114 μg/liter, rather than several milligrams per liter, and the biological seed was primary sewage effluent, rather than a mixed soil population.

The chemical oxidation reaction of hydroxy- and carboxyl-substituted benzene compounds with manganese dioxide has been reported (27,28). It was found that compounds with strong electron withdrawing substituents lowered the reaction rate with manganese dioxide, whereas electron-donating groups increased the reaction rate.

The objectives of this study were to compare microbial degradation of naphthol, naphthalene, and acenaphthene by soil microorganisms under aerobic, anaerobic (i.e., no oxygen or nitrate), and denitrification conditions. Chemical degradation of naphthol and naphthalene in the presence of a manganese oxide was also studied.

3.3. Materials and Methods

Soil. The soil used in this study was an undisturbed, subhumid grassland soil of the Barnes-Hamerly Association, obtained by William C. Dahnke, Agricultural Experiment Station, North Dakota State University, Fargo. The soil was collected from the A soil horizon at the SW1/4 of Section 16, T 139N, R 55 W in Cass County, N.D. The soil was air dried, screened to pass a U.S. standard sieve no. 10 (2.0 mm), and then placed in refrigerated storage.

Mineral Medium. The mineral medium used in the biodegradation tests was prepared in deionized water with salts to provide buffering capacity, microbial nutrients, and sustaining electrolyte. The mineral medium was prepared such that after dilution with stock PAH solution the background electrolyte was 0.01 N $CaCl_2$ with the following salts (in milligrams per liter): KH_2PO_4, 8.5; K_2HPO_4, 21.75; $Na_2HPO_4 \cdot 7H_2O$, 33.4; $FeCl_3 \cdot 6H_2O$, 0.25; NH_4Cl, 1.7; and $MgSO_4 \cdot 7H_2O$, 22.5. The mineral medium pH was 6.80. At the initiation of an experiment, mineral medium was combined with soil and stock PAH solution. The purpose of the 0.01 N $CaCl_2$ electrolyte was to assist centrifugation and separation of the solid phase at the completion of a test.

Chemical Reagents. Chemical reagents were obtained from Fisher Scientific Co., Pittsburgh, Pa., and Aldrich Chemical Co., Milwaukee, Wis. Scintillation grade or certified grade acenaphthene, naphthalene, and naphthol were obtained as crystalline powders. The name naphthol refers to the compound α-naphthol.

Instrumentation and Analyses. Solute analyses were performed with a high pressure liquid chromatograph (HPLC) system manufactured by The Perkin-Elmer Corporation, Norwalk, Conn. A Series 3 liquid chromatograph unit and Model 204-S fluorescence detector were used, and the results were recorded and integrated on an LC-100 Laboratory Computing Integrator. Shaking was performed with a wrist action shaker (model 74; Burrell Co., Pittsburgh, Pa.), and centrifuging was performed at 875 x *g* with a clinical centrifuge (International Equipment Co., Needham Heights, Mass.).

The PAH compounds were analyzed on an LC-PAH column (Supelco Inc., Bellefonte, Pa.) by direct aqueous injection of 1 to 10 μl samples which were eluted under isocratic conditions with 60% high-pressure liquid chromatography grade acetonitrile and 40% deionized water. Each sample point was injected at least three times. Prior to use in high-pressure liquid chromatography analysis, acetonitrile and water were filtered through Teflon and cellulose filters respectively (pore size, 0.45 μm), degassed by vacuum treatment, and purged with helium. Acenaphthene and naphthalene were detected by setting the fluorescence excitation and emission wavelengths at 280 and 340 nm, respectively, whereas for naphthol the settings were adjusted to 310 and 340 nm, respectively. The PAH detection limit was 0.01 mg/liter.

Dissolution of PAH. The PAH compounds used in these tests exist as crystalline solids at room temperature. Stock solutions of these compounds were prepared by placing a known amount of solid in deionized water and then dissolving it overnight by magnetic stirring in a closed glass container covered with aluminum foil. The solution was then filtered through an extra thick glass fiber filter (no. 66077; Gelman Sciences Inc., Ann Arbor, Mich.) to remove any undissolved, suspended crystals. The filtered stock solutions were analyzed by high-pressure liquid chromatography techniques to assess the preparation procedures. Typically, these techniques resulted in stock solutions containing the PAH compounds in the desired range of about 1 to 10 mg/liter.

Sample Preparation. Pyrex centrifuge tubes (50 ml; Corning Glass Works, Corning,

N.Y.) were utilized to contain the test samples, controls, and blanks. Each tube was sealed with a Teflon-lined septum (model 2-3281, Supelco) and secured with an open-port screw cap. Test samples were composed of a mixture of mineral medium and PAH stock solution with 1.0000 gm (dry weight) of soil and filled to zero headspace. Immediately after being filled, the tubes were secured with the Teflon-lined septum and open-port screw cap, and covered with aluminum foil. The tubes were shaken for 4 h per day on a wrist action shaker.

Sterile blank and control samples were run concurrently with the test samples. Blanks contained mineral medium and PAH stock solution in sterilized glassware without soil. Sterile control samples contained mineral medium, PAH stock solution, and 1 g of soil. Sterilization was carried out by autoclaving the glassware and soil at 121°C and 20 lb/in^2 steam pressure for 1 h and then adding $HgCl_2$ such that the concentration of $HgCl_2$ in the control samples was 400 mg/liter. Sample blanks were used to confirm no loss of PAH compounds through volatilization, photodegradation, or interaction with the Teflon-lined septum, whereas sample controls were used to confirm the results obtained from the sample blanks as well as to verify no loss of PAH compounds through abiotic degradation. The experiments were conducted in a batch mode with test samples, blanks, and controls being prepared simultaneously. Approximately 36 separate tubes were set up at the initiation of a single experiment. The tubes were withdrawn individually for analysis during the course of an experiment and then removed from service after being analyzed.

Soil-water samples were centrifuged for 1 h before the aqueous phase was analyzed for PAH compounds. The aqueous-phase samples were obtained by puncturing the septum with an injection syringe equipped with a removable gas chromatography needle (series 800, Hamilton Co., Reno, Nev.) and immediately analyzing the sample on the HPLC. Therefore, test samples, blanks, and controls remained closed and secure from the external environment from the initiation of the experiment through sample analysis. The samples were maintained at room temperature during the experiments.

3.3.1. Degradation Test Conditions.

(I) Aerobic degradation. PAH stock solution and oxygen-saturated mineral medium were combined in a 50-ml centrifuge tube containing 1 g (dry weight) of soil. The relative volumes of mineral medium to PAH solution were 3:2, 4:1, and 4:1 for acenaphthene, naphthalene, and naphthol, respectively. The larger proportion of acenaphthene stock

solution to mineral medium was necessary to provide sufficient aqueous-phase PAH concentrations following sorption equilibrium of acenaphthene with soil.

Separate measurements were performed to determine the dissolved oxygen concentration in the test samples at the beginning of a run. Dissolved oxygen was measured by iodometric titration procedures (1). This confirmed the presence of sufficient oxygen for possible mineralization of the PAH compound. Selected test samples were analyzed for residual dissolved oxygen at the conclusion of an experiment after sampling for the PAH compound. The final dissolved oxygen measurement showed that dissolved oxygen was present throughout the test. For example, in the aerobic test with the the solute naphthol, the initial dissolved oxygen concentration was approximately 30 mg/liter, and this was decreased to approximately 5.3 mg/liter by the conclusion of the experiment.

(ii) Anaerobic degradation. Similar experimental protocols as in the aerobic tests were used in the experiments to assess PAH degradation under anaerobic conditions, except that oxygen was removed from the samples by first degassing the mineral medium by vacuum treatment, and then purging the mineral medium with helium for 30 min. Mineral medium was then combined with PAH stock solution and purged further with helium for 1 h before it was transferred to 50-ml centrifuge tubes. Iodometric titration measurements for dissolved oxygen were conducted on selected samples at the beginning and at the conclusion of a test run. These measurements confirmed the absence of oxygen in the anaerobic samples.

(iii) Denitrification. The experiments to evaluate PAH compound degradation under denitrification conditions involved similar procedures to those used in the anaerobic experiments, except that $NaNO_3$ was added to the mineral medium. The initial nitrate concentration in the test samples was approximately 75 mg of NO_3^- as nitrate per liter. As in the anaerobic tests, the absence of dissolved oxygen was monitored by iodometric titrametric procedures.

(iv) Chemical degradation. Chemical degradation tests were done by experimental procedures described elsewhere (27). The manganese oxide suspension was prepared from oxygenation of Mn^{2+}, after which the oxide was deoxygenated by purging with nitrogen for 90 min. Then 10 ml of the oxide suspension was immediately combined with 40 ml of PAH solution. In these tests, the PAH solution consisted of a buffer and electrolyte solution containing (milligrams per liter) KH_2PO_4, 17.0; K_2HPO_4, 43.5; and $Na_2HPO_4 \cdot 7H_2O$, 66.8;

sufficient NaCl to maintain an ionic strength of 0.01 N NaCl in the final sample was also added. The manganese oxide concentration in an individual sample, after being combined with PAH stock solution, was 2×10^{-3} M. The pH of the samples was adjusted to 5.9 for the test with the solute naphthol and to 5.0 and 8.0 for the tests with naphthalene. Blanks were prepared with PAH stock solution without manganese oxide. The centrifuge tubes were sealed with Teflon-lined septum tops, covered with aluminum foil, and rotated six times daily.

3.4. Results

In the following presentation of data, each sample point represents the average of two to five individual samples. After analysis for PAH compounds, selected samples were monitored for dissolved oxygen and pH. The individual samples were discarded after sampling for PAH compound, because the septum was punctured in the sampling process. Nondetectable levels of a PAH compound refer to an aqueous concentration of less than 0.01 mg of the PAH compound per liter.

Figure 1 shows microbial degradation of naphthol, naphthalene, and acenaphthene under aerobic conditions. The aqueous-phase naphthol concentration decreased from approximately 9 mg/liter to nondetectable levels in 3 days with no observed acclimation period. Naphthalene was degraded from approximately 7 mg/liter to nondetectable levels in 10 days, and acenaphthene degraded from approximately 1 mg/liter to nondetectable levels in 10 days. Naphthalene and acenaphthene showed acclimation periods of approximately 2 days before degradation occurred. Blanks containing no soil and controls which contained sterilized soil showed no significant loss in aqueous-phase PAH concentration through the duration of the tests (data not shown).

Figure 2 shows results of microbial degradation tests with naphthol, naphthalene, and acenaphthene under anaerobic conditions. Naphthol was degraded from an initial aqueous-phase concentration of approximately 9 mg/liter to nondetectable levels in 15 days. No acclimation period was evident for microbial degradation of naphthol. The aqueous-phase naphthalene concentration did not change significantly over a time span of approximately 50 days; it remained at approximately 1.3 mg/liter for the duration of the experiment. The aqueous-phase acenaphthene concentration did not change from approximately 1 mg/liter over the 70 day duration of the anaerobic experiment. Blanks and controls remained at constant concentration for each of the three sets of anaerobic tests.

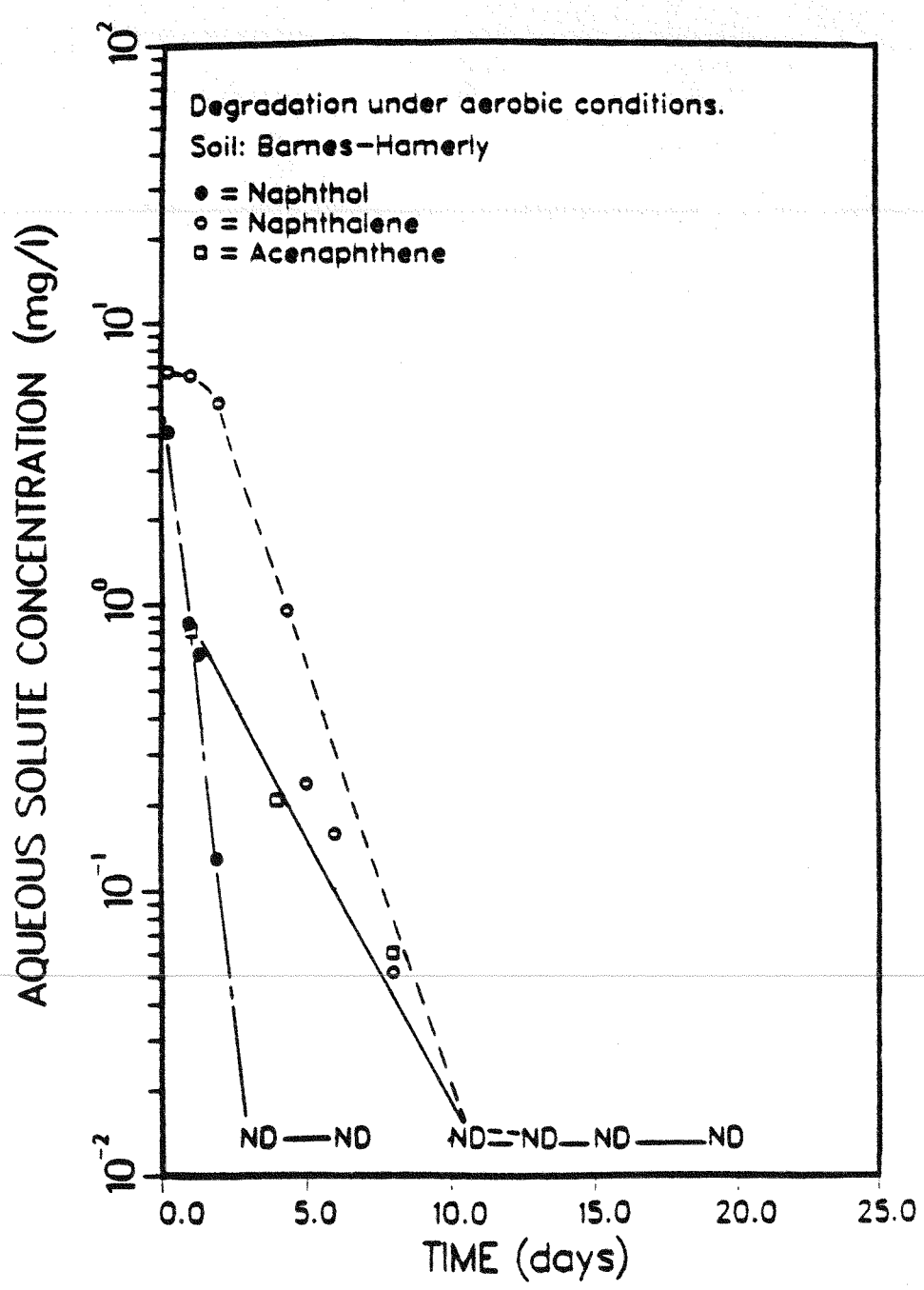

Figure 1. Microbial degradation of naphthol, naphthalene, and acenaphthene under aerobic conditions. Initial aqueous naphthol, naphthalene, and acenaphthene concentrations were 9, 7, and 1 mg/liter, respectively. ND, Nondetectable levels.

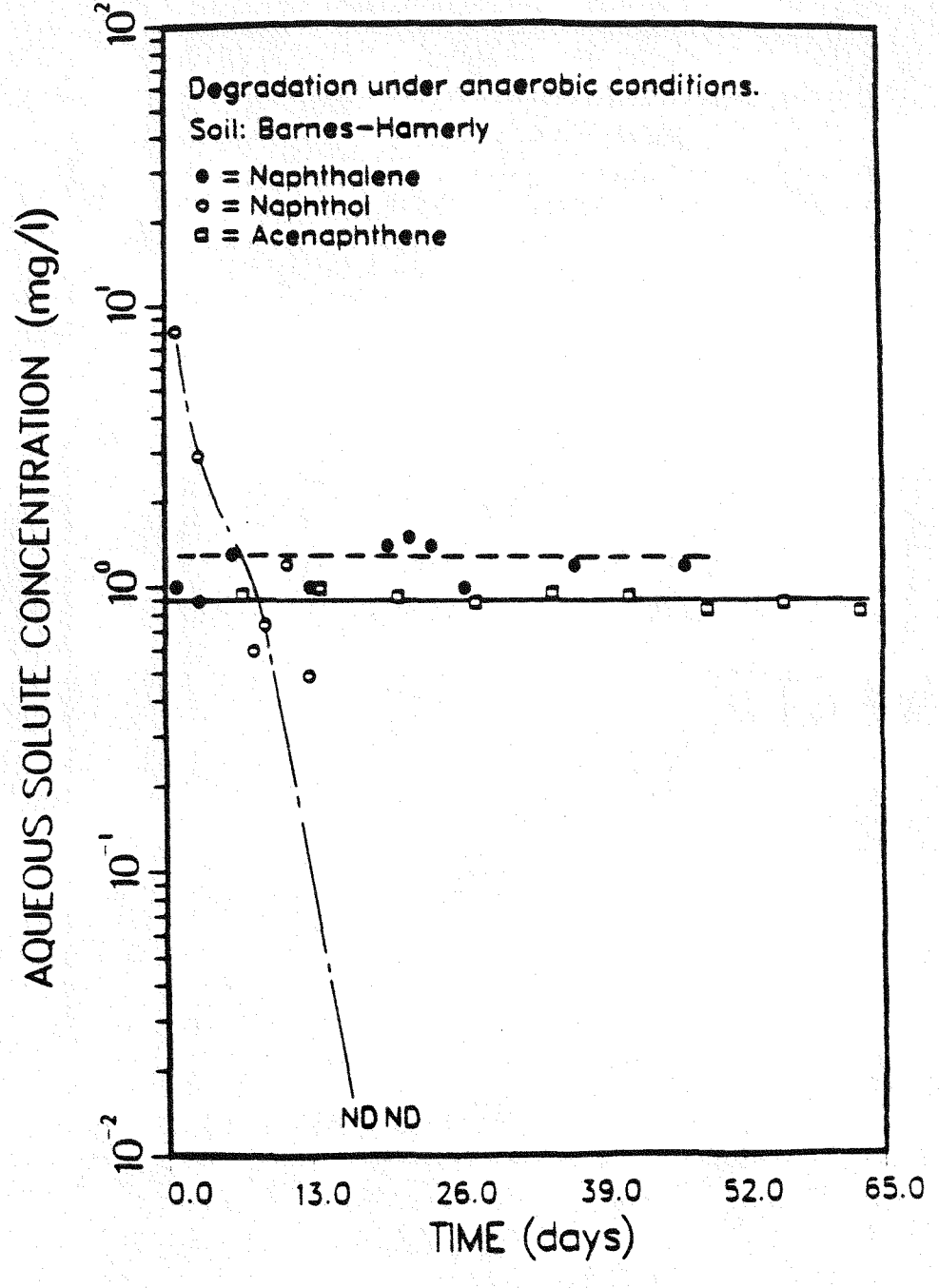

Figure 2. Microbial degradation of naphthol, naphthalene, and acenaphthene under anaerobic conditions. Initial aqueous naphthol, naphthalene, and acenaphthene concentrations were 8, 1.3, and 1 mg/liter, respectively. ND, Nondetectable levels.

Figure 3 shows microbial degradation under denitrification conditions for the solutes naphthol, naphthalene, and acenaphthene. These experiments were performed to assess the microbial degradation of PAH in the presence of nitrate, which may serve as an alternate electron acceptor to oxygen. At neutral pH values, the microbial process of oxidation of organic solute via denitrification is only slightly less favorable energetically than that via aerobic respiration, but considerably more favorable than the anaerobic processes of oxidation of organic solutes via sulfate reduction or methane fermentation (23). Naphthol was degraded from an initial aqueous-phase concentration of 8 mg/liter to nondetectable levels in less than 16 days (Fig. 3). In this test no acclimation period was evident. The aqueous-phase naphthalene concentration decreased from an initial concentration of 7 mg/liter to nondetectable levels in 45 days. In this test an acclimation period of approximately 10 days was observed prior to the occurrence of significant degradation. The initial aqueous-phase concentration of acenaphthene, approximately 0.4 mg/liter, decreased to nondetectable levels in 40 days with an acclimation period of approximately 15 to 20 days. As in the previous tests, the sample blanks and controls remained unchanged through the denitrification experiments. For example for the test conducted with acenaphthene, blank concentrations were 0.45 and 0.48 mg/liter, whereas control concentrations were 0.39 and 0.32 mg/liter at time zero and 45 days, respectively.

Figure 4 shows the naphthol reaction in the presence of manganese oxide at a pH of 5.9. The abiotic degradation reaction began immediately, without a lag time, and the aqueous-phase naphthol concentration decreased from approximately 9 mg/liter to nondetectable levels in approximately 9 days. Analogous experiments were conducted to assess naphthalene reactivity in the presence of manganese oxide. Naphthalene exhibited no significant degradation reaction with manganese oxide over a time period of 9 weeks at pH values of either 5.0 or 8.0. Sample blanks remained constant for the experiments with either solute.

3.5. Discussion

The experimental data gave results on the microbial degradation of naphthol, naphthalene, and acenaphthene under aerobic, anaerobic, and denitrification conditions in natural soil-water systems. Also presented were results on the chemical degradation of naphthol and naphthalene in the presence of a manganese oxide. These results demonstrate that the redox environment is an important factor in assessing the persistence of PAH compounds in soil-water systems.

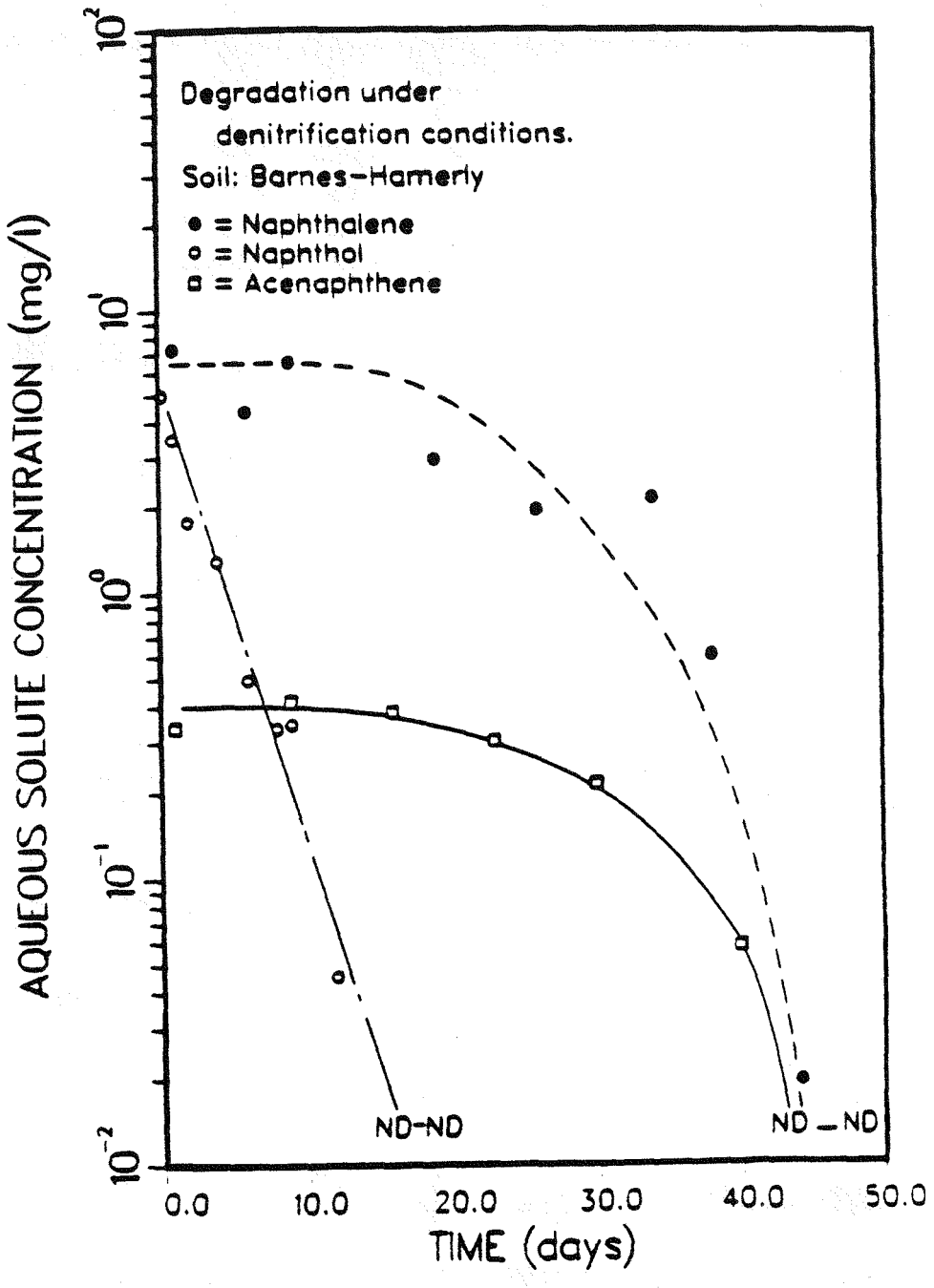

Figure 3. Microbial degradation of naphthol, naphthalene, and acenaphthene under denitrification conditions. Initial aqueous naphthol, naphthalene, and acenaphthene concentrations were 8, 7, and 0.4 mg/liter, respectively, and the initial nitrate concentration was 75 mg/liter in all tests. ND, Nondetectable levels.

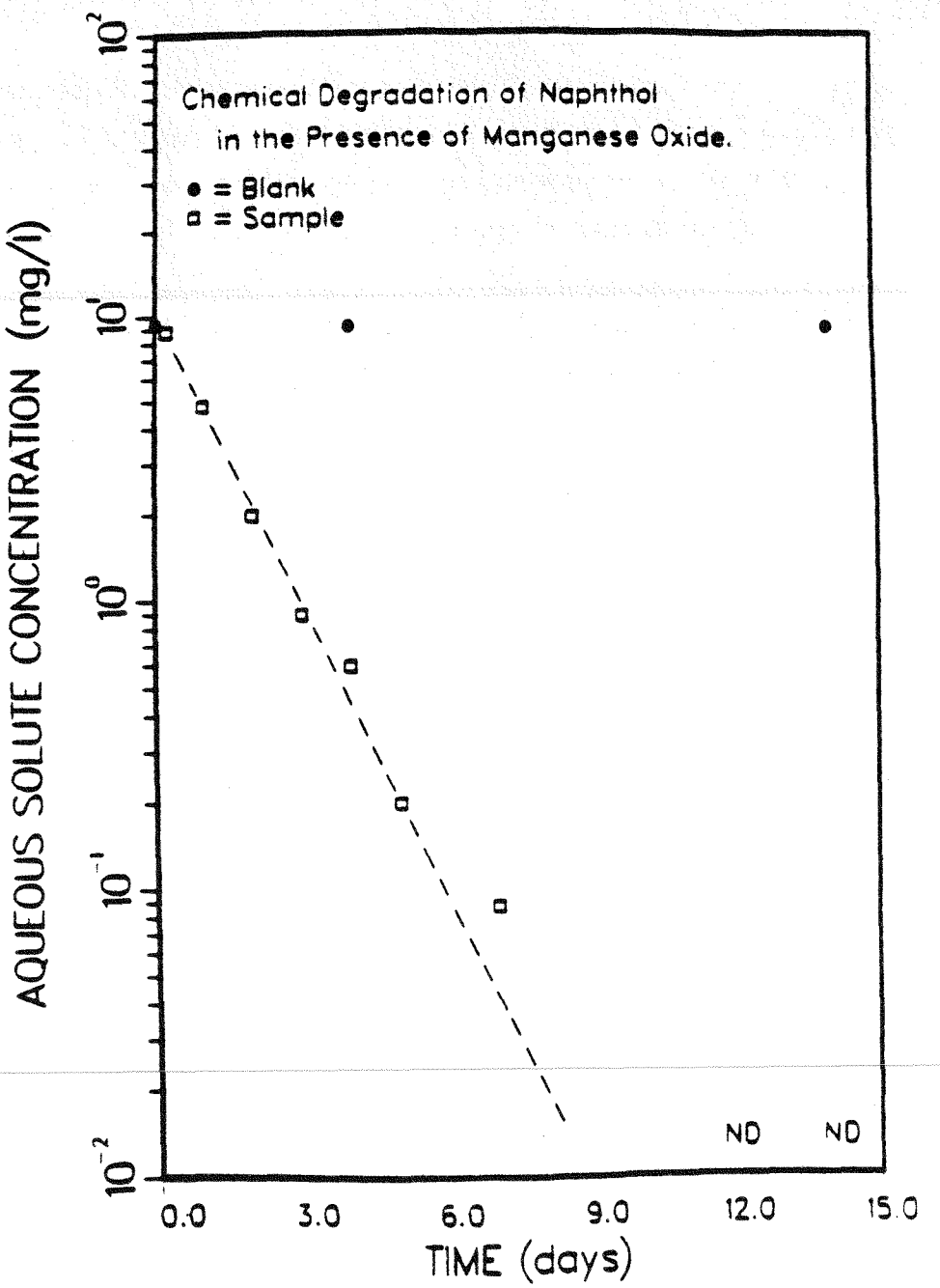

Figure 4. Chemical degradation of naphthol in the presence of manganese oxide. The initial concentrations of manganese oxide and naphthol were 2 x 10^{-3} M and 6.25 x 10^{-5} M respectively. A sample blank was used for comparison. ND, Nondetectable levels.

Reaction with manganese oxide. The chemical processes by which manganese oxides are reduced and solubilized by reaction with aromatic hydrocarbons have been discussed by Stone and Morgan (27,28). Reactive organic solutes include species which may form surface complexes with the oxide surface. Electron-donating substituents on aromatic solutes, such as -OH on naphthol, increase the reaction rate. The rate of the reaction depends on pH, solute concentration, and the concentration of the oxide suspension, as well as other parameters such as suspension age and the presence of competing sorbates. Data in Fig. 4 can be used to obtain an estimate of a second-order rate constant for degradation of naphthol in the presence of manganese oxide, assuming first-order dependence with respect to both the solute and the oxide (28). The experiment was performed with a 32-fold molar excess of manganese oxide, assuming a uniequivalent reaction between manganese and naphthol, and thus the manganese oxide concentration can be considered constant in the experiment. These assumptions provide a second-order naphthol reaction rate constant of approximately 3×10^{-3} liters/mol per s for pH 5.9 and other conditions specified earlier. This rate is in the range of that reported by Stone and Morgan (28) for reaction of resorcinol and salicylate with manganese oxide, although it is recognized that the results are not strictly comparable owing to the somewhat different experimental conditions.

The significance of the test results with manganese oxide is that naphthol may reduce and solubilize manganese from manganese oxide-bearing soils and sediments. However, the results of the microbial degradation tests indicate that the fate of naphthol in soil systems is more likely to be dependent on microbial degradation processes, regardless of aerobic, anaerobic, or denitrification conditions, rather than on abiotic degradation reactions with manganese oxide. This is because naturally occurring manganese oxide may exhibit different reactivity from that of the freshly prepared material used in these studies and because manganese is a minor constituent of soils, being present at about 0.1 % by weight (21). However, the reactivity with manganese may be important even at low concentrations if manganese can be rapidly recycled between oxidized and reduced phases. Another complicating factor in understanding the role of manganese is the possibility of microbial reduction of manganese (13).

Microbial degradation. Acenaphthene, naphthalene, and naphthol were degraded microbially under aerobic conditions to nondetectable levels in 10 days or less. These observations are consistent with several other studies which have reported on the microbial degradation of naphthalene (3,10,16,17) and anthracene (3,17) in natural soils and sediments.

Naphthol was degraded under all microbial test conditions through either aerobic, anaerobic, or denitrification processes. The aqueous naphthol concentration attained nondetectable levels most rapidly under aerobic microbial degradation conditions, with the compound depleted to less than 0.01 mg/liter in 3 days. Although naphthol was the only substituted PAH compound examined in this study, it is evident that the substituent hydroxyl group causes naphthol to be more biologically reactive than the unsubstituted parent compound, naphthalene. The higher reactivity of naphthol than naphthalene under aerobic conditions is expected because the initial steps in microbial metabolism of naphthalene when catalyzed by microbial oxygenases is believed to entail dihydroxylation followed by cleavage of the aromatic ring (9,14).

In contrast to naphthol, naphthalene and acenaphthene showed no microbial degradation under anaerobic conditions for test durations of up to 10 weeks. These observations are similar to the results of other studies which have reported the stability of PAH compounds such as naphthalene and anthracene in the absence of oxygen (3,10). Hence, the data support the current view that anaerobic degradation of unsubstituted PAH compounds by microorganisms at best proceeds at low rates in sediments (2). However, the soil used in this study was obtained from an upper soil horizon and therefore may not be truly representative of the activity of microbial populations from anaerobic soils.

Previous research has shown that the presence of oxygen on the PAH aromatic ring or ring substituent is apparently a basic requirement for cleavage of the aromatic ring under anoxic conditions (2,4). In this regard, the most significant result of this study is the demonstration that microbial degradation of naphthalene and acenaphthene may occur under denitrification conditions, although this may require acclimation periods of several weeks prior to the onset of microbial degradation. In this study it is important to note the stability of blanks containing no soil and of sterilized controls containing soil, which demonstrated no loss of compound across, or reaction with, the Teflon-lined septum. Furthermore, stable test samples under anaerobic conditions indicate that oxygen intrusion across the Teflon-lined septum was not occurring.

Although anaerobic degradation of oxygen-substituted benzenes, e.g., derivatives of phenol and benzoic acid, and oxygen-substituted PAH compounds has been demonstrated previously, this investigation presents the first evidence of microbial degradation of unsubstituted PAH compounds under denitrification conditions. Likewise, the degradation of

p-, *m*-, and *o*-xylene by a mixed microbial population under nitrate reducing conditions has recently been reported (20, 30). These studies demonstrated in an analogous manner that alkyl-substituted benzenes, which also were believed previously to be microbially inert in the absence of molecular oxygen, were degraded under denitrification conditions.

The results of this study and those of Kuhn et al. (20) and Zeyer et al. (30) show the significance of denitrification as a mechanism for microbial degradation of aromatic hydrocarbons containing no oxygen substituents. This work suggests pathways for microbial restoration of anoxic soils, sediments, and groundwater systems contaminated with PAH compounds. A companion paper (22) further examines the microbial degradation of acenaphthene and naphthalene under denitrification conditions, discusses the role of solute sorption-desorption on microbial degradation, and evaluates the roles of nitrate and naturally occurring soil organic carbon on the microbial degradation of PAH compounds.

3.6. References

1. **American Public Health Association.** 1985. Standard methods for the examination of water and wastewater, p. 418-419, 16th ed. American Public Health Association, Washington, D.C.
2. **Atlas, R.M.** 1981. Microbial degradation of petroleum hydrocarbons: an environmental perspective. Microbiol. Rev. **45**:180-209.
3. **Bauer, J.E., and D.G. Capone.** 1985. Degradation and mineralization of the polycyclic aromatic hydrocarbons anthracene and naphthalene in intertidal marine sediments. Appl. Environ. Microbiol. **50**:81-90.
4. **Bouwer, E.J., and P.L. McCarty.** 1983. Transformations of halogenated organic compounds under denitrification conditions. Appl. Environ. Microbiol. **45**:1295-1299.
5. **Cerniglia, C.E., and D.T. Gibson.** 1978. Metabolism of naphthalene by cell extracts of *Cunninghamella elegans*. Arch. Biochem. Biophys. **186**:121-127.
6. **Cerniglia, C.E., D.T. Gibson, and C. Van Baalen.** 1980. Oxidation of Naphthalene by Cyanobacteria and Microalgae. J. Gen. Microbiol. **116**:495-500.
7. **Cerniglia, C.E., C. Van Baalen, and D.T. Gibson.** 1980. Metabolism of naphthalene by the cyanobacterium *Oscillatoria* sp., strain JCM. J. Gen. Microbiol. **116**:485-494.
8. **Cripps, R.E., and R.J. Watkinson.** 1978. Polycyclic aromatic hydrocarbons: metabolism and environmental aspects, p. 113-134. *In* R.J. Watkinson (ed.), Developments in biodegradation of hydrocarbons-1, Appl. Sci. Publishers, London.
9. **Dean-Raymond, D., and R. Bartha.** 1975. Biodegradation of some polynuclear aromatic petroleum compounds of marine bacteria, Dev. Ind. Microbiol. **16**:97-109.
10. **Delfino, J.J., and C.J. Miles.** 1985. Aerobic and anaerobic degradation of organic contaminants in Florida groundwater. Proc. Soil Crop Sci. Soc. Fla. **44**:9-14.
11. **Dzombak, D.A., and R.G. Luthy.** 1984. Estimating adsorption of polycyclic aromatic hydrocarbons on soils. Soil Sci. **137**:292-308.
12. **Ensley, B.D., D.T. Gibson, and A.L. Laborde.** 1982. Oxidation of naphthalene by a multicomponent enzyme system from *Pseudomonas* sp. strain NCIB 9816. J. of Bacteriol. **149**:948-954.
13. **Ghiorse, W.C.** 1987. Microbial reduction of manganese and iron, *In* A.J.B. Zehnder (ed.) Environmental microbiology of anaerobes, John Wiley and Sons, Inc., New York.
14. **Gibson, D.T.** 1976. Microbial degradation of carcinogenic hydrocarbons and related compounds, p. 225-237. *In* Proc. Symp. Sources, Effects, and Sinks of Hydrocarbons in Aquatic Environment. American Institute of Biological Sciences, Washington, D.C.
15. **Hambrick, G.A., R.D. DeLaune, and W.H. Patrick.** 1980. Effect of estuarine sediment pH and oxidation-reduction potential on microbial hydrocarbon degradation. Appl. Environ. Microbiol. **40**:365-369.

16. **Heitkamp, M.A., J.P. Freeman, and C.E. Cerniglia.** 1987. Naphthalene biodegradation in environmental microcosms: estimates of degradation rates and characterization of metabolites. Appl. Environ. Microbiol. **53**:129-136.

17. **Herbes, S.E., and L.R. Schwall.** 1978. Microbial transformation of polycyclic aromatic hydrocarbons in pristine and petroleum contaminated sediments. Appl. Environ. Microbiol. **35**:306-316.

18. **Jeffrey, A.M., H.J.C. Yeh, D.M. Jerina, T.R. Patel, J.F. Davey, and D.T. Gibson.** 1975. Initial reactions in the oxidation of naphthalene by *Pseudomonas putida*. Biochem. **14**:575-584.

19. **Kiyohara, H., and K. Nagao.** 1978. The Catabolism of phenanthrene and naphthalene by bacteria. J. Gen. Microbiol. **105**:69-75.

20. **Kuhn, E.P., P.J. Colberg, J.L. Schnoor, O. Wanner, A.J.B. Zehnder, and R.P. Schwarzenbach.** 1985. Microbial transformations of substituted benzenes during infiltration of river water to groundwater: laboratory column studies. Environ. Sci. Technol. **19**:961-968.

21. **Lindsay, W.L.** 1979. Chemical equilibrium in soils, John Wiley & Sons, Inc., New York.

22.) **Mihelcic, J.R., and R.G. Luthy.** 1988. Microbial degradation of acenaphthene and naphthalene under denitrification conditions in soil-water systems. Appl. Environ. Microbiol. **54**.

23. **Morel, F.M.M.** 1983. Principles of aquatic chemistry. John Wiley & Sons, Inc., New York.

24. **Ribbons, D.W., and R.W. Eaton.** 1982. Chemical transformations of aromatic hydrocarbons that support the growth of microorganisms. p. 72-84. *In* A.M. Chakrabarty (ed.), Biodegradation and detoxification of environmental pollutants. CRC Press, Inc., Boca Raton.

25. **Schocken, M.J., and D.T. Gibson.** 1984. Bacterial oxidation of the polycyclic aromatic hydrocarbons acenaphthene and acenaphthylene. Appl. Environ. Microbiol. **48**:10-16.

26. **Sims, R.C., and M.R. Overcash.** 1983. Fate of polynuclear aromatic compounds (PNAs) in soil-plant systems. Residue Rev. **88**:1-68.

27. **Stone, A.T., and J.J. Morgan.** 1984. Reduction and dissolution of manganese (III) and manganese (IV) oxides by organics. 1. reaction with hydroquinone. Environ. Sci. Technol. **18**:450-456.

28. **Stone, A.T., and J.J. Morgan.** 1984. Reduction and dissolution of manganese (III) and manganese (IV) oxides by organics. 2. survey of reactive organics. Environ. Sci. Technol. **18**:617-624.

29. **Wilson, J.T., and J.F. McNabb.** 1983. Biological transformation of organic pollutants in groundwater. Trans. Am. Geophys. Union. **64**:503-506.

30. **Zeyer, J., E.P. Kuhn, and R.P. Schwarzenbach.** 1986. Rapid microbial mineralization of toluene and 1,3-dimethylbenzene in the absence of molecular oxygen. Appl. Environ. Microbiol. **52**:944-947.

Chapter 4

Microbial Degradation of Acenaphthene and Naphthalene under Denitrification Conditions in Soil-Water Systems

4.1. Abstract

This study examined the microbial degradation of acenaphthene and naphthalene under denitrification conditions at soil-to-water ratios of 1:25 and 1:50 with soil containing approximately 10^5 denitrifying organisms per g of soil. Under nitrate-excess conditions, both acenaphthene and naphthalene were degraded from initial aqueous-phase concentrations of about 1 and several mg/liter, respectively, to nondetectable levels (< 0.01 mg/liter) in less than 9 weeks. Acclimation periods of 12 to 36 days were observed prior to the onset of microbial degradation in tests with soil not previously exposed to polycyclic aromatic hydrocarbon (PAH) compounds, whereas acclimation periods were absent in tests with soil reserved from prior PAH degradation tests. It was judged that the apparent acclimation period resulted from the time required for a small population of organisms capable of PAH degradation to attain sufficient densities to exhibit detectable PAH reduction, rather than being a result of enzyme induction, mutation, or use of preferential substrate. About 0.9 % of the naturally occurring soil organic carbon could be mineralized under denitrification conditions, and this accounted for the greater proportion of the nitrate depletion. Mineralization of the labile fraction of the soil organic carbon via microbial denitrification occurred without an observed acclimation period and was rapid compared with PAH degradation. Under nitrate-limiting conditions the PAH compounds were stable owing to the depletion of nitrate via the more rapid process of soil organic carbon mineralization. Soil sorption tests showed at the initiation of a test that the total mass of PAH compound was divided in comparable proportions between solute in the

---

This chapter has been accepted for publication in *Applied and Environmental Microbiology*.

aqueous phase and solute sorbed on the solid phase. The microbial degradation of the PAH compound depends on the interrelationships between (i) the desorption kinetics and the reversibility of desorption of sorbed compound from the soil, (ii) the concentration of PAH-degrading microorganisms, and (iii) the competing reaction for nitrate utilization via mineralization of the labile fraction of naturally occurring soil organic carbon.

4.2. Introduction

Polycyclic aromatic hydrocarbon (PAH) compounds are a generally hazardous class of organic compounds which may be produced as the result of combustion or pyrolysis of fossil fuels or other organic matter. PAH contamination of groundwater and soil environments from anthropogenic sources has been documented for water and sediment samples collected in the vicinity of coal conversion facilities, petroleum plants, and waste disposal sites (14,19,32). Because many PAH compounds are toxic and/or carcinogenic, there is interest in understanding the physicochemical processes and microbial degradation reactions that affect the transport and fate of these compounds in groundwater and soil-sediment systems. In groundwater and soil environments, microbial transformations may largely determine the persistence of PAH compounds and thus affect their degree of hazard to the environment (20). In general, organic-contaminated soil-water systems are anoxic, and therefore subsurface microbial degradation of PAH compounds depends on the availability of suitable nutrients and soil microorganisms which can degrade the compounds through utilization of electron acceptors other than molecular oxygen.

A companion paper (26) reported on the microbial degradation of PAH compounds under various redox conditions in soil-water systems. It was demonstrated that naphthalene and acenaphthene were degraded under denitrification conditions, but were otherwise stable under the anaerobic test conditions. Those results indicated that PAH compounds may persist or degrade slowly in anoxic soil-water systems in the absence of nitrate or a suitable substituent group on the aromatic ring. The soil used in those tests was obtained from an upper soil horizon, from which the microorganisms may be more indicative of a denitrifier population than a fermentative population. Denitrification entails biologically mediated processes whereby oxidized forms of nitrogen may be reduced while organic carbon is oxidized. The organic carbon may be contributed from natural material, as in the case of a labile fraction of soil organic carbon, or from an organic contaminant, as in the case of PAH compounds. Thus, upon introduction into a soil-water environment, an organic contaminant

may, or may not, become the dominant source of organic carbon for use in microbial denitrification reactions, depending on the characteristics of the organic carbon content of the soil and the amount and the nature of the organic contaminant.

Microbial degradation may also depend on the PAH sorption-desorption reactions with soil and on the role of naturally occurring soil organic carbon, as a sorbent. Aqueous concentrations of hydrophobic organic compounds such as PAH compounds are highly dependent on soil sorption-desorption equilibria (13). The sorption of hydrophobic organic solutes onto soils and sediments has been well documented and shown to be dependent on the organic carbon content of the soil (16,21,22,25). Typical mineral soils may contain on the order of 0.5 to 5 % organic carbon (dry weight).

The role of soil organic carbon as an electron donor in the denitrification process has been widely recognized (29). The amount of soil organic carbon participating in these reactions has been correlated with denitrification rates, such that an increase in denitrification rate is observed with increasing soil organic carbon content (8,11,29,38). Approximately 0.6 to 1.4 % of the total naturally occurring organic carbon content of soil may be mineralized by denitrifying soil microorganisms (29); thus, much of the organic carbon content of soils is resistant to mineralization. Several researchers have reported a higher rate of denitrification upon addition of labile organic carbon to soil (10,28). Organic amendments may influence microbial degradation of xenobiotic compounds in soil; for example, exposure to amino acids has been shown to enhance aerobic degradation of *m*-cresol, *m*-aminophenol, and *p*-chlorophenol, whereas experimental results with naphthalene were inconclusive (33).

Much of the available information on microbial degradation of aromatic compounds under nitrate-reducing conditions has been obtained with phenolic or benzoate derivatives (6,7,15,34,40). Few investigations on microbial denitrification have addressed degradation of aromatic compounds having no oxygen substituent groups, although recently *p*-, *m*-, and *o*-xylene have been shown to be degraded under denitrification conditions (24, 45). In contrast, dichlorobenzenes have been found to be stable under denitrification conditions (9,24). The biotransformation of aromatic compounds having no oxygen on the ring or ring substituent is particularly important from the viewpoint of soil and groundwater contamination. Unlike phenolics, benzoates, and related compounds, which may be degraded in anaerobic as well as in denitrifying environments, it is currently believed that aromatic compounds which lack oxygen as a substituent are stable or degrade at negligible rates in anaerobic systems (5,26).

The objectives of this study were to evaluate the microbial degradation of naphthalene and acenaphthene under denitrification conditions in soil-water systems and to understand the nitrate demand exerted by both the PAH compound and the available soil organic carbon. This was accomplished by enumerating the denitrifier population, assessing the nitrate demand exerted by naturally occurring soil organic carbon, evaluating naphthalene and acenaphthene sorption onto the soil, and comparing PAH degradation under both nitrate-limiting and nitrate-excess conditions.

4.3. Materials and Methods

The soil, reagents, equipment, and procedures used in this study are described in the accompanying paper (26). The water used for cleaning glassware and experimentation was produced by a MegaPure High Capacity Deionizer (Corning Glass Works, Corning, N.Y.) and then distilled and passaged through four ultrapure (mixed-bed) cartridges (D8902; Barnstead, Boston, Mass.).

Sorption isotherm tests. The soil used in these and other tests was undisturbed, subhumid grassland soil from the Barnes-Hamerly Association, Cass County, N.D. The soil was collected from the A soil horizon and then air dried and screened to pass a U.S. standard sieve no. 10 (2.0 mm) (26). Sorption isotherms of naphthalene and acenaphthene onto the soil were determined to estimate solute partitioning to the solid phase with an aqueous phase consisting of the PAH compound, mineral medium, and 0.01 N $CaCl_2$. The soil was autoclaved for 1 h at 121°C and under steam pressure of 20 lb/in^2. The sorption isotherm tests were performed in a batch mode at room temperature with 50-ml glass centrifuge tubes fitted with Teflon-lined septums and open-port screw caps. The samples contained various amounts of soil and an initial aqueous-phase solute concentration ranging from approximately 0.2 to 10 mg/liter depending on the solubility of the solute in water. The amount of soil was varied from 1.5 to 25.0 g, (weighed to 10^{-4} g) per 50 ml to produce a range of aqueous-phase solute concentrations after equilibration. The soil was placed in a centrifuge tube, and then an aqueous mixture containing mineral medium and solute was added, with the volume recorded to 10^{-2} ml. Samples were filled to zero headspace, sealed with Teflon-lined septums and screw caps, and covered with aluminum foil to prevent photodegradation. Blanks without soil were run concurrently.

After sample preparation, the sealed centrifuge tubes were transferred to a wrist action

shaker and shaken for an equilibrium period of 24 h. Previous studies had indicated that the sorption process was not significantly time dependent after approximately 4 h and that sorption equilibrium was attained in less than 1 day. After equilibration, the tubes were centrifuged for 30 min and the separated aqueous phase was analyzed by high-pressure liquid chromatographic methods by sampling directly through the septum.

Soil Organic carbon utilization. Batch experiments were used to determine the evolution of CO_2 from a nitrate-rich soil-water mixture. A 500-ml Erlenmeyer flask was fitted with a side port at the top for purging the system with nitrogen gas, and one at the bottom for withdrawing a sample of the suspension. Soil and water were added to the flask at a soil-to-water ratio of 1:25 (g/ml) so that the initial amount of soil was 14.07 g (dry weight). A soil-to-water ratio of 1:25 was used because there were no difficulties with mixing. This was the same ratio used in the naphthalene microbial degradation tests. Companion soil organic carbon utilization tests performed at soil-to-water ratios of 1:3 and 1:10 resulted in lower values of cumulative CO_2 evolution owing to difficulty in maintaining the system completely mixed.

The soil suspension was magnetically stirred in darkness at room temperature. The system was purged with nitrogen gas for 3 h prior to nitrate addition and purged continuously thereafter for the duration of the experiment. Sodium nitrate was added such that the initial nitrate concentration was approximately 800 mg NO_3^- as nitrate per liter. The flask was immediately sealed and connected to a CO_2 trap which contained 100 ml of 0.025 N KOH solution. A portion of soil suspension was removed periodically from the bottom side port, centrifuged, filtered, and analyzed for nitrate by colorimetric procedures. The caustic solution in the CO_2 trap was replaced daily and titrated with standard acid. Blank flasks without soil were run concurrently to monitor the purity of the nitrogen gas and to verify nitrate reduction due to microbiological processes.

Most-probable-number tests. The denitrifying cell population was enumerated by a most-probable-number method described by Alexander (1). Two different bacterial growth media were used for comparison (1,4). Positive tubes were indicated by a color change, due to an increase in alkalinity, in conjunction with the formation of gaseous nitrogen.

PAH degradation under denitrification conditions. Stock PAH and mineral medium solutions (1 liter each) were prepared separately. The stock PAH solution consisted of a saturated PAH solution in deionized water. A mineral medium-phosphate buffer solution was

prepared which consisted of $NaNO_3$ and the following salts (in milligrams per liter): KH_2PO_4, 17.0; K_2HPO_4, 43.50; $Na_2HPO_4 \cdot 7H_2O$, 66.8; $FeCl_3 \cdot 6H_2O$, 0.50; NH_4Cl, 3.4; sufficient $CaCl_2$ so that a final ionic strength of 0.01 N $CaCl_2$ was obtained in each individual sample was also added.

The mineral medium solution was degassed by vacuum treatment for 30 min and then purged with helium for 30 min. The saturated PAH solution was filtered through an extra-thick glass fiber filter (Gelman Sciences, Inc., Ann Arbor, Mich.), and then both solutions were combined and purged with helium for 1 h. The pH of the final solution was adjusted to 7.0 by the addition of 1 N HCl or 1 N NaOH as needed. The absence of dissolved oxygen was verified by titrimetric procedures (3).

Aliquots were transferred to 50-ml glass centrifuge tubes which typically contained 1 or 2 g (dry weight) of Barnes-Hamerly soil for acenaphthene and naphthalene experiments respectively. The samples were sealed immediately with Teflon-lined septums and open-port screw caps, and the tubes were covered with aluminum foil. No headspace was visible in the tubes. Samples were shaken for 3 h per day on a wrist action shaker and maintained at room temperature. Periodically, individual samples were withdrawn, centrifuged at 875 x g, and sampled directly through the septum for analysis of aqueous PAH compound concentration by high-pressure liquid chromatographic methods with fluorescence detection. Nitrate, nitrite, and sulfate were analyzed by either colorimetric or ion chromatographic (IC) methods after analysis for PAH compound. Individual samples were withdrawn for analysis during the course of an experiment and then removed from service after being analyzed, except for some samples in the special experiments in which additional nitrate was introduced into the system following depletion of nitrate.

Sterilized blanks containing no soil and controls containing sterilized soil were run concurrently. Sterilization consisted of autoclaving samples on three consecutive days for 1 h at 121°C under steam pressure of 20 lb/in^2. Heat sterilization was supplemented in later experiments by the addition of $HgCl_2$ at 200 mg/liter. Heat sterilization was effective in inhibiting microbial degradation of PAH compounds, whereas addition of $HgCl_2$ with autoclaving was required to completely inhibit nitrate reduction.

Initially, analysis for nitrate was performed spectrophotometrically by reduction of nitrate to nitrite, followed by diazotization and coupling of nitrite with N-[1-naphthyl]ethylenediamine

(Bausch & Lomb, Inc., Rochester, N.Y.). Nitrite was analyzed similarly but with the absence of the preceding reduction step. In all later tests, aqueous-phase nitrate, nitrite, and sulfate concentrations were analyzed by IC methods with a Dionex IC 14 equipped with an AS3 separator column and a 35350 anion fiber suppressor column (Dionex Corp., Sunnyvale, Calif.). An eluent of 0.0015 M $NaHCO_3$ and 0.0012 M Na_2CO_3 was used. Prior to analysis by IC methods, organic constituents were removed by passing 15 ml of aqueous sample through a C_{18} cartridge (Waters Associates, Inc., Milford, Mass.). Samples were then stored in a freezer prior to IC analysis. Ammonia was analyzed by a colorimetric automated phenate method (41). A detection limit of 0.01 mg/liter was observed for all anions. Nitrate and other compound analyses are reported as compound, e.g., milligrams per liter as NO_3^-.

Tests with acclimated soil. Experiments were performed to determine whether the acclimation period was affected by using soil which had been previously exposed to naphthalene. Individual centrifuged samples were reserved and stored under refrigeration at the conclusion of a set of degradation tests which showed that a nondetectable aqueous-phase concentration of naphthalene had been reached. These samples were used in a subsequent test by adding an aqueous solution containing deoxygenated PAH compound and mineral medium and resuspending the solid phase. The aqueous solution consisted of a mixture of naphthalene stock solution combined with an aqueous phase decanted from former test samples containing mineral nutrients, $NaNO_3$, and electrolyte described previously.

4.4. Results

Experiments were conducted to evaluate the microbial degradation of naphthalene and acenaphthene under denitrification conditions in soil-water systems. The study included experiments to examine the partitioning of acenaphthene and naphthalene between the solid and the aqueous phases, the role of soil organic carbon in nitrate reduction, and the significance of nitrate-limiting conditions on microbial degradation of PAH compounds via nitrate reduction.

Solute sorption. Figure 1 shows a linear sorption isotherm for naphthalene and Barnes-Hamerly soil. Various laboratory studies have shown for sparingly soluble, hydrophobic organic solutes that sorption onto soils can be described by a linear isotherm (13,21):

$$S = K_p C$$

where S is the amount of solute sorbed (in milligrams of solute per gram of soil), C is the equilibrium aqueous solute concentration (in milligrams per liter), and K_p is the linear sorption partition coefficient (in liters per gram or per kilogram). For the sorption of acenaphthene and naphthalene onto Barnes-Hamerly soil, K_p was 52 (r^2 = 96.4 %) and 12 (r^2 = 99.1 %) liters/kg, respectively.

The sorption of hydrophobic organic solutes onto soils can be correlated with the organic carbon content of a given soil. The role of soil organic matter in sorption of hydrophobic aromatic solutes onto soil has been studied extensively and is similar to that of an organic solvent in solvent extraction; thus, the partitioning of a relatively nonpolar compound between soil organic matter and water should correlate well with the partitioning of that solute between water and an immiscible organic solvent (13). A normalized soil sorption coefficient can be defined as follows:

$$K_{oc} = K_p / OC \qquad [1]$$

where OC is the fractional mass of organic carbon in a soil. Various researchers have presented relationships between values of K_{oc} and the solute octanol/water partition coefficient, K_{ow}, for nonpolar aromatic compounds (21,22,25,31). For sorption of relatively hydrophobic organic solutes, the relationship between K_{oc} and K_{ow} is usually given by a linear regression in the following form:

$$\log K_{oc} = a \log K_{ow} + b \qquad [2]$$

where a and b are regression coefficients. The correlations between K_{oc} and K_{ow} result in a somewhat divergent set of relationships which may be attributed to various factors including kinetic or steric effects, as well as hydrophobic contributions to sorption.

Measured values of log K_{ow} for naphthalene are about 3.36 (18,22). Log K_{ow} for acenaphthene may be estimated as 4.03 on the basis of molecular structure by using atomic group hydrophobic fragment constants (13,44). From equations 1 and 2, it is expected that the ratio of the values of K_{ow} for acenaphthene and naphthalene, 4.7, should be similar to the ratio of the experimental values of K_p for the two solutes, 4.3, as evidenced here. The organic carbon content of the soil was measured by the Walkley-Black method (2) and found to be 2.9 ± 0.28, which resulted in a predicted value of K_{oc} which agrees within a factor of about 1.5 of that given by equation 2 with regression coefficients suggested by Schwarzenbach and Westall (31).

Most-probable-number tests. Most-probable-number tests were performed to

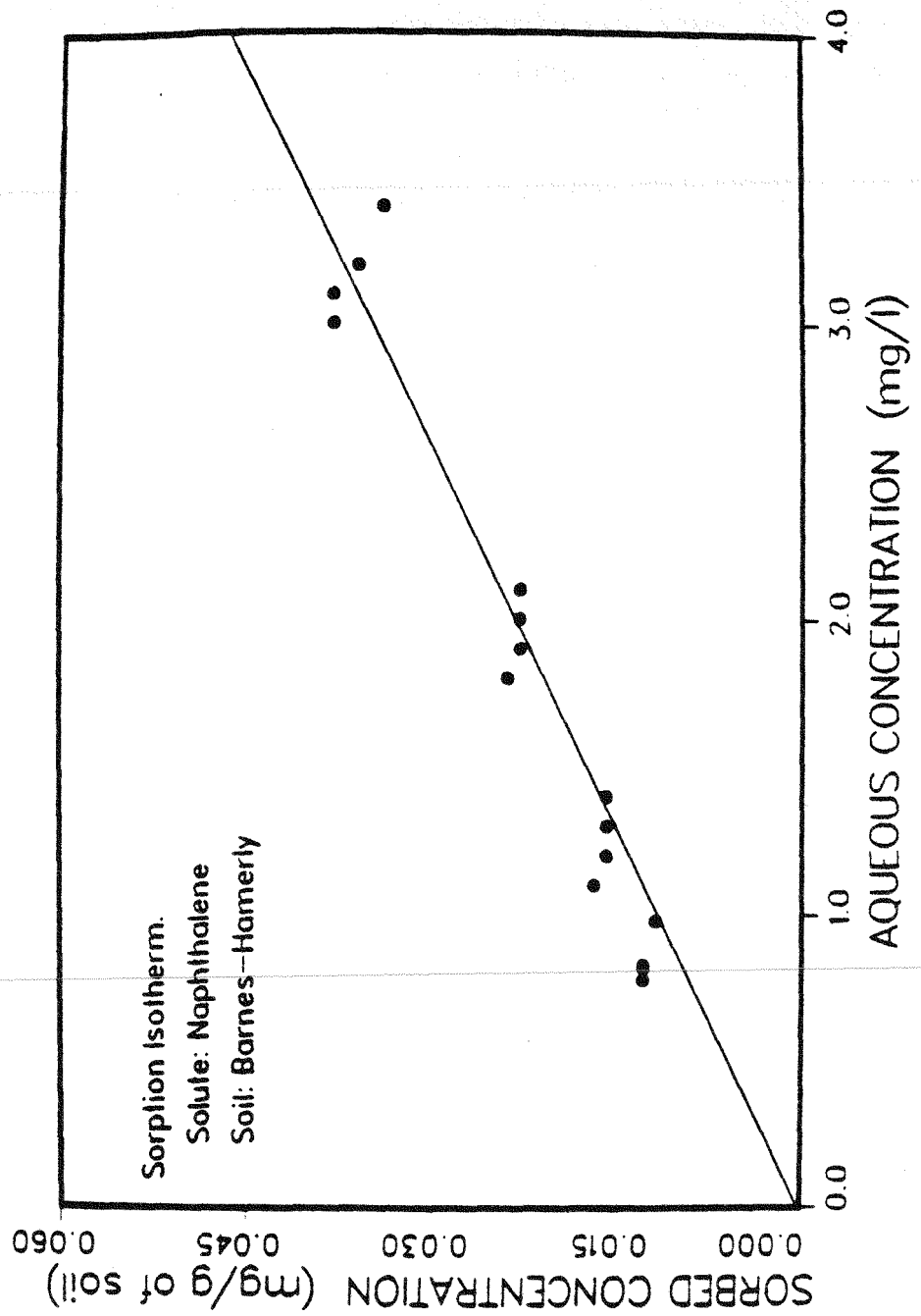

Figure 1. Sorption isotherm for the solute naphthalene onto Barnes-Hamerly soil. K_p = 12 liters/kg with r^2 = 99.1 %.

enumerate nitrate-reducing microorganisms in soil samples prior to their use in the degradation experiments. The average value for five individual most-probable-number tests by the method of Alexander (1) was $1.2 \times 10^5 \pm 6 \times 10^4$ denitrifying organisms per g of soil. Most-probable-number tests, conducted with a second growth medium (4), also yielded an average number of 1.2×10^5 denitrifying organisms per g of soil.

Microbial utilization of soil organic carbon. Figure 2 shows results of experiments to assess the mineralization of soil organic carbon by denitrifying microorganisms. Figure 2 presents the average results for three individual tests conducted simultaneously for cumulative CO_2 evolution over 20 days at a soil-to-water ratio of 1:25 (g/ml). These data show that the denitrification process was initiated immediately. Soil organic carbon utilization was assumed to follow first-order kinetics (29), and hence carbon mineralization can be described as follows:

$$dC/dt = -k_c C \qquad [3]$$

where C is the available carbon remaining in the soil (in milliequivalents CO_2), k_c is a first-order carbon mineralization coefficient (in reciprocal hours) and t is time (in hours). Integration of equation 3 yields

$$C = C_{max}\exp(-k_c t) \qquad [4]$$

where C_{max} is defined as the maximum available soil organic carbon (in milliequivalents CO_2). Since C equals C_{max} minus the evolved CO_2, substitution of this expression into equation 4 and rearranging yields the following equation describing the cumulative evolution of CO_2.

$$CO_2 = C_{max}[1 - \exp(-k_c t)]$$

The data in Figure 2 were used to estimate k_c and C_{max} as 0.0049 hr^{-1} and 0.63 meqv (0.27 mg of C per g of soil), respectively (r^2=88%). The fitted parameters, k_c and C_{max}, were found by using a nonlinear, parameter estimation program (P.S. McCroskey, and G.J. McRae, PAREST, A Computer Program for Estimation of Parameters in Algebraic and Ordinary Differential Equation Models, Carnegie Mellon University, Pittsburgh, Pa., 1987).

PAH degradation. The datum points shown in Fig. 3 to 9 for blanks, controls, and test samples represent the average values of analysis of two or three individual samples. The individual samples were removed from the experiment after analyses. The data for the sample blanks show no change for the duration of any of the experiments for either PAH compound or nitrate, for experiments lasting up to 84 days. This demonstrates that there was no loss of PAH compound or nitrate via the Teflon-lined septum, or PAH degradation owing to photolysis. Sterile controls were also stable for the duration of the experiments, which

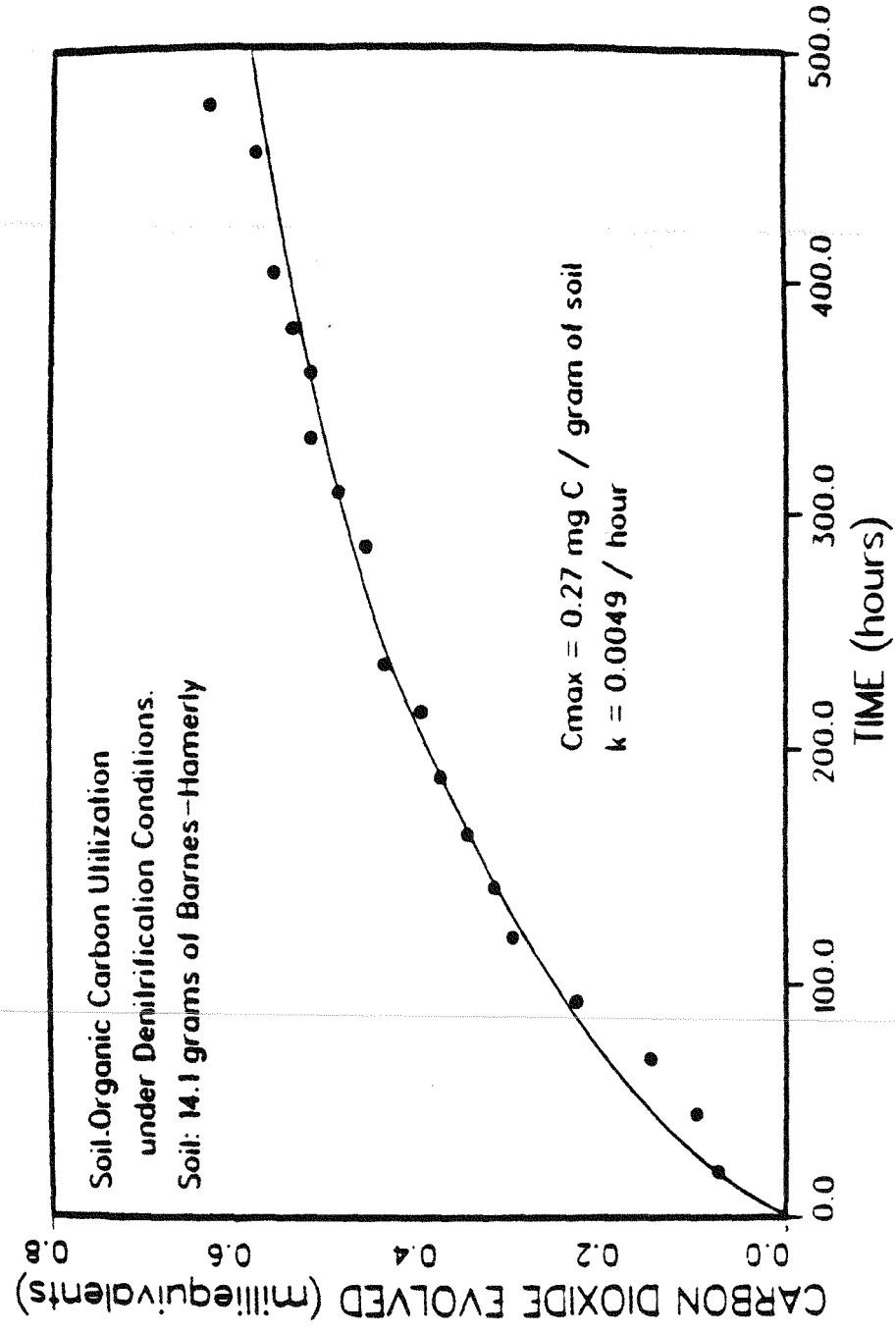

Figure 2. Soil organic carbon utilization under denitrification conditions with a soil-to-water ratio of 1:25 (g/ml).

confirms the absence of PAH loss across the Teflon-lined septum, as well as lack of significant abiotic degradation reaction with the soil.

The experiments to examine the microbial degradation of naphthalene and acenaphthene under denitrification conditions encompassed a time span of nearly 1 year. The results of the experiments shown in Fig. 3 to 9 were performed with soil samples withdrawn from a single large batch, and therefore the soil aged over the approximate 1-year duration of the microbial degradation tests. The chronology of the experiments progressed from results shown in Fig. 3 and 4, to 5, and to 6 through 9. The data show that the acclimation period associated with the onset of naphthalene degradation increased with soil age from approximately 12 days (Fig. 3) to about 24 days (Fig. 6). Similar results were evident for acenaphthene, in which the acclimation period increased with soil age from approximately 12 days (26) to about 36 days (Fig. 8). In all cases, nitrate reduction via mineralization of soil organic carbon was observed to be initiated immediately with no acclimation period even with aged soil.

Figure 3 shows naphthalene degradation under nitrate-reducing conditions for two samples sets in concurrent experiments, each with a soil-to-water ratio of 1:50 (g/ml). The results show the aqueous-phase naphthalene concentration decreasing from approximately 4 and 3 mg/liter to nondetectable levels in 47 and 33 days for sample sets 1 and 2, respectively. An acclimation period of approximately 2 weeks was observed prior to evidence of significant degradation of naphthalene. The decrease in nitrate concentration over the duration of the experiment was in the range of 40 and 18 mg of NO_3^- per liter, for sample sets 1 and 2, respectively, as determined by colorimetric procedures. The residual nitrate concentration in the test samples at the conclusion of the experiment was 110 and 66 mg of NO_3^- per liter; therefore, there was excess nitrate in the samples through the duration of the microbial degradation reactions. The results shown in Fig. 3 were supplemented by monitoring selected samples for ammonia to assess nitrate assimilation to ammonium. The aqueous-phase ammonia concentration in the test samples exhibiting naphthalene degradation was similar to that in the blanks and controls (i.e. < 1.0 mg/liter).

Acenaphthene degradation under denitrification conditions is shown in Fig. 4 for two concurrent sample sets. In these tests the initial nitrate concentration was adjusted to provide for less than half the nitrate demand observed for the sample sets in Fig. 3. The initial nitrate concentration was 11 and 9 mg of NO_3^- per liter for sample sets 1 and 2, respectively. In both

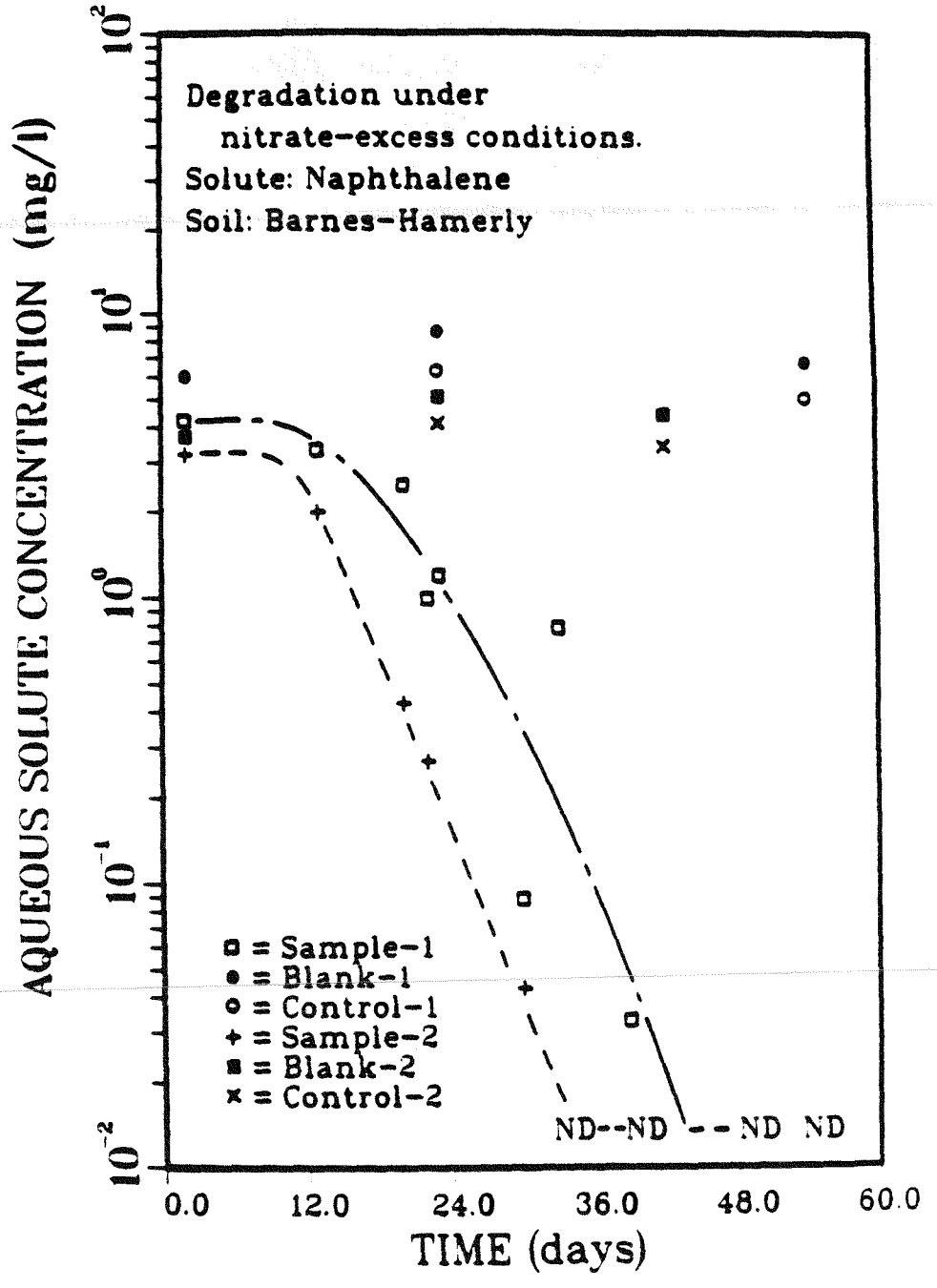

Figure 3. Microbial degradation of naphthalene under denitrification conditions with 1 g of Barnes-Hamerly soil per 50-ml centrifuge tube. ND, Nondetectable levels.

sample sets, nitrate was depleted to nondetectable levels in approximately 2 weeks; thereafter, the microbial denitrification degradation reactions were restricted owing to the lack of nitrate. The initial aqueous acenaphthene concentrations were approximately 0.60 and 0.40 mg/liter for sample sets 1 and 2 respectively. Sample set 1 showed no significant degradation of acenaphthene over a time span of 12 weeks, whereas sample set 2 showed a small decrease in acenaphthene concentration to approximately 0.2 mg/liter over a period of about 40 days, after which the acenaphthene concentration remained constant for the final month of the experiment. In agreement with results shown in Fig. 3 for naphthalene and with results presented for acenaphthene in the accompanying paper (26), there was no substantial degradation of acenaphthene under nitrate-limiting conditions.

Additional experiments were conducted to assess the role of nitrate on microbial degradation of naphthalene. In these and subsequent tests, nitrate, nitrite, and sulfate analyses were performed by IC methods. The analysis for aqueous sulfate concentration was used to determine whether the observed PAH degradation was related to sulfate reduction. Sulfate was not added to samples intentionally, but was present as a result of its natural occurrence in the soil. In the following experiments with naphthalene, 2 g of Barnes-Hamerly soil were used in 50-ml samples, which resulted in an initial aqueous sulfate concentration in the range of 4 to 7 mg/liter. The sulfate concentration did not change from the initial levels through the course of the experiments. Nitrite was nondetectable (< 0.01 mg/liter) in almost all of the samples, except during days 1 and 2 when nitrite was observed in many samples at concentrations less than 1 mg/liter. Selected samples were monitored throughout the experiment for pH, and the pH values in the completed samples ranged from 6.8 to 7.2.

Figure 5 shows aqueous naphthalene and nitrate concentrations over time for an experiment in which a small amount of nitrate was added to the test samples initially. After the initial nitrate was depleted to nondetectable levels (< 0.01 mg/liter), additional nitrate was introduced to the samples by injection through the septum with a syringe equipped with a removable gas chromatography needle. Approximately 8 μl of 3.0 M nitrate solution was added to the samples, which increased the aqueous nitrate concentration to 28.5 mg/liter. As a precaution against possible naphthalene volatilization losses due to the puncturing of the Teflon-lined septum, the septum was sealed with a drop of silicone glue, although independent screening tests had shown no loss of naphthalene over a 10 day period from test blanks which had been punctured eight times with the syringe needle.

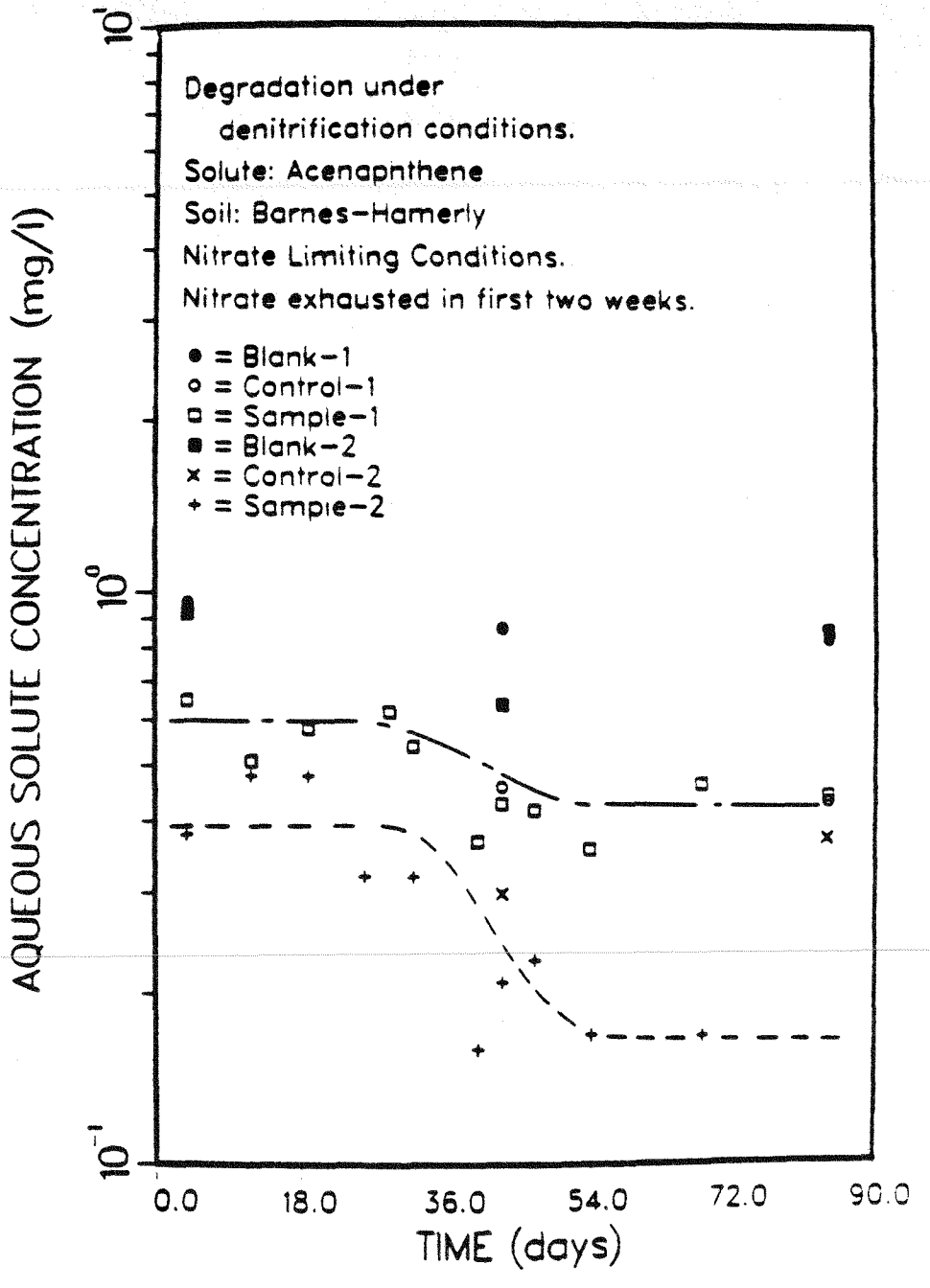

Figure 4. Microbial degradation of acenaphthene under denitrification conditions for a case in which nitrate was limiting. The initial nitrate concentration was depleted to nondetectable levels in the first 2 weeks.

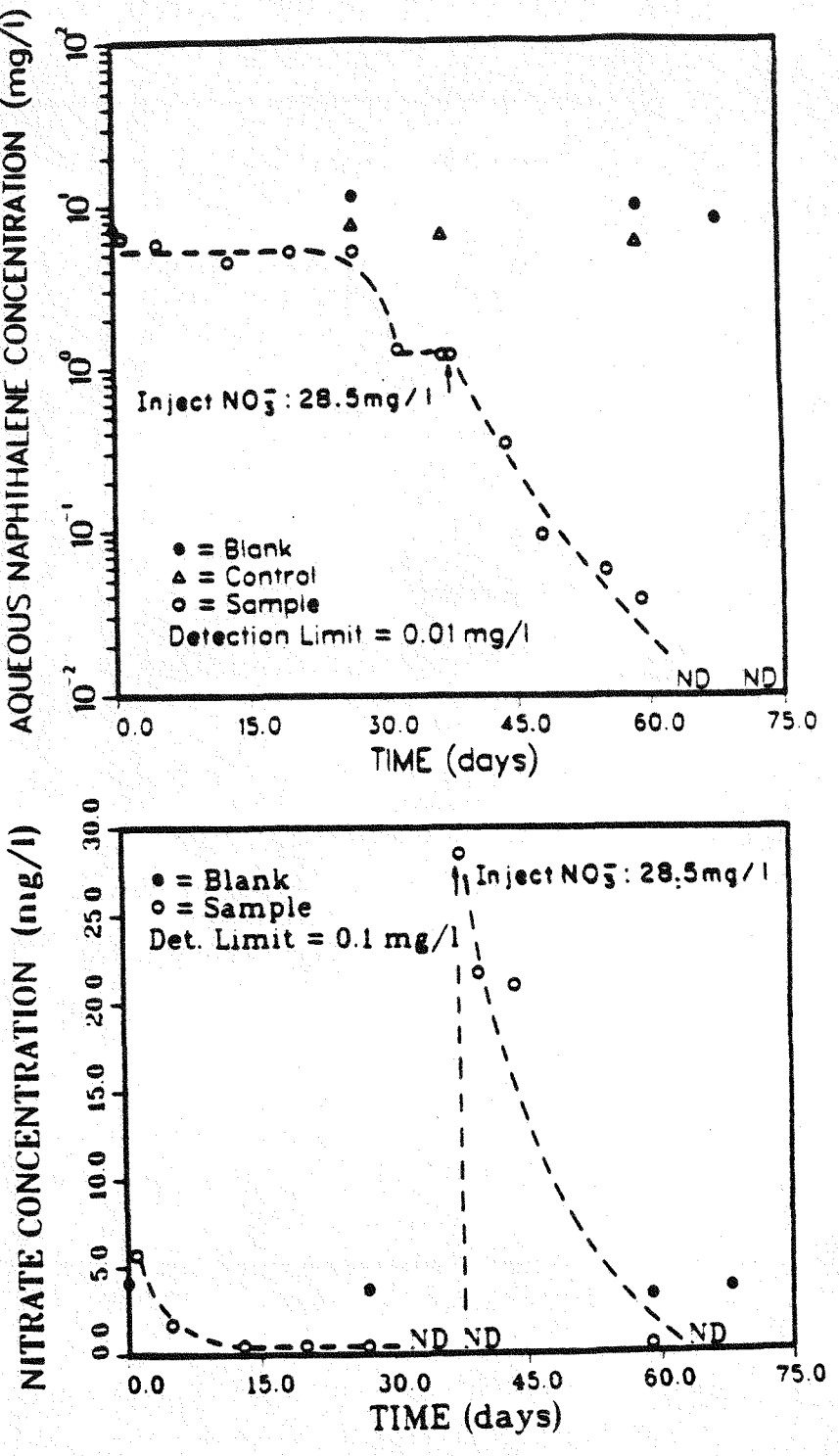

Figure 5. Aqueous naphthalene and nitrate concentrations under denitrification conditions. The nitrate was exhausted in 30 days, and this resulted in the cessation of naphthalene degradation. After reintroduction of nitrate on day 38, the denitrification reactions resumed. ND, Nondetectable levels.

was reduced from about 5 to 1.5 mg/liter. The naphthalene concentration remained constant from days 30 to 38 owing to the depletion of nitrate. Following injection of nitrate on day 38, the microbial degradation of naphthalene was resumed and naphthalene attained nondetectable levels 3 weeks after the reintroduction of nitrate into the samples.

Figures 6 and 7 show a set of confirmation tests for microbial degradation of naphthalene under nitrate-excess and nitrate-limiting conditions, respectively, with 2 g soil per 50 ml. Sufficient nitrate was available through the duration of the test, and the nitrate concentration was decreased from approximately 95 to 40 mg/liter (Fig.6). During the first 2 weeks of the test, 55 mg of nitrate per liter was depleted owing to oxidation of the mineralizable portion of soil organic carbon, and after approximately 1 month of the experiment there was a 16-mg/liter decrease in nitrate concentration. The latter decrease in nitrate levels coincided with a decrease in the aqueous naphthalene concentration from approximately 4.4 mg/liter to nondetectable levels in 3 to 4 weeks following a 30 day acclimation period. In contrast, under nitrate-limiting conditions, the aqueous naphthalene concentration remained constant at 6 mg/liter for 11 weeks (Fig. 7). In this test the initial nitrate concentration was 9 mg/liter and nitrate was reduced to nondetectable levels in 20 days. The sample blanks and controls remained at constant levels for the duration of the test, which again confirmed the stability of the samples with respect to volatilization or abiotic degradation. Furthermore, the stability of the test samples in Fig. 7 confirmed that there was no oxygen intrusion across the septum.

Figures 8 and 9 show an analogous set of confirmatory tests with acenaphthene and 1 g of soil per 50 ml under nitrate-excess and nitrate-limiting conditions respectively. Acenaphthene degraded from an initial aqueous-phase concentration of approximately 0.60 mg/liter to near nondetectable levels in 80 days following an acclimation period of approximately 42 days (Fig. 8). The nitrate concentration decreased from approximately 55 to 15 mg/liter over the duration of the test, with most of the nitrate depletion occurring in the first 2 weeks. Figure 9 shows the aqueous-phase acenaphthene concentration under nitrate-limiting conditions. In this test the initial nitrate concentration was 58 mg/liter and this was reduced to nondetectable levels in approximately 22 days. There was no degradation of acenaphthene over a period of 83 days, and the aqueous phase acenaphthene concentration remained at approximately 0.60 mg/liter throughout the test. As observed in previous experiments, the stability of blanks, controls, and test samples confirms the integrity of individual samples and the absence of volatilization and/or oxygen intrusion.

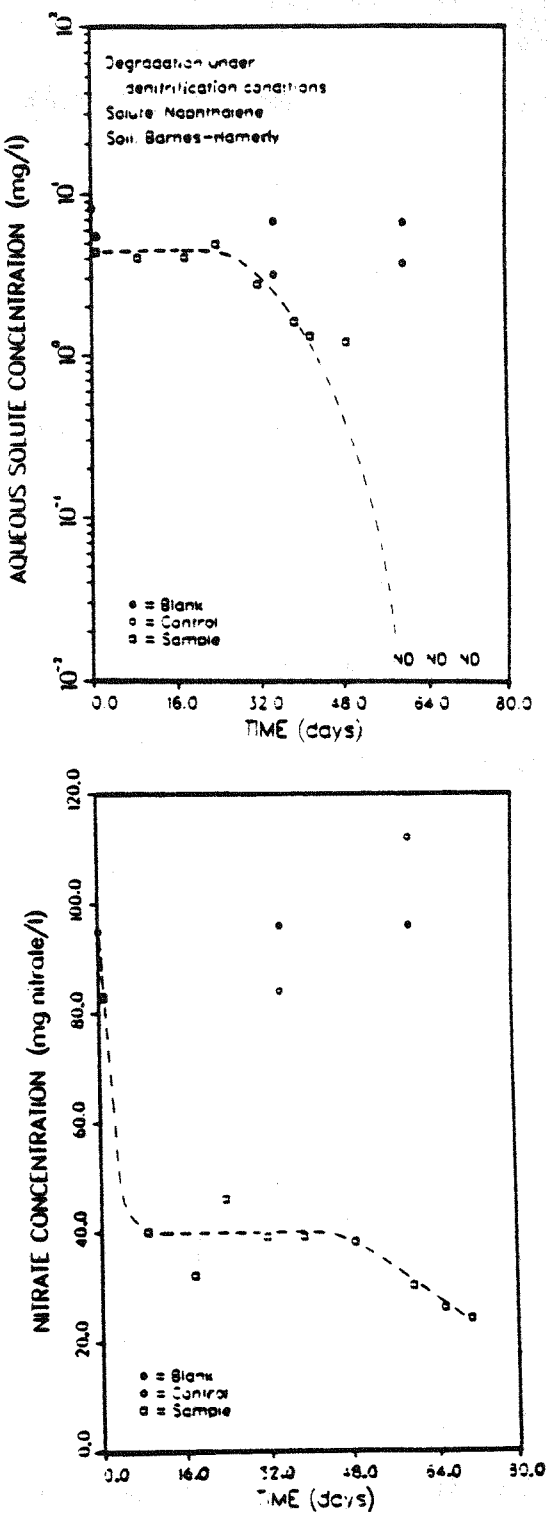

Figure 6. Aqueous naphthalene and nitrate concentrations under denitrification conditions for a case in which nitrate was in excess. Naphthalene degraded from an initial concentration of 4.5 mg/liter to nondetectable levels (ND) in 60 days, with an acclimation period of approximately 30 days.

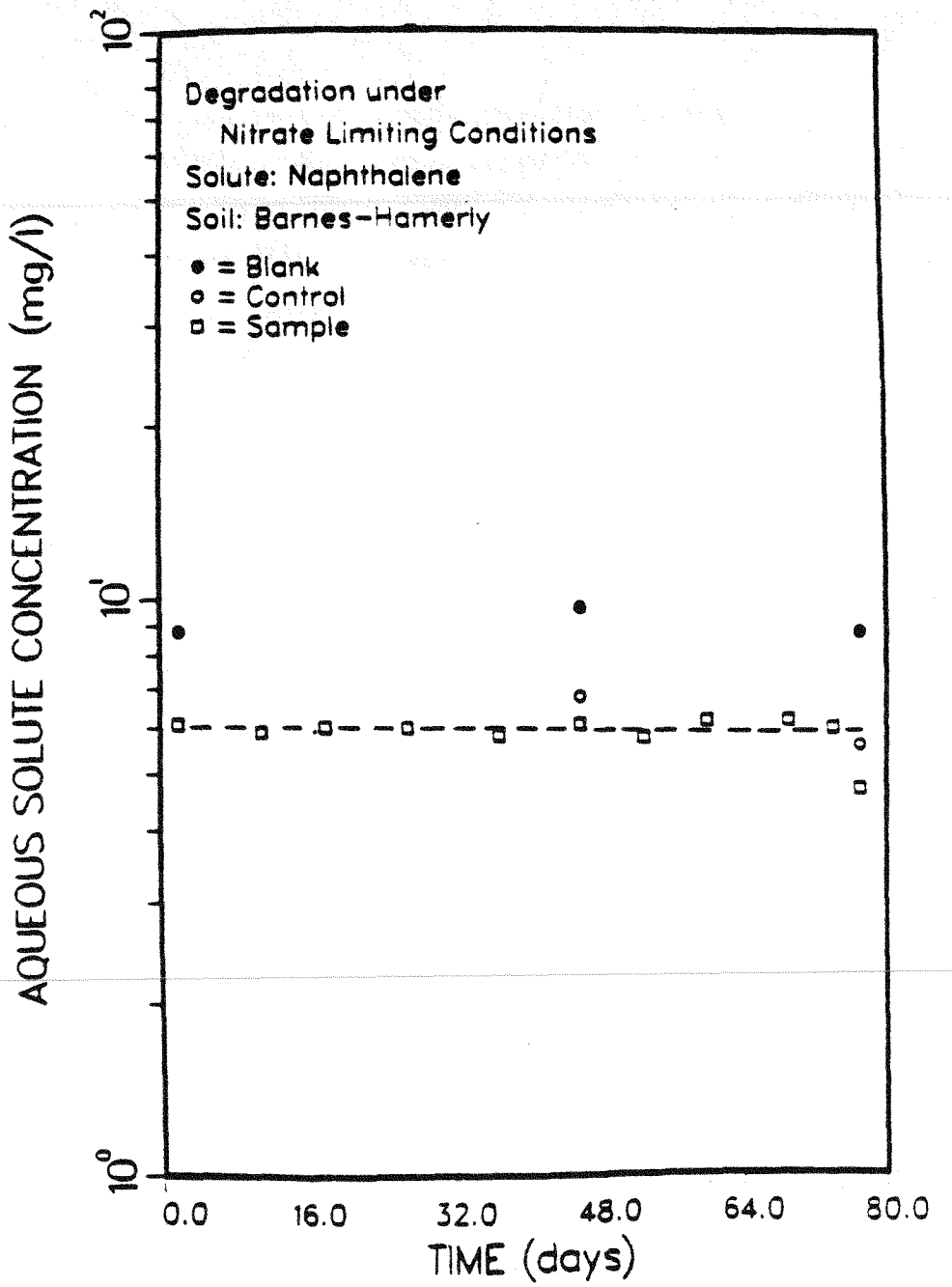

Figure 7. Microbial degradation of naphthalene under denitrification conditions for a case in which nitrate was limiting. The aqueous naphthalene concentration remained at 6 mg/liter for 11 weeks. The initial nitrate concentration of 9 mg/liter was depleted to nondetectable levels in 20 days.

acenaphthene over a period of 83 days, and the aqueous phase acenaphthene concentration remained at approximately 0.60 mg/liter throughout the test. As observed in previous experiments, the stability of blanks, controls, and test samples confirms the integrity of individual samples and the absence of volatilization and/or oxygen intrusion.

A concluding set of tests were performed to determine whether the acclimation period associated with naphthalene degradation could be eliminated if acclimated soil was used in the experiment in lieu of field soil. Samples showing naphthalene degradation from the tests shown in Fig. 6 were used in this experiment. The results are shown in Fig. 10; the aqueous-phase naphthalene concentration decreased from approximately 3.0 mg/liter to nondetectable levels in approximately 16 days. No acclimation period was observed in this experiment, and the nitrate concentration decreased from approximately 37 to 17 mg/liter.

4.5. Discussion

This study evaluated the microbial degradation of naphthalene and acenaphthene in soil-water systems under denitrification conditions. Acenaphthene and naphthalene were degraded microbially to nondetectable levels under denitrification conditions in systems in which nitrate was not a limiting constituent. An evaluation of the manner in which the PAH compounds may be degraded by soil microorganisms under nitrate-reducing conditions requires an understanding of the relevant fractions of organic carbon in the soil-water system. With regard to the tests described here, carbon may exist as four entities: (i) soil organic carbon available for mineralization, (ii) soil organic carbon refractory to mineralization, (iii) PAH compound in the aqueous phase, and (iv) PAH compound in the sorbed phase. The nature of these entities influenced the results of this study.

Sorption and degradation. Sorption isotherms demonstrated the partitioning of the PAH solute between sorbed and aqueous phases. As expected, acenaphthene exhibited a greater tendency to sorb than naphthalene, and the extent of solute sorption at equilibrium was correlated with the organic carbon content of the soil and the octanol/water partition coefficient of the solute. It is anticipated that solute sorption is important in our understanding of the mechanistic processes which may govern the microbial degradation of sorbable, hydrophobic organic solutes such as PAH compounds. Intracellular degradation of PAH compounds depends in part on the availability of the organic compound to the microorganisms. If an organic compound were irreversibly sorbed to soil organic matter, it

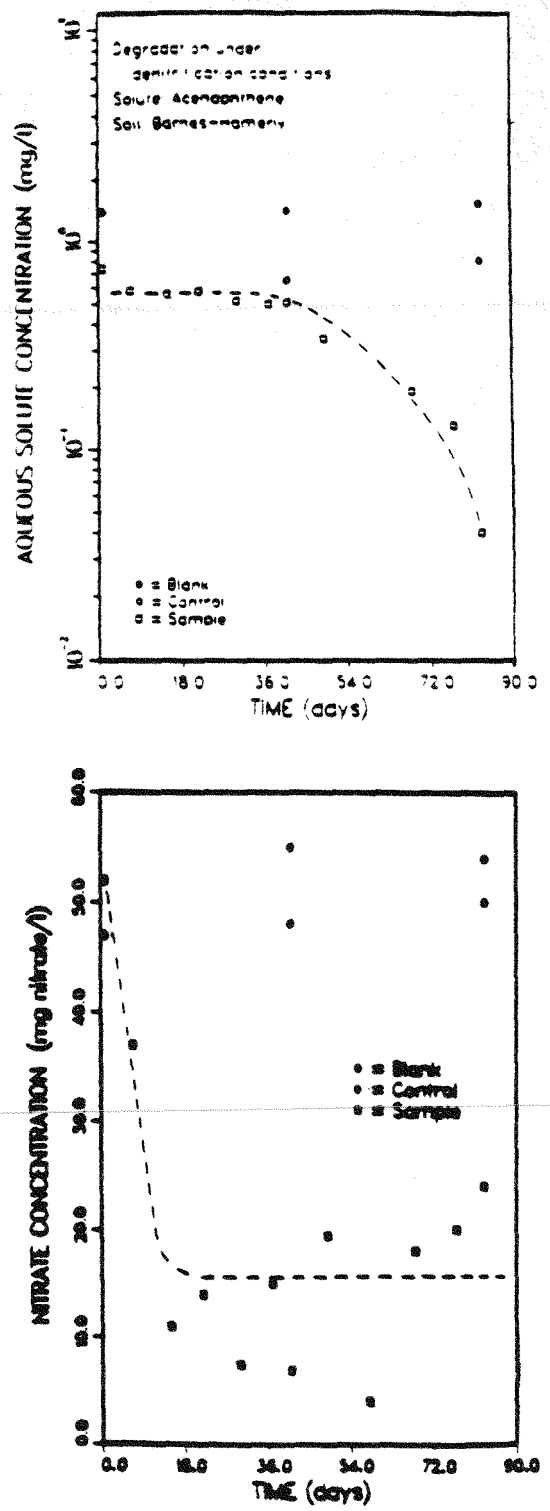

Figure 8. Aqueous acenaphthene and nitrate concentrations under nitrate-excess conditions. Acenaphthene degraded from an initial concentration of 0.60 mg/liter to nondetectable levels in 80 days, with an acclimation period of approximately 42 days.

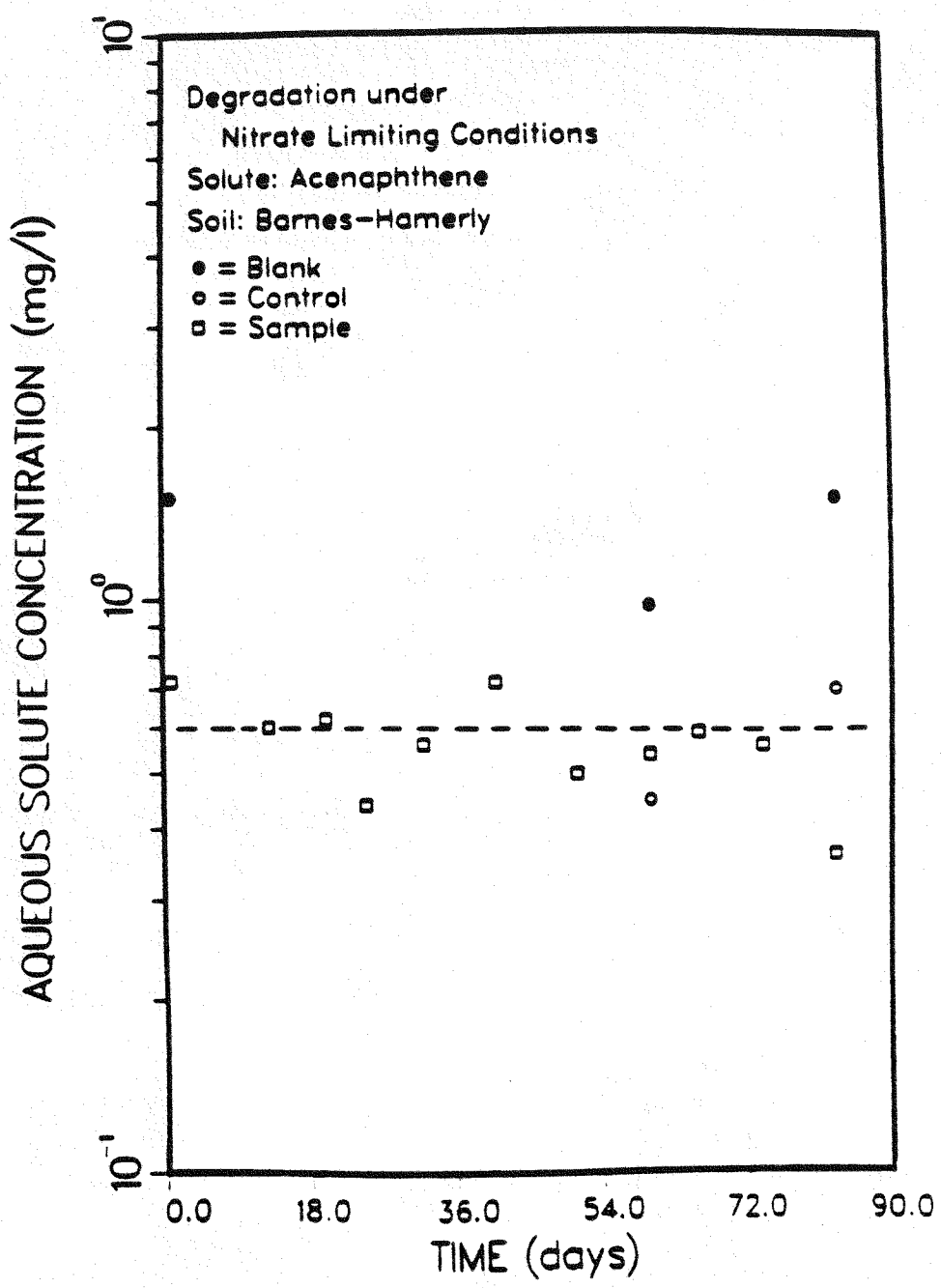

Figure 9. Microbial degradation of acenaphthene under nitrate-limiting conditions. The aqueous acenaphthene concentration remained at 0.6 mg/liter for 83 days.

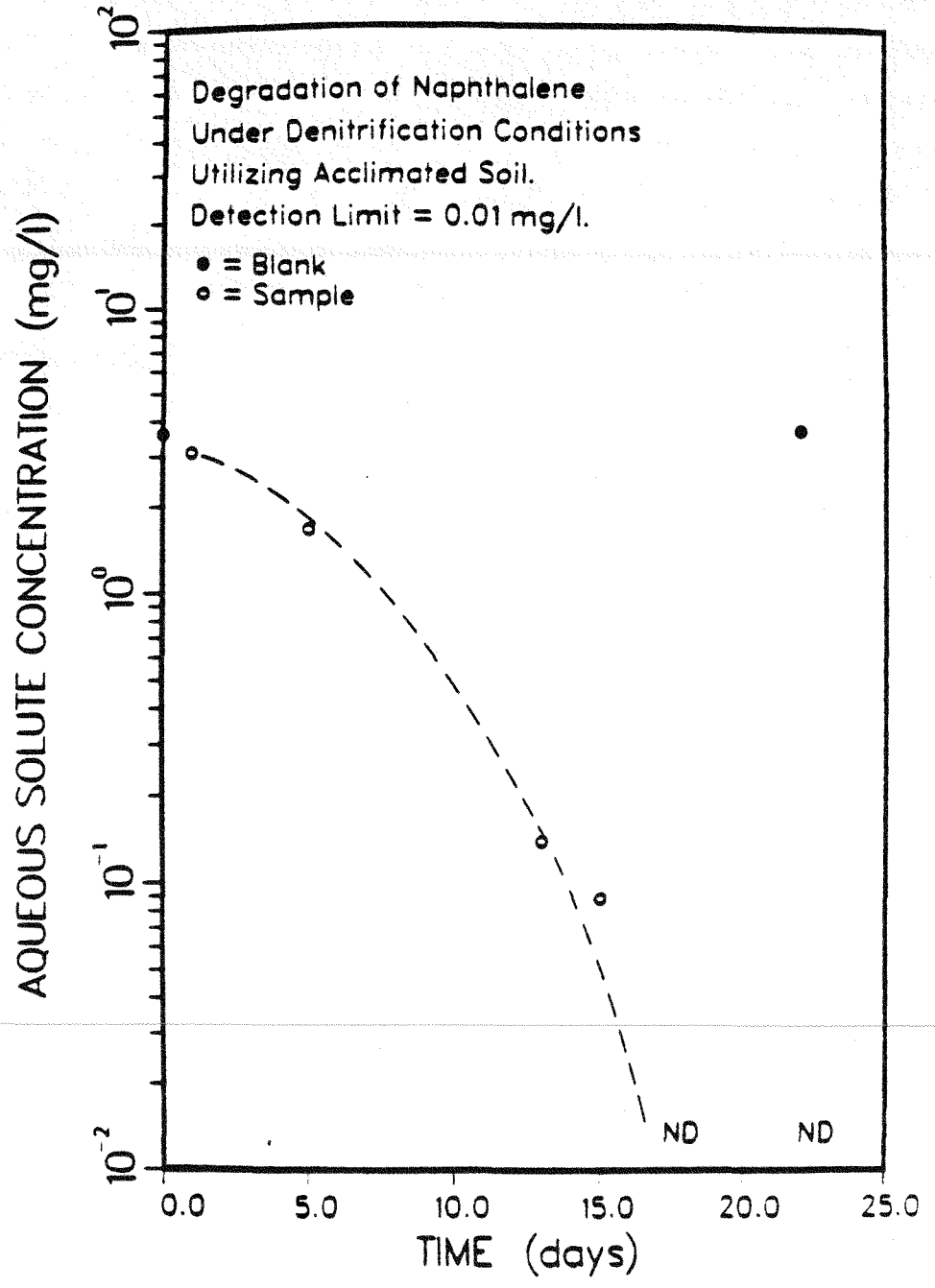

Figure 10. Microbial degradation of naphthalene under denitrification conditions with acclimated soil. The initial aqueous naphthalene concentration was reduced from 3.1 mg/liter to nondetectable levels (ND) in 16 days. No acclimation period was evident.

may be isolated and protected from intracellular degradation. Alternatively, if the organic compound were reversibly sorbed to soil organic matter, the solute would desorb from the soil organic carbon in response to a decrease in the aqueous-phase concentration. Thus solute desorption and diffusion through the aqueous phase would increase the accessibility of the solute to microorganisms. It may be hypothesized that surface diffusion and surface scavenging of sorbed organic solute by sorbed microorganisms may occur; however, the current perception is that soil microbial degradation reactions are inhibited or significantly slowed for a sorbed-phase solute than for an aqueous-phase solute.

The role of organic solute sorption in microbial degradation is not well understood, although available evidence suggests that sorption decreases the total amount of the organic solute available to microorganisms for degradation (27). Steen et al. (39) have presented results for the degradation of chlorpropham and di-*n*-butyl phthalate in soil, for which it was assumed that sorption rendered the sorbed solute unavailable for degradation. Ogram et al. (27) evaluated the effects of sorption of both bacteria and a herbicide (2,4-dichlorophenoxyacetic acid) on microbial degradation in soil. It was concluded that sorbed 2,4-dichlorophenoxyacetic acid was completely protected from microbial degradation. If these findings are applicable to soil-water systems with the solutes naphthalene and acenaphthene, the reversibility and kinetics of desorption of the PAH compounds from soil will affect the rate of degradation of the PAH compounds in a soil-water environment. This issue is currently being investigated by experimental and modeling activities in our laboratory to assess the kinetics and reversibility of PAH desorption in conjunction with the kinetics of microbial degradation. Initial observations with the solute naphthalene have indicated that the soil sorption-desorption process is reversible; this finding is supported by the work of Gschwend and Wu with chlorobenzenes (17). Therefore, for these lower-molecular-weight PAH compounds, the total amount of PAH in the soil-water system, i.e., aqueous phase plus sorbed phase, may be potentially available to the soil microorganisms.

Mineralization of soil organic carbon. Aside from the PAH compound, a portion of the soil organic carbon is also utilized by soil-denitrifying microorganisms. Many of the degradation tests reported here were performed at a soil-to-water ratio of 1:25 (g/ml), and it was found in separate experiments that the maximum amount of mineralizable soil organic carbon (C_{max}) under denitrification conditions was 0.27 mg of C per g of Barnes-Hamerly soil. The soil used in this study had an organic carbon content of 2.9 %. Thus, 0.9 % of the total organic carbon was available for mineralization by the soil denitrifiers. This agrees with other

work which has shown that C_{max} may range from about 0.6 to 1.4 % of the total organic carbon for various mineral and organic soils (29). Thus, much of the naturally occurring organic matter in soil is resistant to microbial decomposition under denitrification conditions, and therefore the mineralization of soil organic carbon via denitrification should have minimal effect on the bulk of the soil carbon phase associated with PAH sorption.

The total mass contributions of potentially degradable PAH compound and labile soil organic carbon are comparable in magnitude in the tests reported here. In an experiment with an initial aqueous solute concentration of naphthalene of 7.0 mg/liter, 2 g of soil per 50 ml, and an experimentally determined K_p of 12 liters/kg, the mass of degradable naturally occurring organic carbon is about 0.54 mg, whereas the total amount of degradable naphthalene is about 0.52 mg. For the solute acenaphthene, with 1 g of soil per 50 ml, an initial equilibrium concentration of 1 mg/liter, and an experimentally determined K_p of 52 liters/kg, the amount of degradable naturally occurring soil organic carbon is approximately 0.27 mg, with the total amount of acenaphthene being about 0.15 mg. There is insufficient evidence to judge conclusively the extent to which the PAH compound may be mineralized to CO_2 via microbial denitrification. Nonetheless, as discussed below, the nitrate demand per milligram of PAH compound may be comparable to the nitrate demand per milligram of soil organic carbon for naphthalene degradation under nitrate-excess conditions.

Nitrate demand. The tests with unacclimated soil showed that the mineralizable portion of the soil organic carbon is utilized quickly in comparison with the PAH compound. At approximately 20 days, this supply of soil organic carbon is depleted, assuming slow conversion of residual refractory soil organic carbon to mineralizable soil organic carbon. If the assumption is made that soil organic carbon can be described by a carbohydrate equivalent (29), the mineralization of soil organic carbon under nitrate-reducing conditions can be described as follows:

$$5CH_2O + 4NO_3^- + 4H^+ = 2N_{2(g)} + 5CO_{2(g)} + 7H_2O$$

In this case, 0.8 mol of NO_3^- is reduced per mol of CO_2 produced. This relationship may be used to estimate the nitrate demand from soil organic carbon assuming that the labile fraction of the soil organic carbon is completely mineralized, as given by C_{max}. It is predicted that approximately 45 mg of NO_3^- per liter should be reduced during the initial phase of the test owing to the demand exerted by the soil organic carbon contributed by 2 g of soil. This relationship was generally followed in the experiments. For example, from the data in Fig. 6 at a soil-to-water ratio of 1:25 (g/ml), nitrate was depleted from approximately 95 to 40 mg/liter during the first 3 weeks of the test.

Although there are insufficient data to clearly assess the extent of mineralization of the PAH compounds, the results in Fig. 6 and 10 suggest qualitatively that much of the naphthalene was mineralized under nitrate-excess conditions. The data in Fig. 6 show, following the mineralization of soil organic carbon, that nitrate was depleted during the period of naphthalene degradation from about 40 to 24 mg/liter, or by about 0.065 meqv, assuming reduction to molecular nitrogen:

$$NO_3^- + 6H^+ + 5e^- = 0.5\ N_{2(g)} + 3H_2O$$

Aqueous-phase naphthalene was depleted from about 4.5 mg/liter to nondetectable levels, for a total of 2.3 μmol assuming reversible desorption from the 2 g of soil with a K_p of 12 liters/kg. If the naphthalene was completely mineralized the nitrate demand would be 0.12 meqv according to the following equation:

$$C_{10}H_8 + 20H_2O = 10CO_{2(g)} + 48H^+ + 48e^-$$

A similar comparison is evident from the data in Figure 10 with acclimated soil, assuming that the nitrate demand results from the added naphthalene rather than from the residual, refractory soil organic carbon. These data show a nitrate demand of 0.081 meqv (20 mg of NO_3^- per liter) for 0.086 meqv total naphthalene (3.1 mg of initial aqueous-phase PAH per liter, 2 g of soil, and K_p of 12 liters/kg). Hence, from these considerations it appears that about 50 and 90 % of the naphthalene may have been mineralized to CO_2 for the experiments shown in Fig. 6 and 10, respectively.

Data in Fig. 3 cannot be evaluated as readily to assess the extent of naphthalene mineralization, owing to the uncertainty associated with precise determination of nitrate in a soil-water suspension by colorimetric procedures. This is evidenced since the nitrate demand for sample set 2 is less than that which may be attributed to mineralization of the labile fraction of the soil organic carbon. However, results for sample set 1 suggest that a significant portion of the naphthalene may have been mineralized to CO_2, since nitrate decreased by approximately 40 mg/liter of which approximately 22 mg/liter may be ascribed to the mineralization of the labile fraction of the soil organic carbon. The nitrate data shown in Fig. 8 correspond to acenaphthene degradation under nitrate-excess conditions. Unlike the results in Fig. 6, these data do not show a demarcation between the nitrate reduction due to mineralization and PAH degradation. Nonetheless, the depletion of 40 mg of NO_3^- per liter can not all be attributed to the nitrate demand anticipated for labile soil organic carbon.

Nitrate reduction. The reduction of nitrate in the soil-water systems was found not to entail dissimilatory reduction to ammonium, as indicated by measurement of aqueous phase

ammonium concentration. This observation is consistent with results of a study of soil carbon mineralization and denitrification kinetics in which there was very little reduction of nitrate to ammonium when using an experimental apparatus similar to those used here for determination of C_{max} and k_c (29). Dissimilatory reduction of nitrate has been shown to be significant in glucose-amended soils, but not in nonamended soils (12,37). Both assimilatory and dissimilatory nitrate reduction may be significant in the case of marine sediments (23,35).

Acclimated soil. Experiments with acclimated soil showed that the degradation of naphthalene under denitrification conditions commenced without a several week acclimation period. The occurrence of an acclimation period may result from various factors (43), including enzyme induction, genetic mutation, insufficient supply of inorganic nutrients, preferential utilization of other organic compounds, and the time necessary for a small microbial population to increase in size to be able to degrade observable quantities of the organic compound. For the results reported here, it is believed that the acclimation period is not due to insufficient nutrients, owing to the use of the mineral medium. The acclimation periods were much longer than the time usually required for enzyme induction, which is typically minutes or hours (30). Although the period for enzymes to be induced may be longer at low substrate concentrations, other studies have concluded that long acclimation periods are not likely explained by induction (42,43).

Acclimation periods which have reproducible durations among replicate tests are thought not to be the result of mutation or the appearance of new genotypes (43). For this reason, genetic mutation is probably not the cause of the acclimation period, owing to the reproducibility of the acclimation period among individual samples of any one batch experiment, as well as the reproducibility among sample sets initiated at the same period (data in Fig. 3, for example). The acclimation period may not be directly related to the preferential utilization of the mineralizable fraction of soil organic carbon over the PAH compound. Experiments which measured CO_2 evolution from the mineralization of soil organic carbon showed that most of the labile soil organic carbon was utilized by soil-denitrifying microorganisms in less than 3 weeks, whereas the acclimation periods observed prior to PAH degradation varied from about 2 weeks to 1 month and more.

It is most probable that the acclimation period is a result of the time necessary for an initially small population of PAH-degrading organisms to grow to sufficient levels to produce a detectable loss of substrate PAH compound. This reasoning is consistent with the work of

Wiggins et al. (43), who arrived at a similar conclusion for the case of microbial degradation of *p*-nitrophenol. This may also explain the increase in acclimation period with soil age. Over the period of 1 year in which the PAH compound microbial degradation experiments were conducted, the acclimation period preceding naphthalene degradation increased from approximately 2 to 4 weeks, whereas that for acenaphthene increased from about 2 to 6 weeks. This was probably a result of soil drying and storage on microbial activity. It has been shown by Sparling and Chesire (36) that initial microbial populations and their growth rates decreased with storage time over a period of 6 months.

4.6. Conclusion

The results of this study indicate that microbial degradation of acenaphthene and naphthalene under denitrification conditions may be an important process for assessing the fate of PAH compounds in anoxic soil-water systems. The significance of this potential activity in the field depends on the availability of nitrate, as well as on the ratio of PAH compound to other mineralizable carbon sources. In this study the masses of both the PAH compound and the mineralizable fraction of the soil organic carbon were comparable, and nitrate depletion due to the mineralizable fraction of the soil organic carbon could arrest microbial degradation of the PAH compound under nitrate-limiting conditions. The sorption-desorption interactions with soil may limit the amount of total PAH compound available to the microorganisms; this is a subject of further study.

4.7. References

1. **Alexander, M.** 1965. MPN test. p. 1467-1472, and 1484-1486. *In* C.A. Black (ed.), Methods of soil analysis, part II: chemical and microbiological properties. American Society of Agronomy, Inc., Madison, Wis.
2. **Allison, L.E.** 1965. Organic carbon, p. 1372-1375. *In* C.A. Black (ed.), Methods of soil analysis, part II: Chemical and microbiological properties. American Society of Agronomy, Inc., Madison, Wis.
3. **American Public Health Association.** 1985. Standard methods for the examination of water and wastewater, p. 418-419. 16th ed. American Public Health Association, Washington, D.C.
4. **Argaman, Y., and A. Brenner.** 1986. Single-sludge nitrogen removal: modeling and experimental results. J Water Pollut. Control Fed. **58**:853-860.
5. **Atlas, R.M.** 1981. Microbial degradation of petroleum hydrocarbons: an environmental perspective. Microbiol. Rev. **45**:180-209.
6. **Bakker, G.** 1977. Anaerobic degradation of aromatic compounds in the presence of nitrate. FEMS Microbiol. Lett. **1**:103-108.
7. **Bassert, I.D., and L.Y. Young.** 1986. Anaerobic oxidation of *p*-cresol by a denitrifying bacterium. Appl. Environ. Microbiol. **52**:1117-1122.
8. **Batonda, J., and S.A. Waring.** 1984. Denitrification in relation to soil carbon for soils of the Darling Downs, Queensland. Rev. in Rural Sci. **5**:231-239.
9. **Bouwer, E.J., and P.L. McCarty.** 1983. Transformations of halogenated organic compounds under denitrification conditions. Appl. Environ. Microbiol. **45**:1295-1299.
10. **Bowman, R.A., and D.D. Focht.** 1974. The influence of glucose and nitrate concentrations upon denitrification rates in sandy soils. Soil Biol. Biochem. **6**:297-301.
11. **Burford, J.R., and J.M. Bremner.** 1975. Relationships between the denitrification capacities of soils and total, water-soluble and readily decomposable soil organic matter. Soil Biol. Biochem. **7**:389-394.
12. **Caskey, W.H., and J.M. Tiedje.** 1979. Evidence of clostridia as agents of dissimilatory reduction of nitrate to ammonium in soils. Soil Sci. Soc. Am. J. **43**:931-936.
13. **Dzombak, D.A., and R.G. Luthy.** 1984. Estimating adsorption of polycyclic aromatic hydrocarbons on soils. Soil Sci. **137**:292-308.
14. **Elder, V.A., B.L. Proctor, and R.A. Hites.** 1981. Organic compounds found near dump sites in Niagara Falls, New York. Environ. Sci. Technol. **15**:1237-1243.
15. **Evans, W.C.** 1977. Biochemistry of the bacterial catabolism of aromatic compounds in anaerobic environments. Nature (London). **270**:17-22.
16. **Fu, J.K., and R.G. Luthy.** 1986. Effect of organic solvent on sorption of aromatic solutes onto soils. J. Environ. Eng. **112**:346-366.

17. **Gschwend, P.M., and S.C. Wu.** 1985. On the constancy of sediment-water partition coefficients of hydrophobic organic pollutants. Environ. Sci. Technol. **19**:90-96.

18. **Hansch, C., and A. Leo.** 1979. Substituent constants for correlation analysis in chemistry and biology. John Wiley & Sons, Inc., New York.

19. **Herbes, S.E.** 1977. Partitioning of polycyclic aromatic hydrocarbons between dissolved and aqueous phases in natural waters. Water Res. **11**:493-496.

20. **Herbes, S.E., and I.R. Schwall.** 1978. Microbial transformation of polycyclic aromatic hydrocarbons in pristine and petroleum-contaminated sediments. Appl. Environ. Microbiol. **35**:306-316.

21. **Karickhoff, S.W.** 1984. Organic pollutant sorption in aquatic systems. J. Hydraulic Engineering. **110**:707-735.

22. **Karickhoff, S.W., D.S. Brown, and T.A. Scott.** 1979. Sorption of hydrophobic pollutants on natural sediments. Water Res. **13**:241-248.

23. **Kolke, I., and A. Hattori.** 1978. Denitrification and ammonia formation in anaerobic coastal sediments. Appl. Environ. Microbiol. **35**:278-282.

24. **Kuhn, E.P., P.J. Colberg, J.L. Schnoor, O. Wanner, A.J.B. Zehnder, and R.P. Schwarzenbach.** 1985. Microbial transformations of substituted benzenes during infiltration of river water to groundwater: laboratory column studies. Environ. Sci. Technol. **19**:961-968.

25. **Means, J.C., S.G. Wood, J.J. Hassett, and W.L. Banwart.** 1980. Sorption of polynuclear aromatic hydrocarbons by sediments and soils. Environ. Sci. Technol. **14**:1524-1528.

26. **Mihelcic, J.R., and R.G. Luthy.** 1988. Degradation of polycyclic aromatic hydrocarbon compounds under various redox conditions in soil-water systems. Appl. Environ. Microbiol. **54**.

27. **Ogram, A.V., R.E. Jessup, L.T. Ou, and P.S.C. Rao.** 1985. Effects of sorption on biological degradation rates of (2,4-dichlorophenoxy)acetic acid in soils. Appl. Environ. Microbiol. **49**:582-587.

28. **Reddy, K.R., W.H. Patrick Jr., and R.E. Phillips.** 1978. The role of nitrate diffusion in determining the order and rate of denitrification in flooded soil I. Experimental results. Soil Sci. Soc. Am. J. **42**:268-272.

29. **Reddy, K.R., P.S.C. Rao, and R.E. Jessup.** 1982. The effect of carbon mineralization on denitrification kinetics in mineral and organic soils. Soil Sci. Soc. Am. J. **46**:62-68.

30. **Richmond, M.H.** 1968. Enzymic adaption in bacteria: its biochemical and genetic basis. Essays Biochem. **4**:105-154.

31. **Schwarzenbach, R.D., and J. Westall.** 1981. Transport of nonpolar organic compounds from surface water to groundwater. Laboratory sorption studies. Environ. Sci. Technol. **15**:1360-1367.

32. **Sims, R.C., and M.R. Overcash.** 1983. Fate of polynuclear aromatic compounds (PNA's) in soil-plant systems. Residue Rev. **88**:1-68.

33. **Shimp, R.J., and F.K. Pfaender.** 1985. Influence of easily degradable naturally occurring carbon substrates on biodegradation of monosubstituted phenols by aquatic bacteria. Appl. Environ. Microbiol. **49**:394-401.

34. **Sleat, R., and J.P. Robinson.** 1984. The bacteriology of anaerobic degradation of aromatic compounds. J. Appl. Bacteriol. **57**:381-394.

35. **Sorensen, J.** 1978. Capacity for denitrification and reduction of nitrate to ammonia in a coastal marine sediment. Appl. Environ. Microbiol. **35**:301-305.

36. **Sparling, G.P., and M.V. Cheshire.** 1979. Effects of soil drying and storage on subsequent microbial growth. Soil Biol. Biochem. **11**:317-319.

37. **Stanford, G., J.O. Legg, S. Dzienia, and E.C. Simpson, Jr.** 1975. Denitrification and associated nitrogen transformations in soils. Soil Sci. **120**:147-152.

38. **Stanford, G., R.A. Vander Pol, and S. Dzienia.** 1975. Denitrification rates in relation to total and extractable soil carbon. Soil Sci. Soc. Am. Proc. **39**:284-289.

39. **Steen, W.F., D.F. Paris, and G.L. Baughman.** 1980. Effects of sediment sorption on microbial degradation of toxic substances, p. 477-482. *In* R.A. Baker (ed.), Contaminants and sediments, Vol. 1. Fate and transport, case studies, modeling, toxicity. Ann Arbor Science, Ann Arbor, Mich.

40. **Taylor, B.F., W.L. Campbell, and I. Chinoy.** 1970. Anaerobic degradation of the benzene nucleus by a facultatively anaerobic microorganism. J. Bacteriol. **102**:430-437.

41. **U.S. Environmental Protection Agency.** 1979. Methods for chemical analysis of water and wastes, EPA-600/4-79-020, method 350. U.S. Environmental Protection Agency, Washington, D.C.

42. **Varma, M.M., L.W. Wan, and C. Prasad.** 1976. Acclimation of wastewater bacteria by induction or mutation selection. J. Water Pollut. Control Fed. **48**:832-834.

43. **Wiggins, B.A., S.H. Jones, and M. Alexander.** 1987. Explanations for the acclimation period preceding the mineralization of organic chemicals in aquatic environments. Appl. Environ. Microbiol. **53**:791-796.

44. **Yalkowsky, S.H., and S.C. Valvani.** 1979. Solubilities and partitioning 2. Relationships between aqueous solubilities, partition coefficients, and molecular surface areas of rigid aromatic hydrocarbons. J. Chem. Eng. Data. **24**:127-129.

45. **Zeyer, J., E.P. Kuhn, and R.P. Schwarzenbach.** 1986. Rapid microbial mineralization of toluene and 1,3-dimethylbenzene in the absence of molecular oxygen. Appl. Environ. Microbiol. **52**:944-947.

Chapter 5

Hydrophobic Aromatic Solute Sorption-Desorption in Soil-Water Systems

5.1. Introduction

Upon introduction into a soil-water system, an organic compound will partition itself between solid and aqueous phases, depending on the physical and chemical properties of the organic compound and the soil or sediment. This phenomenon influences the transport and fate of organic contaminants in soil-water systems. Some issues related to this phenomenon, and its potential impact on microbial degradation, are discussed in this chapter for the sorption-desorption characteristics of lower-molecular-weight polycyclic aromatic hydrocarbons (PAH) in a soil-water system. The discussion includes a general review of the sorptive process, and experimental data are presented for lower-molecular-weight PAH to demonstrate the nature of the partitioning process for hydrophobic compounds between solid and aqueous phases. Included is an examination of the reversibility of the sorption isotherm and the kinetics of the sorptive and desorptive process.

The experimental results were evaluated by a radial diffusion model. This model was used to confirm experimental evidence that the sorption and desorption kinetics were rapid for the lower-molecular-weight compounds used in these tests. The model was also used to obtain a preliminary assessment of the effects of particle size and solute hydrophobicity on sorption kinetics. The modeling results were then used to provide an indication of the types of systems for which PAH sorption and desorption kinetics may entail relatively long equilibration periods.

5.1.1. Hydrophobic Solute Sorption onto Soil

The role of naturally occurring soil organic carbon as a sorbent for hydrophobic solutes such as PAH compounds has been well documented. The sorption process has been shown to be dependent on the weight fraction of organic carbon of the soil and the hydrophobicity of the PAH compound, as expressed by physical or chemical properties such as molecular surface area, aqueous solubility, or octanol/water partition coefficient (Fu and Luthy, 1986; Karickhoff et al., 1979; Karickhoff, 1980; Means et al., 1980).

Though the process of hydrophobic solute sorption onto soils and sediments is thought to consist of only weak attractive forces (Chio et al., 1983; Karickhoff, 1984), many researchers have viewed soil sorption as entailing a partial irreversible process in which a certain fraction of the initially sorbed organic compound is resistant to desorption (Di Toro, and references within, 1985). These conclusions were formulated on experimental and modeling efforts for sorbates such as pesticides, herbicides, and PCB's, and sorbents such as soils and sediments. In contrast to those investigators, Gschwend and Wu (Gschwend and Wu, 1985; Wu and Gschwend, 1986) have presented experimental and modeling evidence which suggests that hydrophobic solute sorption onto natural sediments is a reversible process and that the previously observed irreversible phenomena were due in part to experimental artifacts associated with the separation of the solid and liquid phases before solute analysis. They concluded that noncentrifugeable and/or nonfilterable microparticles, or organic macromolecules were not removed in the separation process and thus remained in the aqueous phase. This produced erroneously high aqueous-phase concentrations, particularly for very hydrophobic solutes, e.g. PCB's at trace concentrations. Wu (1986) also explained that the process of solute sorption and desorption is dependent on intra-aggregate diffusion, and that the partitioning of solute between the aqueous and solid phases may not have attained equilibrium in some of the previously performed studies which examined the reversibility of hydrophobic solute partitioning.

In view of these developments, work was carried out in this study to understand the sorption and desorption characteristics of a PAH compound and Barnes-Hamerly soil system as utilized previously in the microbial degradation experiments. Laboratory experiments and modeling were employed to understand the partitioning of the solute between sorbed and aqueous phases, and the reversibility of the sorption process. These results will be utilized in the following chapter for examination of the effect solute sorption and desorption have on microbial degradation.

5.2. Experimental Methods

5.2.1. Sorption Isotherm Tests

The soil, reagents, equipment, and procedures used in the following studies are described in Chapters 3 and 4. Sorption isotherms for naphthol, naphthalene, and acenaphthene onto the soil were determined to estimate solute partitioning to the solid phase with an aqueous phase consisting of PAH, mineral medium, and 0.01 N $CaCl_2$. The soil was sterilized by autoclaving for one hour at a temperature of 121°C and a steam pressure of 20 lb/in^2. The sorption isotherm tests were performed in a batch mode at room temperature with 50-ml glass centrifuge tubes fitted with Teflon-lined septums and open-port screw caps. The samples contained various amounts of soil and an initial aqueous-phase solute concentration ranging from approximately 0.2 to 10 mg/liter, depending on the solute's solubility in water. The amount of soil was varied from 1.5 to 25.0 grams, weighed to 10^{-4} grams, per 50 ml to produce a range of aqueous-phase solute concentrations after equilibration. The soil was placed in a centrifuge tube and then an aqueous mixture containing mineral medium and solute was added with the volume recorded to 10^{-2} ml. Samples were filled to zero headspace, sealed with Teflon-lined septums and screw caps, and covered with aluminum foil to prevent photodegradation. Blanks without soil were run concurrently.

After sample preparation, the sealed centrifuge tubes were transferred to a wrist action shaker and equilibrated for 24 hours. Previous studies had indicated that the sorption process was not significantly time dependent after approximately four hours, and that sorption equilibrium was attained in less than one day. After equilibration, the tubes were centrifuged for thirty minutes and analysis of the separated aqueous phase was performed by high-pressure liquid chromatographic (HPLC) methods by sampling directly through the septum.

5.2.2. Desorption Isotherm Tests

Desorption isotherms were performed with a system containing Barnes-Hamerly soil and the solute naphthalene. The experiments were conducted in a batch-sample mode similar to that for the sorption isotherm tests. Heat sterilization was supplemented by chemical sterilization so that each individual sample had 200 mg/liter $HgCl_2$ at the initiation of the test. Glass centrifuge tubes, with Teflon-lined septums, contained either 5, 10, 15, or 20 grams of soil with an aqueous solution containing naphthalene plus 0.01 N $CaCl_2$ electrolyte. During the

sorption mode of the test, samples were equilibrated for periods of 1, 3, or 36 days in three individual experiments. This was followed by successive desorption experiments as described by Di Toro and Horzempa (1982). A successive desorption test consisted of decanting the aqueous phase containing naphthalene and replacing it with deionized water containing 0.01 N $CaCl_2$. All liquid volumes were measured to 10^{-2} ml since the calculations of solute mass desorbed included a correction for the pore water which had been entrapped during the solid separation process. The samples were then placed on the wrist action shaker and equilibrated again for 8 hours. Samples were then centrifuged and the aqueous phase was analyzed then for naphthalene concentration. This process was repeated to obtain successive desorption measurements. This process was repeated until no significant desorption was observed from the soil particles.

5.2.3. Sorption and Desorption Kinetic Tests

A set of tests was performed in an attempt to measure the rate at which naphthalene was sorbed and desorbed from Barnes-Hamerly soil. These tests were performed in a batch mode. Samples contained 1 or 3 grams of Barnes-Hamerly soil per 50 ml, and blanks containing no soil were run concurrently. The experimental procedures for the sorption and desorption kinetic tests were similar to those described above, in which samples were shaken, centrifuged, and analyzed by HPLC procedures. Since apparatus for continuous monitoring of a sample was not available in the laboratory, the experiment could not measure aqueous-phase concentrations for time increments as short as several minutes. In an effort to minimize the interval prior to the time of the first sampling point, the time scale for initial equilibration on the wrist action shaker and subsequent centrifuging was abbreviated by equilibrating the first sample for one half hour followed by centrifuging for one half hour, prior to analysis on the HPLC. After analysis by HPLC methods, the soil samples were then employed for desorption tests by reserving the solids which contained naphthalene, adding solute-free aqueous phase, and resuspending.

5.3. Experimental Results

5.3.1. Sorption Isotherms

As described previously in Chapter 4, the aqueous-phase concentration of a hydrophobic organic solute in a soil-water system is dependent on the sorptive-desorptive equilibrium with a sorbent present within the system. This phenomenon has been described by various investigators, including Fu and Luthy (1986).

In Chapter 4, the Freundlich sorption model was shown to be useful in describing the sorption characteristics of organic solutes in sediment-water and soil-water systems (Means et al., 1979; Karickhoff et al., 1979). The Freundlich sorption isotherm can be expressed as:

$$\frac{S}{M} = K_p \; C^{1/n} \qquad [1]$$

where S equals the total mass of the solute sorbed, mg, M is the mass of solids, g or kg, C is the equilibrium concentration in the aqueous phase, mg/liter, and K_p is the partition coefficient, liters/g or liters/kg. K_p and 1/n are empirical constants which are characteristic of the solute and sorbent. Many laboratory studies of organic solute sorption onto soils, sediments, and suspended solids have found that a linear sorption isotherm (i.e. 1/n =1) could describe hydrophobic organic solute sorption on these materials (Hamaker and Thompson, 1972; Karickhoff, 1984). Karickhoff et al. (1979) showed for various PAH, that n equals unity for a range of equilibrium aqueous-phase concentrations up to approximately one half the compound's solubility in water or about 10^{-5} M, whichever is lowest.

Sorption isotherms for Barnes-Hamerly soil and the solutes naphthol, naphthalene, and acenaphthene are presented in Figures 5-1, 5-2, and 5-3 respectively. Each data point in these figures represents the average of approximately 5 individually prepared sorption samples. The average and standard deviation of the samples are listed in Appendix E of this report. The results for Figures 5-1 to 5-3 were characterized by a linear sorption model. The sorption data were reduced by linear-least-squares regression analysis to determine the regression equation and a statistical measure of the fit of the curve, as shown in each figure. For the solutes acenaphthene and naphthalene the regression line was forced through the zero intercept. For Barnes-Hamerly soil, the following values were obtained for the sorption partition coefficient, K_p, from the isotherms shown in Figures 5-1 to 5-3: acenaphthene, 52 liters/kg; naphthalene, 12 liters/kg; and naphthol, 6.8 liters/kg. The results show the solute dependence on sorption with the least soluble solutes having a greater sorption capacity.

Figure 5-1: Adsorption isotherm for naphthol.

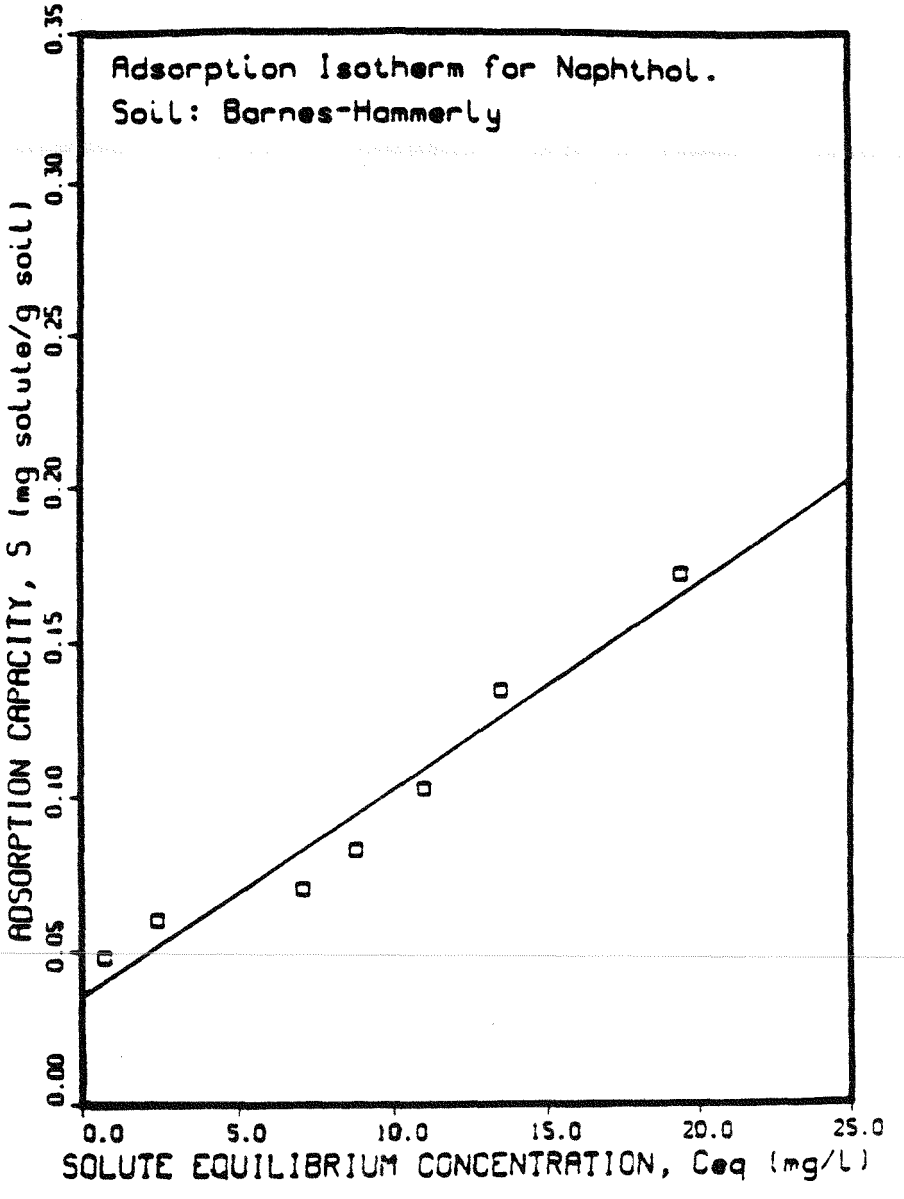

$S = 0.0353 + 0.0068\ C_{eq}$

sum of squares / total sum of squares = 95.0%

$R^2 = 94.0$

Figure 5-2: Adsorption isotherm for naphthalene.

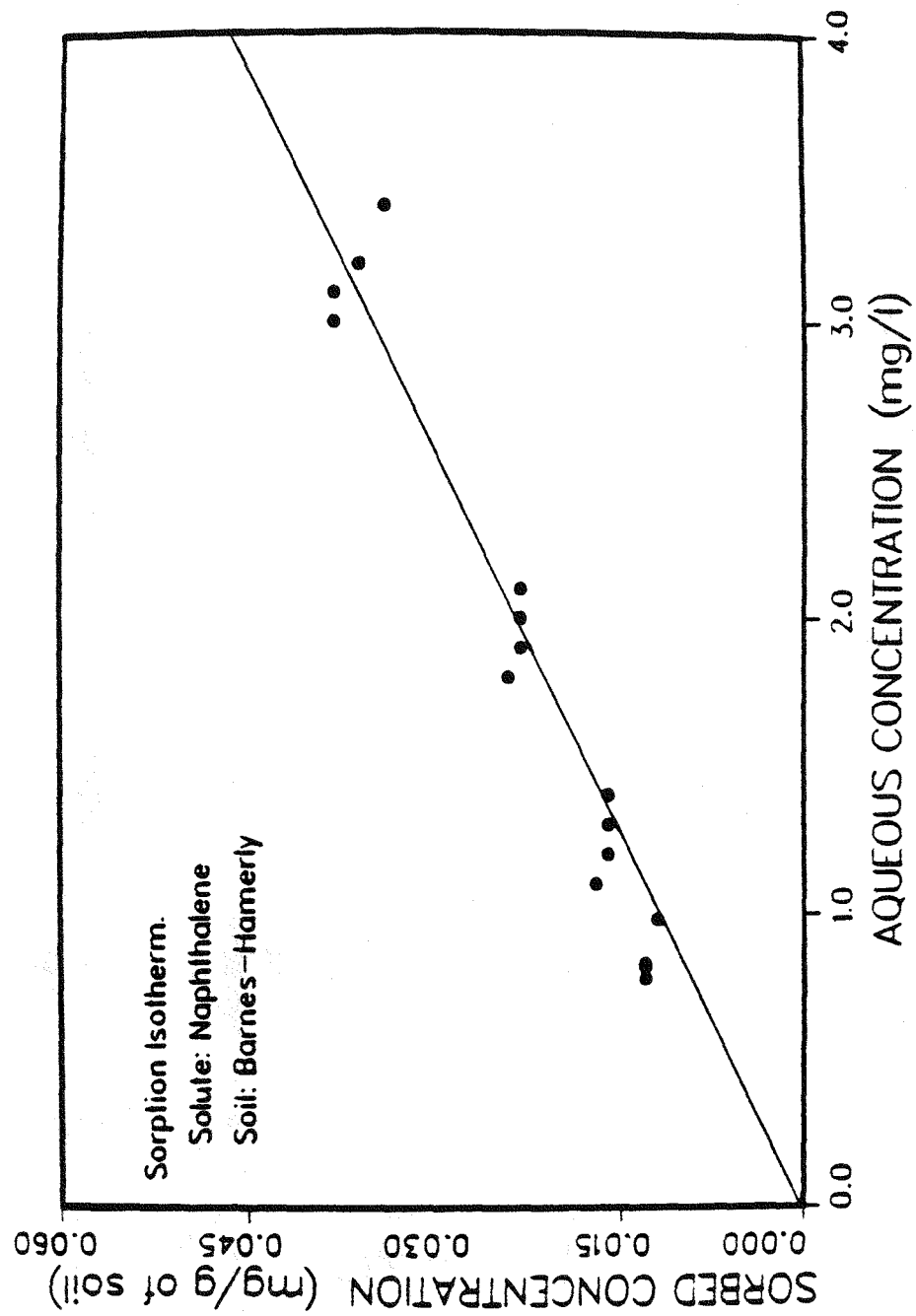

$S = 0.012\ C_{eq}$

sum of squares / total sum of squares = 98.7%

Figure 5-3: Adsorption isotherm for acenaphthene.

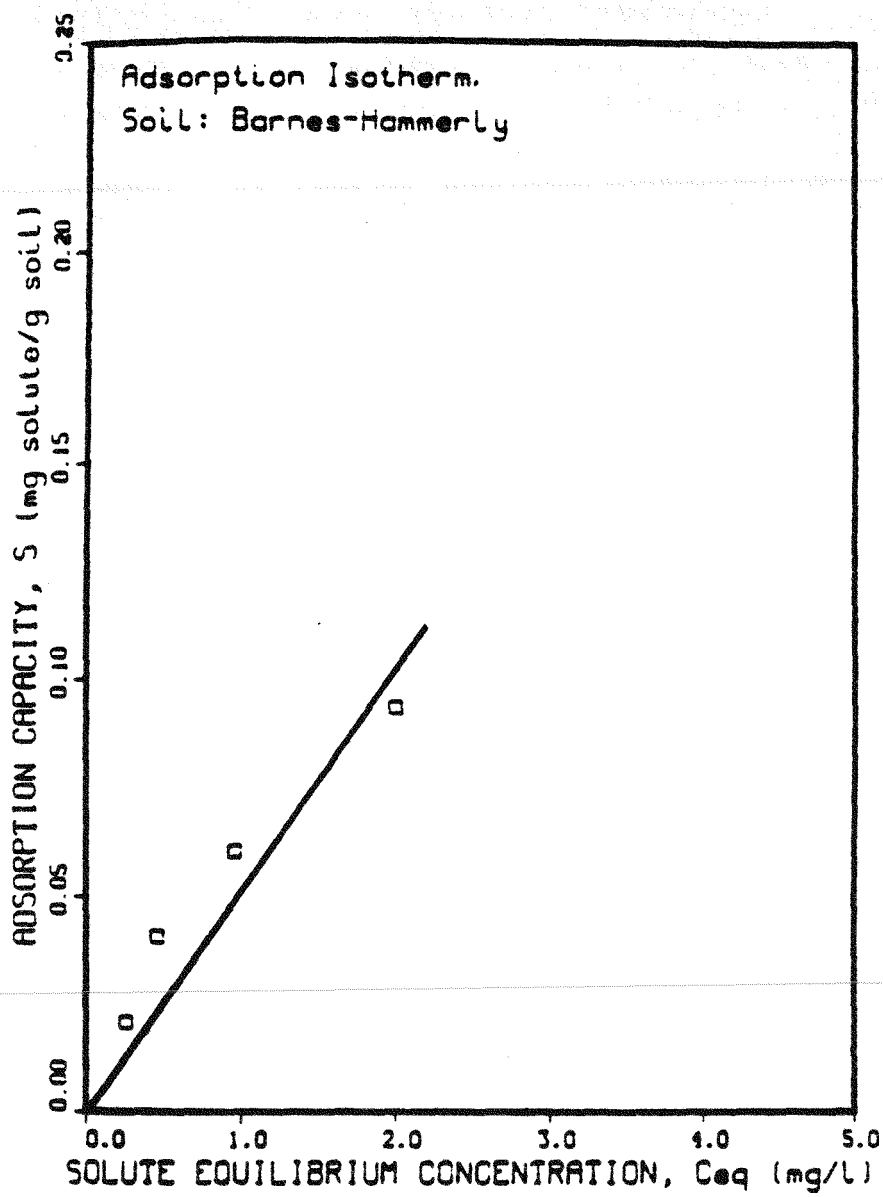

$S = 0.052\ C_{eq}$

sum of squares / total sum of squares = 96.4%

Naphthol sorption onto Barnes-Hamerly soil gave a distinct nonzero intercept. This is attributed to naphthol sorbing through both hydrophobic and nonhydrophobic sorption interaction with the soil. Nonhydrophobic sorption interactions are evident at low solute equilibrium concentrations which are believed to be a result of the hydroxyl group participating in site-specific interactions with the sorbent, possibly through hydrogen bonding. Fu and Luthy (1986) and Hasset et al. (1981) also examined naphthol sorption onto various soils and sediments. Their data suggested that the sorption of naphthol could be described with a linear isotherm with an intercept in the range of 0.7 mg/g for solute equilibrium concentration less than or equal to several mg/liter. Thus, except for the lower intercept value, the sorption data of Barnes-Hamerly soil with the solute naphthol agreed with those studies.

5.3.2. The Reversibility of the Sorption Isotherm

Figures 5-4, 5-5, and 5-6 show sorption and desorption isotherms for a system containing the solute naphthalene and Barnes-Hamerly soil for initial equilibrium periods of 1, 3, and 36 days respectively. Each point in the figures represents an individual sample. These three figures show that even with an initial sorption equilibrium of 36 days, the sorption and desorption isotherms have very similar slopes. The results suggest that the naphthalene sorption process is reversible, and that the kinetics are at least as rapid as the time allocated for desorption equilibration which was 8 hours in these experimental studies.

These tests were conducted for the case of initial sorption equilibrium periods as long as 36 days in order to assess naphthalene desorption for an equilibration period comparable to the longest acclimation lag interval observed in the microbial degradation tests. It was believed that the longer equilibration period may have had an effect on the extent to which naphthalene may be released from the soil. Karickhoff (1980) suggested that the ease of recovering sorbed PAH from soil by solvent extraction decreased with increasing equilibration period. Karickhoff also reported on results of release of naphthalene from sediments by sparging the system and trapping the PAH on a chromatography column. Sorbed naphthalene was recovered (> 90 percent) in minutes to a few hours, while hexachlorobenzene required 10 to 30 days for sorption equilibration times ranging from 5 to 58 days. Karickhoff (1980) concluded from his work, and the work of others, that intraparticle diffusion may have occurred, whereby a sorbent is slowly incorporated into a porous aggregated particle. The results shown in Figures 5-4 to 5-6 are consistent with Karickhoff's (1984) observations with naphthalene.

Figure 5-4: Naphthalene sorption and desorption isotherms with initial one day sorption equilibrium.

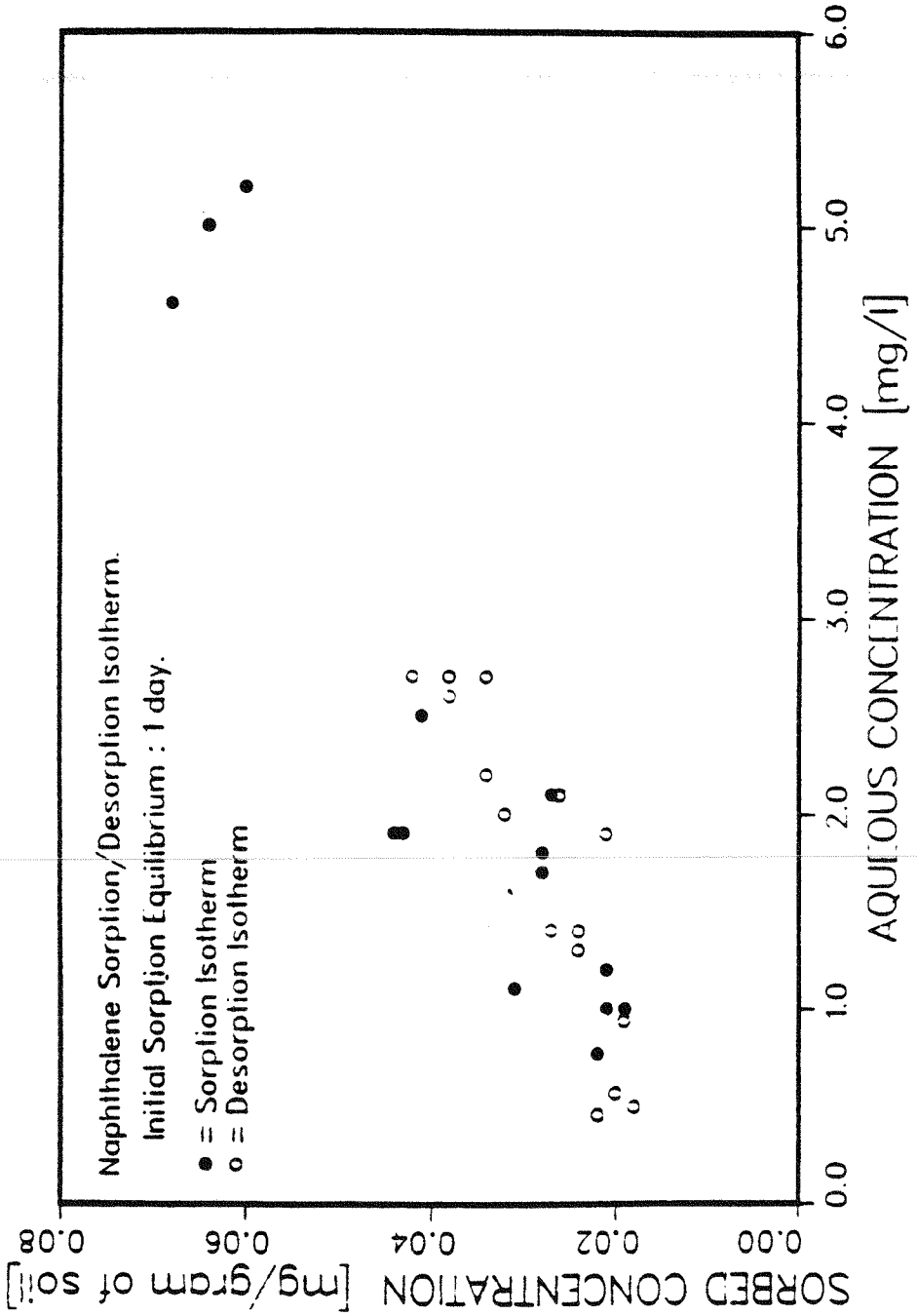

Figure 5-5: Naphthalene sorption and desorption isotherms with initial three day sorption equilibrium.

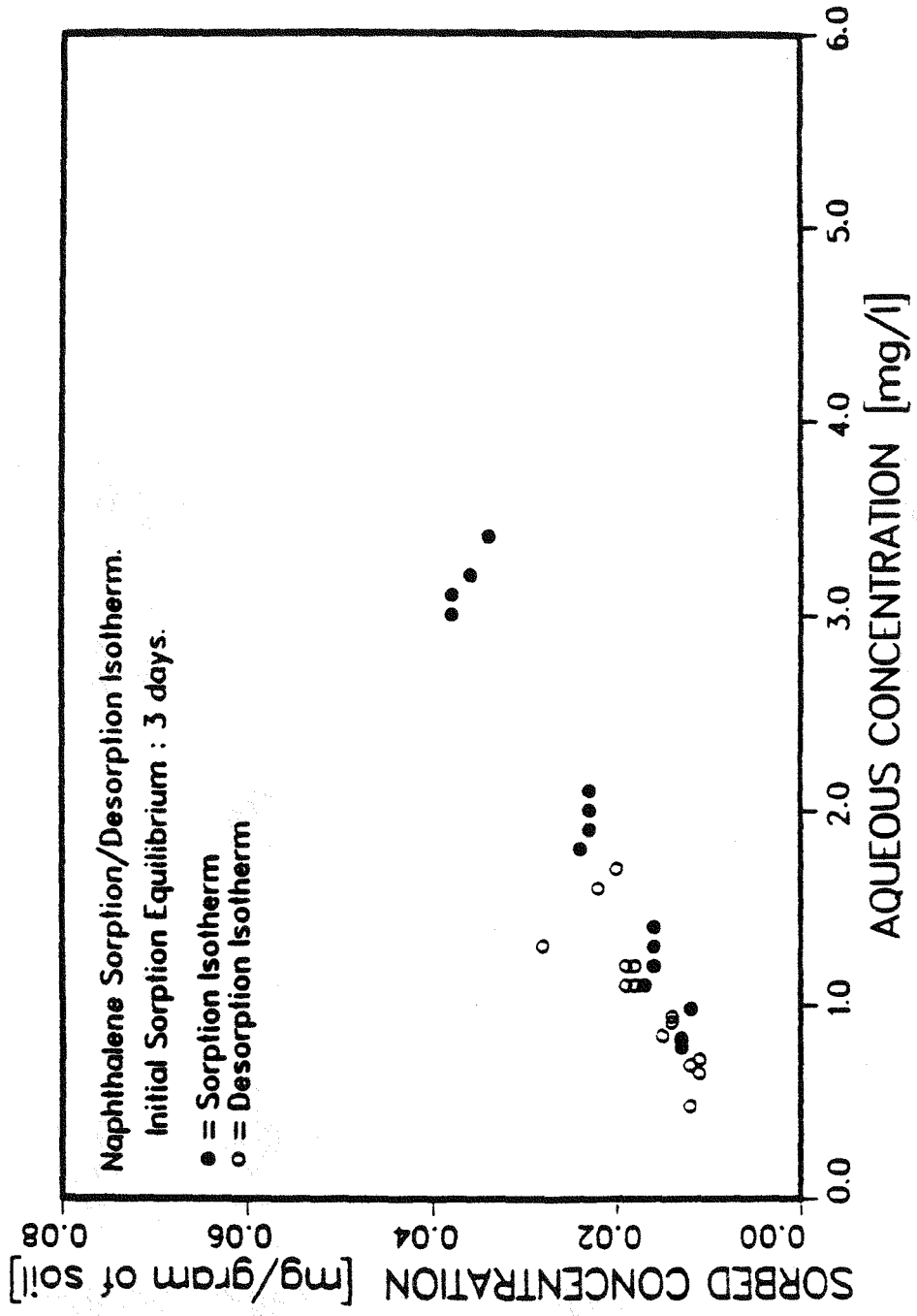

Figure 5-6: Naphthalene sorption and desorption isotherms with initial thirty-six day sorption equilibrium.

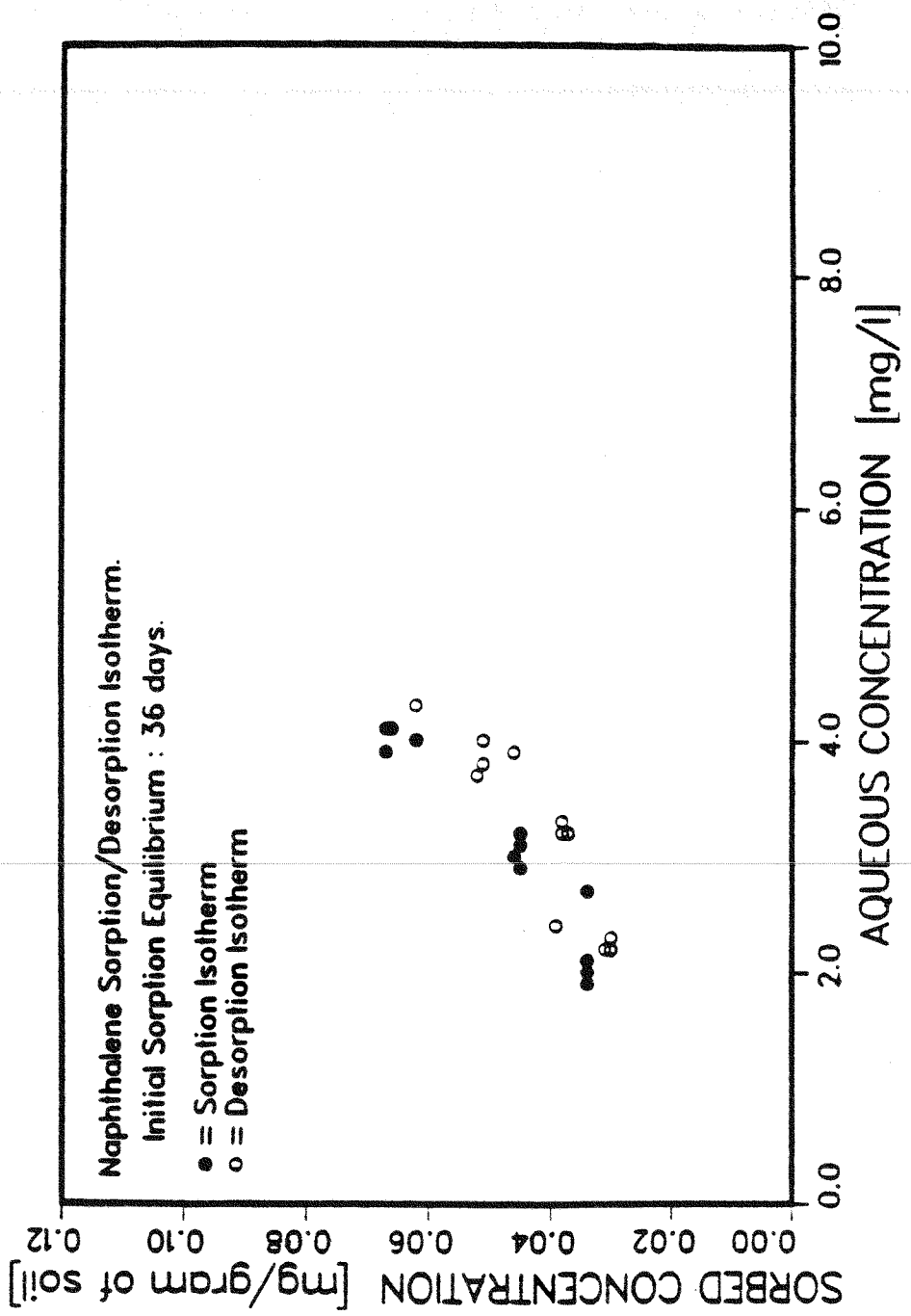

The work of Gschwend and Wu (1985), Wu and Gschwend (1986), and Wu (1986) also support the findings in Figures 5-4 through 5-6. Wu (1986) showed through modeling the sorption-desorption process as an intra-aggregate radial diffusion process, for a compound with a K_{ow} of 10^4 and a mean particle diameter of as great as 0.0232 cm, that the solute may not be equilibrated after 1 day of desorption, thus causing a higher observed K_p when conducting a consecutive desorption experiment. As explained below, the intra-aggregate solute diffusion concept gives predictions consistent with the results of this study for naphthalene sorption and desorption equilibrium.

5.3.3. Sorption and Desorption Kinetic Tests

Experimental data for naphthalene sorption and desorption kinetics with Barnes-Hamerly soil are presented in Table 5-1. Aqueous solute concentrations are presented for sorption times ranging from 1.5 to 24 hours for samples containing 1 and 3 grams of soil (Samples 1S and 3S, respectively) and desorption equilibration periods from 1 to 26 hours for samples containing 1 and 3 grams of soil previously sorbed with naphthalene (samples 1D and 3D, respectively). The values presented in Table 5-1 are the average of 2 to 5 samples and the standard deviation is presented in parenthesis. Sample 3S contained a greater initial aqueous concentration of naphthalene than sample 1S, which accounts for the similarity in the final concentration after sorption. The results show that the aqueous-phase concentration of naphthalene did not change with time after the first sampling point. For sorption the first sample was obtained at 90 minutes after sample preparation, while for the desorption tests the first sample was obtained 60 minutes after desorption was initiated. Thus, it appears that desorption equilibrium was attained in these experiments in time periods less than approximately one hour.

Wu and Gschwend (1986) utilized a radial diffusion model to describe chlorinated benzene compound sorption into porous soil and sediment aggregates. Experimentally, they showed that 90 percent sorption equilibrium for 1,4-dichlorobenzene (log K_{ow} = 3.4) was attained in less than 100 minutes for particles with a larger diameter than used in the tests reported here. In this study naphthalene (log K_{ow} = 3.3) attained close to 100 percent equilibrium in time span of less than or equal to 90 minutes. The experimental results presented in Table 5-1, and studies by others (Karickhoff, 1980, 1984), appear to support the belief that naphthalene sorption onto soil is a reversible process and the rate of desorption is relatively fast. This finding is important later in this work when modeling the rate of microbial degradation of naphthalene in a soil-water systems.

Table 5-1: Sorption and desorption for naphthalene in soil for different equilibration periods.

Sorption

	Aqueous Solute Concentration (mg/liter)	
Equilibration Time (hours)	Sample 3S	Sample 1S
1.5	19.6 (0.20)	19.5 (0.85)
2.5	18.2 (0.40)	20.0 (1.6)
3.5	17.6 (0.60)	19.4 (0.20)
7	19.5 (0.05)	18.5 (0.20)
24	20.3 (2.4)	21.5 (1.7)

Desorption

	Aqueous Solute Concentration (mg/liter)	
Equilibration Time (hours)	Sample 3D	Sample 1D
1	7.5 (0.050)	6.3 (0.30)
1.5	8.2 (0.20)	6.4 (0.20)
3	6.7 (0.30)	6.2 (0.05)
8	7.4 (2.3)	5.9 (0.30)
26	7.1 (1.7)	6.8 (0.62)

Samples 1S and 1D: 1 gram of soil per 50 ml; Samples 3S and 3D: 3 grams of soil per 50 ml

5.3.4. Methods of Particle Size Analysis

In order to model sorption and desorption kinetics, and to assess the effect of these kinetics on microbial degradation, it was necessary to obtain an accurate particle size distribution of the soil particles employed in the prior experiments. Many methods are available to obtain a particle size distribution. This section will briefly describe methods of measuring particle size. It should be noted that regardless of the method, care should be taken during the sample preparation so as to not alter the size distribution of the particles.

Particle size determination may be performed by filtration, sedimentation, and instrument counting techniques. Filtration procedures can measure particle size down to the 0.1 to 12 μm range (Murphy, 1984) . This method requires a series of cascading filters, much as in dry-sieving methods employed in the area of soil science. Hydrometer and centrifugation methods employ sedimentation principles (Lambe, 1953; Lloyd, 1968; Scarlett, 1968). The Reynold's number limits the upper sized particles which can be measured by this procedure, as the particles are to be at their terminal velocity for analysis. In water with a solid density of 2 g/cm^3, the maximum size detectable by sedimentation procedures is approximately 71 μm. A hydrometer test can be used to detect particles down to 0.2 μm (Lambe , 1953). These tests provide a particle size distribution on a percent finer by weight basis, rather than by a number count.

Stream scanning instrument methods pass a liquid or gaseous suspension through a small sensing zone where the particles are counted and sized (Lloyd, 1968). An example of this type of instrument is the Coulter Counter. Problems with this method include a second particle reaching the sensing zone while a preceding particle is still being sensed, and counting particles with diameter greater than 40 percent of the tube diameter.

Scanning Electron Microscopy (SEM) employs an electron beam to search for particles by moving along a search grid. Particles are then detected on the search grid by monitoring the variation in contrast of a backscattered electron signal. Particles greater than square root of 2 times the grid size are counted 100 percent of the time while particles less than this are not always counted. SEM allows one to obtain percent-by-number data and to analyze a large sample size accurately. This method also can provide information on volume, area, and width-to-length ratios. For these reasons this method was selected for use in this work.

The soil particles used in this study were characterized in order to confirm their

aggregate nature, to determine their particle size distribution, and to assess whether the particle size distribution changed significantly over the duration of a typical microbial degradation test.

Electron microscopy (EM) was performed by the Carnegie Mellon University, Department of Material Sciences, in order to obtain electron micrographs of the soil particles. Samples were prepared by combining 2 grams of Barnes-Hamerly soil and approximately 50 ml of deionized water containing 0.01 N $CaCl_2$ in a 50-ml glass centrifuge tube. This sample was sealed with a Teflon-lined septum top and shaken on a wrist action shaker overnight. Figure 5-7 shows two representative electron micrographs obtained from EM analysis. These micrographs provide a qualitative assessment of the aggregate nature and diameter of the particles. Figure 5-7 indicates that many particles have a width in the range of a fraction of a micron to tens of microns, the particles appear to have an aggregate nature and contain interior voids, and the particles are irregularly shaped.

Scanning electron microscopy was performed on soil samples to obtain a particle size distribution of the soil utilized in the microbial degradation tests and to assess if the distribution changed during a one-month period of shaking in a 50-ml centrifuge tube without headspace. Samples were prepared by combining 2 grams Barnes-Hamerly soil and approximately 50 ml of aqueous phase containing 0.01 N $CaCl_2$. Two sample sets were prepared with two samples per set. The time of contact of soil and aqueous phase prior to preparation of the sample for SEM analysis was 4 hours (1 total hour shaking) for the first sample set, and one month (8 hours per day shaking on a wrist action shaker) for the second sample set.

The samples were prepared for SEM analysis by transferring the contents of the centrifuge tube into a 50-ml beaker and gently stirring with a magnetic stirrer. A small volume of sample was removed by a glass eyedropper and approximately 2 drops were added to 20 ml of deionized water in a 50-ml glass beaker. This suspension was filtered through a 0.2-μm nuclepore filter (Nuclepore Corp., Pleasanton, Cal.) resting atop a 0.2-μm millipore filter (Millipore Corp., Bedford, Mass.). The glass beaker was carefully rinsed out with deionized water to remove all solids. The nuclepore filter was then allowed to dry and approximately a 5 x 10 mm segment was mounted on an aluminum stub using an amorphous graphite suspension (Conductive Carbon Paint, SEEVAC, Pittsburgh, Pa.). Particle size distribution was then performed by an ISI SS-40 scanning electron microscope with software developed by LeMont Scientific (State College, Pa.). The scanning electron microscope used in this

Figure 5-7: Electron microscopy micrographs of soil particles.

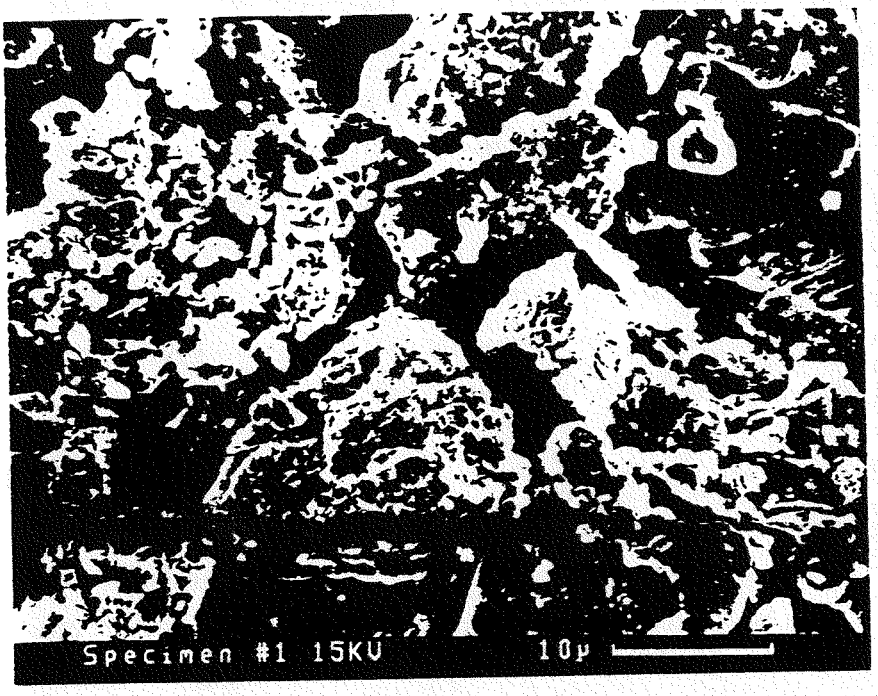

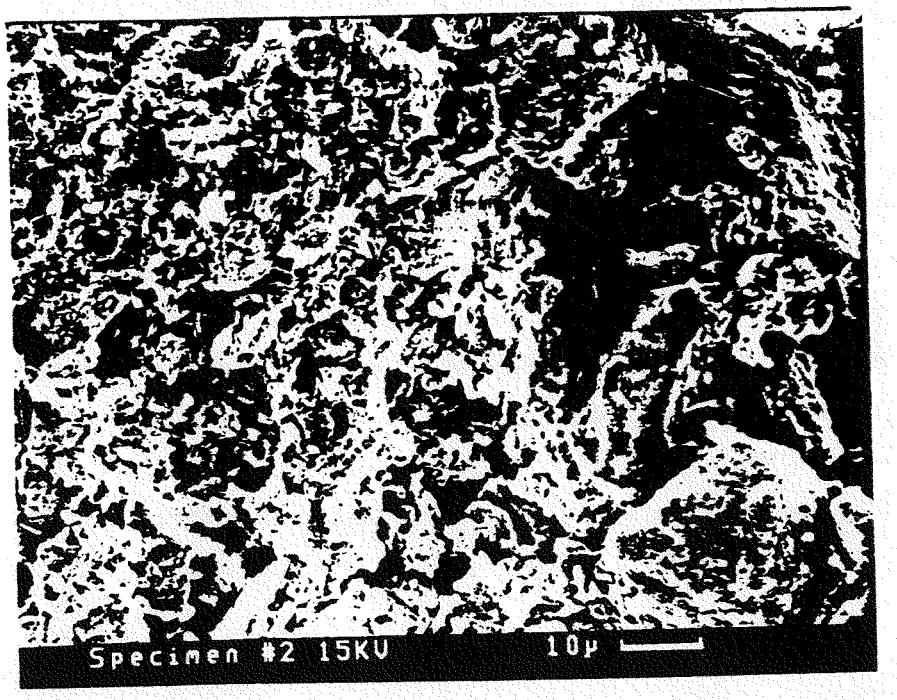

study calculates the particle diameter by placing 8 diagonals on the particle and taking the average of the 8 measurements. Particle volume was calculated assuming that each particle was a prolate ellipse with the major and minor axes becoming length and width, respectively. Particles greater than 0.37 μm were counted 100 percent of the time.

Figure 5-8 shows the particle size distribution and geometric mean diameter obtained by the SEM method for the four separate samples with the abscissa being the percent of total particles counted. Figures 5-8a and 5-8b show results for the samples which were equilibrated for 4 hours while Figure 5-8c and 5-8d show results for the samples which were equilibrated for 30 days. The size range of the particles is between 0.40 and 25 μm in diameter. Geometric mean diameters were 1.50, 1.48, 1.38, and 1.50 μm for samples 1, 2, 3, and 4, respectively. Particle volume distributions for samples 1, 2, 3, and 4 are shown in Figures 5-9a, b, c, and d, respectively. It appears that the particle volume distribution did not shift to a lower range after one month of shaking.

For use in the model simulation, the volume mean radius was required, not the number mean radius. The volume mean diameter was found from the number mean diameter by the following relationship (Seinfeld, 1986):

$$log(\overline{dp})_V = log(\overline{dp})_N + 6.9(log\sigma_g)^2 \qquad [2]$$

where $(\overline{dp})_V$ is the volume mean diameter, μm, $(\overline{dp})_N$ is the number mean diameter, μm, and σ_g is the geometric standard deviation. The volume mean diameter is taken such that the total volume of a system with this diameter equals the actual total volume of the original system. From the experimentally determined number mean diameter, the volume mean diameter for sample 1 was calculated to be 35 μm. The cumulative number and volume distributions corresponding to sample 1 are shown in Figure 5-10. Figure 5-10 and Figure 5-8 indicate that the particle size distribution is log-normally distributed.

Width-to-length ratios for all four samples were also obtained by SEM analysis. The average width-to-length ratio from the distributions were 0.433, 0.442, 0.419, and 0.423 for samples 1, 2, 3, and 4, respectively. These results indicate that the particles are more ellipsoid than spherical, although a spherical diffusion model is utilized in the modeling work.

Cumulative distributions for particle diameter were plotted to compare the reproducibility of sample preparation procedure and the effect of equilibration time on the particle size

Figure 5-8: Particle diameter size distributions.

a.) Particle Size Distribution, Sample 1

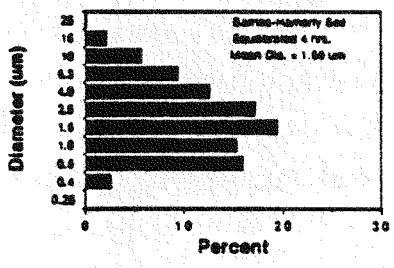

b.) Particle Size Distribution, Sample 2

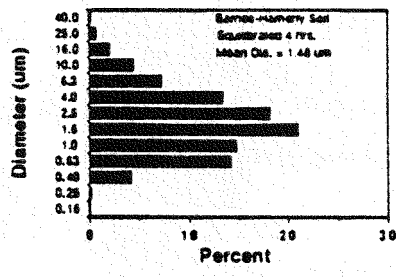

c.) Particle Size Distribution, Sample 3

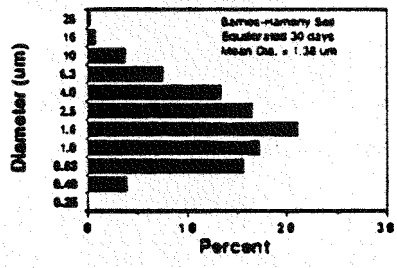

d.) Particle Size Distribution, Sample 4

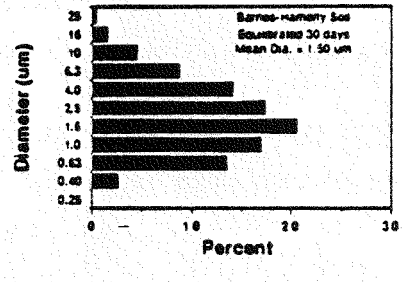

Figure 5-9: Particle volume size distributions.

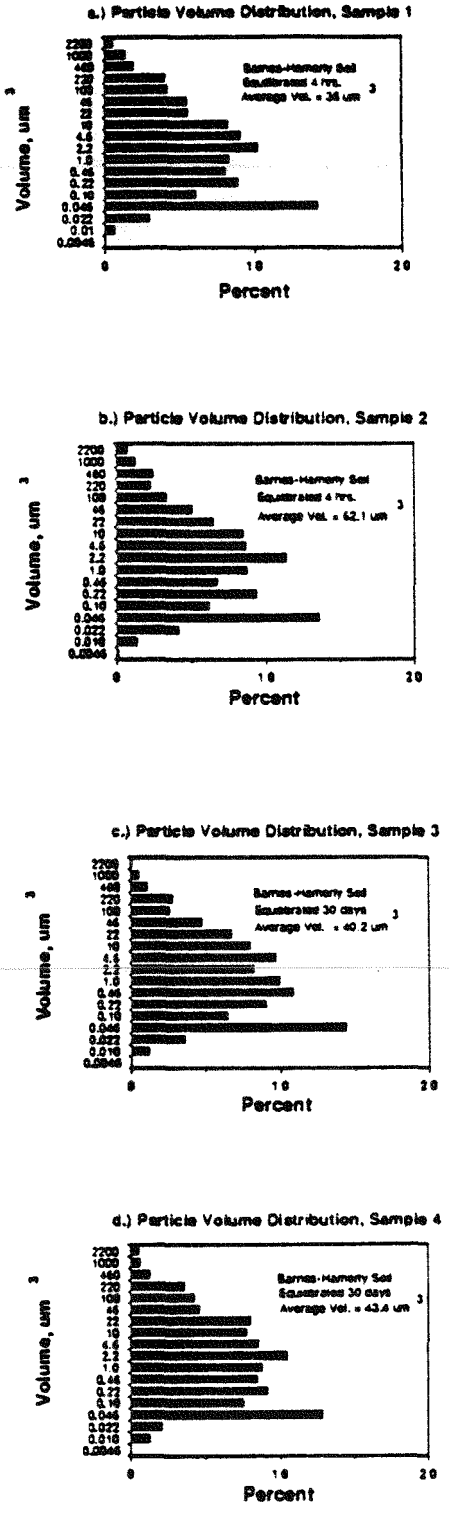

Figure 5-10: Cumulative number and volume distributions of a soil sample typical of that employed in the microbial degradation studies.

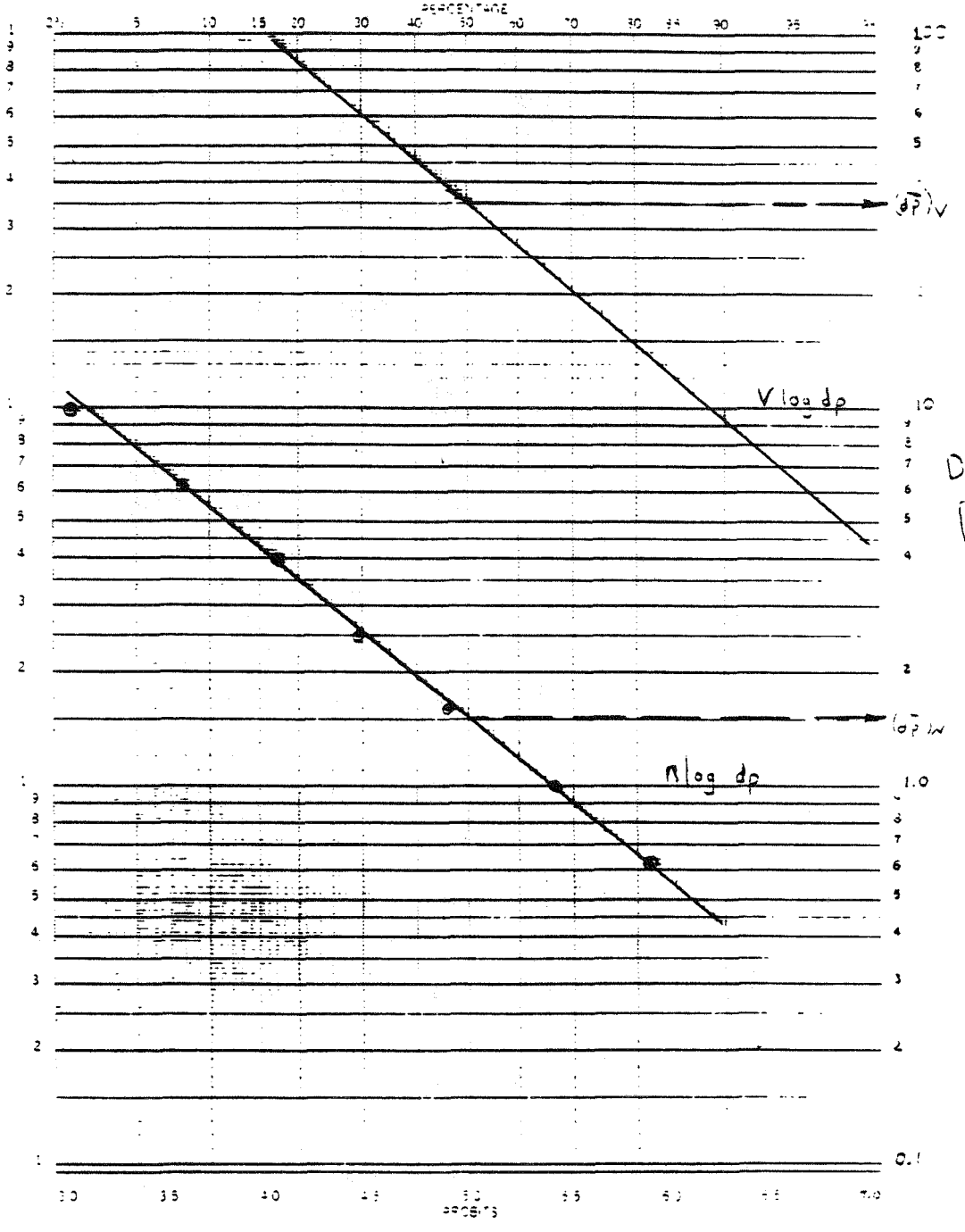

distribution. Figure 5-11 shows cumulative distributions comparing replicate samples 1 and 2, and replicate samples 3 and 4. The replicates were run concurrently with equal equilibration times. Figure 5-12 shows a cumulative distribution comparing samples 1 and 4 to determine whether the particle size distribution changed significantly over one month of shaking. These figures show that the cumulative size distributions are very similar. The Kolmogrov-Smirnov statistic, a quantitative measure of fit, can be used to test whether two samples did not come from the same distribution. The sample sizes for sample 1, 2, 3, and 4 were 1267, 1213, 1043, and 1767, respectively. At a 0.01 significance level the maximum expected difference between observed values can be estimated as 0.065, 0.064, and 0.060 when comparing samples 1 and 2, samples 3 and 4, and samples 1 and 4, respectively (Benjamin and Cornell, 1970). Maximum observed differences were 0.028, 0.042, and 0.024 respectively which is much less than the expected differences. Thus it appears that the reproducibility of the sample preparation and SEM analysis was good, and that the particle size distribution did not change significantly over a one-month period of shaking.

5.4. Modeling of Sorption and Desorption of Hydrophobic Compounds in Soil-Water Suspensions

Modeling was undertaken to confirm the experimental results which showed the rapidity of naphthalene sorption and desorption in the tests with Barnes-Hamerly soil. Modeling was also performed to assess conditions for which PAH solute may require relatively long time intervals to attain sorption or desorption equilibrium.

The modeling approach employed in this section assumed that the irregular-shaped soil particles may be represented as spherical aggregates. While this assumption may not be exactly correct for the case of the experimental system, it is shown later that this assumption has little consequence owing to the rapidity of predicted sorption and desorption equilibrium compared to the time scale of the experimental measurements.

Various Modeling Approaches. Various models have been proposed to describe sorption kinetics of hydrophobic organic compounds to natural soils and sediments. Three such sorption kinetic models are illustrated in Figure 5-13 (Wu and Gschwend, 1986). The models are:

(a) a one-box (or one-compartment) model in which the sorptive process is described by

Figure 5-11: Comparison of cumulative distributions of samples equilibrated for same time periods.

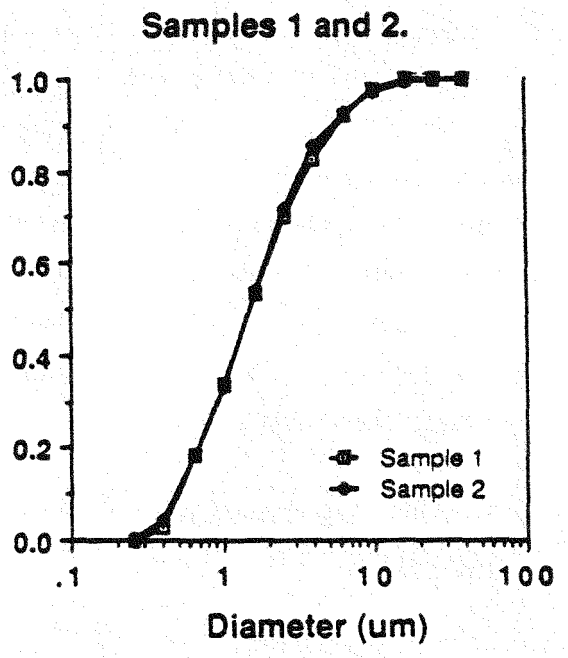

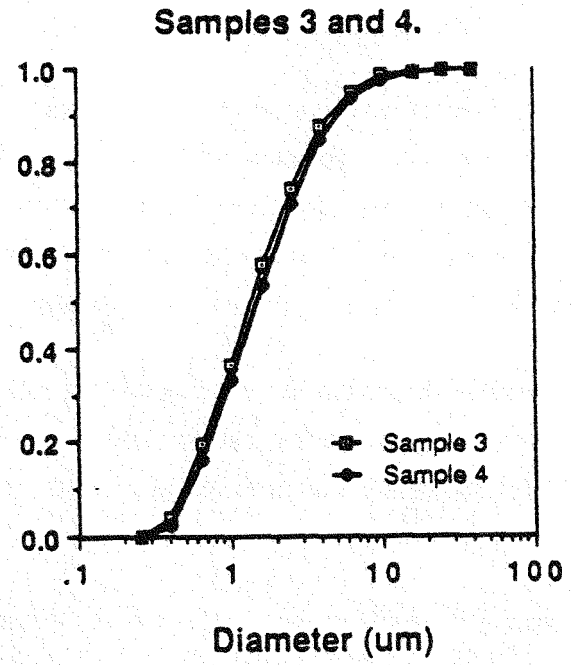

Figure 5-12: Comparison of cumulative distributions of samples equilibrated for 4 hours and 30 days.

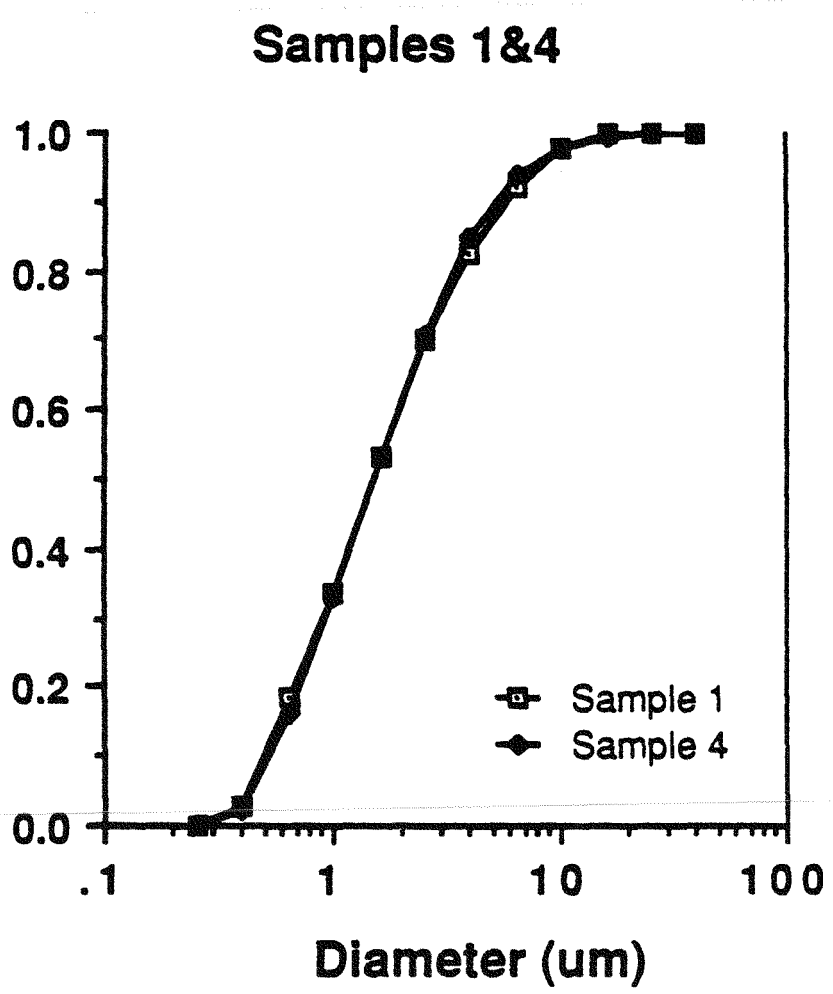

first-order kinetics. This model assumes that the sorptive process is limited by only one process, such as mass transfer or sorption site specificity, and the sorbent may be visualized as a completely mixed compartment.

(b) a two-box (or two-compartment) model in which it is envisioned that there are two types or classes of sorption sites; one easily accessible to solute and the other slowly accessible.

(c) a porous aggregate (or radial diffusion) model in which the soil is viewed as material with a porous structure in which the accessibility of the solute to the surface is dependent on solute migration through intraparticle pore fluid.

The inadequacies of the first two conceptual models have been described by Gschwend and Wu (1986). The one-box model does not fit experimental data well, as strongly hydrophobic solutes demonstrate a rapid initial uptake, or release, followed by slower approach to equilibrium. The two-box model overcomes this problem and fits experimental data quite well. Karickhoff (1980) utilized this method successfully to model the sorption of naphthalene, phenanthrene, and pyrene onto sediments. However, this model suffers from the need to provide three independent parameters which lack fundamental justification and which must usually be evaluated on a case-by-case basis.

Development of the Radial Diffusion Model. For a long period of time chemical engineers have considered intraparticle diffusion the rate-limiting step in sorption of organic compounds by activated carbons, synthetic resins, and porous catalysts, while recently soil scientists have incorporated this theory into transport of chemicals in naturally aggregated soils (Wu and Gschwend, 1986; Wu, 1986). Diffusion is the net transfer of material within a single phase in the absence of mixing. It results from pressure, temperature, and concentration gradients, and external force fields. The sorptive process can be visualized as one in which the solute radially penetrates the porous particles, but is retarded on the local level within the pore fluid according to a partition coefficient. Wu (1986) has developed a model based on the theory of diffusion of a solute into a porous aggregate to explain the sorption and desorption of organic compounds from soils and sediments. This approach has also been utilized by Rao et al. (1980) to analyze experimental data for diffusion of chloride ion from a porous sphere. The intraparticle diffusion approach incorporates important physical and chemical parameters [i.e., molecular diffusion and phase partitioning], and has

Figure 5-13: Comparison of models which describe the rate of sorption and desorption.

Kinetics Models	Independent Kinetics Fitting Parameters (derived parameters)
One-box model 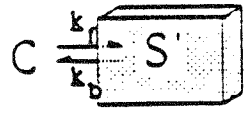	k_f $(k_b = k_f / K_p)$
Two-box model 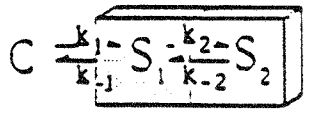 size x_1 x_2	k_1, k_2, x_1 $(k_{-1} = k_1 / K_p)$ $(k_{-2} = k_2)$ $(x_2 = 1 - x_1)$
Diffusion model 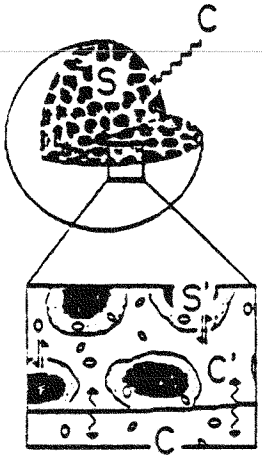	D_{eff}

From Wu and Gschwend, 1986

advantages over the one- or two-compartment models mentioned in the previous paragraph. Major advantages include only one fitting parameter and fundamental justification (Wu and Gschwend, 1986).

The following assumptions are made for the porous aggregate diffusion model. The model assumes that: 1.) sediment and soil particles are spherical aggregates (see references in Wu, 1986, for a discussion of this assumption), 2.) the molecular diffusivity of the solute is not a function of solute concentration, 3.) the particles are assumed to consist of internally homogeneous media, 4.) the bulk fluid is assumed to be sufficiently turbulent so that sorptive exchange is not limited by an exterior boundary layer, 5.) the entire sorptive area is available for mass flux, 6.) the pathlength of diffusion for natural soil can be accommodated by a pore geometry, or tortuosity factor.

The intra-aggregate radial diffusion model is developed as follows (Wu, 1986). The diffusion equation for radially orientated paths can be written in spherical coordinates according to Crank (1975):

$$\frac{\partial S(r)}{\partial t} = D_m n \left[\frac{\partial^2 C'(r)}{\partial r^2} + \frac{2}{r}\frac{\partial C'(r)}{\partial r}\right] \qquad [3]$$

where D_m is the pore diffusivity of the solute, cm^2/s, n is the porosity of the sorbent, cm^3 fluid/cm^3 total, and C'(r) is the dissolved solute concentration in the pore fluid, mol/cm^3, and changing with radial distance r, cm.

S is the total volumetric concentration of the solute in the porous sorbent, mol/cm^3, and can be expressed as:

$$S(r) = (1-n)\ \rho_s\ S'(r) + nC'(r) \qquad [4]$$

where S'(r) is the concentration of the immobile bound sorbate, mol/g, and ρ_s is the sorbent's specific gravity, g/cm^3.

At equilibrium the pore fluid concentration and the sorbed concentration can be related by the linear sorption isotherm

$$S'(r) = K_p C'(r) \qquad [5]$$

where K_p is the equilibrium partition coefficient, cm^3/g.

Equation [5] can be substituted into Equation [4] to obtain the total volumetric concentration of the solute in the sorbent:

$$S(r) = [(1-n)\rho_s K_p + n]C'(r) \quad [6]$$

The time rate of change of the sorbed compound can then be expressed as:

$$\frac{\partial S(r)}{\partial t} = \frac{D_m n}{(1-n)\rho_s K_p + n}\left[\frac{\partial^2 S(r)}{\partial r^2} + \frac{2}{r}\frac{\partial S(r)}{\partial r}\right] \quad [7]$$

The effective intraparticle diffusivity, D'_{eff}, can be defined as:

$$D'_{eff} = \frac{D_m n}{(1-n)\rho_s K_p + n} \quad [8]$$

and when $K_p >> n$, which is true for hydrophobic compounds, D'_{eff} can be written as:

$$D'_{eff} = \frac{D_m n}{(1-n)\rho_s K_p} \quad [9]$$

Substitution for the effective diffusivity into Equation [7] yields:

$$\frac{\partial S(r)}{\partial t} = D'_{eff}\left[\frac{\partial^2 S(r)}{\partial r^2} + \frac{2}{r}\frac{\partial S(r)}{\partial r}\right] \quad [10]$$

The diffusional path in natural aggregated soils is not straight nor radially orientated, and thus D'_{eff} must be modified to account for the pore geometry. This may be achieved by defining the effective diffusivity, D_{eff}, as a function of intra-aggregate porosity and tortuosity, t, which for the case of natural silts and sediments may be given as:

$$D_{eff} = D'_{eff}\, f(n,t) \quad [11]$$

Ullman and Aller (1982) have observed that $f(n,t) = n^i$ where i is between 1 and 2. Wu (1986) arbitrarily set i = 1 so that Equation [10] can be written as follows:

$$\frac{\partial S(r)}{\partial t} = D_{eff}\left[\frac{\partial^2 S(r)}{\partial r^2} + \frac{2}{r}\frac{\partial S(r)}{\partial r}\right] \quad [12]$$

Equation [12] can be solved with the following initial condition and two boundary conditions. At time equal to zero the total volumetric solute concentration is given as:

$S(r=0,t=0) = S_o$

The concentration at the aggregate surface is given by:

$$S(r=R) = [(1-n)\rho_s K_p + n]C$$

and the concentration at the center of the sphere as:

$$\frac{\partial S}{\partial r} = 0$$

The change in aqueous-phase concentration can be developed as follows from a mass balance relationship in a closed well-mixed system. The aqueous concentration, C, can be determined from:

$$V\frac{dC}{dt} = -V_s\frac{d\overline{S}}{dt} \qquad [13]$$

where V is solution volume, cm^3, V_s is the solid phase volume, cm^3, and $\overline{S}$ is the average concentration in a particle given by the integration over a sphere as follows:

$$\overline{S} = \frac{3}{4\pi R^3}\int_0^R 4\pi r^2 S(r)dr \qquad [14]$$

Analytical solutions for this description of solute diffusion into a porous medium with sorption are limited to simple situations such as there being a uniform particle size distribution with the bulk-aqueous phase being well-mixed (Crank, 1975). Wu (1986) has provided a numerical solution to Equation [12] for the intra-aggregate radial diffusion of a solute for the case of several classes of particle sizes and the bulk aqueous concentration allowed to vary. Particle sizes are differentiated on the basis of volumetric radius. Wu's original model was recoded in Fortran77 for use in this study, and a copy is available in Appendix B of this document.

The numerical solution of Wu (1986) was compared to the analytical solution (Crank, 1975) for verification. Table 5-2 compares the analytical and numerical solutions for two examples. Results are presented as the fractional approach of aqueous-phase concentration to completion to equilibrium, M_t/M_∞, which equals $(C_{initial} - C_t)/(C_{initial} - C_{equilibrium})$. The input parameters are taken from the experimental and simulation results presented in Wu and Gschwend (1986), corresponding to experiments 5 and 6 which examined 1,2,3,4-tetrachlorobenzene sorption onto Charles River sediments for an assumed mono-disperse

suspension. The numerical and analytical solution provided similar results except at the earliest time increments. At early times there is an error in the numerical integration procedure as extra weight is given to the surface grid point which is assumed equilibrated with the bulk-aqueous phase at time equal to zero. This error could be decreased by increasing the number of grid points used in the simulation. Wu (1986) provides a graphical means to estimate error in the numerical procedure as a function of grid number from knowledge of D_{eff} and the particle radius.

In the model simulations which follow, D_m for the organic solute in water at a temperature of 25 °C was calculated from the Hayduk and Minhaus correlation from the solute's molar volume and solvent viscosity (Hayduk and Minhaus, 1982; as recommended by Reid et al., 1987). Molar and critical volumes were estimated by the Lydersen, and Tyn and Calus methods, respectively (Lyman et al, 1982).

5.4.1. Model Simulations of the Sorption-Desorption Kinetics for Systems Comparable to Those Used in the Experiments with Extension to Unexplored Systems

The radial diffusion model of Wu (Wu, 1986) was utilized to assess the kinetics of sorption and desorption for systems similar to ones which were utilized in the experimental microbial degradation tests. This model was also employed to evaluate the effect of particle size, intraparticle porosity, and solute K_{ow} on sorption and desorption kinetics for particle sizes and solutes not experimentally evaluated.

Figure 5-14 shows a comparison of predicted sorption kinetics using either the volume mean particle radius or the particle volumetric radius size distribution of Figure 5-8a separately with the radial diffusion model. The number size distribution of Figure 5-8a was converted to a volumetric radius distribution by the relationship in Equation [2]. The volume mean radius was 17.5 μm. Five particle size groups, containing 20 percent of the total system volume, were selected to represent the volumetric radii distribution, and consisted of volumetric radii of 4.6, 10.25, 17.6, 30.5, and 63.5 μm. Fifteen grids were used for the volumetric radius and 10 grids for the particle size distribution radii. D_m for acenaphthene and naphthalene was 6.06 and 7.24 x 10^{-6} cm^2/sec, respectively, while K_p was 52 and 12 liters/kg, respectively. Other input parameters for the experimental system were ρ_s = 2.5 g/cm^3, n = 0.13, and solids concentration = 0.04 g/ml (i.e., 2g/50ml). These parameters are comparable to that for the

Table 5-2: Comparison of the analytical and numerical solutions for an intra-aggregate radial diffusion model.

		M_t / M_∞	
Experiment	Time (minutes)	Numerical	Analytical
5	5	0.186	0.272
5	10	0.278	0.314
5	100	0.644	0.639
5	500	0.907	0.903
5	1000	0.974	0.973
6	5	0.152	0.158
6	10	0.162	0.168
6	100	0.291	0.291
6	500	0.540	0.540
6	1000	0.677	0.678
6	5000	0.956	0.957

For experiment number 5, input parameters were as follows:

K_p = 1520 cm^3/g, r = 9.6 x 10^{-3} cm, 10 grids,

D_{eff} = 2.5 x 10^{-10} cm^2/sec,

solids concentration = 0.0010 g/ml,

and $C_{initial}$ = 3.2 x 10^{-9} mol/ml.

$C_{equilibrium}$ was calculated to be 1.25 x 10^{-9} mol/ml.

For experiment number 6, input parameters were as follows:

K_p = 1390 cm^3/g, r = 2.32 x 10^{-2} cm, 10 grids,

D_{eff} = 3.3 x 10^{-10} cm^2/sec,

solids concentration = 4.42 x 10^{-4} g/ml,

and $C_{initial}$ = 3.70 x 10^{-9} mol/ml.

$C_{equilibrium}$ was calculated to be 2.29 x 10^{-9} mol/ml.

$M_t/M_\infty = (C_{initial}-C_t)/(C_{initial}-C_{equilibrium})$

experimental systems used in the microbial degradation tests of this work. In the following figures the ordinates are plotted as [Co - C]/[Co - Ce] which represents the fraction of completion to equilibrium.

From Figure 5-14 it is seen that by using the measured particle size distribution, rather than the measured volume mean radius, the model predicts an initial higher sorbed concentration and a slower approach to equilibrium. This difference can be explained by the work of Cooney et al. (1983). Cooney et al. investigated the effect of particle size distribution on sorption kinetics by modeling the adsorption of *p*-nitrophenol onto activated carbon. The authors concluded that the particle size distribution was not of great importance with a narrow range of particle sizes in an infinite bath system (aqueous-phase solute > > solid-phase solute) but was important in finite bath systems and for highly non-Gaussian particle size distributions. In a finite bath system the aqueous solution concentration decreases with sorption; thus, the mass transfer driving force, i.e. the concentration gradient, also decreases with time. Cooney et al. explained that at early times, when the concentration gradient was greatest and the smallest particles were approaching equilibrium quickly, the finite-bath response was similar to the infinite-bath case. Furthermore a broad particle size distribution would contain more larger-than-average particles which would have a slower response towards equilibrium, thus, slowing down the total system's response towards equilibrium. The authors suggested that even though the effect of the particle size distribution on modeling accuracy is less than one might expect, greater accuracy is obtained for tests using a narrow Gaussian size distribution, and when investigating sorption kinetics experimentally, it is desirable that an investigator should use a uniform sieved fraction of the sorbent. Wu (1986) concluded from use of his numerical model that usage of the geometric mean of the volumetric size distribution was reasonable if the total size distribution was within one order of magnitude.

Rao et al. (1982) studied whether solute diffusion in nonspherical aggregates could be approximated by equivalent spherical aggregates and whether a nonuniform size distribution could be replaced by a single-weighted-average size. They concluded that solute diffusion from cubic aggregates could be described by equivalent spheres and that a volume-weighted average radius of equivalent spheres could replace a nonuniform size distribution of cubic-shaped aggregates.

Figure 5-15 shows the predicted effect of varying the volume mean particle size on

Figure 5-14: Comparison of the modeled sorption kinetics using the measured particle volume mean radius and the particle size distribution.

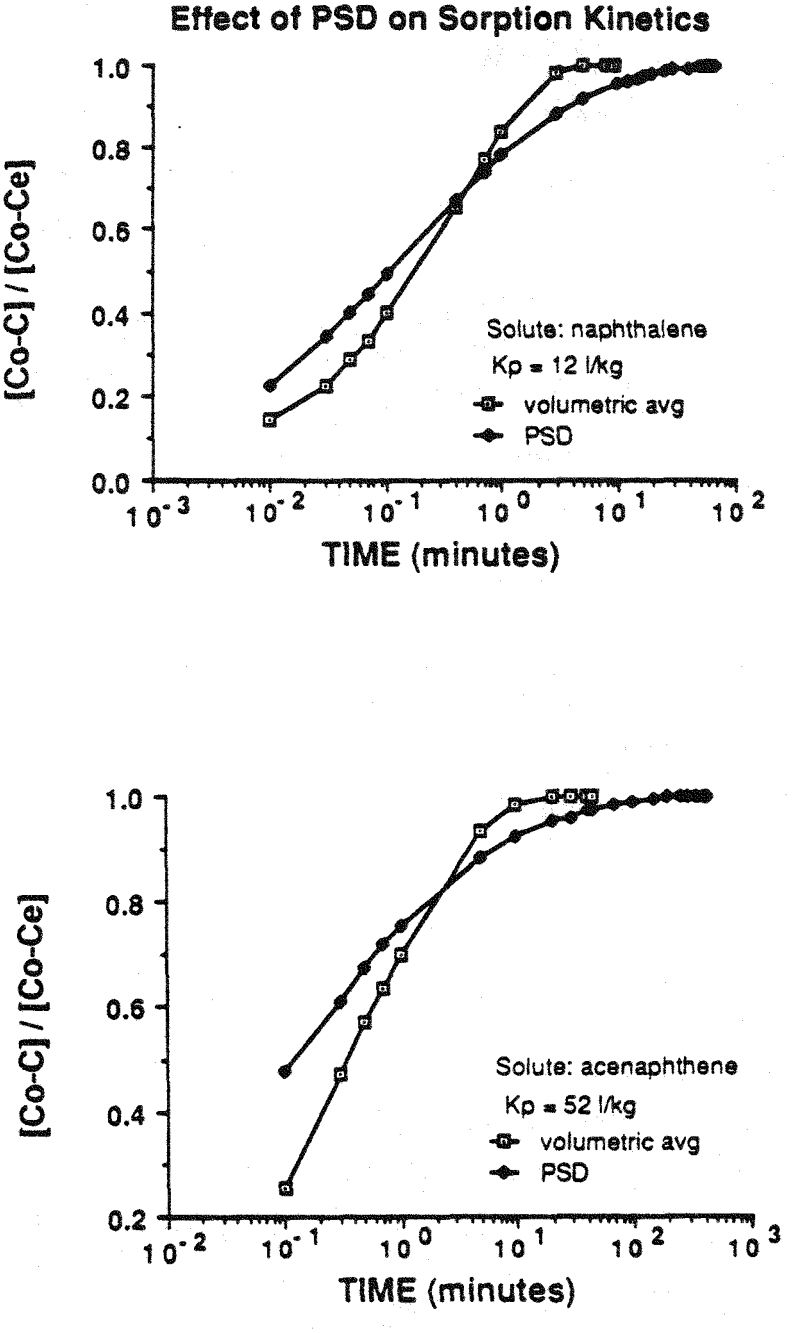

sorption uptake for a system described by the following input parameters: log K_{ow} = 3.36 (e.g., naphthalene), n = 0.13, ρ_s = 2.5, solids concentration = 1.75 x 10^{-5} g/ml, f_{oc} = 0.029, and D_m = 7.24 x 10^{-6} cm^2/sec. Log K_{ow} was used to estimate K_p according to Schwarzenbach and Westall (1979) by the equation, log K_{oc} = log K_{ow} - 0.21. From Figure 5-15 it is seen that the sorption uptake rate increased by a factor of 100 with a 10-fold decrease in volume mean particle radius. This is an expected result as the dimensionless time scale in the finite difference model is given as follows:

$$T = D_{eff}\ t/r^2 \qquad [15]$$

Thus sorption and desorption rates rates are dependent on the inverse of the square of the particle radius.

Figure 5-16 shows a comparison of predicted sorption and desorption kinetics associated with the solutes naphthalene and acenaphthene using measured value of volumetric mean radius. These results show model predictions for the systems similar to that used in the experimental studies with Barnes-Hamerly soil. Input parameters were n = 0.13, ρ_s = 2.5 g/cm^3, solids concentration = 0.04 g/ml (i.e., 2g/50 ml), and volume mean particle radius = 0.00175 cm. D_m for acenaphthene and naphthalene was 6.06 and 7.24 x 10^{-6} cm^2/sec, respectively. Log K_{ow} (3.36 and 4.03 for naphthalene and acenaphthene, respectively) was inputted into the equation log K_{oc} = log K_{ow} - 0.21, with f_{oc} = 0.029, to estimate the partition coefficients for naphthalene and acenaphthene. As seen in Figure 5-16 for the modeled experimental system, the solute sorption and desorption processes have similar time scales and are very rapid compared to the time scales of the microbial degradation experiments. The modeling predictions confirm the results presented in Table 5-1. Thus for purposes of preliminary assessment it is a reasonable assumption to model the irregular-shaped particles as spherical aggregates.

Notice that for naphthalene and a volumetric mean particle size as observed in the experiments, that over 90 percent of the approach to sorption and desorption equilibrium may be attained in a time scale of thirty minutes. Although the batch experimental system could not be utilized to continuously monitor sorption-desorption kinetics for time scales on the order of several minutes, the prediction was confirmed in part by the experimental results which showed that sorption equilibrium was attained in time periods less than an hour.

Figure 5-17 presents an evaluation of the sensitivity of the predicted sorption kinetics for naphthalene with respect to the intraparticle porosity, n, utilizing the mean particle volumetric

Figure 5-15: Predicted effect of volumetric mean particle radius on naphthalene sorption kinetics.

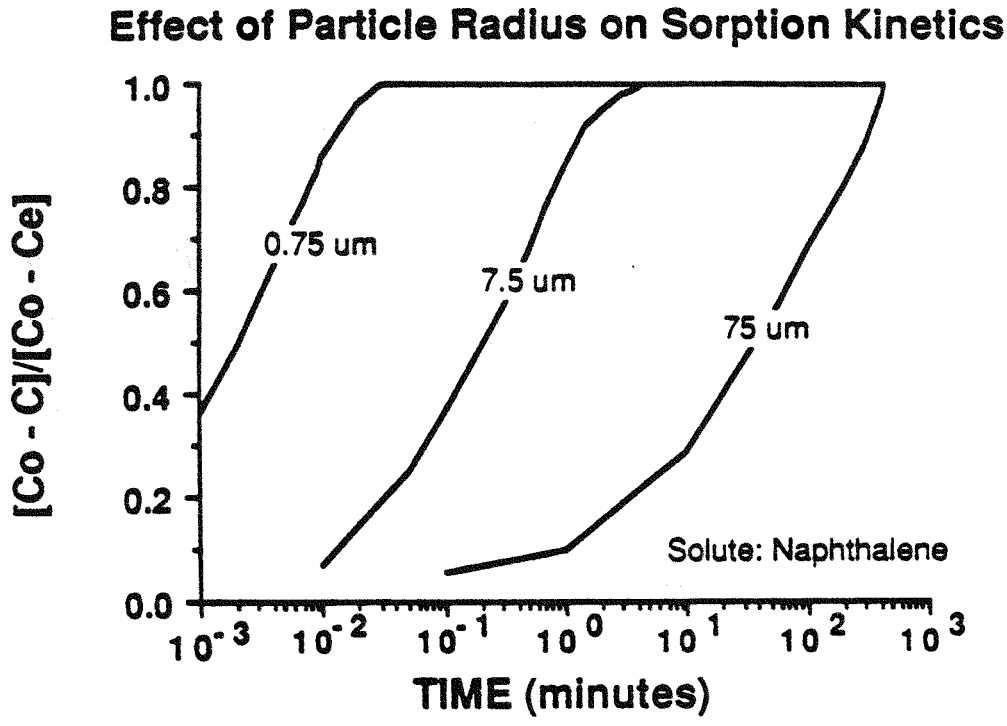

Figure 5-16: Comparison of the predicted rate of solute sorption and desorption using the measured value of the volumetric mean radius.

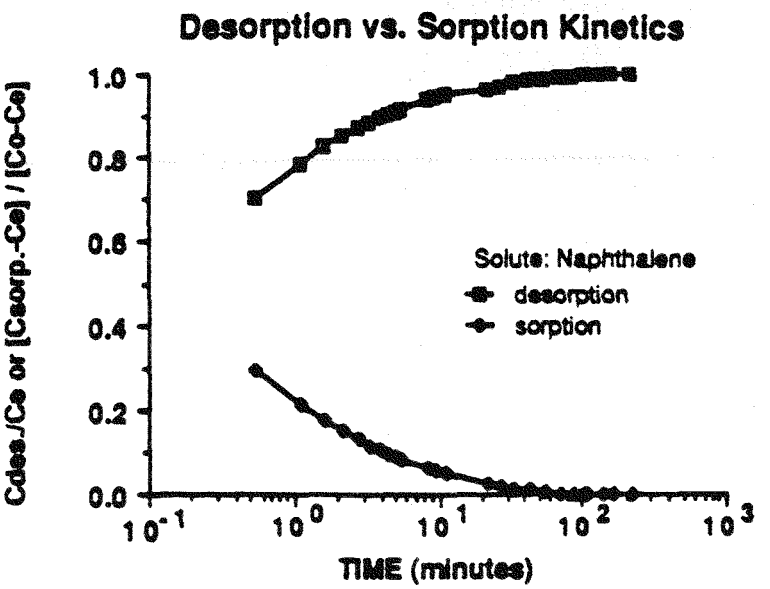

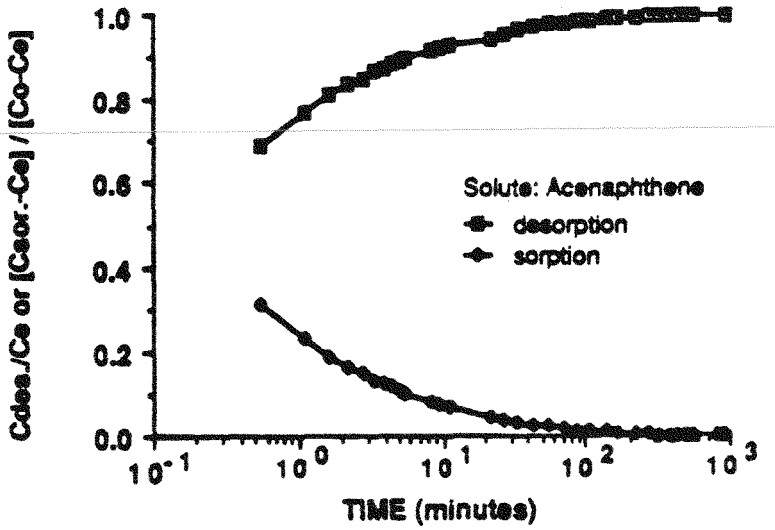

radius for the size distribution shown in Figure 5-8a. Input parameters were chosen to represent an experimental system containing the solute naphthalene and 2 grams of Barnes-Hamerly soil per 50-ml centrifuge tube. Wu and Gschwend (1986) found that the average intraparticle porosity for different sediment types was 0.13± 0.04. It is seen that decreasing this average value of n by a factor of 2 increases the time to 100 percent equilibrium by approximately a factor of 2.3 while increasing the average value n by a factor of 2 decreases the time to 100 percent equilibrium by approximately a factor of 2.3. This is a consequence of Equations [9] and [15] in which D_{eff} is a function of $n^2/(1-n)$ which in turn is incorporated in the equation for the dimensionless time step. As the intraparticle porosity, n, decreases, more of the total solid volume consists of solid phase instead of liquid phase. Thus more of the contaminant can become associated with the immobile solid phase which causes the sorption kinetics to decrease. These results show that the predicted sorption kinetics are much more dependent on the volume mean radius than the intraparticle porosity.

A model simulation was conducted to examine the predicted effect of solute K_{ow} on sorption kinetics. Figure 5-18a, b, and c show the approach to sorption equilibrium as a function of time for three PAH compounds. The solutes selected where naphthalene (log K_{ow} = 3.36), anthracene (log K_{ow} = 4.54), and benzo(*a*)pyrene (log K_{ow} = 6.50). Simulation parameters were n = 0.13, solids concentration = 1.75 x 10^{-5} g/ml, and ρ_s = 2.5 g/cm^3. The particle radii used were 17.5, 175, and 1,750 μm with 15 grids. In Figure 5-18a it is seen that naphthalene, anthracene, and benzo(*a*)pyrene reached 100 percent equilibrium in approximately 25, 460, and 1.3 x 10^5 minutes respectively, for a volume mean radius of 17.5 μm, while for volume mean radii of 175 and 1,750 μm, the time periods to attain 100 percent equilibrium were approximately 2,400, 46,000 and 8.2 x 10^6 minutes and 2.4 x 10^5 (0.45), 4.6 x 10^6 (8.8), and 9.2 x 10^8 (1,700) minutes (years) respectively for the solutes naphthalene, anthracene, and benzo(*a*)pyrene. Although these predicted results were not confirmed by experiment, the predicted trends are consistent with the work of Wu and Gschwend (1986) and Karickhoff (1980) who examined the effect of hydrophobicity on sorption uptake rate and concluded from their own experimental work that compounds with a higher hydrophobicity had much slower uptake rates.

Sorption equilibrium was predicted to be attained with naphthalene in under one half hour due to the small volume mean particle size of 17.5 μm. Consistent with this result are the data of Wu and Gschwend (1986) who found by experimental and modeling work that sorption of tetrachlorobenzene (log K_{ow} = 4.6) onto Charles River sediments (f_{oc} = 8.5 percent, mean

Figure 5-17: Predicted effect of intra-aggregate porosity on naphthalene sorption kinetics.

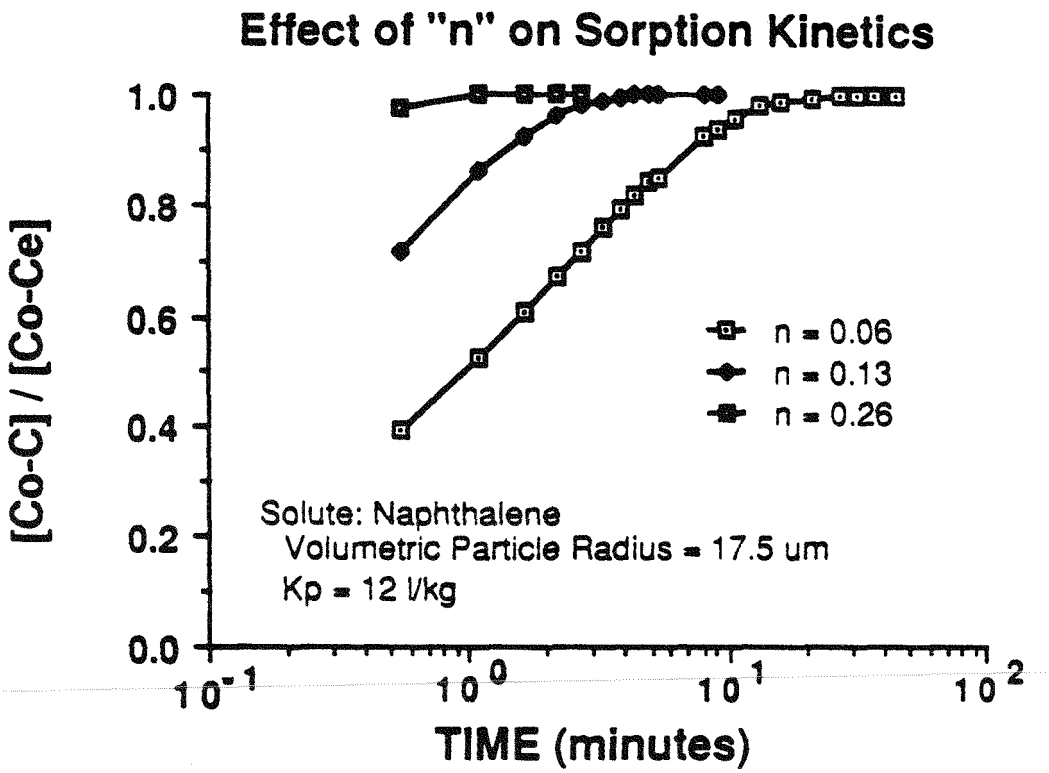

Figure 5-18: Predicted effect of octanol/water partition coefficient on the rate of sorption.

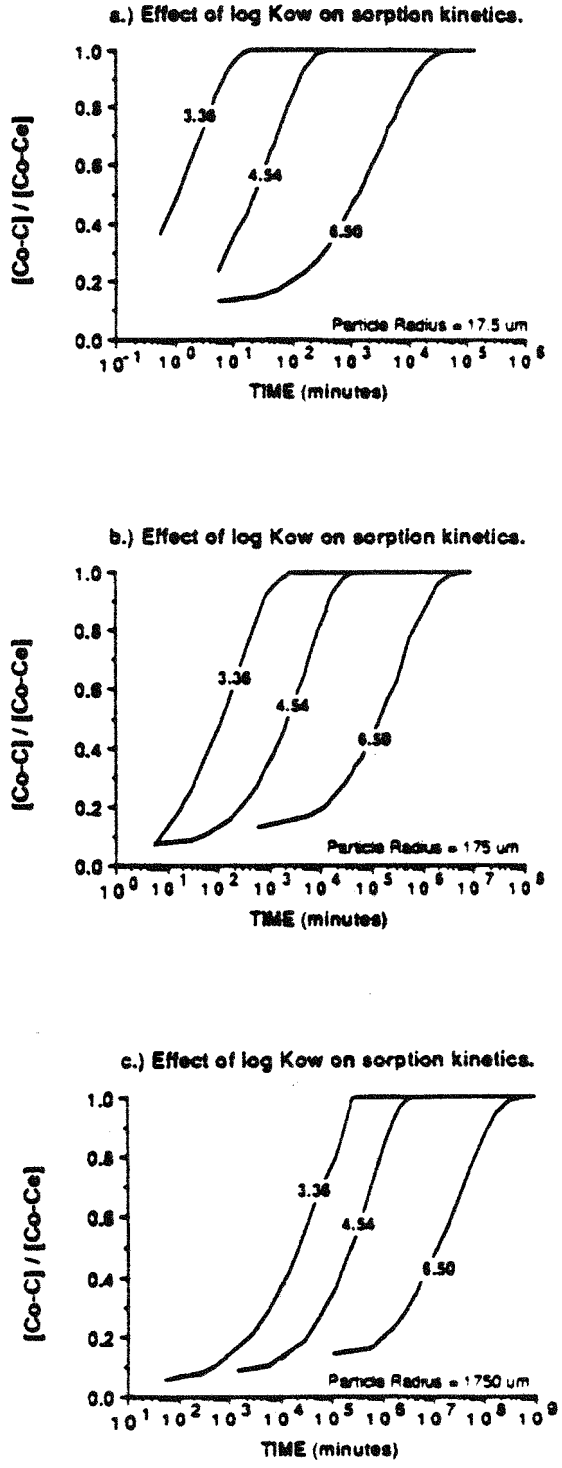

particle diameter = 96 μm) reached 90 percent equilibrium in a time span of approximately 100 minutes. In contrast, an interesting result from the predictions with the experimentally measured volume mean particle size of 17.5 μm, the solutes anthracene and benzo(*a*)pyrene are predicted to attain sorption equilibrium over periods of 7.7 hours and 6 days respectively, which when compared to naphthalene is significant.

The radial diffusion model predicts that the organic compound with the higher partition coefficient will attain equilibrium slower. This is a result of local sorption equilibrium being reached between molecules dissolved in pore fluids and molecules sorbed locally so the solutes with a higher K_p are theorized to penetrate slower into a natural porous aggregate if diffusive transport is occurring in the pore fluids. This can also be explained as a consequence of higher partitioning decreasing D_{eff} since more of the contaminant is fixed to immobile particles at higher levels of sorption. Thus a smaller fraction of the contaminant is dissolved and free to diffuse. Higher molecular weight compounds also have lower diffusivities. For example, the estimated D_m for the solutes naphthalene and benzo(*a*)pyrene in water at 25 °C are 7.24 and 3.30 x 10^{-6} cm^2/sec respectively. The difference is small "since D_m is inversely proportional to the one third power of molar volume" (Wu and Gschwend, 1986). Therefore the hydrophobicity of the compound dominates the sorption uptake rate shown in Figures 5-18a, b, and c.

This section described the use of a radial diffusion model to evaluate the rates of sorption and desorption of hydrophobic compounds onto/from soils and sediments for both simulated experimental and unexplored conditions. Influential parameters which were addressed included the effect of particle size, particle size distribution, intraparticle porosity, and solute hydrophobicity. The modeling supported the experimental evidence which demonstrated the reversibility and the relatively rapid kinetics of sorption and desorption of the solute naphthalene with the Barnes-Hamerly soil used in this study. This modeling showed the long time durations which may be required for sorption or desorption equilibrium in a system containing larger soil aggregates and a strongly hydrophobic PAH solute.

5.5. Conclusions

This chapter examined the sorption and desorption characteristics of PAH compounds in soil-water systems. Both experimental and modeling work were conducted which showed that naphthalene is reversibly sorbed and that the kinetics of sorption and desorption are rapid for the particle size employed in the experiments. For the case of the experimental portions of this work, the small average particle size resulted in rates of sorption and desorption being relatively rapid; on a time scale of minutes to an hour. Although the soil particles in these experiments were irregular-shaped aggregates, a spherical radial diffusion model was employed for preliminary assessment of the potential effect of particle size and solute hydrophobicity on rates of sorption and desorption. This demonstrated the importance of particle size and solute hydrophobicity on sorption-desorption kinetics for PAH solutes. These topics are addressed further in the following chapter in which the effect of desorption on the rate of microbial degradation is examined.

5.6. References

1. Benjamin, J.R., and C.A. Cornell, *Probability, Statistics, and Decision for Civil Engineers,* McGraw-Hill Book Company, New York, 1970.
2. Chio, C.T., P.E. Porter, D.W. Schmedding, "Partition Equilibrium of Nonionic Organic Compounds between Soil Organic Matter and Water," *Environmental Science and Technology,* Vol. 17, p. 227-231, 1983.
3. Cooney, D.O., B.A. Adesanya, and A.L. Hites, "Effect of Particle Size Distribution on Adsorption Kinetics in Stirred Batch System," *Chemical Engineering Science,* Vol. 38, p. 1535-1541, 1983.
4. Crank, J., The Mathematics of Diffusion, 2nd ed., Clarendon Press, Oxford, England, 1975.
5. Di Toro, D.M., "A Particle Interaction Model of Reversible Organic Chemical Sorption," *Chemosphere,* Vol. 14, p. 1503-1538, 1985.
6. Di Toro, D.M., and L.M. Horzempa, "Reversible and Resistant Components of PCB Adsorption-Desorption: Isotherms," *Environmental Science and Technology,* Vol. 16, p. 594-602, 1982.
7. Fu, J.K., and R.G. Luthy, "Effect of Organic Solvent on Sorption of Aromatic Solutes onto Soils," *Journal of Environmental Engineering,* Vol. 112, p. 346-366, 1986.
8. Gschwend, P.M., and S.C. Wu, "On the Constancy of Sediment-Water Partition Coefficients of Hydrophobic Organic Pollutants," *Environmental Science and Technology,* Vol. 19, p. 90-96, 1985.
9. Hamaker, J.W., and J.M. Thompson, "Adsorption," in *Organic Chemicals in the Soil Environment,* Vol. 1, Eds: C.A.I. Goring and J.W. Hamaker, Marcel-Dekker, New York, 1972.
10. Hayduk, W., and B.S. Minhaus, *Canadian Journal of Chemical Engineering,* Vol. 60, p. 295, 1982.
11. Hassett, J.J., W.L. Banwart, S.G. Wood, and J.C. Means, "Sorption of α-Naphthol: Implications Concerning in the Limits of Hydrophobic Sorption," *Soil Sci. Soc. Am. J.,* Vol. 45, p. 38, 1981.
12. Karickhoff, S.W., D.S. Brown, and T.A. Scott, "Sorption of Hydrophobic Pollutants on Natural Sediments," *Water Research,* Vol. 13, p. 241-248, 1979.
13. Karickhoff, S.W., "Sorption Kinetics of Hydrophobic Pollutants in Natural Sediments, 193-205. *In* R.A. Baker (ed.), *Contaminants and Sediments. Volume 2. Fate and Transport Case Studies, Modeling, Toxicity,* Ann Arbor Science, Ann Arbor, Michigan, 1980.
14. Karickhoff, S.W., "Organic Pollutant Sorption in Aquatic Systems," *Journal of Hydraulic Engineering,* Vol. 110, p. 707-735, 1984.
15. Lambe, T.W., *Soil Testing for Engineers,* John Wiley and Sons, Inc., New York, p. 29-42, 1967.
16. Lloyd, P.J., "Stream Scanning Methods," Chapter 3, presented at the Particle Characteristics Conference, Department of Chemical Engineering, Loughborough University of Technology, September, 1968.
17. Lloyd, P.J., "Gravity Sedimentation Methods," Chapter 14, presented at the

Particle Characteristics Conference, Department of Chemical Engineering, Loughborough University of Technology, September, 1968.

18. Lyman, W.J., W.F. Reehl, and D.H. Rosenblatt, *Handbook of Chemical Property Estimation Methods,* McGraw-Hill Book Company, New York, pp. 12.33 - 12.39, 1982.

19. Means, J.C., S.G. Wood, J.J. Hassett, W.L. Banwart, "Sorption of Polynuclear Aromatic Hydrocarbons by Sediments and Soils," *Environmental Science and Technology,*" Vol. 14, p. 1524-1528, 1980.

20. Murphy, C.H., *Handbook of Particle Sampling and Analysis Methods,* Verlag Chemie International, Inc., Deerfield Beach, Florida, p. 44-49, 1984.

21. Rao, P.S.C., R.E. Jessup, D.E. Rolston, J.M. Davidson, and D.P. Kilcrease, "Experimental and Mathematical Description of Nonadsorbed Solute Transfer by Diffusion in Spherical Aggregates," *Soil Sci. Soc. Am. J.,* Vol. 44, p. 684-688, 1980.

22. Rao, P.S.C., R.E. Jessup, and T.M. Addiscott, "Experimental and Theoretical Aspects of Solute Diffusion in Spherical and Nonspherical Aggregates," *Soil Science,* Vol. 133, p. 342-349, 1982.

23. Reid, R.C., J.M. Prausnitz, and B.E. Poling, *The Properties of Gases and Liquids, 4th Edition,* McGraw-Hill Book Company, New York, p. 577-631, 1987.

24. Scarlett, B., "Centrifugal Sedimentation" Chapter 15, presented at the Particle Characteristics Conference, Department of Chemical Engineering, Loughborough University of Technology, September, 1968.

25. Schwarzenbach, R.P., and J. Westall, "Transport of Nonpolar Organic Compounds From Surface Water to Groundwater. Laboratory Sorption Studies," *Environmental Science and Technology,* Vol. 15, p. 1360-1367, 1981.

26. Seinfeld, J.H., *Atmospheric Chemistry and Physics of Air Pollution,* John Wiley and Sons, New York, 1986.

27. Ullman, W.J., and R.G. Aller, "Diffusion Coefficients in Nearshore Marine Sediments," *Limnology and Oceanography,* Vol. 27, p. 552-556, 1982.

28. Wu, S., and P.M. Gschwend, "Sorption Kinetics of Hydrophobic Organic Compounds to Natural Sediments and Soils," *Environmental Science and Technology,* Vol. 20, p. 717-725, 1986.

29. Wu, S., "Transport of Hydrophobic Organic Compounds Between Water and Natural Sediments," Ph.D. Thesis, Department of Civil Engineering, Massachusetts Institute of Technology, Boston, Massachusetts, 1986.

Chapter 6

Modeling the Degradation of PAH Compounds and the Associated Nitrate Reduction in Soil-Water Suspensions under Denitrification Conditions

Knowledge of the fate and transport of pollutants which have been discharged into soil-water systems is important for understanding the effects of environmental contaminants in the subsurface environment. Mihelcic and Luthy (1988a, 1988b) have recently reported experimental evidence on the microbial degradation of low-molecular-weight polycyclic aromatic hydrocarbons (PAH) under denitrification conditions. In that work it was shown that acenaphthene and naphthalene were microbially degraded under nitrate-excess conditions, but not under anoxic nitrate-limiting conditions.

This chapter begins with a presentation of some relevant literature pertaining to i.) the mineralization of naturally occurring soil organic carbon in soil, ii.) the modeling of nitrate depletion in soil environments, and iii.) the modeling of organic contaminant utilization in aquatic and soil-water systems. This information is incorporated into models which describe the change in concentration of naturally occurring soil organic carbon, nitrate, and PAH compound with time for a soil-water suspension under denitrification conditions. The experimental procedures are described and this is followed by a presentation and discussion of the experimental data and model predictions.

The purpose of the model simulations was to develop initial understanding of the manner in which PAH sorption-desorption kinetics may effect the bio-availability of PAH compounds during microbial degradation. For this purpose it was assumed that the microbial degradation of the PAH compounds in a soil-water suspension occurs through solute residing in the aqueous phase, and that the irregular-shaped soil particles could be represented as spherical aggregates with the sorption-desorption process described by an intra-aggregate radial diffusion process. The chapter concludes with a discussion of model simulations which

examine the effect of particle size and PAH compound hydrophobicity on microbial degradation of PAH solutes in soil-water suspensions.

6.1. Background

The following discussion is relevant to understanding some of the microbially-induced interactions which may occur as a result of naturally occurring soil organic carbon mineralization, PAH degradation, and nitrate reduction in a soil-water suspension.

Studies have indicated that the rate of nitrate reduction in both wastewater and soil systems was a function of the type of available organic material (Lewandoswki, 1982; Jacobson and Alexander, 1980). For this reason some researchers have incorporated into denitrification models various fractions of organic carbon, each with their own rate of decomposition (Jenkinson and Rayner, 1977; Reddy et al., 1980, Molina et al., 1983). The organic carbon fraction which is mineralizable under denitrification conditions, and not the total organic carbon content of soil, has been strongly correlated to denitrification rates (Stanford et al., 1975; Burford and Bremner, 1975; Beauchamp et al., 1980; Reddy et al., 1982, Batonda et al., 1984).

The denitrification rate in soils has been modeled as a first-order reaction (Stanford et al., 1975; Stars and Parlange, 1975), zero-order reaction (Stammers et al., 1983) and mixed-order reaction (Bowman and Focht, 1974; Kohl et al., 1976; Oren and Blackburn, 1979; Reddy et al., 1982; Ryden et al., 1983) with respect to nitrate concentration, and first- or mixed-order with respect to carbon substrate (Reddy et al., 1982; Rolston et al., 1984). An explanation for these various rate relationships must recognize that these studies employed various concentrations of nitrate and various experimental protocols including column studies, completely-mixed batch reactors, and flooded and unflooded unmixed soil systems.

For example, many of the references which have reported denitrification kinetics in soil being dependent on nitrate concentration were conducted in flooded soil experiments. The effect of flooded and non-flooded soil conditions on the order of the denitrification reaction with respect to nitrate concentration has been studied by experiments and modeling for unmixed soil systems with standing water (Reddy et al., 1978; Phillips et al., 1978). It was concluded from tests with fifteen soils that experiments which were conducted with stagnant floodwater exhibited first-order kinetics while non-flooded soils exhibited zero-order kinetics. The

difference was attributed to a diffusion-limiting reaction in the flooded soil system, i.e., the rate of denitrification was faster than the rate of NO_3-N flux diffusing to the soil.

Table 6-1 compares the results of various investigations which have examined the rate and order of the denitrification reaction in soil. From Table 6-1, it appears for batch degradation tests with the suspension being agitated periodically, that the rate of nitrate reduction will be zero-order with respect to nitrate for aqueous-phase nitrate concentrations greater than several µg NO_3^- per g of soil.

In general, when modeling the fate of organic compounds in a soil-water or aquatic system, the rate of microbial removal of an organic compound can be described according to Monod kinetics as follows:

$$\frac{dS}{dt} = -\frac{\mu_m \; S \; B}{Y \; (K_s + S)} \qquad [1]$$

where S is the substrate concentration, mol/liter, μ_m is the maximum growth rate, hr^{-1}, B is the bacteria population, organisms/liter, Y is a yield factor for conversion of substrate to biomass, organisms/mol of substrate, and K_s is the half saturation constant for growth which equals the substrate concentration at which the rate equals 1/2 μ_m.

Paris et al. (1975, 1981) have utilized a modified form of Monod kinetics to describe the microbial removal rate of malathion, chlorpropham, and the butoxy-ethyl ester of 2,4-D in natural waters. The authors assumed that the bacteria concentration remained constant over time and that the low solubility of the hydrophobic organic compounds in water resulted in $S << K_s$. By grouping the rate constants and incorporating these assumptions, Equation [1] can be written as:

$$\frac{dS}{dt} = -k_1 \; S \qquad [2]$$

where k_1 is a pseudo-first-order rate constant equal to $\mu_m B/YK_s$, hr^{-1}.

If substrate concentration is higher than K_s, and if biological growth is neglible (i.e. B is constant), Equation [1] reduces to a zero-order equation with respect to substrate and can be written as:

$$\frac{dS}{dt} = \frac{-\mu_m}{Y} B \qquad [3]$$

Paris et al. (1975, 1981) concluded that the model presented as Equation [2] could

Table 6-1: Review of studies examining the kinetics of denitrification.

Nitrate Dependence	Experimental System	Reference
K_m=170 mg/l NO_3^--N K_m=1000 mg/l NO_3^--N	50 g soil, 50 ml aqueous (unmixed), 2 soils	Bowman and Focht, (1974)
first order	10 g soil, 25 ml aqueous (unmixed)	Stanford et al., (1975)
first order	soil column studies	Stars and Parlange, (1975)
K_m=48.7 mg/l NO_3^--N	75 g soil, 125 ml aqueous	Kohl et al. (1976)
first order	flooded soil	Reddy et al. (1978)
K_m=21 mg/l NO_3^--N	flooded soil	Oren and Blackburn, (1979)
zero order	saturated soil no floodwater	Reddy et al. (1978)
zero order	column studies	Stammers et al., (1983)
K_m= 5-10 µg/g soil	field measurements	Ryden (1983)

describe the degradation of the three organic compounds in aquatic systems. By varying the initial bacterial concentration by orders of magnitude, the authors also showed proportional changes in the rate constant, k_1.

Other researchers have incorporated bacterial growth kinetics for the modeling of soil and water systems in which microbial growth influenced the shape of the substrate disappearance curve (Robinson and Tiedje, 1983; Simkins and Alexander, 1984; Brunner and Focht, 1984; Focht and Brunner, 1985; Simkins et al., 1986; Suflita et al., 1987). This and other factors which affect the shape of the substrate disappearance curve have been reviewed by Alexander (1985).

As discussed by Mihelcic and Luthy (1988b), the role of organic solute sorption on microbial degradation may decrease the total amount of solute available to microorganisms for degradation (Ogram et al., 1985), as well as result in the entrapment of a solute in soil micropores for long periods of time (Steinberg et al., 1987). The effect of the desorption rate from bentonite clay on microbial degradation of *n*-decylamine has been studied experimentally, with the conclusion for that particular system, that the rate of desorption did not limit the rate of degradation (Wszolek and Alexander, 1979). Other researchers have incorporated sorption kinetics into a model which described substrate disappearance, by assuming that the sorption kinetics were rapid when compared to the rate of microbial degradation. The role of solute sorption was assumed to affect the system by reducing the degradable aqueous-phase concentration of the organic compound (Steen et al., 1980).

Summary. The various literature may be summarized as follows. The effect of carbon concentration on carbon utilization during denitrification in soil has been expressed by subdividing the carbon into different forms, each which has a varying rate of degradation ascribed to it. Utilization of naturally occurring soil organic carbon has been successfully modeled by first-order kinetics. The denitrification rate is thought to be a function of the mineralizable carbon concentration and independent of nitrate concentration in completely-mixed soil-water systems. The degradation of an organic compound in a soil-water system can be successfully modeled by Monod growth kinetics with either no-growth or growth kinetics of the microorganisms incorporated into the model. Sorption of a hydrophobic solute may limit the total amount of solute available to microorganisms and affect the degradation rate if the rate of desorption becomes the rate-limiting step.

The objectives of this portion of the work were to develop models which describe the change in nitrate concentration and PAH concentration with time while accounting for any effects of sorption and desorption on the microbial degradation of PAH, and to verify these concepts experimentally. This was followed by simulations of unexplored conditions in order to examine the influence of particle size on degradation, through its effect on solute desorption and bio-availability.

6.2. Model Development

6.2.1. Soil Organic Carbon Utilization

The mineralization of naturally occurring soil organic carbon under denitrification conditions has been modeled successfully by many researchers as explained in Mihelcic and Luthy (1988b). This is accomplished by a first-order reaction with respect to mineralizable soil organic carbon:

$$C_c = C_{max}\ exp(-k_c t) \qquad [4]$$

where C_c is the available soil organic carbon at time t, mol/liter C, C_{max} is the maximum available, naturally occurring soil organic carbon, mol/liter C, k is the first-order kinetic coefficient, hr^{-1}, and t is time, hr.

6.2.2. Nitrate Reduction

In a soil-water system the denitrification rate can be modeled as a function of carbon substrate concentration and denitrifying cell population. In the experimental work described in this portion of the study, acclimated soil was used, hence the growth of the active microorganisms was assumed to be neglible. Thus the denitrification rate, which depends on the initial active microbial cell population, was hypothesized to be related to the soil-to-water ratio of the experimental system. The denitrification rate can then be written as follows:

$$dN/dt = - k_N\ C_T \qquad [5]$$

where k_N is the first-order kinetic rate constant, mol N /mol C -hr, C_T is the total carbon concentration in mol C/l. An organic solute such as PAH, when introduced into a soil environment, contributes another source of carbon to an already complex mixture of carbon sources. Assuming that the available, naturally occurring soil organic carbon is utilized as a single source, and letting the total available organic carbon substrate be comprised of available soil organic carbon and soluble PAH, Equation [5] can be expanded as follows:

$$dN/dt = - k_N\ [C_c + C] \qquad [6]$$

where C_c is the contribution of organic carbon from the soil and C is the aqueous concentration of PAH, mol/liter. Substitution of Equation [4] into Equation [6] for C_c yields the following expression for nitrate utilization:

$$dN/dt = - k_N [C_{max} exp(-k_c t) + C] \quad [7]$$

From Equation [7] it is seen that one form of organic carbon substrate can dominate the loss of nitrate from a soil-water system. For example, if a small amount of PAH is present in a soil of average organic carbon content value, then $C_{max} > > C$. For the case of the experimental results presented in Mihelcic and Luthy (1988a, b), C_{max} and C were of near equal magnitudes. However, in tests which utilized acclimated soil, the available soil organic carbon was assumed completely mineralized since previous experiments had shown that C_{max} was depleted in approximately three weeks, during which the associated nitrate demand was exerted. Thus in the tests which were conducted with acclimated soil, C_{max} was approximately zero, assuming slow conversion of residual soil organic carbon to labile organic carbon.

6.2.3. Microbial Degradation of Polycyclic Aromatic Hydrocarbons

It is envisioned in this work for a soil-water system maintained under gentle suspension which utilizes an acclimated active microorganism population, that the microbial degradation of the PAH compound will occur through the solute residing in the bulk aqueous phase, and that the rate of degradation may be proportional to the substrate concentration in the bulk aqueous phase and the initial active cell population. This situation is depicted in Figure 6-1. As the bulk aqueous-phase concentration begins to decrease, a concentration gradient develops which allows sorbed solute to diffuse from the porous aggregate into the bulk phase. In this development it is also assumed that the bulk-phase concentration is uniform and that there is sufficient turbulence so that an outside boundary layer resistance between the bulk phase and the particle is not significant. This assumption is appropriate for the experiments conducted in this work with soil-water suspensions. It is also assumed that there is no mass transfer resistance between a compound desorbing from the solid phase through a biofilm which may be on, or near, the particle surface, nor mass transfer resistance for compound diffusion to the microorganisms from the bulk aqueous phase.

As seen in Chapter 5, the change in aqueous PAH solute concentration with time for the case of sorption and desorption can be written as follows:

Figure 6-1: Description of coupled desorption-degradation model.

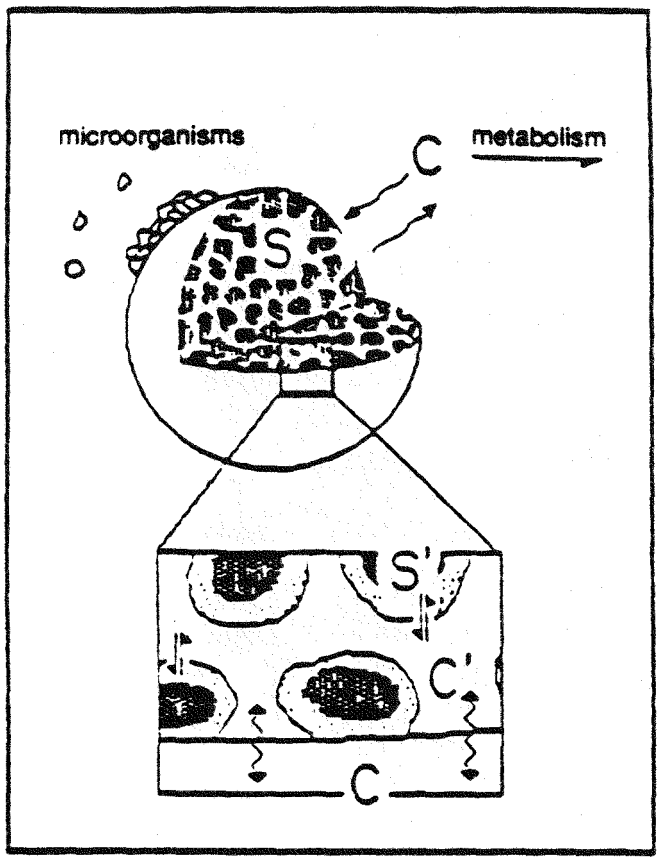

Adapted from Wu and Gschwend, 1986

$$\frac{dC}{dt} = -\frac{V_s}{V}\frac{d\bar{S}}{dt} \qquad [8]$$

where C is the aqueous concentration of PAH, mol/ml; $\bar{S}$ is the average solute concentration in the solid integrated over the sphere, mol/cm^3 total; V_s is the volume of the solid, cm^3 total and equals $V\rho/(1-n)\rho_s$ where ρ is the soil-to-water ratio, g solid/cm^3 liquid, and ρ_s is the specific weight of the solid, g solid/cm^3; n is the intra-aggregate porosity of the solid, cm^3 liquid/cm^3 total; V is the volume of the liquid phase, cm^3 liquid; and t is time, min.

Monod reaction kinetics are used to describe substrate depletion from the aqueous phase, so the change of PAH solute is given by coupling the change due to sorption and desorption from soil with substrate depletion in the aqueous phase:

$$\frac{dC}{dt} = -\frac{V_s}{V}\frac{d\bar{S}}{dt} - \frac{K_{max}\ C}{K_s + C} \qquad [9]$$

where K_{max} is the maximum rate of the reaction, mol/ml-min (mg/liter-day), and is equal to $\mu_m B/Y$, and K_s is the half-saturation coefficient, mol/ml (mg/l). K_s is the substrate concentration for which the rate is equal to one half of the maximum rate.

It is assumed that the microbial population is constant and proportional to the mass of soil in the system so that K'_{max} can be defined as the maximum rate, K_{max}, divided by the soil-to-water ratio, ρ, g/ml. The units of K'_{max} are mol/g-min (mg/g-d). The assumption of a constant active microbial population and proportionality between microbial population and soil-to-water ratio is appropriate for the experiments performed in this study which employed small amounts of acclimated soil.

For the solute naphthalene and the particles used in the experimental portion of this work, the solute residing in the sorbed and aqueous phases can be assumed in equilibrium over the course of the experiment. This assumption was justified because the solid was maintained in gentle suspension, and it was shown that microbial degradation occurred over time periods of days, whereas supplemental experiments and modeling showed that sorption and desorption occurred over a time period of approximately one hour. Thus, the change in average sorbed-phase concentration with time can be related to the aqueous-phase concentration by a partition coefficient:

$$\frac{d\bar{S}}{dt} = K_p\ \rho_s(1 - n)\ \frac{dC}{dt} \qquad [10]$$

where K_p is the partition coefficient, cm^3 liquid/g solid, and n is the intra-aggregate porosity, cm^3 liquid/cm^3 total. Substitution of Equation [10] into Equation [9] and a reduction of terms yields:

$$\frac{dC}{dt} = - \frac{K_{max}\ C}{K_s + C} (1 + \rho\ K_p)^{-1} \qquad [11]$$

Because of the rapidity with which naphthalene may attain sorption and desorption equilibrium in the experiments performed in this study, K_{max} and K_s were estimated from the experimental aqueous-phase concentration versus time data by Equation [11] using the nonlinear parameter estimation program of McCroskey and McRae (1987). This program utilizes principles of Bayes and Maximum Likelihood to fit parameters in both algebraic or differential equation models. This method involved applying the estimation program to Equation [11] using data describing aqueous-phase naphthalene concentration over time. The experimentally determined value of K_p (12 cm^3/g) and the soil-to-water ratios used in a particular experiment were employed for the parameter estimation.

The model described by Equation [9] was used to verify the equilibrium assumption for estimating K_{max} and K_s. Equation [9] was also used for the evaluation of the effect of sorption and desorption kinetics on the microbial degradation for unexplored conditions. The radial diffusion model of Wu (1986) was modified to include the microbial degradation terms included in Equation [9] and is referred to as a coupled solute desorption-degradation model. This numerical model couples a retarded radial diffusion mechanism for sorption and desorption with microbial decay in finite difference form. This model allows the user to easily input known physical, chemical, and biological parameters of the system, The computer code for this program is listed in Appendix C and can be easily modified to describe first-order microbial degradation if required.

6.3. Materials and Methods

The following experiments were conducted with the purpose of examining the effect of the initial nitrate concentration and the soil-to-water ratio on the rate of degradation of PAH compound. For a more detailed description of the experimental procedure and methods of analyses, the reader is referred to Mihelcic and Luthy (1988a, 1988b). For the experiments

described in this chapter, acclimated soil was utilized in order to eliminate the acclimation period. This also served to justify the assumption that C_{max} was neglible for modeling nitrate reduction, and that the bacterial population could be assumed constant over the duration of the experiment for modeling both nitrate reduction and microbial degradation of PAH compound.

6.3.1. Preparation of Acclimated Soil

Acclimated soil was prepared by two separate methods. The first method entailed placement of a saturated naphthalene solution containing mineral medium and buffer solution, and nitrate in a 1-liter glass jar. This mixture was purged with helium gas for one hour and 100 grams of Barnes-Hamerly soil were then added. The system was purged for another one half hour after which the jar was sealed with very little initial headspace. Aluminum foil was place between the seal and the aqueous mixture. The slurry was mixed three hours daily by a magnetic stirrer. Aqueous-phase naphthalene and nitrate concentrations were analyzed periodically by briefly opening the seal and placing a helium purge in the sample while collecting approximately 15 ml of sample. This sampling method typically resulted in the sample being exposed for intervals less than one minute. The soil was considered acclimated when naphthalene had reached nondetectable levels and nitrate concentration had attained a value consistent with that predicted by consideration of the oxidation of naturally occurring soil organic carbon and naphthalene. This process entailed the reduction of several hundred mg/liter nitrate in the system. Aqueous naphthalene concentrations remained constant for approximately 2 weeks after which degradation occurred. The acclimation period was consistent with that which had been observed in previous tests with unacclimated soil.

Acclimated soil was also obtained by reserving soil samples from prior tests in which naphthalene had attained nondetectable levels. This method was the same as employed previously (Miheldic and Luthy, 1988b) for an experiment which studied the acclimation period.

6.3.2. Effect of Nitrate Concentration on the Degradation Rate

Experiments were conducted to assess if the degradation of PAH compound was independent of nitrate concentration. Samples were prepared with initial nitrate concentrations of 35 to 135 mg/liter NO_3^-. All other initial experimental parameters were the same as experiments conducted with 2 grams of soil in previous tests which studied the

microbial degradation of PAH compounds under nitrate-excess and nitrate-limiting conditions (Mihelcic and Luthy, 1988b). Aqueous-phase naphthalene and nitrate concentrations were monitored over time as previously reported (Mihelcic and Luthy, 1988a).

6.3.3. Effect of Soil-to-Water Ratio on the Degradation Rate

Experiments were conducted with soil-to-water ratios of approximately 1, 2, and 5 grams per 50-ml centrifuge tube in order to examine the proportionality of the maximum rate, K_{max}, with respect to the mass of acclimated soil. The mass of soil was taken to be proportional to the initial concentration of active PAH-degrading bacteria. All other initial experimental parameters were the same as experiments conducted previously and the aqueous PAH compound and nitrate concentrations were monitored over time as previously reported (Mihelcic and Luthy, 1988a, 1988b).

6.4. Results

Six individual tests were performed which examined the degradation of the solute naphthalene over time. Three of the tests used acclimated soil obtained from a single large batch of soil which had been exposed to naphthalene, whereas three of the tests used acclimated soil obtained from samples reserved from prior tests after nondetectable levels of naphthalene had been attained. Both, blanks containing no soil, and controls which contained sterilized soil, remained constant over the duration of the tests. The experimental data are presented in Appendix D.

6.4.1. Naphthalene Biodegradation

The results of biokinetic parameter estimation for experimental data obtained from various tests which were conducted over a time period of 9 months are shown in Table 6-2. Shown in the table are the maximum rates and half-saturation coefficients along with the initial conditions of the experiments. The goodness-of-fit of the parameter estimate was judged by inspection of the model prediction versus experimental data, and by the standard deviation of the residuals between the measured and predicted responses which were 0.36, 0.074, 0.016, 0.68, 0.51, and 0.29 for Experiments 1 to 6, respectively.

The estimation of the parameters K_{max} and K_s, by the estimation program, employed all data having values above the detection level of 0.01 mg/liter, as well as the first nondetectable

data point which was taken as 0.10 mg/liter. Sensitivity analysis was performed to examine what effect decreasing the time of occurrence of the nondetectable point would have on the estimation of the two parameters. This was performed by varying the time for the first measured nondetectable concentration to the time of the lowest detectable concentration.

For data of Experiment 6 (Figure 6-7) the nondetectable point was changed from 19 to 17 days. This caused K_{max} to increase from 0.83 to 0.85 mg/liter-day while K_s remained at 0.54 mg/liter. Likewise in Experiment 3 (Figure 6-2), the time of occurrence of the nondetectable point was changed from 18 to 17 and 16 days. This caused K_{max} to change from 0.75 to 0.74 and 0.74 mg/liter-day, respectively, whereas K_s remained at 1.0 mg/liter. This slight change in the estimated parameters did not affect the error residual in the parameter estimation program between the predicted model response and the experimental data. Experiments 1, 2, and 4 (Figures 6-3, 6-4, and 6-5, respectively) would show similar insensitivity to the placement in time of the nondetectable level point since these curves show a similar set of experimental data where the aqueous concentration data points span two orders of magnitude.

The parameters for Experiment 5 (Figure 6-6), however were fit from five experimental data points, four of which had an aqueous concentration greater of 1 mg/liter, and one which was nondetectable. Sensitivity analysis on the parameters estimated for this experiment showed that as the time of nondetection decreased from 23 to 22, 20, and 18 days, K_{max} decreased from 0.35 to 0.34, 0.32, and 0.32 mg/liter-day, respectively, while K_s decreased from 0.36 to 0.24, 0.16, and 0.10 mg/liter, respectively. This was an unexpected occurrence since the decrease in the time of nondetection was expected to slightly increase K_{max} or K_s. However, the small difference in the range of the predicted parameters for the 5 day time increment was only 0.32 to 0.34 mg/liter-day for K_{max} and 0.10 to 0.36 mg/liter for K_s. From this work, it was concluded that the parameters K_{max} and K_s were insensitive to the time of measurement of the first nondetectable point, especially for the situations in which the aqueous concentration experimental data spanned about two orders of magnitude.

The results in Table 6-2 support the conclusion from data in the literature that the reaction rate is independent of nitrate concentration for nitrate concentrations greater than several milligrams per liter. Initial nitrate concentration was varied by a factor of approximately three and one half, from 37 to 135 mg/liter, for experiments 1, 4, 5, and 6, yet the maximum rate normalized to account for the amount of soil (K'_{max}) remained relatively constant in the

range of 7.9 to 9.75 mg/g-liter. Tests 2 and 3 show values of K'_{max} that are outside this range, but the values vary inversely with respect to nitrate. For this reason it was judged that the variation is not attributable to nitrate-dependent microbial kinetics. The half-saturation coefficient, K_s, remained constant over the range of tests except for Experiment 3, for which the variation may be a result of the experiment being conducted approximately 7 months prior to the other five experiments. For all six tests, the average value of K_s was found to be 0.48 mg/liter with a standard deviation of 0.28 mg/liter. If the samples reserved from the large batch acclimation procedure are considered, the average K_s was equal to 0.37 mg/liter with a standard deviation of 0.17 mg/liter. This average value agrees with the result from Experiment 1 for which it was estimated that there was 100 percent mineralization of naphthalene.

The parameter K'_{max} was obtained by dividing the maximum rate by the soil-to-water ratio of a 50-ml centrifuge tube. The average value of K'_{max} for all six samples was found to be 9.8×10^{-3} mg/g-day with a standard deviation of 4.8×10^{-3} mg/g-day. If only the three samples prepared from the large batch of acclimated soil are used, the average value of K'_{max} was 8.8×10^{-3} mg/g-day with a standard deviation of 0.95×10^{-3} mg/g-day. This average value also agrees with the result from Experiment 1 for which it was estimated that there was 100 percent mineralization of naphthalene. As hypothesized, K_{max} was found to be dependent on the initial amount of acclimated soil originally placed within the experimental system. This result agrees with the work of Paris et al. (1981).

An estimate of the percent naphthalene mineralized is also presented in Table 6-2. The estimation procedure (Mihelcic and Luthy, 1988b) is based on the amount of nitrate reduced over the course of an experiment. It was estimated that the extent of naphthalene mineralization ranged from 55 to 100 percent assuming that degraded naphthalene is mineralized to carbon dioxide and water.

Verification of the rapid desorption kinetic assumption inherent to Equation [11] was performed by comparing the predicted results from the models expressed by Equations [9] and [11]. This comparison is presented in Table 6-3. These results were obtained from input parameters obtained from Experiment 2 which utilized 5.2789 grams of soil per 50-ml centrifuge tube for a soil suspension having a mean volumetric radius of 17.5 μm. Table 6-3 shows that the solutions to both approaches are essentially identical. This is a result of the rate of intraparticle diffusion being rapid compared to the kinetics of microbial degradation for the soil used in these tests. The conceptual desorption-degradation model developed from

Table 6-2: Experimentally determined biokinetic coefficients and initial conditions for modeling the microbial degradation of naphthalene under denitrification conditions.

Experiment	% Mineralized[d]	Grams of Soil	K_{max} mg/l-d	K'_{max}[e] mg/g-d	K_s mg/l	C_i[f] mg/l	N_i[g] mg/l
1[a]	100	1.1104	0.20	9.00	0.33	2	134
2[a]		5.2789	0.47	4.48	0.40	2	135
3[b]	93	2.0000	0.75	18.8	1.0	3.1	35
4[c]	55	2.0000	0.39	9.75	0.20	5.6	37
5[c]	100	2.0000	0.35	8.75	0.36	4.0	50
6[c]	100	5.2789	0.83	7.90	0.54	3.6	37

a - experiments conducted with soil samples reserved from previous experiments which examined the microbial degradation of naphthalene

b - experimental results from Chapter 4, Figure 10

c - tests employed from a single large batch of acclimated soil

d - estimation of the percent of total naphthalene mineralized

e - K'_{max} is K_{max} normalized for the soil-to-water ratio

f - C_i is the aqueous naphthalene concentration after one day sorption equilibrium

g - N_i reported as mg NO_3^-/liter

Equation [9] was used later for comparison of model predictions to actual experimental data since it allowed the user to incorporate the particle size into the model for comparison later with simulations of unexplored conditions.

Figures 6-2 to 6-7 compare actual data to the model predictions described by the coupled desorption-degradation model of Equation [9] for Experiments 1 through 6, respectively, for examination of the microbial degradation of naphthalene in systems containing acclimated Barnes-Hamerly soil. Initial soil-to-water ratios were 0.04, 0.0222, 0.105, 0.04, 0.04, and 0.105 g/ml, respectively. It is seen that the model predictions agree closely to the experimental data for all six tests. In these figures, ND represents an analytical determination which was less than the detection limit of 0.01 mg/liter (7.81×10^{-11} mol/ml for naphthalene). Each data point represents the determination from one or two individual samples which were discarded after sample analyses.

The predicted results in Figures 6-2 to 6-7 were generated by use of the kinetic parameters for naphthalene biodegradation and known physical and chemical parameters of the solute and the soil with the coupled desorption-degradation model, described by Equation [9]. This prediction combines naphthalene desorption kinetics and Monod microbial degradation kinetics to describe naphthalene depletion from the aqueous phase. A mean volumetric particle radius of 17.5 μm was used in the calculations as obtained from particle size analyses described in Chapter 5. The partition coefficient, K_p, was taken to be 12 cm^3/g as measured experimentally (Mihelcic and Luthy, 1988b). An intra-aggregate porosity of 0.13 was used, as obtained by Wu and Gschwend (1986). These authors obtained this value by averaging fitted values of intra-aggregate porosities obtained from three different types of sediments and four solutes when analyzing the sorption and desorption of chlorinated benzene compounds with sediments. This value was confirmed to some extent by the authors fitting their model to another researcher's experimental data. The molecular diffusivity for naphthalene in water at a temperature of 25 °C was estimated to be 7.24×10^{-6} cm^2/sec by the Hayduk and Minhaus correlation from the solute's molar volume and solvent viscosity (Hayduk and Minhaus, 1982) as recommended by Reid et al. (1987). In any event, as shown in Table 5-1 and Table 6-3, the experimental data already demonstrate that the rate of microbial degradation was not affected by the rates of sorption and desorption for the soil-water suspensions employed in this investigation.

The results shown in Figures 6-5 to 6-7 were obtained from experiments initiated from a

Table 6-3: Comparison of the instantaneous desorption equilibrium assumption and the coupled desorption-degradation model for an experimental soil-water suspension.

The aqueous-phase concentrations are expressed as x 10^{-6} mol/ml.

Time (days)	Coupled Desorption-Degradation. Equation [9]	Instantaneous Desorption Equilibrium. Equation [11]
1	1.56	1.56
2	1.42	1.40
3	1.29	1.27
4	1.16	1.14
5	1.04	1.02
6	0.912	0.893
7	0.793	0.775
8	0.679	0.661
9	0.570	0.554
10	0.468	0.453
11	0.374	0.361
12	0.290	0.278
13	0.216	0.206
14	0.155	0.147
15	0.107	0.100
16	0.0704	0.0660
17	0.0448	0.0418
18	0.0277	0.0257
19	0.0168	0.0156
20	0.0100	0.00927
21	0.00592	0.00548
22	0.00348	0.00322
23	0.00204	0.00189
24	0.00119	0.00100

Figure 6-2: Predicted model response versus experimental data from experiment no. 3 for naphthalene degradation.

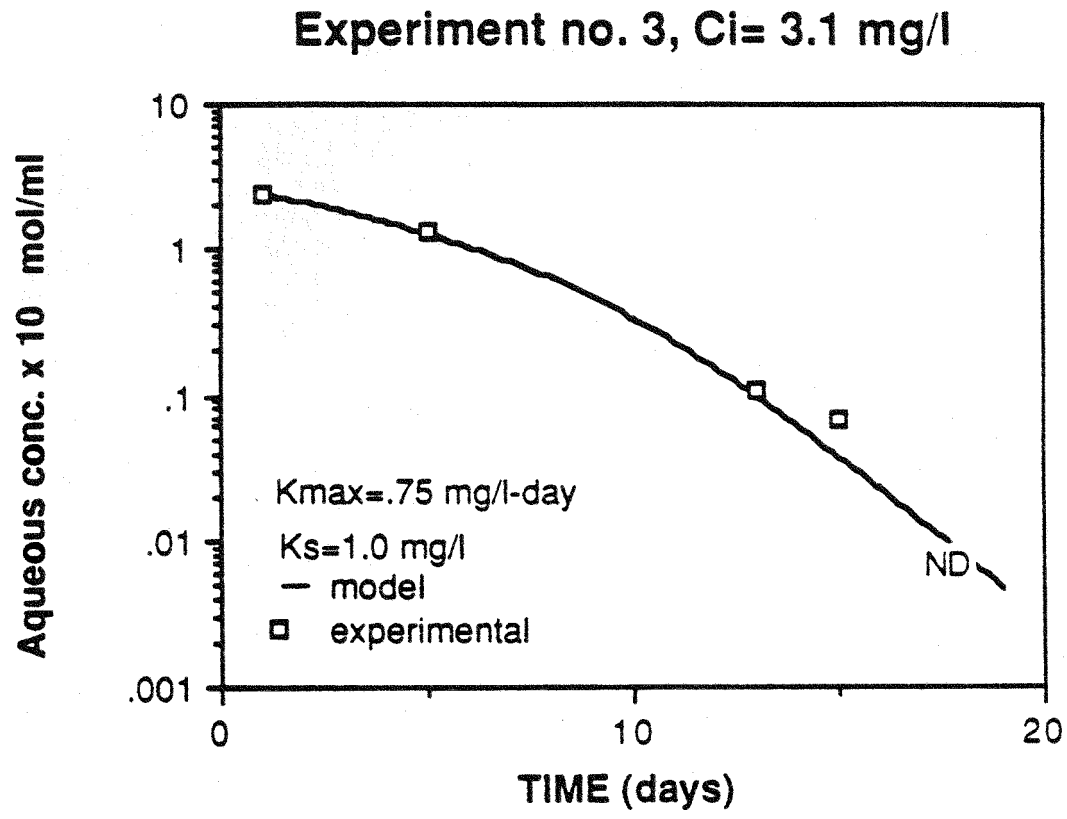

Figure 6-3: Predicted model response versus experimental data from experiment no. 1 for naphthalene degradation.

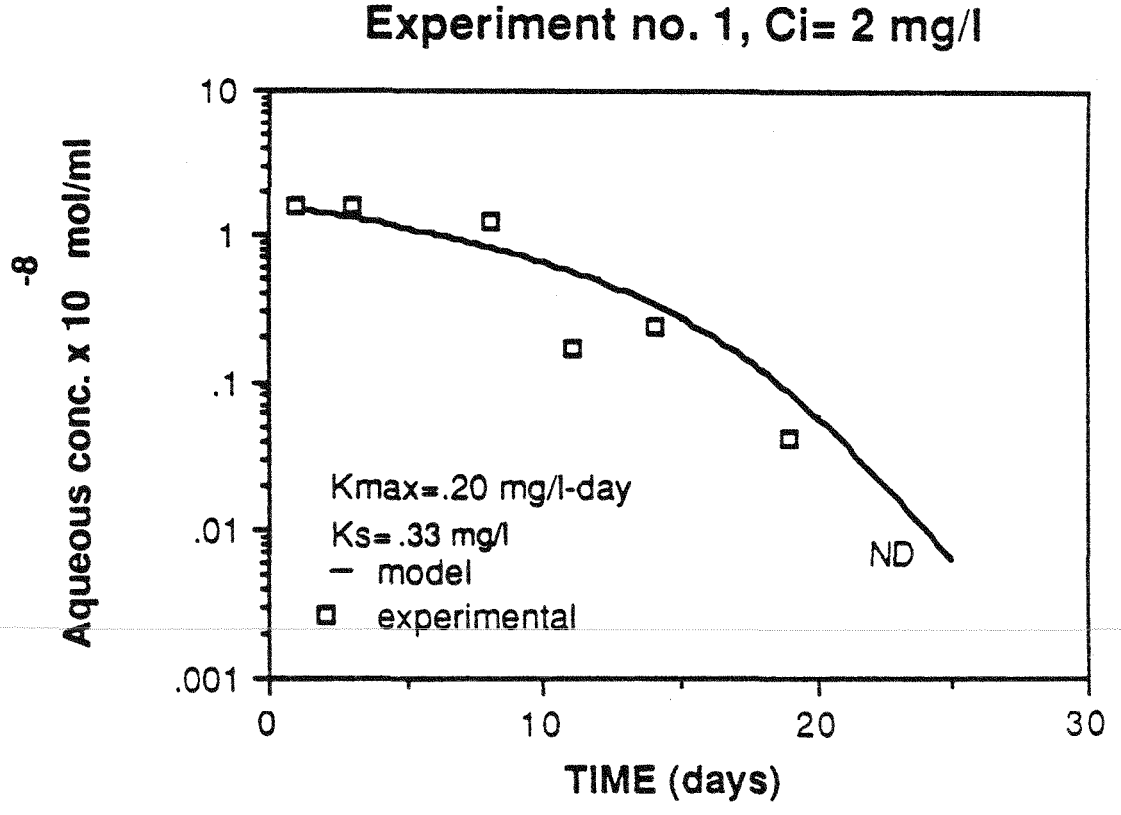

Figure 6-4: Predicted model response versus experimental data from experiment no. 2 for naphthalene degradation.

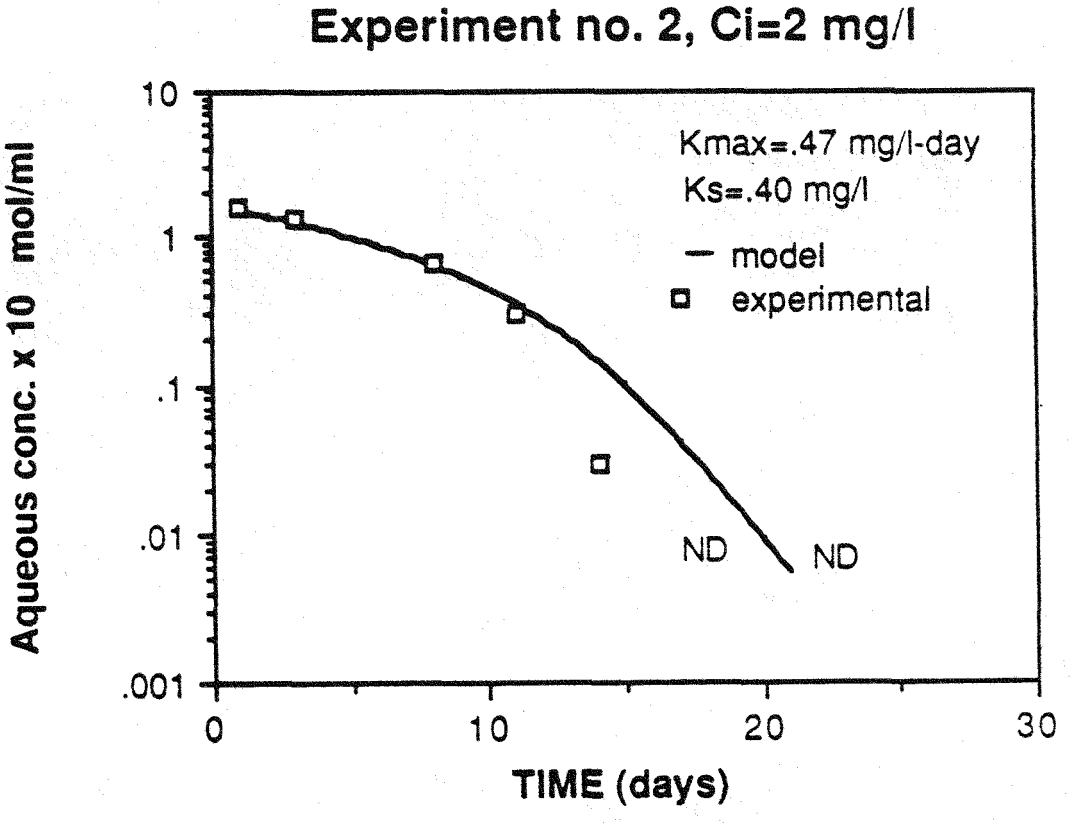

Figure 6-5: Predicted model response versus experimental data from experiment no. 4 for naphthalene degradation.

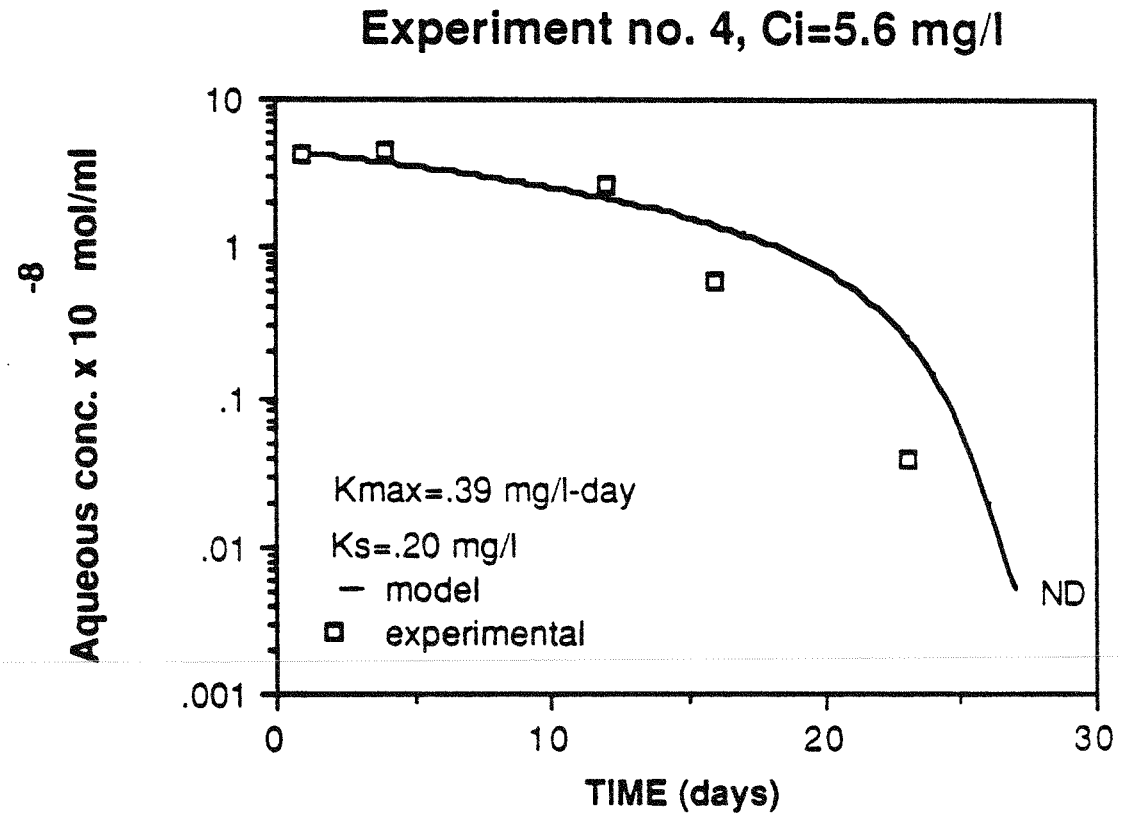

Figure 6-6: Predicted model response versus experimental data from experiment no. 5 for naphthalene degradation.

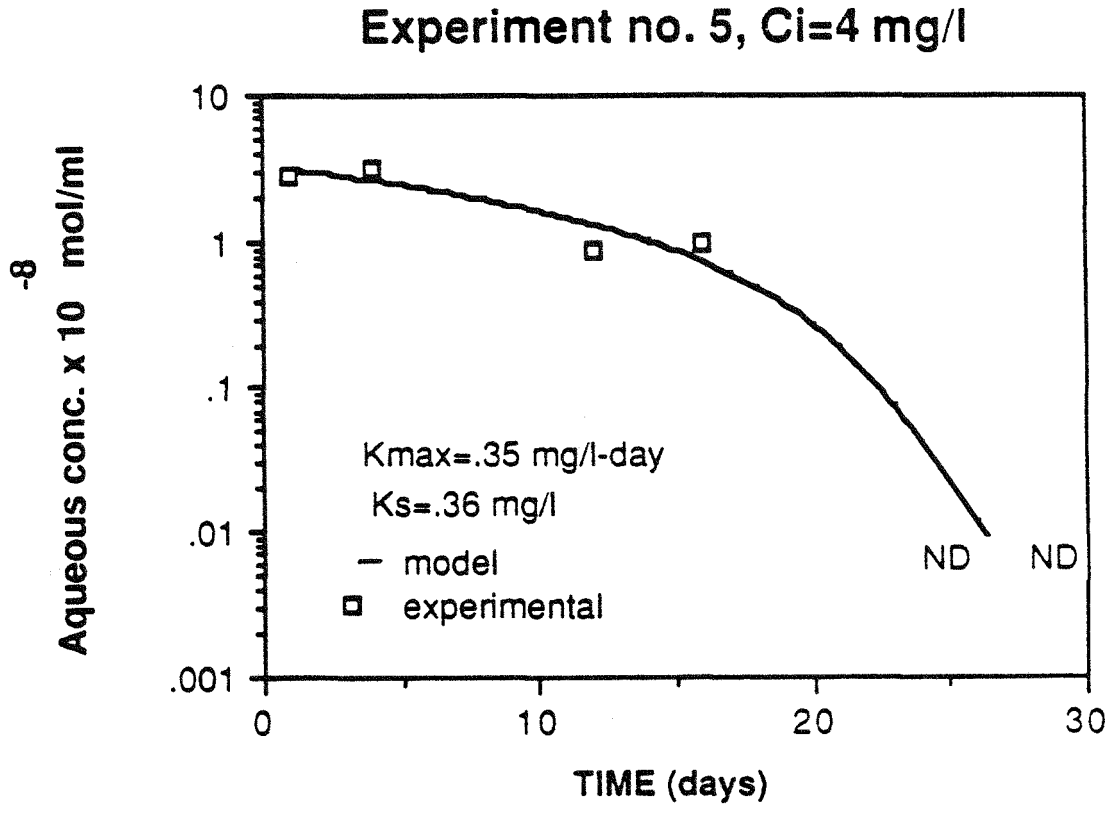

Figure 6-7: Predicted model response versus experimental data from experiment no. 6 for naphthalene degradation.

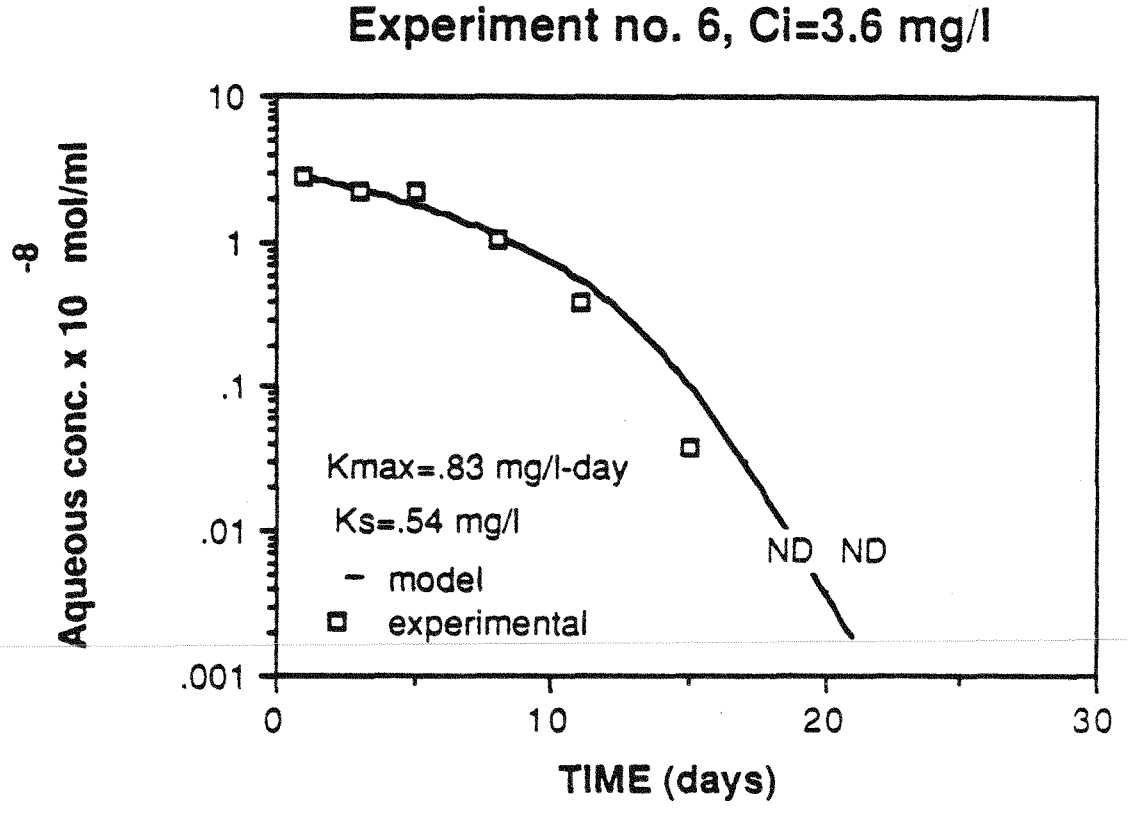

large batch of acclimated soil. The maximum rates in Figures 6-5 and 6-6, with 2 grams of soil, were 0.39 and 0.35 mg/liter-day, respectively, whereas the maximum rate in Figure 6-7 for a system with 5.2789 grams of soil was 0.83 mg/liter-day. It may be expected that the system with 5.2789 grams of soil would have a maximum rate of 2.6 times greater than the system with 2 grams of soil since it was hypothesized that the maximum rate was a function of the initial active cell population. In fact, the estimated maximum rate was approximately 2.2 times greater in the system with 5.2789 grams of soil compared to the system with 2 grams of soil. This does not imply that the time required to attain nondetectable aqueous-phase concentration would be more than twice as rapid for tests with 5.2789 grams of soil versus 2 grams of soil. In the comparison of Figure 6-7 with Figures 6-5 and 6-6, which had similar initial aqueous naphthalene concentrations after sorption equilibrium was attained between the aqueous and solid phases, one notices that Experiment 6 did not reach nondetectable levels 2.2 times faster than Experiment 4 and 5. In fact, the rate was only slightly more rapid as nondetectable levels were reached in 28 and 23 days, respectively for Experiments 4 and 5, and 19 days for Experiment 6. The similarity in these results is a consequence of the mass of solute associated with the solid phase. Measured initial aqueous-phase mass of solute was approximately 2.2, 1.6, and 1.4 x 10^{-6} mol for Experiments 4, 5, and 6 respectively while the estimated mass in the sorbed phase was 1.0, 0.75, and 1.8 x 10^{-6} mol, respectively. Thus it is seen that the test with 5.2789 grams of soil had a greater amount of naphthalene sorbed to the solid phase and that desorption of naphthalene to the aqueous phase prolonged the time to deplete naphthalene to nondetectable levels than may otherwise be anticipated for a system for which there was no desorption effect.

6.4.2. Nitrate Reduction

The purpose of developing the following model was to estimate the initial nitrate reduction associated with microbial degradation of PAH compounds under denitrification conditions. Acclimated soil was utilized in the experiments reported in this chapter and thus the nitrate demand associated with the naturally occurring soil organic carbon may be assumed neglible relative to the demand from the PAH compound so that Equation [7] can be written as:

$$dN/dt = - k_N C \qquad [12]$$

The majority of the nitrate was depleted during the period in which the rate of

naphthalene biodegradation was in the zero-order region with respect to naphthalene concentration. For this reason these data were used for estimating the rate of nitrate depletion. Also, as the naphthalene concentration was degraded to near nondetectable levels, the nitrate concentration would sometimes fluctuate, rather than demonstrate a consistent trend and for this reason as well, the reduction of nitrate was described by the initial rate data. If the aqueous-phase organic substrate concentration, C, is in the zero-order kinetic range, the equation describing aqueous-phase substrate depletion over time, Equation [11] can be integrated to obtain:

$$C = C_o - \frac{K_{max}\, t}{1 + \rho\ K_p} \qquad [13]$$

Equation [13] can be substituted into Equation [12] with the following limits to obtain:

$$\int_{N_o}^{N} dN = -\int_0^t k_N\ [C_o - \frac{K_{max}}{1 + \rho K_p}\ t]\ dt \qquad [14]$$

where N is the nitrate concentration, mol NO_3^-/liter, N_o is the initial nitrate concentration, mol NO_3^-/liter, and C_o is the initial aqueous naphthalene concentration, mol naphthalene/liter. Integration of Equation [14] yields:

$$N = N_o - k_N\ [C_o t - 1/2\{\ \frac{K_{max}}{1 + \rho K_p}\ t^2\}] \qquad [15]$$

Equation [15] is expressed in linearized form, so that k_N can be found by plotting N versus $[C_o t - 1/2\{K_{max}/(1+\rho K_p)\}t^2]$.

Graphical estimation of k_N for Experiments 1, 2, 4, 5, and 6 is shown in Figures 6-8 a, b, c, d, and e, respectively, along with the regression equation and a statistical measure of the goodness-of-fit. These five experiments were selected for model evaluation as they were run at a similar time. Results from Experiment 3 were not used for analysis of the estimation of the kinetics of nitrate reduction as this test was conducted almost seven months prior to the other five experiments. Table 6-4 shows estimated values of k_N, and estimated values of the rate coefficient normalized for the soil-to-water ratio used in the tests, as well as initial test conditions.

Considering all five tests, and adjusting for the soil-to-water ratio of the test, the average value of k_N' was 80 mol nitrate-ml/mol naphthalene-day-g with a standard deviation of 38. If only the three samples prepared from a large batch of acclimated soil were compared, the average value of k_N' was was 53 mol nitrate-ml/mol naphthalene-day-g with a standard

Figure 6-8: Graphical estimation of the biokinetic parameter, k_N, to describe nitrate reduction in soil-water suspensions.

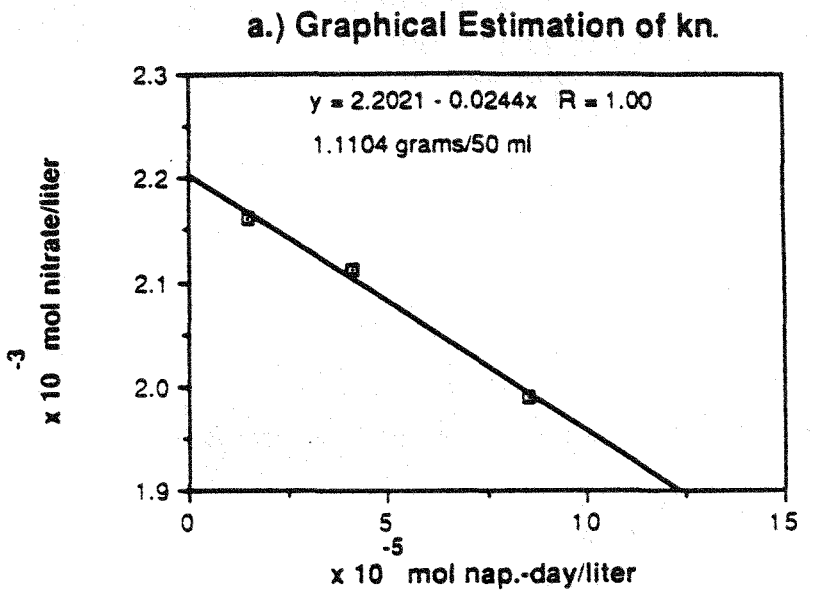

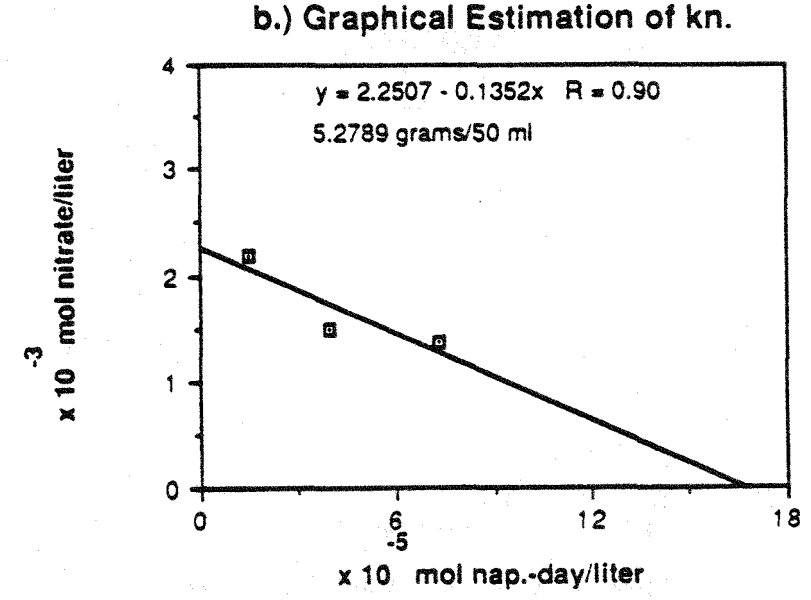

c.) Graphical Estimation of kn.

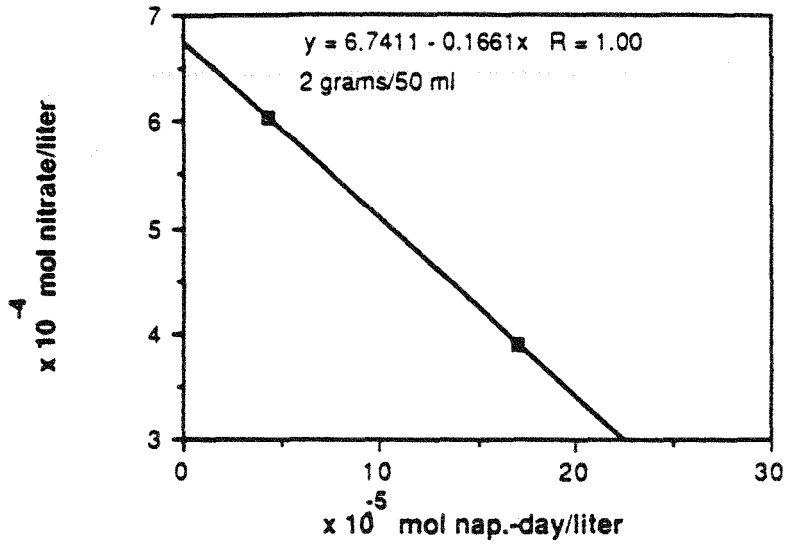

d.) Graphical Estimation of kn.

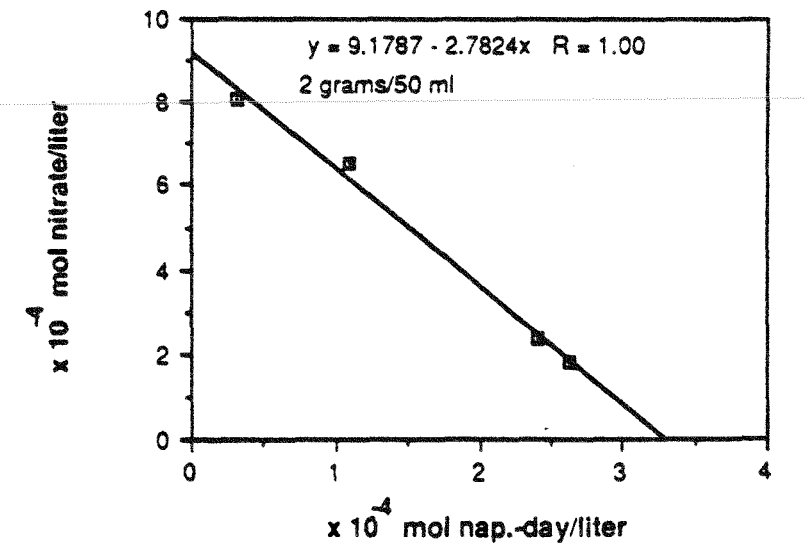

e.) Graphical Estimation of kn.

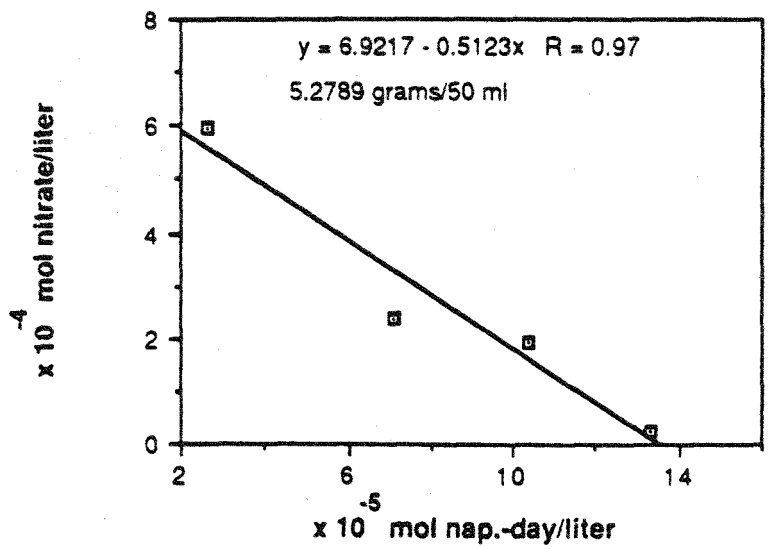

Table 6-4: Biokinetic parameters for nitrate reduction for various experiments.

The parameters and corresponding units are:

k_N: mol nitrate per mol of naphthalene-day,

k_N': mol nitrate-ml per mol naphthalene-day-g,

$C_{initial}$: mg per liter,

$N_{initial}$: mg nitrate per liter.

Experiment	soil-to-water ratio (g/ml)	k_N	k_N'	$C_{initial}$	$N_{initial}$
1	0.0222	2.44	110	2	134
2	0.105	13.5	128	2	135
4	0.040	1.66	41.5	5.6	37
5	0.040	2.78	69.5	4.0	50
6	0.105	5.12	48.8	3.6	37

deviation of 14.5. k_N' was expected to be a function of the soil-to-water ratio employed in the 50-ml centrifuge tube since, as in the modeling of PAH degradation with acclimated soil, the rate of nitrate reduction was hypothesized to be a function of the size of the active denitrifying population, which was proportional to the soil-to-water ratio. The results show that k_N' was independent of nitrate concentration as shown in the comparison of Experiments 4 and 5 which were conducted under similar initial conditions but with different initial nitrate concentrations.

Comparison of results of actual nitrate data and the model prediction are shown in Figures 6-9 a, b, c, d, and e which correspond to naphthalene degradation of Experiments 1, 2, 4, 5, and 6, respectively. It is seen that in general the model prediction describes the experimental data as in Experiments 5 and 6. The estimation procedure did not describe the nitrate data after a time period of approximately 10 days for Experiments 1, 2, and 4 owing to the scatter of the nitrate data. The nitrate demand which is associated with the zero-order range of naphthalene degradation could be modeled by the approach expressed by Equation [15] as shown in Experiments 5 and 6, and this is the interval over which the greatest nitrate demand occurred. This provides an estimate of the total nitrate demand due to naphthalene degradation.

6.5. Simulation of the Microbial Degradation of PAH in Soil-Water Suspensions using the Coupled Desorption-Degradation Model

This section employs the coupled solute desorption-degradation model to examine the effect of particle size and the amount of acclimated soil on the degradation of PAH in simulated experimental soil-water suspensions. Also examined were situations in which three PAH compounds of various hydrophobicity were added to a soil-water system and the aqueous- and sorbed-phase concentrations were modeled over time. The simulation approach incorporates a Monod biodegradation kinetic model with a radial diffusion solute sorption-desorption model, as was developed from Equation [9].

The purpose of the following simulations was to obtain preliminary insights into the manner in which PAH solute interactions with soil may influence the bio-availability of solute to an active microorganism population. For this purpose it was assumed that irregular-shaped soil particles may be represented as spherical aggregates with the interaction of solute and soil being described by a radial diffusion model. This discussion develops the principal

Figure 6-9: Predicted model responses versus experimental data for the nitrate reduction associated with the microbial degradation of PAH.

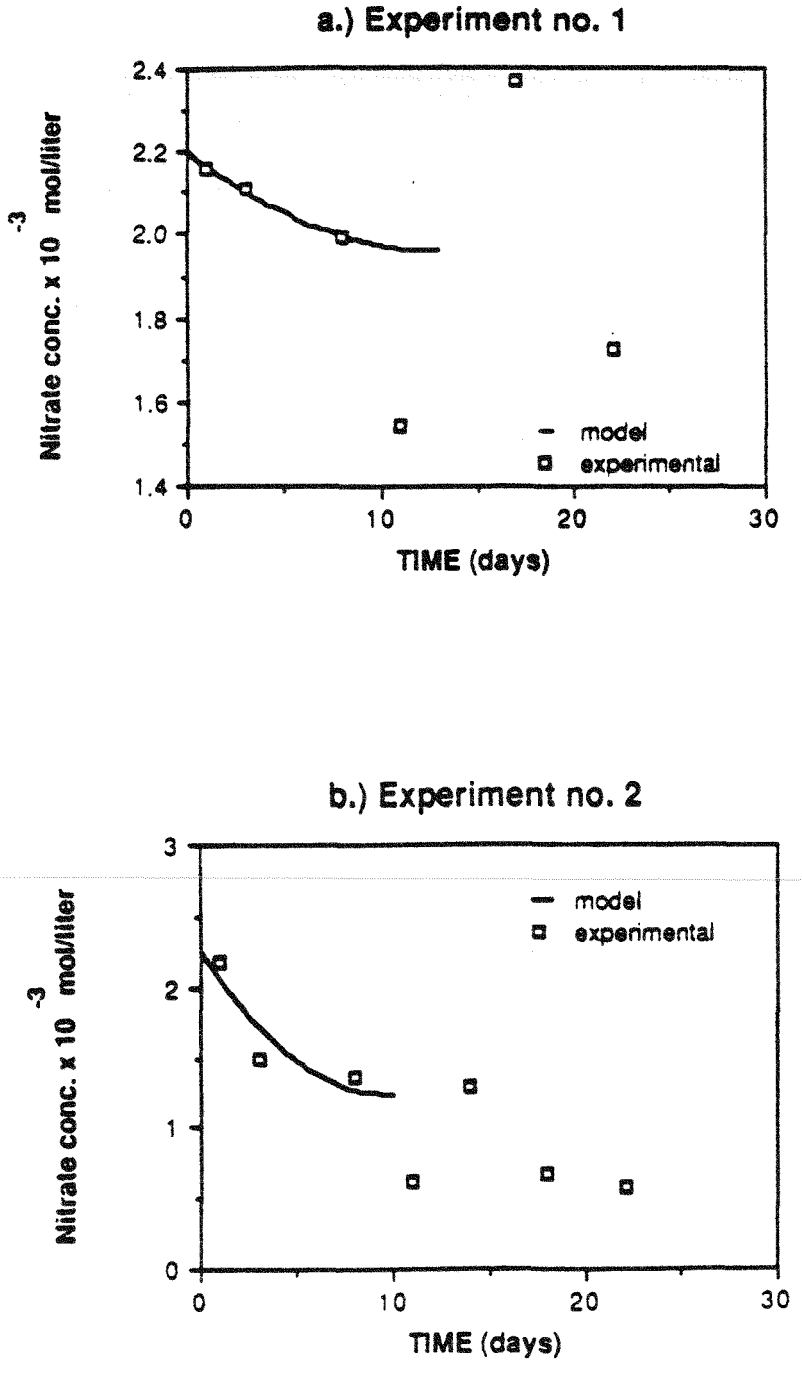

c.) Experiment no. 4

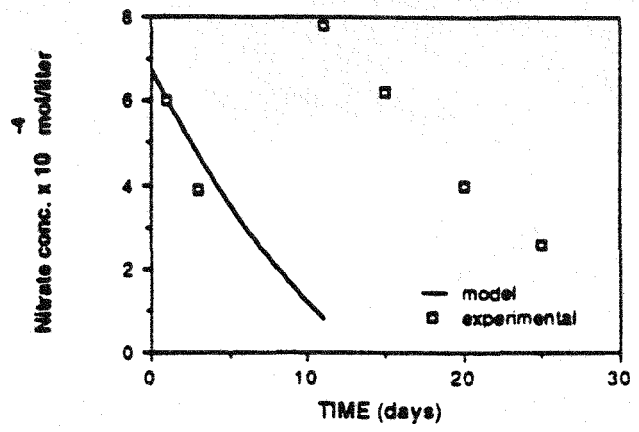

d.) Experiment no. 5

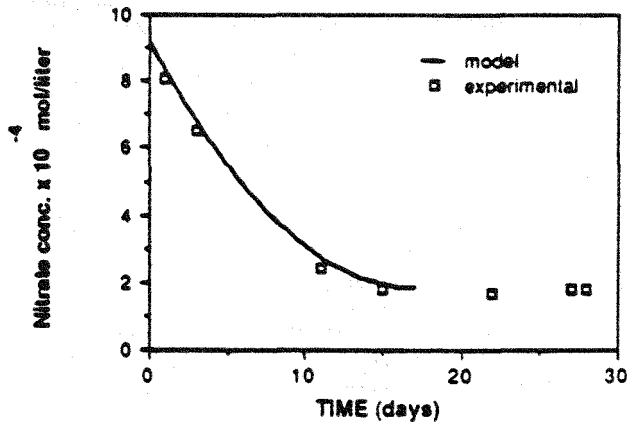

e.) Experiment no. 6

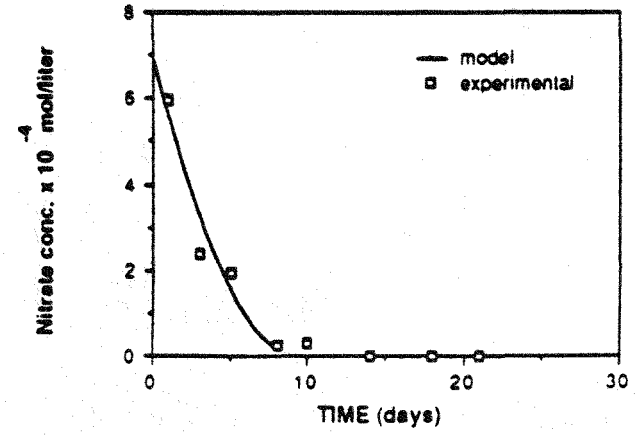

concept referred to in the model development, i.e., that the amount of sorbed PAH influences the microbial degradation of hydrophobic organic compounds. This effect may be evident in both laboratory experiments and field tests depending on the influence which the soil particle size may have on microbial degradation of hydrophobic organic contaminants in a soil-water suspensions.

Input parameters for the model were the soil specific gravity, ρ_s = 2.5 g/cm^3 for experimental systems, and ρ_s = 2.6 g/cm^3 for the case of comparison among different solutes, and an intra-aggregate porosity of n = 0.13 for all cases. The partition coefficient, K_p, was taken as either the experimentally determined value for naphthalene, K_p = 12 cm^3/g, or for the case for comparison among different solutes, the relationship of Schwarzenbach and Westall (1981), i.e., log K_{oc} = log K_{ow} - 0.21. The organic fraction of the soil, f_{oc}, was taken as 0.029, as determined in previous experiments (Mihelcic and Luthy, 1988b). Molecular diffusivities were estimated to be 7.24, 5.45, and 3.88 x 10^{-6} cm^2/sec for the solutes naphthalene, anthracene, and benzo(*a*)pyrene, respectively. Log K_{ow} was 3.36, 4.54, and 6.50 for the solutes naphthalene, anthracene, and benzo(*a*)pyrene, respectively (from table in Walters and Luthy, 1984). The solids concentration was taken to vary from 0.01 to 0.20 gram per ml for simulation of unexplored conditions, and 1 gram per ml for simulation of conditions for comparison among various solutes.

6.5.1. Simulation of naphthalene degradation with various amounts of soil and different mean volumetric radii

Figure 6-10 depicts a system in which the initial equilibrated aqueous naphthalene concentration was 3.0 mg/liter and the soil-to-water ratio was 0.020 and 0.10 g/ml. Input parameters were a mean volumetric radius of 1.75 x 10^{-3} cm (10 grids), K_p = 12 cm^3/g, K'_{max} = 8.80 x 10^{-3} mg/g-day, K_s = 0.37 mg/liter, and a time step of 180 minutes. It is seen that the aqueous-phase concentration in the system with a soil-to-water ratio of 0.10 g/ml decreased at a faster rate when compared to the system with a soil-to-water ratio of 0.020 g/ml. This is a result of the system with solids concentration of 0.10 g/ml assumed to have a five times larger initial active biomass concentration, and thus a maximum rate 5 times greater than the system with a solids concentration of 0.020 g/ml. The system with a solids concentration of 0.10 g/ml showed sorbed-phase concentration decreasing from 2.81 x 10^{-7} to 1.96 x 10^{-11} mol/g in 16 days.

Figure 6-10: Model simulations of naphthalene degradation with soil-to-water ratios of 0.020 and 0.10 g/ml and equal initial aqueous concentrations.

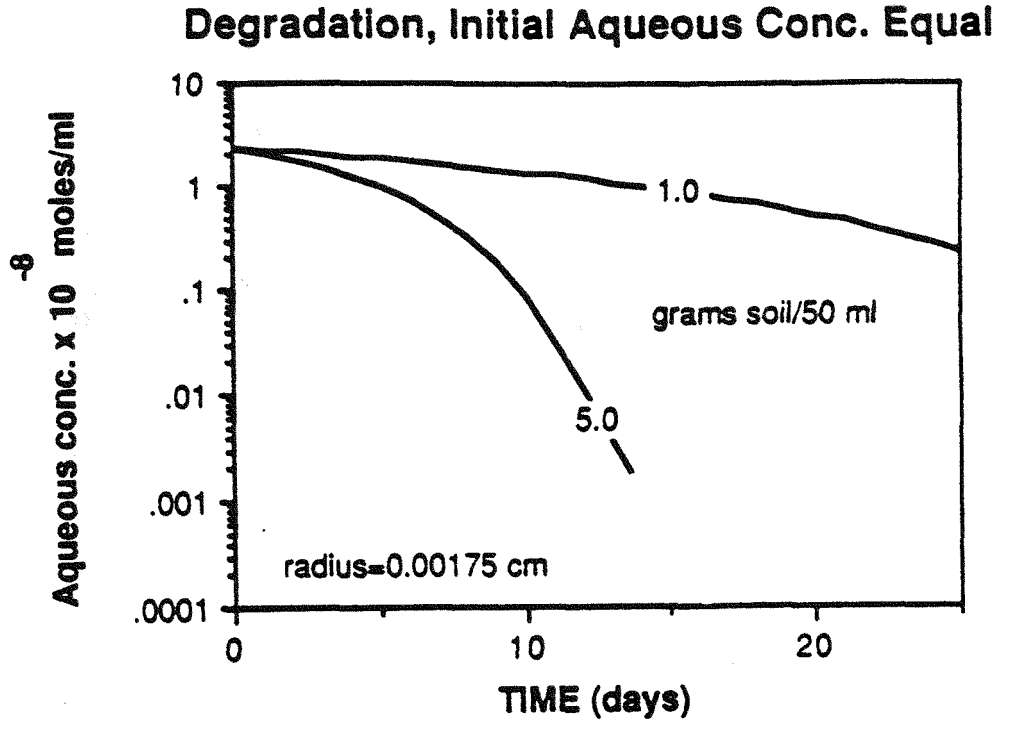

It is intended that the modeling results may be appropriate for aqueous-phase concentrations in the range of several mg/liter to levels of about 0.01 mg/liter and less, as this encompasses the range over which the experimental data were collected. It is not appropriate to extend the modeling evaluations to very low levels of aqueous-phase solute concentration as this was beyond the range for which the biokinetic data were obtained.

Figure 6-11 simulates systems for which the initial total mass of naphthalene was equal but the solids concentration was 0.010, 0.10, and 0.20 g/ml. The mean volumetric radius was set at 17.5 μm (17 grids). The system with a solids concentration of 0.20 g/ml showed a much faster approach to low levels of solute remaining in the system compared to the systems with 0.010 and 0.10 g/ml. At a time of 9 days the system with 0.20 gram of soil per ml had 3.18×10^{-10} mol in the aqueous phase and 1.87×10^{-9} mol in the solid phase. At 9 days the system with 0.10 gram of soil per ml had 2.37×10^{-7} mol in the sorbed phase, and 1.72×10^{-7} mol in the aqueous phase, while the system with 0.010 gram of soil per ml had 2.3×10^{-6} mol in the aqueous phase and 2.8×10^{-7} mol in the sorbed phase. The aqueous-phase concentrations at 9 days were 4.64×10^{-8} (5.9), 3.45×10^{-9} (0.44), and 6.36×10^{-12} (0.001) mol/ml (mg/liter) for the systems with a solids concentration of 0.010, 0.10, and 0.20 g/ml.

As in Figure 6-10, the system with greater amount of soil is predicted to attain a faster approach to solute removal. In these situations solute desorption is not rate limiting as indicated by the much lower mass of solute in both the aqueous and sorbed phase in the system with 0.20 gram of soil per ml versus the systems with 0.10 and 0.010 gram of soil per ml. If desorption was very slow, the system with 0.20 gram of soil per ml would have a much larger mass of solute associated with the soil and much less solute in the aqueous phase.

Figures 6-12a and b present model results for total naphthalene versus time for suspensions of 0.020 and 0.10 gram of soil per ml and particle radius of 0.175 and 1.75 cm (17 grids), respectively. Figure 6-12a shows that the system with 0.10 gram of soil per ml initially has a faster rate of degradation compared with the system with 0.020 gram of soil per ml. However at approximately 40 days the system with 0.020 gram of soil per ml begins to exhibit a faster rate of degradation. This can be explained by the respective aqueous- and sorbed-phase naphthalene concentrations in each system. At 41 days, the system with 0.10 gram of soil per ml has an aqueous-phase concentration of 7.76×10^{-12} mol/ml (0.001 mg/liter) and a sorbed-phase concentration of 1.98×10^{-9} mol/g, whereas the system with 0.020 gram of soil per ml has an aqueous- and sorbed-phase concentrations of 6.08×10^{-9}

Figure 6-11: Model simulations of the effect of the soil-to-water ratio on microbial degradation of naphthalene with equal amounts of initial solute mass.

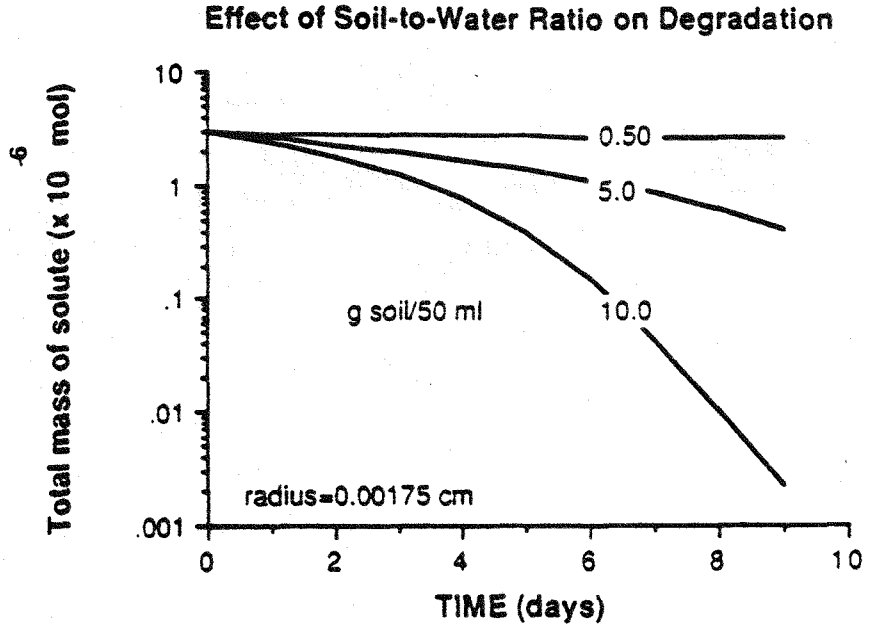

Figure 6-12: Model simulations of the effect of particle radius on naphthalene degradation for two values of soil-to-water ratios.

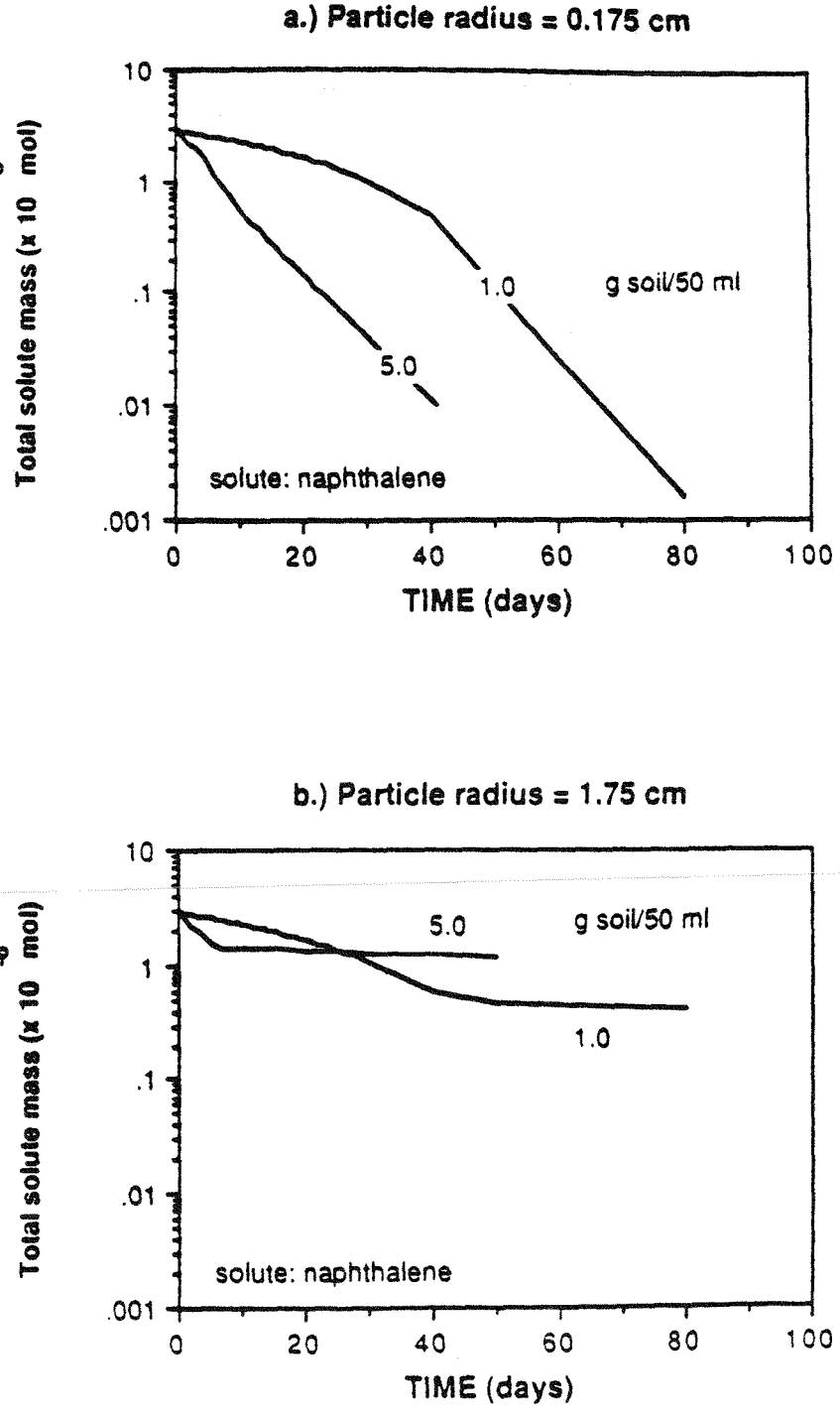

mol/ml (0.78 mg/liter) and 1.26 x 10^{-7} mol/g, respectively. Much of the total initial mass of the system with a soil-to-water ratio of 0.10 g/ml has been removed from the system, and the aqueous-phase concentration is sufficiently low so that the rate of degradation is essentially arrested.

However in Figure 6-12b it is seen that by increasing the mean volumetric particle radius 10-fold to 1.75 cm, the comparative rates of degradation are quite different in contrast with those in Figures 6-12a. At 41 days the system with 0.10 gram of soil per ml had an aqueous-phase concentration of 2.58 x 10^{-11} mol/ml (0.003 mg/liter) and a sorbed-phase concentration of 2.43 x 10^{-7} mol/g, whereas the system with 0.020 gram of soil per ml had aqueous- and sorbed-phase concentrations of 1.84 x 10^{-9} mol/ml (0.24 mg/liter) and 4.67 x 10^{-7} mol/g, respectively. The time at which the rate of solute removal becomes relatively similar corresponds to the situation in which the majority of the solute mass is associated with the slowly desorbing solute. Thus in the system with the larger mean volumetric radius, more solute persists in the system due to the slower desorption process of a system with larger particle size.

Figure 6-12 illustrates the effect which the mean volumetric particle radius can have on the microbial degradation rate by causing a change in the rate-controlling step. As the rate of solute desorption becomes the rate-controlling process, the rate of the reaction will become independent of the active microorganism population as indicated by the similar slopes of the depletion curves for both systems.

Figure 6-13 shows the change in aqueous-phase concentration for microbial degradation of naphthalene with mean volumetric particle radii of 0.00175, 0.0175, 0.175, and 1.75 cm. The radii were divided into 10 grids for the modeling and the time step was selected as 180 minutes. K_s and K_{max} were selected as 0.54 mg/liter and 0.83 mg/liter-day, respectively and the corresponding solids concentration was 0.105 g/ml. Initially the solute associated with solid and liquid phase was assumed in equilibrium, so that the initial aqueous and sorbed concentrations were 2.81 x 10^{-8} mol/ml (3.6 mg/liter) and 3.38 x 10^{-7} mol/g, respectively.

Figure 6-13 shows that particle radii of 0.00175 and 0.0175 cm result in the same trend. This is a consequence of particles with these values of mean volumetric radius having rapid desorption kinetics relative to the kinetics of degradation. As the mean volumetric particle size

Figure 6-13: Simulation of the effect of particle radius on aqueous-phase naphthalene concentration as predicted by the coupled desorption-degradation model.

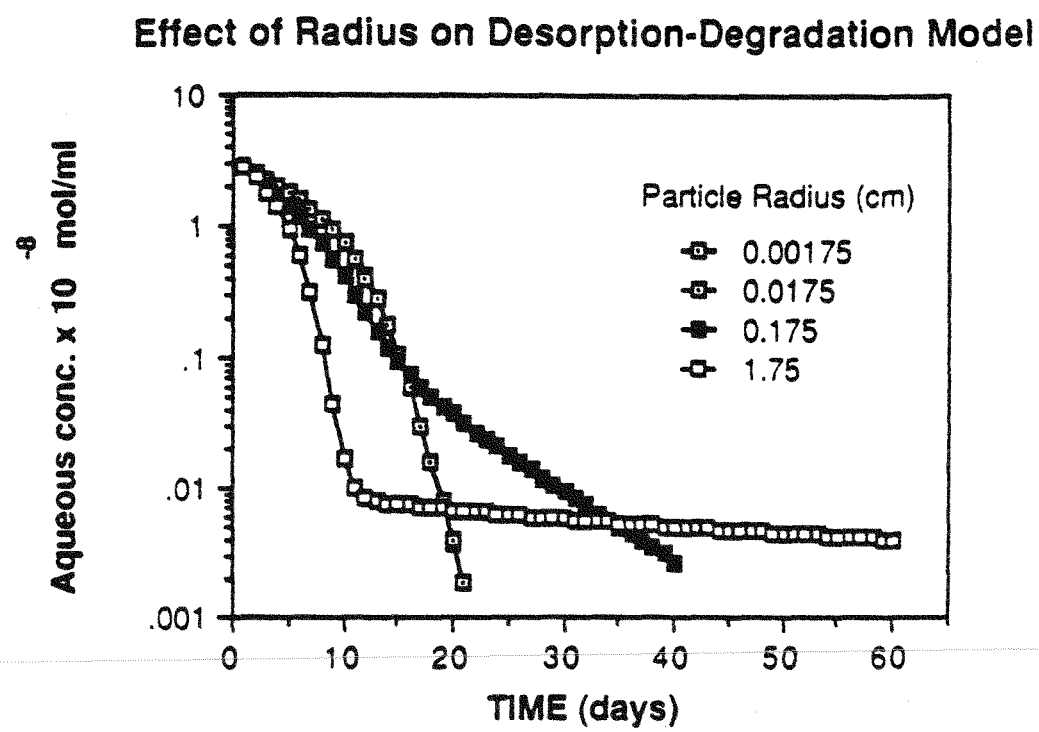

increases to 0.175 and 1.75 cm, the initial aqueous concentration decreases rapidly in the first 10 to 15 days but approaches a level of 0.001 mg/liter at a much slower rate. In fact, the time to reach an aqueous concentration of approximately 0.001 mg/liter for a radius of 0.175 and 1.75 cm is predicted to be 41 and 570 days, respectively. For the system with particle radius of 1.75 cm, at 570 days the mass of solute in the aqueous phase is 3.9×10^{-10} mol (0.001 mg/liter) while that in the sorbed phase is 5.3×10^{-7} mol. This illustrates the impact of the slow rate of desorption on degradation, as over 30 percent of the initially sorbed solute is still associated with the solid phase.

6.5.2. Simulation of the Effect of PAH Hydrophobicity on Microbial Degradation using the Coupled Desorption-Degradation Model

Computer simulations were also performed to examine situations comparing the microbial degradation of PAH compounds of various hydrophobicities in soil-water suspensions. The solutes selected to span a range of hydrophobicities were naphthalene, anthracene, and benzo(*a*)pyrene (log K_{ow} of 3.36, 4.54, and 6.50, respectively). Mean volumetric particle radii were selected as 0.0116 and 0.116 cm (10 grids) and time step of 5, 50, and 1440 minutes were selected for the three solutes, respectively. An average radius of 0.0116 cm was typical for Charles River sediments (Wu and Gschwend, 1986).

It was desired that the microbial degradation rates for the PAH solutes be obtained from a consistent set of experiments which employed careful laboratory protocols. It was for this reason that the microbial degradation rates were chosen from the work of Herbes and Schwall (1978). In that study the authors experimentally determined the rate of microbial degradation of PAH compounds in pristine and petroleum-contaminated stream sediments with use of ^{14}C labeling and mass balance techniques. The soil-to-water ratio in the experiments was 0.5 gram of sediment per 0.5 ml aqueous phase. The authors reported first-order degradation rates for contaminated sediments of 0.14, 2.5×10^{-3}, and 3×10^{-5} /hr for the solutes naphthalene, anthracene, and benzo(*a*)pyrene, respectively. The rate for the solute benzo(*a*)pyrene was judged to be an upper boundary, as the authors noted for those experiments that the observed degradation was barely different than observed in sterilized controls during the sample incubation period of 27 days. It should be noted that in the estimation of these first-order rate constants, Herbes and Schwall did not account for sorption or desorption, so their reported first-order decay coefficient values may be less than values obtained from consideration of soluble phase solute rather than total solute.

These rates are by no means characteristic of all soil-water systems. For example as discussed by Herbes and Schwall (1978), a comparable study (Walker et al., 1976) found the transformation rate of naphthalene to be 100 times slower and that for benzo(*a*)pyrene to be 20 times faster, though sediments suspensions in the Walker et al. study were much more dilute than in the work of Herbes and Schwall.

The model which was developed from Equation [9] was modified to substitute first-order degradation kinetics instead of Monod kinetics for describing biodegradation of the organic contaminant in a soil-water suspension so that:

$$\frac{dC}{dt} = -\frac{V_s}{V}\frac{d\overline{S}}{dt} - kC \qquad [16]$$

where k is a first-order rate constant, hr^{-1}. A working copy of this model can be easily derived as indicated in Appendix C. A simulation for the solute naphthalene was conducted to examine the effect of two particle sizes, as well as a situation in which no solids contributed to a desorption effect. The initial aqueous concentration was set at 0.1 mg/liter (7.81×10^{-10} mol/ml). The sorbed phase at initial equilibrium was estimated to be 3.2×10^{-8} mol per gram of soil for a solids concentration of 1 gram per ml. Figure 6-14 compares the rate of naphthalene degradation for mean volumetric particle radii of 0.0116 and 0.116 cm with degradation if the solids effect is not taken into consideration. Notice that if the large amount of reversibly sorbed solute is not accounted for, the predicted time period for the naphthalene to be degraded is grossly underestimated.

Figures 6-15 to 6-17 show a set of simulations for the situation in which sufficient aqueous-phase naphthalene, anthracene, and benzo(*a*)pyrene were added to a 1 g/ml soil-water system so that after addition and initial partitioning, the initial aqueous concentrations were approximately 7.75×10^{-9} (1), 2.4×10^{-10} (0.04), and 6.9×10^{-12} mol/ml (0.0017 mg/liter), respectively.

Figures 6-15a and 6-15b depict situations in which naphthalene was added at an initial concentration of 4.0×10^{-8} mol/ml (5.1 mg/liter) so that after equilibrium the aqueous-phase concentration would be approximately 1 mg/liter. The particle radii were selected as 0.0116 and 0.116 cm (10 grids) and a time step of 5 minutes was used. Figure 6-15a shows for a particle radius of 0.0116 cm, after initial partitioning for ten minutes, the aqueous and sorbed concentrations were 7.75×10^{-9} mol/ml (0.99 mg/liter) and 3.21×10^{-8} mol/g. The aqueous

Figure 6-14: Simulation of the rate of naphthalene degradation for two particle sizes for a 1:1 soil-to-water ratio.

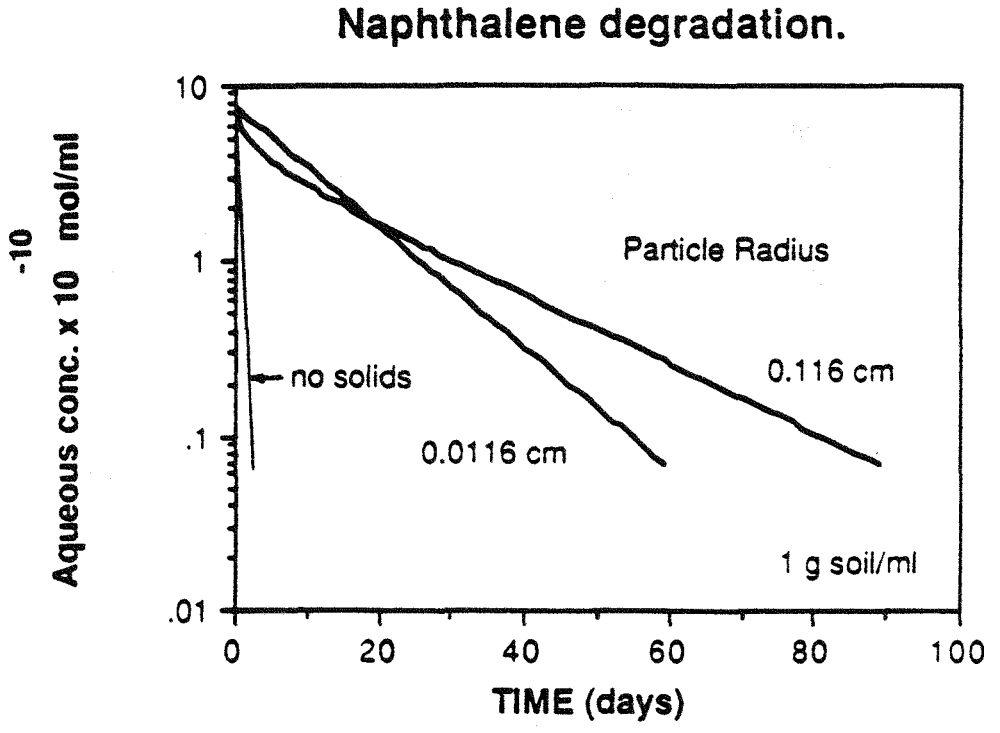

phase showed a continuous decrease for about 100 minutes, which was due mostly to continued sorption, which was followed by a decrease to levels of 0.624×10^{-9} (0.08 mg/liter) after 34 days. The sorbed concentration showed an initial increase to approximately 3.84×10^{-8} mol/g followed by a decrease to 0.260×10^{-8} mol/g in 34 days. At 34 days, approximately 8 percent of the solute mass remained in the system with the majority residing in the sorbed phase.

Figure 6-15b illustrates a comparison situation with a particle size of 0.116 cm. After initial partitioning for 5 minutes, the aqueous and sorbed concentrations were 7.75×10^{-9} mol/ml and 3.21×10^{-8} mol/g. However unlike the system with a particle size of 0.0116 cm, an initial short period of increase in sorbed concentration did not occur. The aqueous phase decreased to 0.573×10^{-9} mol/ml (0.073 mg/liter) over 34 days while the sorbed concentration decreased to approximately 0.418×10^{-8} mol/g. In this case, after 34 days, the total mass of naphthalene which remained in the system was approximately 12 percent with the majority of that in the sorbed phase.

Figure 6-16a and b show the situation in which anthracene was added at an initial level such that after equilibrium the aqueous-phase concentration would be approximately 0.04 mg/liter. Figure 6-16a shows that with a mean volumetric radius of 0.0116 cm, after initial partitioning for 50 minutes, the aqueous and sorbed concentrations were 2.38×10^{-10} mol/ml (0.04 mg/liter) and 1.476×10^{-8} mol/g. The aqueous phase showed a continuous decrease for about 3,800 minutes, mostly due to sorption, which was then followed by a slower decrease to levels of 0.218×10^{-10} mol/ml (0.0039 mg/liter) in 1.5×10^{6} minutes (1,040 days). The sorbed concentration showed an initial increase to approximately 1.50×10^{-8} mol/g followed by a decrease to 1.36 mol/g at 1,040 days. At day 1,040, approximately 91 percent of the total solute mass remained in the system with the majority in the solid phase.

Figure 6-16b shows that with the larger particle size of 0.116 cm, after initial partitioning of 50 minutes, the aqueous- and sorbed-phase concentrations were 2.38×10^{-10} mol/ml and 1.476×10^{-8} mol/g, respectively. After a slight decrease in the aqueous-phase concentration due to continued sorption, the aqueous phase decreased to 0.212×10^{-10} mol/ml after 1.5×10^{6} minutes. The sorbed concentration increased slightly to 1.483 mol/g over the first 14,000 minutes and then steadily decreased to 1.335 mol/g at 1.5×10^{6} minutes. At the end of these simulations, 91 and 89 percent of the initial solute still remained in the systems for solids with a mean volumetric radius of 0.0116 and 0.116 cm, respectively.

Figure 6-15: Simulation of the effect of particle size on the aqueous- and sorbed-phase concentrations when naphthalene is added to a soil-water suspension.

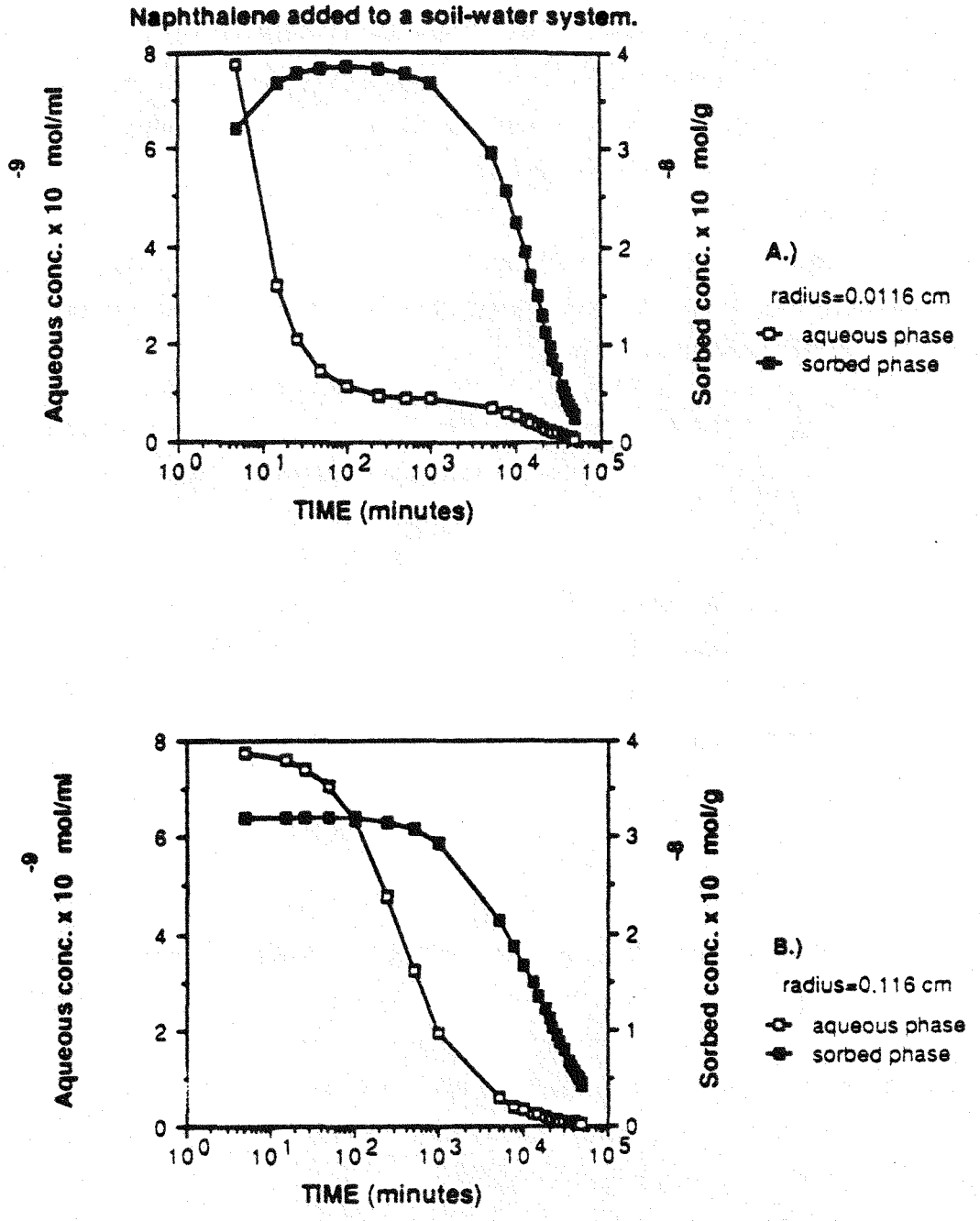

Figure 6-16: Simulation of the effect of particle size on the aqueous- and sorbed-phase concentrations when anthracene is added to a soil-water suspension.

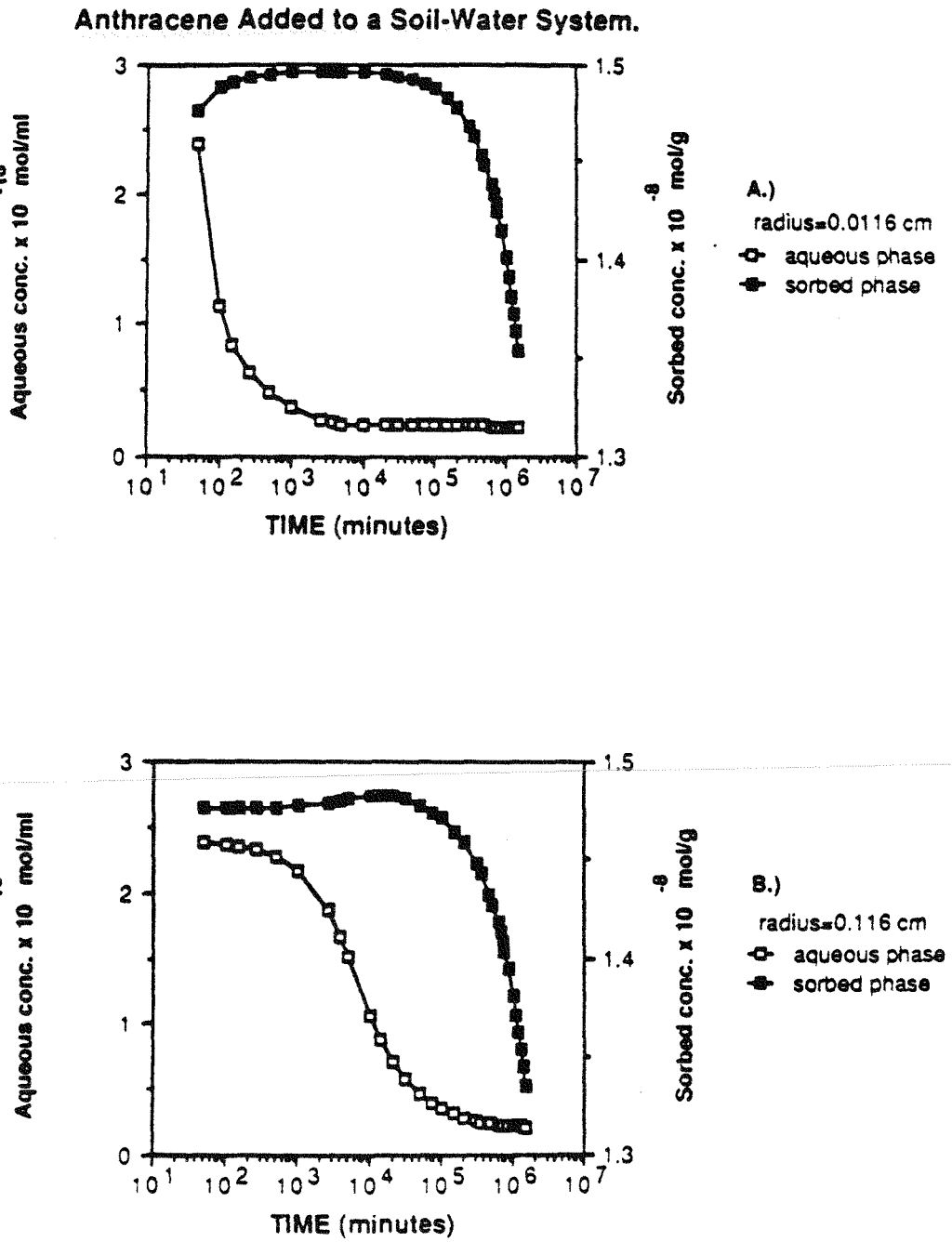

Figure 6-17a shows the case where benzo(*a*)pyrene was added to a 1 g/ml soil-water system, with a mean volumetric radius of 0.0116 cm, so that after a 1 day partitioning period, the aqueous-phase concentration was 6.93 x 10^{-12} mol/ml (0.0017 mg/liter) and the sorbed-phase concentration equaled 3.96931 x 10^{-8} mol/g. The aqueous phase decreased to 0.693 x 10^{-12} mol/ml (0.00017 mg/liter) in 5 x 10^{6} minutes (3,500 days) which was mostly due to sorption since more than 99 percent of the initial solute mass still remained in the system.

Figure 6-17b depicts benzo(*a*)pyrene addition in a system with a volumetric radius of 0.116 cm. After a one-day partitioning period, the initial and sorbed concentrations were 6.93 x 10^{-12} (0.0017 mg/liter) and 3.96931 x 10^{-8} mol/g, respectively. The sorbed-phase concentration continued to increase for almost the whole simulation period as a result of continued sorption from the aqueous phase while the aqueous-phase concentration decreased to 1.51 x 10^{-12} mol/ml (0.00038 mg/liter) over the same time period. At 1.5 x 10^{6} minutes, over 99 percent of the solute still remained in each system.

The results shown in Figures 6-15 to 6-17 are summarized in Tables 6-5, 6-6, and 6-7 for the solutes naphthalene, anthracene, and benzo(*a*)pyrene respectively. Shown in the three tables are simulated aqueous- and sorbed-phase concentrations and the percent total mass which remained in the system as a function of time for each particle radius.

For the system with the solute benzo(*a*)pyrene, it is seen that very little of the solute was removed in a period of 9.5 years. Over 99 percent of the solute remained in the system, mostly in the sorbed phase. The system with a mean volumetric radius of 0.0116 cm experienced a more rapid decrease in the aqueous-phase concentration when compared with the system with a radius of 0.116 cm. This was due to faster desorption kinetics associated with the smaller particle size as explained in Chapter 5 of this report. In both systems, the rate of microbial degradation was extremely slow, thus very little of the solute was removed and sorption-desorption was the rate-controlling step.

With the solute anthracene, it was predicted that 9 and 11 percent of the solute was removed over 1,040 days for the systems with a mean volumetric particle radius of 0.0116 and 0.116 cm, respectively. The initial decrease in aqueous-phase anthracene was due to sorption as indicated in Table 6-6 where time periods of 2.6 and 9.7 days correspond to the maximum sorbed concentration for a system with radii of 0.0116 and 0.116 cm, respectively. The system with a particle size of 0.116 cm had more total solute removed over the course of the

Figure 6-17: Simulation of the effect of particle size on the aqueous- and sorbed-phase concentrations when benzo(*a*)pyrene is added to a soil-water suspension.

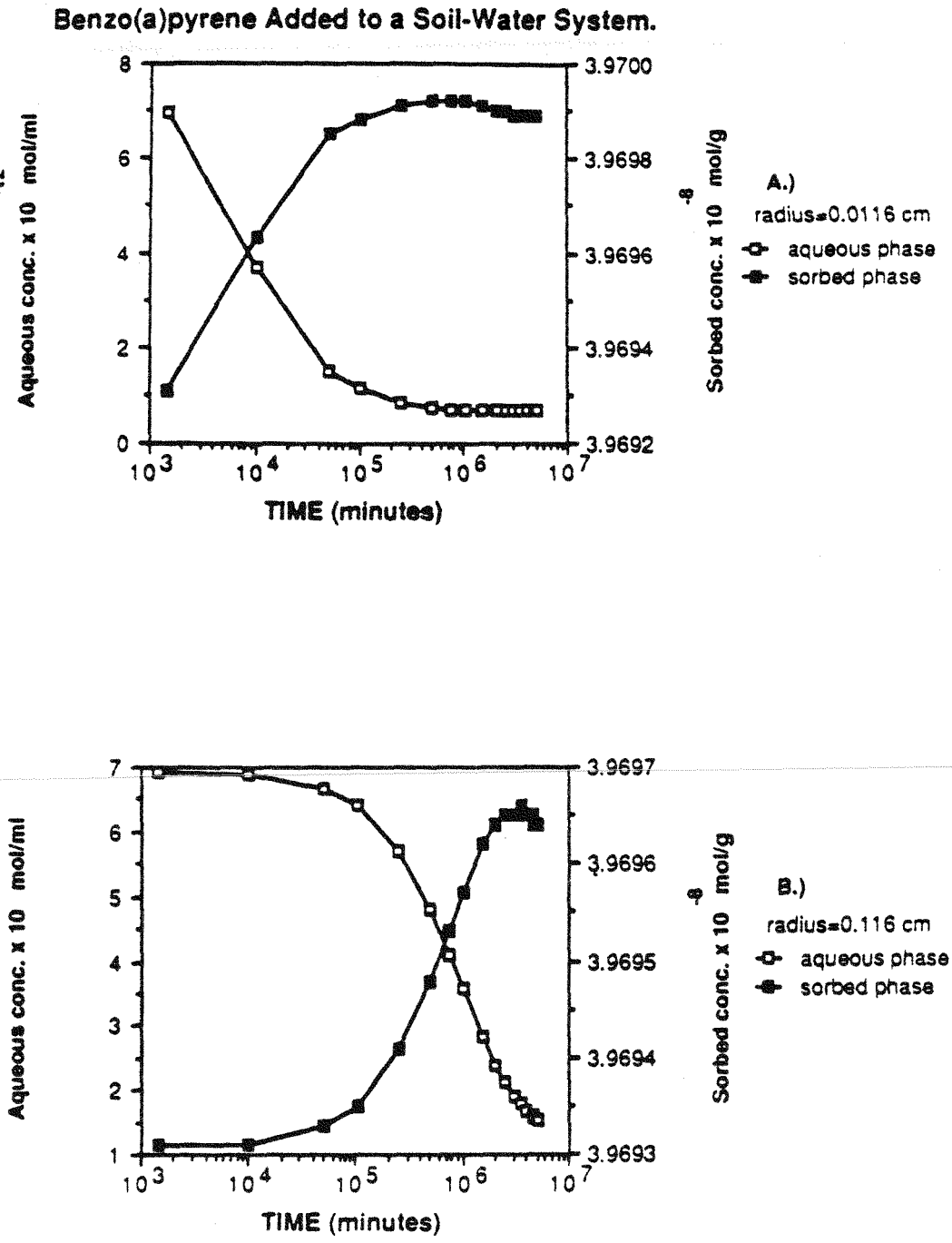

simulation. This was a result of the slower sorption uptake when compared to the system with a radius of 0.0116 cm; thus, more solute was initially in the aqueous phase which caused a greater rate of microbial degradation. However this system showed, as with the system with the solute benzo(*a*)pyrene, that hydrophobic PAH can persist in a soil-water system for long periods of time due to the slow microbial degradation rates and the fact that a sorbed solute may be unavailable to microorganisms as envisioned in this model.

The system with the solute naphthalene showed that much of the solute was removed from both systems after 34 days (93.4 and 89.4 percent total mass removed for particle radius of 0.0116 and 0.116 cm, respectively). After 10,000 minutes (7 days) the system with a mean volumetric particle radius of 0.0116 cm had more solute remaining (69 percent) than the system with a radius of 0.116 cm (42 percent). This was a result of the system with the smaller radius particles having an initial rapid sorption uptake which lasted for approximately 100 minutes. At that point, the solute mass in the aqueous-phase was less than the system with a radius of 0.116 cm, for which there was no net increase in sorbed concentration. Thus the system of 0.116 cm had a faster initial rate of degradation due to the higher solute mass in the aqueous phase. At approximately 30,000 minutes (21 days) that situation reversed itself as there was now higher aqueous-phase concentrations in the system with a radius of 0.0116 cm and thus higher rates of microbial degradation. This was due to the faster rate of desorption associated with the smaller particles.

6.6. Conclusions

The microbial degradation of naphthalene in the experimental soil-water suspensions could be described by a microbial kinetic model which included consideration of the sorbed-phase solute. A coupled solute desorption-degradation model was used to examine unexplored conditions in which PAH sorption-desorption kinetics may dominate the bio-availability of solute to the microorganisms assuming that the sorbed phase was resistant to degradation. This approach combined a radial diffusion model to describe solute sorption and desorption with a model utilizing Monod kinetics to describe the rate of substrate depletion from the bulk aqueous phase assuming the bacterial concentration was constant over the time period of interest. An assumption of fast sorption and desorption kinetics, which was shown to be valid by measurements for the experimental system in this work, was justified by the coupled desorption-degradation model assuming the soil particles could be described as spherical aggregates. The experimental results showed that the rate of degradation was

Table 6-5: Summary of modeling a 1 g/ml soil-water suspension with the solute naphthalene.

initial total mass of naphthalene; 4.0×10^{-8} mol/ml or g

Time min	Aqueous Conc. x 10^{-10} mol/ml	Sorbed Conc. x 10^{-8} mol/g	Percent Total Mass Remaining
radius = 0.0116 cm			
5	77.5	3.21	100
100	11.4	3.84	98.9
10^4	5.36	2.24	69
2.5×10^4	2.34	0.978	25
3.0×10^4	1.78	0.742	19
4.9×10^4	0.624	0.26	6.6
radius = 0.116 cm			
5	77.5	3.21	100
100	63.5	3.20	95.9
10^4	3.30	1.66	42
2.5×10^4	1.38	0.941	23.9
3.0×10^4	1.13	0.796	20.2
4.9×10^4	0.573	0.42	10.6

Table 6-6: Summary of modeling a 1 g/ml soil-water suspension with the solute anthracene.

initial total mass of anthracene; 1.5×10^{-8} mol/ml or g

Time	Aqueous Conc. $\times 10^{-10}$ mol/ml	Sorbed Conc. $\times 10^{-8}$ mol/g	Percent Total Mass Remaining
radius = 0.0116 cm			
50 min	2.38	1.47615	100
2.6 day	0.259	1.49681	99.96
1 yr	0.233	1.44787	96.1
2.8 yr	0.220	1.36287	91.0
radius = 0.116 cm			
50 min	2.38	1.47615	100
9.7 day	0.875	1.48306	99.4
1 yr	0.235	1.42730	95.3
2.8 yr	0.212	1.33535	89.2

Table 6-7: Summary of modeling a 1 g/ml soil-water suspension with the solute benzo(*a*)pyrene.

initial total mass of benzo(*a*)pyrene; 3.97×10^{-8} mol/ml or g

Time min	Aqueous Conc. $\times 10^{-12}$ mol/ml	Sorbed Conc. $\times 10^{-8}$ mol/g	Percent Total Mass Remaining
radius = 0.0116 cm			
1440	6.93193	3.96931	100
5×10^5	0.741949	3.96992	99.99985
1.5×10^6	0.693832	3.96991	99.99948
5×10^6	0.693294	3.96989	99.99897
radius = 0.116 cm			
1440	6.93193	3.96931	100
5×10^5	4.78866	3.96948	99.99896
1.5×10^6	2.84014	3.96962	99.99758
5×10^6	1.50948	3.96964	99.99473

independent of nitrate concentration and proportional to the soil-to-water ratio in the range of 1 to 5 grams per 50 ml employed in the batch microbial degradation experiments.

Nitrate reduction was described by an equation which gave the depletion of nitrate as a function of the soil-to-water ratio and the organic carbon substrate. The model was linearized by predicting nitrate concentrations over the zero-order kinetic range of naphthalene degradation.

Modeling was performed to evaluate the effects of soil-to-water ratio, soil particle size, and solute hydrophobicity on microbial degradation of PAH solute in soil-water suspensions. The purpose was to obtain an initial evaluation of the parameters which may influence the rate of degradation assuming that sorbed-phase solute is resistant to degradation and that a spherical intraparticle radial diffusion model may describe the rate of release of solute to the aqueous phase. Since the model related the maximum rate of degradation to the soil-to-water ratio, the systems with greater amounts of soil showed faster approaches to nondetectable levels. The effect of particle size on the rate of microbial degradation of naphthalene was evident as the mean volumetric radius approached 1 cm and greater.

The effect of PAH compound hydrophobicity on microbial degradation in soil-water suspensions was evaluated for the solutes naphthalene, anthracene, and benzo(*a*)pyrene and particle radii of 0.0116 and 0.116 cm. This modeling showed that the initial rate of sorption can affect the removal rate by lowering the aqueous-phase concentration and thereby decreasing the rate of biodegradation. Furthermore, modeling indicated that very hydrophobic compounds would persist in soil-water systems for long periods because of slow degradation rates and the large portion of the total solute mass associated with the solid phase.

The concepts developed in the coupled desorption-degradation model are important when considering the reactions and fate of hydrophobic organic compounds from soil-water systems. This work provides evidence for the importance of understanding the interactions among the physical, chemical, and biological parameters of the soil-water system. The modeling exercises demonstrated the important role which particle size has on microbial degradation, and justifies the need for additional research on the significance for solubilization of hydrophobic PAH before significant degradation will occur. This has important implications for remedial action when a soil-water system has been contaminated by a hydrophobic organic pollutant such as polycyclic aromatic hydrocarbons.

6.7. References

1. Alexander, M., "Biodegradation of Organic Chemicals," *Environmental Science and Technology,* Vol. 18, p. 106-111, 1985.

2. Batonda, J., and S.A. Waring, "Denitrification in Relation to Soil Carbon for Soils of the Darling Downs," *Review in Rural Science,* Vol. 5, p. 231-239, 1984.

3. Beauchamp, E.G. C. Gale, and J.C. Yeomans, "Organic Matter Availability for Denitrification in Soils of Different Textures and Drainage Classes," *Communications in Soil Science and Plant Analysis,* Vol. 11, p. 1221,1980.

4. Bowman, R.A., and D.D. Focht, "The Influence of Glucose and Nitrate Concentrations Upon Denitrification Rates in Sandy Soils," *Soil Biology and Biochemistry,* Vol. 6, p. 297-301, 1974.

5. Brunner, W., and D.D. Focht, "Deterministic Three-Half-Order Kinetic Model for Microbial Degradation of Added Carbon Substrates in Soil," *Applied and Environmental Microbiology,* Vol. 47, p. 167-172, 1984.

6. Burford, J.R., and J.M. Bremner, "Relationships Between the Denitrification Capacities of Soils and Total, Water-Soluble and Readily Decomposable Soil Organic Matter," *Soil Biology and Biochemistry,* Vol. 7, p. 389-394, 1975.

7. Focht, D.D., and W. Brunner, "Kinetics of Biphenyl and Polychlorinated Biphenyl Metabolism in Soil," *Applied and Environmental Microbiology,* Vol. 50, p. 1058-1063, 1985.

8. Hayduk, W., and B.S. Minhaus, *Canadian Journal of Chemical Engineering,* Vol. 60, p. 295, 1982.

9. Herbes, S.E., and L.R. Schwall, "Microbial Transformation of Polycyclic Aromatic Hydrocarbons in Pristine and Petroleum Contaminated Sediments," *Applied and Environmental Microbiology,* Vol. 35, p. 306-316, 1978.

10. Jacobson, S.N., and N. Alexander, "Nitrate Loss from Soil in Relation to Temperature, Carbon Source, and Denitrifier Population," *Soil Biology and Biochemistry,* Vol. 12, p. 501-505, 1980.

11. Jenkinson, D.S., and J.H. Rayner, "The Turnover of Soil Organic Matter in Some of the Rothamsted Classical Experiments," *Soil Science,* Vol. 123, p. 298-305, 1977.

12. Kohl, D.H., F. Vithaysthil, P. Whitlow, G. Shearer, and S.H. Chien, "Denitrification Kinetics in Soil Systems: The Significance of Good Fits of Data To Mathematical Forms," *Soil Science Society of America Proceeding,* Vol. 40, p. 249-253, 1976.

13. Lewandoswki, Z. "Temperature Dependency of Biological Denitrification with Organic Materials Addition," *Water Research,* Vol. 16, p. 19-22, 1982.

14. McCroskey, P.S., and G.J. McRae, "PAREST, A Computer Program for Estimation of Parameters in Algebraic and Ordinary Differential Equation Models," Department of Chemical Engineering, Carnegie Mellon University, Pittsburgh, Pa., May, 1987.

15. Mihelcic, J.R., and R.G. Luthy, "Degradation of Polycyclic Aromatic Hydrocarbons Under Various Redox Conditions in Soil-Water Systems," *Applied and Environmental Microbiology,*, Vol. 54, 1988a.

16. Mihelcic, J.R., and R.G. Luthy, "Microbial Degradation of Acenaphthene and Naphthalene Under Denitrification Conditions in Soil-Water Systems," *Applied and Environmental Microbiology*,, Vol. 54, 1988b.

17. Molina, J.A.E., C.E. Clapp, M.J. Shaffer, F.W. Chichester, and W.E. Larson, "NCSOIL, A Model of Nitrogen and Carbon Transformations in Soil: Description, Calibration, and Behavior," *Soil Science Society of America Journal*, Vol. 47, p. 85-91, 1983.

18. Ogram, A.V., R.E. Jessup, L.T. Ou, and P.S.C. Rao, "Effects of Sorption on Biological Degradation Rates of (2,4-Dichlorophenoxy)acetic Acid in Soils," *Applied and Environmental Microbiology*, Vol. 49, p. 585-587, 1985.

19. Oren, A., and T.H. Blackburn, "Estimation of Sediment Denitrification Rates at In Situ Nitrate Concentrations," *Applied and Environmental Microbiology*, Vol. 37, p. 174-176, 1979.

20. Paris, D.F., D.L. Lewis, and N.L. Wolfe, "Rates of Degradation of Malathion by Bacteria Isolated From Aquatic System," *Environmental Science and Technology*, Vol. 9, p. 135-138, 1975.

21. Paris, D.F., W.C. Steen, G.L. Baughman, and J.T. Barnett Jr., "Second-Order Model to Predict Microbial Degradation of Organic Compounds in Natural Waters," *Applied and Environmental Microbiology*, Vol. 41, p. 603-609, 1981.

22. Phillips, R.E., K.R. Reddy, and W.H. Patrick, "The Role of Nitrate Diffusion in Determining the Order and Rate of Denitrification in Flooded Soil: II. Theoretical Analysis and Interpretation," *Soil Science Society of America Proceedings*, Vol. 42, p. 272-278, 1978.

23. Reddy, K.R., W.H. Patrick, and R.E. Phillips, "The Role of Nitrate Diffusion in Determining the Order and Rate of Denitrification in Flooded Soil: I. Experimental Results," *Soil Science Society of America Proceedings*, Vol. 42, p. 268-272, 1978.

24. Reddy, K.R., R. Khaleel, and M.R. Overcash, "Carbon Transformations in the Land Areas Receiving Organic Wastes in Relation to Nonpoint Source Pollution: A Conceptual Model," *Journal of Environmental Quality*, Vol. 9, p. 434-442, 1980.

25. Reddy, K.R., P.S.C. Rao, and R.E. Jessup, "The Effect of Carbon Mineralization on Denitrification Kinetics in Mineral and Organic Soils," *Soil Science Society of America Journal*, Vol. 46, p. 62-68, 1982.

26. Reid, R.C., J.M. Prausnitz, and B.E. Poling, *The Properties of Gases and Liquids, 4th Edition*, McGraw-Hill Book Company, New York, p. 577-631, 1987.

27. Robinson, J.A., and J.M. Tiedje, "Nonlinear Estimation of Monod Growth Kinetics Parameters From a Single Substrate Depletion Curve," *Applied and Environmental Microbiology*, Vol. 45, p. 1453-1458, 1983.

28. Rolston, D.E., P.S.C. Rao, J.M. Davidson, and R.E. Jessup, "Simulation of Denitrification Losses of Nitrate Fertilizer Applied to Uncropped,. Cropped, and Manure-Amended Field Plots," *Soil Science*, Vol. 137, p. 270-279, 1984.

29. Ryden, J.C., "Denitrification Loss From a Grassland Soil in the Field Receiving Different Rates of Nitrogen as Ammonium Nitrate," *Journal of Soil Science*, Vol. 34, p. 355-365, 1983.

30. Schwarzenbach, R.P., and J. Westall, "Transport of Nonpolar Organic

Compounds From Surface Water to Groundwater. Laboratory Sorption Studies," *Environmental Science and Technology,* Vol. 15, p. 1360-1367, 1981.

31. Simkins, S. and M. Alexander, "Models for Mineralization Kinetics with the Variables of Substrate Concentration and Population Density," *Applied and Environmental Microbiology,* Vol. 47, p. 1299-1306, 1984.

32. Simkins, S., R. Mukherjee, and M. Alexander, "Two Approaches to Modeling Kinetics of Biodegradation by Growing Cells and Application of a Two-Compartment Model for Mineralization Kinetics in Sewage," *Applied and Environmental Microbiology,* Vol. 51, p. 1153-1160, 1986

33. Stammers, W.N., J.B. Robinson, and H.R. Whiteley, "Characterization of the Kinetics of Denitrification," In T.D. Fontaine, and S.M. Bartell (eds.) *Dynamics of Lotic Ecosystems,* Ann Arbor Science, Ann Arbor, p. 479-486, 1983.

34. Stanford, G. R.A. Vander Pol, and S. Dzienia, "Denitrification Rates in Relation to Total and Extractable Soil Carbon," *Soil Science Society of America Proceedings,* Vol. 39, p. 284-289, 1975.

35. Stars, J.L. and J.Y. Parlange, "Nonlinear Denitrification Kinetics with Continuous Flow in Soil Columns," *Soil Science Society of America Proceedings,* Vol. 39, p. 875, 1975.

36. Steen, W.F., D.F. Paris, and G.L. Baughman, "Effects of Sediment Sorption on Microbial Degradation of Toxic Substances," pp. 477-482. *In* R.A. Baker (ed.), *Contaminants and Sediments. Volume 1. Fate, and Transport Case Studies, Modeling, Toxicity,* Ann Arbor Science, Ann Arbor, Michigan, 1980.

37. Steinberg, S.M., J.J. Pignatello, and B.L. Sawhney, "Persistence of 1,2-Dibromoethane in Soils: Entrapment in Intraparticle Micropores," *Environmental Science and Technology,* Vol. 21, p. 1201-1208, 1987.

38. Suflita, J.M., W.J. Smolnski, and J.A. Robinson, "Alternative Nonlinear Model for Estimating Second-Order Rate Coefficients for Biodegradation," *Applied and Environmental Microbiology,* Vol. 53, p. 1064-1068, 1987.

39. Walker, J.D., R.R. Colwell, and L. Petrakis, "Biodegradation of Petroleum by Chesapeake Bay Sediment Bacteria," *Canadian Journal of Microbiology,* Vol. 22, p. 423-428, 1976.

40. Walters, R.W., and R.G. Luthy, "Liquid/Suspended Solid Phase Partitioning of Polycyclic Aromatic Hydrocarbons in Coal Coking Wastewaters," *Water Research,* Vol. 18, p. 795-809, 1984.

41. Wszolek, P.C., and M. Alexander, "Effect of Desorption Rate on the Biodegradation of *n*-Alkylamines Bound to Clay," *Journal of Agricultural Food Chemistry,* Vol. 27, p. 410-414, 1979.

42. Wu, S.C., and P.M. Gschwend "Sorption Kinetics of Hydrophobic Organic Compounds to Natural Sediments and Soils," *Environmental Science and Technology,* Vol. 20, p.717-725, 1986.

43. Wu, S., "Transport of Hydrophobic Organic Compounds Between Water and Natural Sediments," Ph.D. Thesis, Department of Civil Engineering, Massachusetts Institute of Technology, Boston, Massachusetts, 1986.

Chapter 7
Summary and Conclusions

This report presented results of a study which examined the microbial degradation of lower-molecular-weight polycyclic aromatic hydrocarbons (PAH) under denitrification conditions in soil-water suspensions, and assessed the effect which soil sorption and desorption may have on the rate of microbial degradation through model simulations. The investigation consisted of both experimental and modeling activities. The results of the microbial degradation experiments were interpreted by combining an intra-aggregate radial diffusion model to describe the sorption and desorption of hydrophobic organic solutes from a soil suspension with a Monod kinetic model to describe the rate of substrate depletion from the bulk aqueous phase.

Batch experiments with soil-water suspensions were conducted to examine the degradation of acenaphthene, naphthalene, and naphthol under various redox conditions. The soil selected for this study was characteristic of a sub-humid grassland soil of eastern North Dakota. The solutes which were evaluated were selected on the basis of analytical considerations, as well as to represent some varying degree of hydrophobicity. The presence of an oxygen-containing substituent group was the reason for the selection of naphthol. Under aerobic conditions, all three compounds were degraded to nondetectable levels (< 0.01 mg/l) in less than two weeks, whereas, under anaerobic conditions naphthol was degraded whereas acenaphthene and naphthalene showed no significant degradation for time periods of 70 and 50 days respectively. All three compounds were degraded under denitrification conditions with the time until nondetectable levels were attained greater than in the aerobic experiments. In the presence of a manganese oxide, naphthalene showed no significant change over nine weeks while naphthol decreased to nondetectable levels in less than two weeks. This portion of the study showed the importance of the redox environment on the degradation of PAH compounds in soil-water systems. The results indicated that the degradation of PAH compounds under denitrification conditions was worthy of additional study. This work provided

the first reported evidence of the microbial degradation of PAH compounds under denitrification conditions.

The microbial degradation of acenaphthene and naphthalene under denitrification conditions was examined more extensively. It was found that no degradation occurred under nitrate-limiting conditions due to the rapid depletion of nitrate associated with the demand from the labile fraction of naturally occurring soil organic carbon. Under nitrate-excess conditions, however, both solutes were degraded to nondetectable levels following an acclimation period. The reduction of nitrate was shown to entail the oxidation of both the labile fraction of naturally occurring soil organic carbon and the PAH compound. This information was used to estimate the extent of PAH compound mineralization and to determine the nitrate demand associated with PAH-containing soil-water suspensions. The acclimation period which was observed in the experiments prior to microbial degradation was explained by the time necessary for an active microbial population to increase in number before significant degradation could be observed.

Experimental and modeling work showed that the sorption process for naphthalene was reversible and that the rate of sorption and desorption was relatively rapid when compared to the rate of microbial degradation. For example, the experimental studies indicated that naphthalene sorption and desorption equilibrium were attained in under one hour which was confirmed by modeling. The model selected to describe solute sorption and desorption was an intra-aggregate radial diffusion model in which the solute was visualized as diffusing through a porous spherical soil particle while undergoing local partitioning. This type of model allowed the user to examine the effects of intraparticle porosity, solute hydrophobicity, and soil particle size on the rate of sorption and desorption. The solutes which were examined in this particular portion of the study were naphthalene, anthracene, and benzo(*a*)pyrene. These solutes were selected due to their range of hydrophobicities and the availability of some information regarding the rate of microbial utilization of these compounds in soil-water systems. It was concluded that soil particle size had a large effect on the rate of sorption and desorption with the dimensionless time step being proportional to the inverse of the radius squared, whereas solute hydrophobicity affected the kinetics of soil-water partitioning by increased degree of local partitioning. The radial diffusion model predicted that long time spans were required to completely reach sorption or desorption equilibrium for large soil aggregates and/or extremely hydrophobic solutes, such as benzo(*a*)pyrene.

Experimental data were used to develop a model to describe the concentration of aqueous-phase naphthalene in a soil-water suspension by combining the rate of desorption and microbial degradation. The model incorporated a radial diffusion model to describe solute desorption and Monod or first-order kinetics to describe solute depletion from the bulk aqueous phase. Acclimated soil was used to obtain the biokinetic parameters for naphthalene degradation under denitrification conditions. The biokinetic parameters of the Monod model were estimated for the experimental systems by recognizing that the desorption kinetics were rapid compared to the microbial degradation kinetics. This assumption was judged to be valid based on desorption studies and on modeling the rate of solute desorption using a particle size distribution with a volumetric mean particle radius of 17.5 μm. The Monod half-saturation coefficient was shown to be almost equal for the various experimental systems while the maximum rate of degradation was proportional to the soil-to-water ratio and independent of nitrate concentration. Nitrate reduction was described by a model in which nitrate depletion was first-order with respect to the available organic carbon substrate and the active microbial population.

The coupled desorption-degradation model was used to estimate the effect which the soil particle size had on the rate of microbial degradation in soil-water systems. In computer simulations of conditions similar to the batch tests employed in the experimental portion of this work, it was found for naphthalene that the particle size became important when the volumetric mean radius approached 1 cm. For the case of acclimated systems with large-sized particles, samples which contained less soil and therefore less active microorganisms were predicted to approach lower total solute levels in shorter time periods since less solute mass was associated with the sorbed phase from which solute removal was controlled by slow desorption kinetics rather than the rate of microbial degradation.

Computer simulations were also performed to assess the aqueous- and solid-phase components for the solutes naphthalene, anthracene, and benzo(*a*)pyrene in a soil-water suspension. This provided an initial understanding of the manner in which the rates of sorption and desorption of solute with soils and sediments may affect the microbial degradation of solute in the bulk aqueous phase. First-order microbial degradation rates for these three solutes were obtained from the literature and inputted into the coupled desorption-degradation model to predict aqueous- and sorbed-phase solute concentration over time. It was found that most of the mass of the more hydrophobic solutes partitioned to the sorbed phase where it was assumed to be unavailable to microorganisms. This phenomenon, along

with the inherently slow rate of microbial degradation of the more hydrophobic solutes, caused these solutes to persist for long periods of time. The effect of soil particle size on the systems with the more hydrophobic PAH compounds was to cause the system with greater particle size to have an initially higher aqueous-phase concentration which was due to a slower initial rate of sorption. Thus, this system had a faster rate of microbial degradation compared to the system with smaller size particles. For the solute naphthalene the effect of soil particle size was to cause the system with larger particle size to exhibit a faster initial rate of microbial degradation, whereas at later time periods, when desorption became important, the rate of microbial degradation with larger particle size was slower in comparison to systems with smaller particle sizes.

This study evaluated the microbial degradation of naphthol, naphthalene, and acenaphthene in soil-water suspensions under denitrification conditions. A model was developed which incorporated both sorption-desorption and microbial degradation to simulate the aqueous- and sorbed-phase PAH components over time. These concepts are important in helping to understand the transport and fate of hydrophobic organic solutes in soil-water systems where the rate-limiting step may be either solute sorption, desorption or microbial degradation, depending on the physical, chemical, and biological characteristics of the system.

Appendix A

Physical and Chemical Characteristics of Barnes-Hamerly Soil

Several characteristics of Barnes-Hamerly soil were evaluated. These included organic carbon content, specific gravity, and air moisture content. A size distribution of the soil was also obtained by dry sieve analysis. The particle size distribution of the soil-water suspension was presented in Chapter 5.

Particle Size Analysis. Soil particle size analysis has practical value, including dependencies on soil permeability and capillarity properties. If nearly all grains are so large that they cannot pass through square openings of 0.074 mm (No. 200 sieve), sieve analysis is preferred. This method is described by Lambe (Lambe, T.W., *Soil Testing for Engineers,* John Wiley and Sons, New York, N.Y., 1951) It should be noted that grain analysis by sieving does not determine individual particle sizes but rather determines the percent by weight of soil particle sizes in a range of diameters.

Sieve analysis is accomplished by passing a known weight of soil through a series of sieves. The soil is shaken mechanically and sieved for fifteen minutes. After sieving, the amount of soil retained by each sieve is expressed as a percentage of the soil sample's total mass. The averaged results of the sieve analysis on Barnes-Hamerly soil are presented in Table A-1. A particle size distribution curve can then be constructed from this analysis. Figure A-1 presents this curve on semilogarithmic paper. The median grain size (D_{50}) is defined as that for which 50 percent of the soil by weight is finer and 50 percent is coarser. The effective grain size (D_{10}) is defined as the maximum diameter of the smallest 10 percent by weight of the soil particles. For Barnes-Hamerly soil the median grain size was 0.41 mm and the effective grain size was found to be less than 0.12 mm as shown in Figure A-1. It is important to note that the accuracy of the distribution curve is arbitrary since particle size depends on the degree of disaggregation which is employed before mechanical testing.

Specific Gravity Analysis. The specific gravity of a soil is often used in relating a

Table A-1: Particle size analysis of Barnes-Hamerly soil by a dry-sieve technique.

sieve no.	sieve opening [mm]	total % retained %	total % passing %
10	2.00	0.0	100.
40	0.42	45.16	54.84
70	0.210	75.47	24.53
100	0.149	85.18	14.82
140	0.105	89.96	10.04
200	0.074	95.30	4.70
pan	<0.074	100.	0.0

Figure A-1: Particle Size Distribution of Barnes-Hamerly Soil.

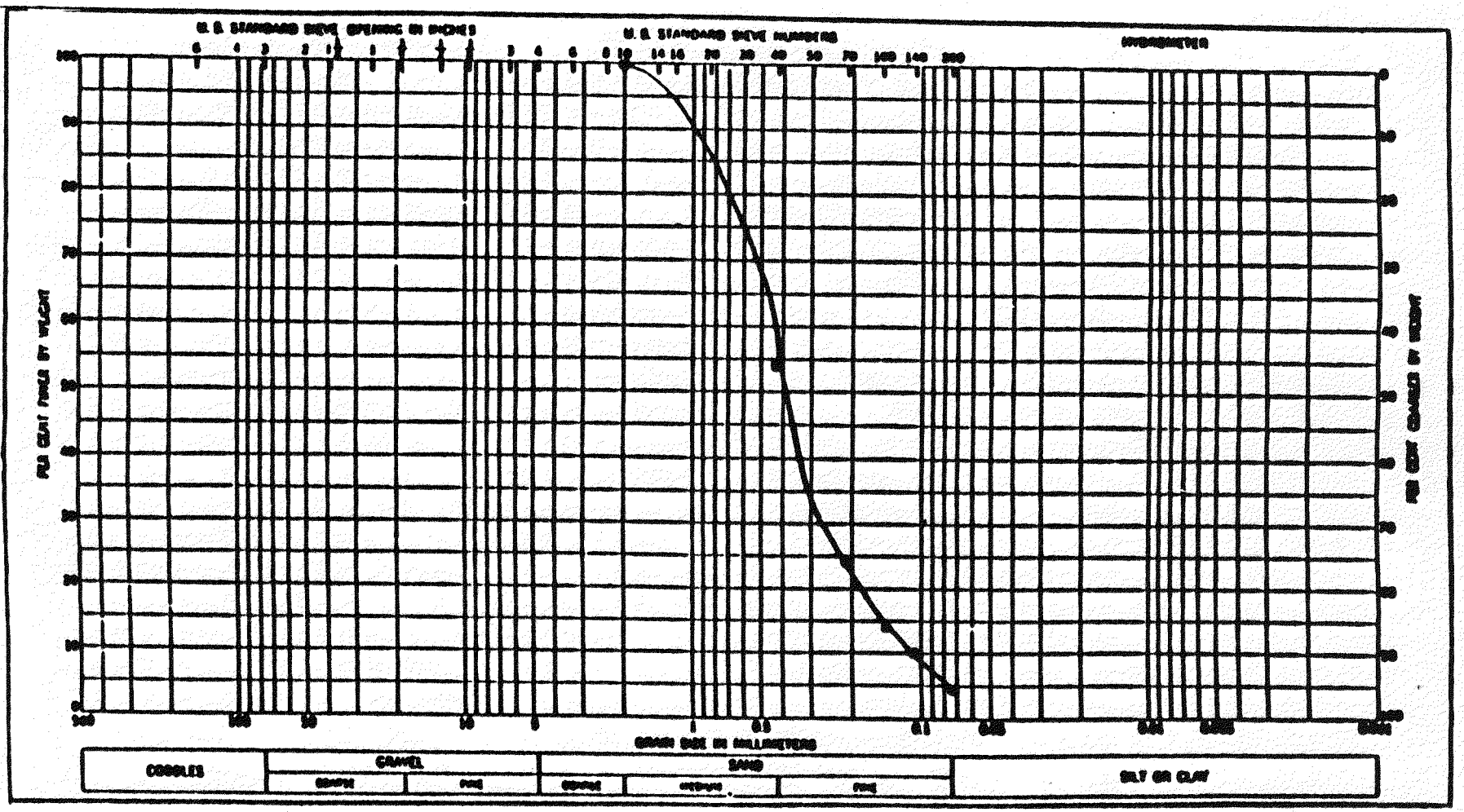

weight of soil to its volume, if the void ratio and degree of saturation are also known. The specific gravity of a soil refers to the ratio of the weight in air of a given volume of soil particles to the weight in air of an equal volume of distilled water at a temperature of 4°C (Lambe, 1951).

A 1000-ml pycnometer is normally employed to measure a soil's specific gravity but in this study a 250-ml volumetric flask was used for the measurement. This adjustment could be made since the soil sample was large enough to compensate for any decrease in precision in measuring the fluid volume. The test consisted of first placing 50 grams of oven-dried soil in a 250-ml volumetric flask. Care was taken to clean the flask's outside, and the neck of any soil deposited during transfer. The flask was then filled approximately one-half full with deaired, distilled water. Entrapped air was removed by gently boiling the mixture for several minutes, after which the flask was cooled to room temperature, and filled with deaired, deionized water. The flask was then weighed and the temperature of the soil-water mixture measured. Finally the flask, filled with deaired, deionized water at the same room temperature, was weighed. The specific gravity of the soil was calculated as follows:

$$\frac{W_s G_T}{W_s - W_1 + W_2}$$

where W_s is the dry weight of the soil, G_T is the specific gravity of distilled water at the temperature, W_1 is the weight of the flask, soil, and water, and W_2 is the weight of the flask plus water. The specific gravity of Barnes-Hamerly soil was measured as 2.5.

Moisture Content. The moisture content of air-dried Barnes-Hamerly soil was determined by placing a known amount of soil in a dish and placing this sample in an oven at 105°C for one hour. Samples are then weighed and the moisture content was calculated as follows:

$$moisture\ content = \frac{T_1 - T_2}{T_2 - T}$$

where T_1 is the weight of soil and tare, T_2 is the weight of oven-dried soil and tare, and T is the weight of the tare. Barnes-Hamerly soil, after being air-dried, had a moisture content of 7.96 percent.

Organic Carbon Content. The percent organic carbon of Barnes-Hamerly soil is

important when considering this soil's ability to adsorb hydrophobic organic compounds and support biological activity. Carbon is the main element of soil organic matter which can be measured quantitatively so estimates of organic matter are generally based on measuring organic carbon. Soil organic matter includes fresh plant and animal residues, humus (representing the bulk of resistant organic matter), and inert forms of nearly elemental carbon such as charcoal, coal, or graphite.

In this study, organic carbon was determined by the Walkley-Black method (Allison, L.E., "Organic Carbon," in *Methods of Soil Analysis, Part II: Chemical and Microbiological Properties,* Ed. C.A. Black, American Society of Agronomy, Inc., Madison, Wisconsin, 1965.). A soil sample weighing 0.1 to 0.5 gram was placed in a 500-ml wide Erlenmeyer flask. Ten ml of 1.0 N $K_2Cr_2O_7$ were added and the flask was swirled gently to disperse the soil into the solution. Twenty ml of concentrated H_2SO_4 were then added to the flask and mixed for one minute. After allowing the solution to stand for 30 minutes, 200 ml of deionized water were added, and then the suspension was filtered. Three or four drops of o-phenanthroline indicator were added prior to titration with 0.5 $FeSO_4$. Titration results in a sharp end point, with the color of the solution changing from blue to red. The amount of $FeSO_4$ used in titration was recorded. Blank determinations were made in the same manner to standardize the $K_2Cr_2O_7$ solution.

The organic carbon content can be calculated according to the following formula, using a correction factor, f = 1.33 (Allison, 1965).

$$Percent\ Organic\text{-}C = \frac{(meq\ K_2Cr_2O_7 - meq\ FeSO_4)\ x\ 0.003\ x\ 100\ x\ f}{g\ of\ dry\ soil}$$

where meq represents milliequivalent of the chemical indicated, and the factor 0.003 refers to the number of grams of carbon per milliequivalent for carbon at an average oxidation state of zero. The factor f = 1.33 corrects for the fact that soil organic carbon is at an average oxidation state slightly less than zero. The organic carbon content of Barnes-Hamerly soil, averaging more than twenty independent tests, was found to be 2.9 percent.

Appendix B

Radial Diffusion Model for Sorption and Desorption Kinetics

```
C     ****************************************************************
C           James R. Mihelcic, Department of Civil Engineering
C                              1987
C                 Carnegie Mellon University, Pittsburgh, Pa.
C     ****************************************************************
C        The following program is recoded into fortran77 from
C     a BASIC program contained in the thesis work
C     of S.C. Wu, Department of Civil Engineering, Mass. Inst.
C     of Technology, 1986.  A detailed discussion of the program is
C     contained in Wu's thesis.
C         The program uses a radial diffusion
C     model to describe the sorption and desorption of hydrophobic
C     solutes in porous spherical aggregates.
C     The program uses a finite difference approach and can
C     simulate kinetics with more than one particle size group using a
C     conventional finite difference method. Grid sizes are changeable.
C     Up to 10 particle classes can be used.
C     ****************************************************************
      CHARACTER*1 changeC, knoDeff
      DOUBLE PRECISION one,two,zero,ca,ssp,t1
      INTEGER ngrid(10), num(20)
c      INTEGER ngrid(10), num(10)
      REAL fs(10),rad(10),u(10,201),g(10)
      REAL dx(10),h(10),ut(10,201),gridsize(10),te(20),co(20)
      REAL s1(10),k1(10),Kow,tmint,Kp,Koc,Kow,foc
      one=1
      zero=0
      two=2
      OPEN(UNIT=10,FILE='des.out',STATUS='unknown')
          WRITE(10,967)
967       FORMAT('*****Output from finite difference program*****')
          WRITE(10,968)
968       FORMAT('*****for modeling sorption and desorption*****')
          WRITE(10,969)
969       FORMAT('***************James R. Mihelcic**************')
          WRITE(10,970)
970       FORMAT('***************Carnegie Mellon University*******')
          WRITE(10,971)
971       FORMAT('*************Department of Civil Engineering***')
```

```
          WRITE(10,972)
972       FORMAT(' Up to 10 particle sizes can be obtained')
C     ----------Entering environmental parameters-------------
C     ----------particle size distribution--------------------
      WRITE(*,4)
4     FORMAT('Please enter environmental parameters.',/)
      WRITE(*,5)
5     FORMAT('Enter the number of particle classes   ',$)
      READ(*,*) ng
      DO 9 n=1, ng
      WRITE(*,6)
C     fraction of particle class. If only using average size, fs(n)=1
6     FORMAT('Enter fraction   ',$)
      READ(*,*)fs(n)
      WRITE(*,7)
7     FORMAT('Enter particle radius in cm   ',$)
      READ(*,*)rad(n)
C     The gridsize is the radius divided by the number of grids.
C     Wu's thesis explains the advantages and disadvantages of the
C     number of grids utilized.
      WRITE(*,8)
8     FORMAT('Enter gridsize of class #, cm   ',$)
      READ(*,*)gridsize(n)
9     CONTINUE
      WRITE(*,11)
11    FORMAT('Initial concentration in solid (mole/g) ?   ',$)
      READ(*,*)so
      WRITE(*,12)
12    FORMAT('Simulation starting time (minute) ?   ',$)
      READ(*,*)te(0)
      WRITE(*,14)
14    FORMAT('Printing time step size (minute) ?   ',$)
      READ(*,*)Timestep
      ncycle=0
15    CONTINUE
            ncycle=ncycle+1
            WRITE(*,16)
16          FORMAT('Ending time (minute) ?   ',$)
            READ(*,*)te(ncycle)
17          continue
            WRITE(*,18)
18          FORMAT('Concentration in aqueous phase (mole/ml) ?   ',$)
            READ(*,*)co(ncycle)
      WRITE(*,20)

C     changing the aqueous concentration allows you to reintroduce
C     the contaminant into the system at a specified time.

20    FORMAT('Do you want to change concentration in aqueous phase? ',$)
      READ(*,*)changeC
       IF (changeC .EQ. 'Y'.OR. changeC .EQ. 'y') THEN
       GOTO 15
       END IF
C     ------------------sorbent concentration and Kp---------------
      WRITE(*,22)
22    FORMAT('Sorbent concentration (g/ml) ?   ',$)
      READ(*,*)solid
```

```
C      ---------------------printing input parameters---------------------
       WRITE(10,200)rad
200    FORMAT('radius (cm)=',1PE10.4)
       WRITE(10,205)gridsize
205    FORMAT('gridsize (cm)=',1PE11.5)
       WRITE(10,210)so
210    FORMAT('initial conc. in solid (mole/g)=',1PE10.4)
       WRITE(10,216)co
216    FORMAT('initial aqueous conc. (mole/ml)=',1PE8.2)
       WRITE(10,220)solid
220    FORMAT('sorbent concentration (g/ml)=',0PF8.4)
C      program now goes to subroutines to obtain parameters associated
C      with sorption and hydrophobicity
       GO TO 376
25     CONTINUE
C        ------------------value of Deff-----------------------------------
       GO TO 585
C      -----------------setting coefficients for numerical iterations----
170      p=1.5
C      p is the particle bulk density (g/cm^3)
C      Go to routine to set gridnumbers and maximum time step.
       GOTO 640
175    CONTINUE
C      SettingIntervals
       GOTO 720
185    ts=te(0)
        DO 187 n=1, ng
           DO 188 ni=1, ngrid(n)
             u(n,ni)=dx(n)*(ni-1)*so*ps*(1-poro)
188        CONTINUE
187     CONTINUE
C      -----------------setting parameters for 1st order model ****-------
        DO 190 n1=1, ng
        s1(n1)=so
        k1(n1)=(10.56*solid*Kp+22.7)*d/rad(n1)**2
C       no fraction effect included
190     CONTINUE
        sss1=so
       GOTO 760
340    CONTINUE
       GOTO 375
375    CONTINUE
C      ------------------------------------------------------------------
C                 Subroutine to estimate the value of Kp
C      ------------------------------------------------------------------
376    continue
       WRITE(*,377)
377    FORMAT('What is known? Kp=1, Ce=2, Koc=3 or Kow=4    ',$)
       READ(*,*)k
        IF (k .EQ. 1) THEN
       GOTO 395
         ELSE IF(k .EQ. 2) THEN
         GOTO 405
           ELSE IF(k .EQ. 3) THEN
           GOTO 425
             ELSE IF(k .EQ. 4) THEN
             GOTO 445
```

```
      END IF
C     Input known value of Kp.
395   WRITE(*,397)
397   FORMAT('Enter Kp (cm^3/g)    ',$)
      READ(*,*)Kp
      GOTO 550
C     Estimate Kp from know values of Co and Ce:
405   WRITE(*,407)
407   FORMAT('Reenter Co [moles/ml]    ',$)
      READ(*,*)co(1)
      WRITE(*,410)
410   FORMAT('Enter Ce [moles/ml]  ',$)
      READ(*,*)ce
      Kp=(co(1)+(solid*so)-ce)/(solid*ce)
      GOTO 550
C     Estimate Kp from known values of Koc and foc.
425    WRITE(*,427)
427    FORMAT('Enter Koc(cm^3/g)    ',$)
       READ(*,*)Koc
       WRITE(*,428)
428    FORMAT('Enter foc(g/g)    ',$)
       READ(*,*)foc
       Kp=Koc*foc
       GOTO 550
445    continue
C     ------------------------------------------------------------------
C                        subroutine to estimate Kp from Kow
C     ------------------------------------------------------------------
      WRITE(*,446)
446   FORMAT('Enter Kow    ',$)
      READ(*,*)Kow
      WRITE(*,447)
447   FORMAT('Which equation do you want to use',/)
      WRITE(*,448)
448   FORMAT('eq.1: log Koc=log Kow - 0.21  or',/)
      WRITE(*,449)
449   FORMAT('eq.2: log Koc=0.72 log Kow + 0.49 ?    ',$)
      READ(*,*)eq
520   IF (eq .EQ. 1)THEN
      GOTO 535
      ELSE IF(eq .EQ. 2)THEN
      GOTO 537
      END IF
C535   CONTINUE
C     eq1:
535   Koc=10**(LOG10(Kow)-0.21)
      GOTO 545
537   CONTINUE
C          eq2:
         Koc=10**(0.72*LOG10(Kow)+0.49)
545   WRITE(*,547)
547   FORMAT('Enter foc    ',$)
      READ(*,*)foc
      Kp=Koc*foc
550   continue
      ce=(co(1)+solid*so)/(solid*Kp+one)
       WRITE(10,560)Kp
```

```
560    FORMAT('Kp=',1PE12.4)
       GOTO 25
C      ------------------------------------------------------------------
C         subroutine to determine Deff from Dm, porosity, and dry density
C      ------------------------------------------------------------------
585    continue
       WRITE(*,587)
587    FORMAT('Do you know the value of Deff?   ',$)
       READ(*,*)knoDeff
       IF (knoDeff .EQ. 'N' .OR. knoDeff .EQ. 'n')THEN
       GOTO 615
       END IF
       WRITE(*,610)
610    FORMAT('Enter Deff (cm^2/s)   ',$)
       READ(*,*)DinSecond
       d=DinSecond*60
       GOTO 170
C      Estimate Deff from other parameters.
615    CONTINUE
       WRITE(*,617)
617    FORMAT('Enter the intraparticle porosity   ',$)
       READ(*,*)poro
       WRITE(*,618)
618    FORMAT('Enter the solid dry density   ',$)
       READ(*,*)ps
       WRITE(*,619)
619    FORMAT('Enter the molecular diffusivity (cm^2/sec)   ',$)
       READ(*,*)Dm
        d=Dm*poro**2/Kp/(1-poro)/ps*60
        WRITE(10,625)poro
625     FORMAT('intraparticle porosity=',1PE12.4)
        WRITE(10,635)ps
635     FORMAT('solid dry density=',1PE12.4)
        WRITE(10,636)Dm
636     FORMAT('molecular diffusivity=',1PE15.4)
        WRITE(10,637)
637     FORMAT(' ')
        WRITE(10,638)
638     FORMAT('The following columns are time, aqu conc., sorbed conc.')
        WRITE(10,642)
642     FORMAT('aqu conc. in units of moles/ml and sorbed in moles/gram')
        WRITE(10,639)
639     FORMAT(' ')
       GOTO 170
640    CONTINUE
C      ------------------------------------------------------------------
C          subroutine to set grid numbers and maximum time step
C      ------------------------------------------------------------------
        tmin=TimeStep
        DO 692 n=1, ng
          ngrid(n)=1.0 +INT((rad(n)/gridsize(n)/2))*2
c          ngrid(n)=1.0 +INT((rad(n)/gridsize(n)/2))**2
          tmint=(rad(n)**2/d/(ngrid(n)-1)**2)/2
         IF (tmin .GT. tmint) THEN
         tmin=tmint
         END IF
          dx(n)=one/(ngrid(n)-1)
```

```
        h(n)=fs(n)*solid*dx(n)**2/(ps-ps*poro)
692     CONTINUE
        GOTO 175
C-------------------------------------------------------------------------
C                  set time step sizes and coefficients
C     -------------------------------------------------------------------
720   continue
      DO 735 n=1, ng
730        g(n)=d*tmin/(rad(n)*dx(n))**2
735   CONTINUE
      GOTO 185
C     -------------------------------------------------------------------
C              iteration and output of simulation
C     -------------------------------------------------------------------
C      This part of the program is the actual finite difference program.
760   continue
      DO 965 nc=1, ncycle
        c=co(nc)
        num(ncycle)=INT((te(nc)-te(nc-1))/TimeStep)
        DO 960 nk=1, num(ncycle)
C        This begins the iteration loop.
785   continue
          aa=zero
          bb=zero
          DO 835 ni=1, ng
           sumj=zero
              DO 823 nj=2, ngrid(ni)-1
           ut(ni,nj)=u(ni,nj)+g(ni)*(u(ni,nj+1)-two*u(ni,nj)+u(ni,nj-1))
           sumj=sumj+(3+(-1)**nj)*(nj-1)*(ut(ni,nj)-u(ni,nj))
823           CONTINUE
           aa=aa+h(ni)*(sumj-(ngrid(ni)-1)*u(ni,ngrid(ni)))
           bb=bb+h(ni)*(ngrid(ni)-1)*Kp*ps*(1-poro)
835       CONTINUE
C         ct is the updated aqueous concentration. Equation 3.18 in Wu.
C         the units on ct are moles per cm3 liquid
          ct=(c-aa)/(one+bb)
          ts=ts+tmin
          c=ct
          DO 880 n1=1, ng
              DO 870 nm=1, ngrid(n1)-1
                  u(n1,nm)=ut(n1,nm)
870           CONTINUE
              u(n1,ngrid(n1))=Kp*ps*(1-poro)*c
880       CONTINUE
          IF (ts .LT. te(nc-1)+TimeStep*nk) THEN
          GOTO 785
          END IF
          ss=zero
          DO 925 ni=1, ng
              sumk=zero
                 DO 915 nj=2, ngrid(ni)-1
                    sumk=sumk+(3+(-1)**nj)*(nj-1)*ut(ni,nj)
915              CONTINUE
              ss=ss+fs(ni)*dx(ni)**2*(sumk+(ngrid(ni)-1)*u(ni,ngrid(ni)))
925       CONTINUE
C         The units of ca are moles/cm3 and ssp are moles/cm3 total
          ca=c
```

```
C       ssp is in units of moles/gram of soil since ps is units of
C       grams per cm3 solid and 1-n is cm3 solid per cm3 total
        ssp=ss/(ps-ps*poro)
        t1=ts
         WRITE(*,955)t1,ca,ssp
955      FORMAT(1PE11.5,'              ',1PE11.5,'              '1PE11.5)
         WRITE(10,958)t1,ca,ssp
958      FORMAT(1PE11.5,'    '1PE11.5,'    '1PE11.5)
960     CONTINUE
965   CONTINUE
      END
```

Appendix C

Sorption-Desorption and Degradation Model

The following model incorporates Monod kinetics into a radial diffusion model which describes the sorption and desorption of hydrophobic compounds in soil-water systems. A model with first-order substrate depletion kinetics was also developed but is not included here. To change this program to describe first-order kinetics one would remove the input of a half-saturation coefficient (not used in first-order model) and change the degradation term in line 926 accordingly to first-order kinetics so that line 926 read, ct=c-(tk*c)*TimeStep.

```
C     ****************************************************************
C           James R. Mihelcic, Department of Civil Engineering
C                                1988
C                  Carnegie Mellon Univeristy, Pittsburgh, Pa.
C      ****************************************************************
C         The following program recoded the BASIC program of S.C. Wu,
C      Department of Civil Engineering, Mass. Inst. of Technology, 1986
C      and added the ability to include degradation of the solute from
C      the bulk-aqueous phase. The program couples a radial diffusion
C      model to describe the rate of sorption and desorption, and Monod
C      kinetics to describe the rate of microbial degradation. The
C      finite difference program allows the user to input up to 10
C      particle size groups. Grid sizes are changeable.
C      A detailed discussion of the program can be found in the
C      theses of S.C. Wu and J.R. Mihelcic.
C      This program is written in fortran 77.
C      ****************************************************************

      CHARACTER*1 changeC, knoDeff
      DOUBLE PRECISION one,two,zero,ca,ssp,t1
      INTEGER ngrid(10), num(20)
      REAL fs(10),rad(10),u(10,201),g(10)
      REAL dx(10),h(10),ut(10,201),gridsize(10),te(20),co(20)
      REAL s1(10),k1(10),Kow,tmint,Kp,Koc,Kow,foc,tk,poro,Ks
      one=1
      zero=0
```

```
      two=2
      OPEN(UNIT=10,FILE='deg.output',STATUS='unknown')
          WRITE(10,967)
967       FORMAT('*****Output from finite difference program*****')
          WRITE(10,968)
968       FORMAT('*****for modeling sorption and desorption*****')
          WRITE(10,969)
969       FORMAT('***************James R. Mihelcic**************')
          WRITE(10,970)
970       FORMAT('***************Carnegie Mellon University*******')
          WRITE(10,971)
971       FORMAT('*************Department of Civil Engineering***')
          WRITE(10,972)
972       FORMAT(' Up to 10 particle sizes can be obtained')
C     -----------Entering environmental parameters-------------
C     -----------particle size distribution--------------------
      WRITE(*,4)
4     FORMAT('Please enter environmental parameters.',/)
      WRITE(*,2)
2     FORMAT('Enter half-saturation coefficient, mole/ml   ',$)
      READ(*,*) Ks
      WRITE(*,3)
3     FORMAT('Enter the maximum rate, mole/ml-min  ',$)
      READ(*,*) tk
      WRITE(*,5)
5     FORMAT('Enter the number of particle classes   ',$)
      READ(*,*) ng
      DO 9 n=1, ng
      WRITE(*,6)
6     FORMAT('Enter fraction   ',$)
C     fraction of particle class. If only average size used, fs(n)=1
      READ(*,*)fs(n)
      WRITE(*,7)
7     FORMAT('Enter particle radius in cm   ',$)
      READ(*,*)rad(n)
C     The gridsize is the radius divided by the number of grids.
C     Wu's thesis explains the advantages and disadvantages of the
C     number of grids utilized.
      WRITE(*,8)
8     FORMAT('Enter gridsize of class #, cm   ',$)
      READ(*,*)gridsize(n)
9     CONTINUE
      WRITE(*,11)
11    FORMAT('Initial concentration in solid (mole/g) ?   ',$)
      READ(*,*)so
      WRITE(*,12)
12    FORMAT('Simulation starting time (minute) ?   ',$)
      READ(*,*)te(0)
      WRITE(*,14)
14    FORMAT('Printing time step size (minute) ?   ',$)
      READ(*,*)Timestep
      ncycle=0
15    CONTINUE
                ncycle=ncycle+1
                WRITE(*,16)
16              FORMAT('Ending time (minute) ?   ',$)
                READ(*,*)te(ncycle)
```

```
17            continue
              WRITE(*,18)
18            FORMAT('Concentration in aqueous phase (mole/ml) ?   ',$)
              READ(*,*)co(ncycle)
      WRITE(*,20)
20    FORMAT('Do you want to change concentration in aqueous phase? ',$)
      READ(*,*)changeC
       IF (changeC .EQ. 'Y'.OR. changeC .EQ. 'y') THEN
       GOTO 15
       END IF
C     ------------------sorbent concentration and Kp----------------
      WRITE(*,22)
22    FORMAT('Sorbent concentration (g/ml) ?   ',$)
      READ(*,*)solid
C      --------------------printing input parameters--------------------
       WRITE(10,200)rad
200    FORMAT('radius (cm)=',1PE10.4)
       WRITE(10,205)gridsize
205    FORMAT('gridsize (cm)=',1PE11.5)
       WRITE(10,210)so
210    FORMAT('initial conc. in solid (mole/g)=',1PE10.4)
       WRITE(10,216)co
216    FORMAT('initial aqueous conc. (mole/ml)=',1PE8.2)
       WRITE(10,220)solid
220    FORMAT('sorbent concentration (g/ml)=',0PF8.4)
C     program now goes to subroutines to obtain parameters associated
C     with sorption and hydrophobicity
      GO TO 376
25    CONTINUE
C       -------------------value of Deff-----------------------------------
      GO TO 585
C     -----------------setting coefficients for numerical iterations----
170      p=1.5
C     p is the particle bulk density (g/cm^3)
C     Go to routine to set gridnumbers and maximum time step.
      GOTO 640
175   CONTINUE
C     SettingIntervals
      GOTO 720
185   ts=te(0)
       DO 187 n=1, ng
          DO 188 ni=1, ngrid(n)
            u(n,ni)=dx(n)*(ni-1)*so*ps*(1-poro)
188       CONTINUE
187    CONTINUE
C     -----------------setting parameters for 1st order model ****-------
       DO 190 n1=1, ng
       s1(n1)=so
       k1(n1)=(10.56*solid*Kp+22.7)*d/rad(n1)**2
C      no fraction effect included
190    CONTINUE
       sss1=so
      GOTO 760
340   CONTINUE
      GOTO 375
375   CONTINUE
C     ------------------------------------------------------------------
```

```
C                Subroutine to estimate the value of Kp
C     ------------------------------------------------------------------
376   continue
      WRITE(*,377)
377   FORMAT('What is known? Kp=1, Ce=2, Koc=3 or Kow=4   ',$)
      READ(*,*)k
       IF (k .EQ. 1) THEN
      GOTO 395
        ELSE IF(k .EQ. 2) THEN
        GOTO 405
          ELSE IF(k .EQ. 3) THEN
          GOTO 425
            ELSE IF(k .EQ. 4) THEN
            GOTO 445
      END IF
C     Input known value of Kp.
395   WRITE(*,397)
397   FORMAT('Enter Kp (cm^3/g)   ',$)
      READ(*,*)Kp
      GOTO 550
C     Estimate Kp from know values of Co and Ce:
405   WRITE(*,407)
407   FORMAT('Re-enter Co [moles/ml]   ',$)
      READ(*,*)co(1)
      WRITE(*,410)
410   FORMAT('Enter Ce [moles/ml]  ',$)
      READ(*,*)ce
      Kp=(co(1)+(solid*so)-ce)/(solid*ce)
      GOTO 550
C     Estimate Kp from known values of Koc and foc.
425    WRITE(*,427)
427    FORMAT('Enter Koc(cm^3/g)   ',$)
       READ(*,*)Koc
       WRITE(*,428)
428    FORMAT('Enter foc(g/g)   ',$)
       READ(*,*)foc
       Kp=Koc*foc
       GOTO 550
445    continue
C     ------------------------------------------------------------------
C                        subroutine to estimate Kp from Kow
C     ------------------------------------------------------------------
      WRITE(*,446)
446   FORMAT('Enter Kow   ',$)
      READ(*,*)Kow
      WRITE(*,447)
447   FORMAT('Which equation do you want to use',/)
      WRITE(*,448)
448   FORMAT('eq.1: log Koc=log Kow - 0.21  or',/)
      WRITE(*,449)
449   FORMAT('eq.2: log Koc=0.72 log Kow + 0.49 ?   ',$)
      READ(*,*)eq
520   IF (eq .EQ. 1)THEN
      GOTO 535
      ELSE IF(eq .EQ. 2)THEN
      GOTO 537
      END IF
```

```
C535   CONTINUE
C      eq1:
535    Koc=10**(LOG10(Kow)-0.21)
       GOTO 545
537    CONTINUE
C           eq2:
          Koc=10**(0.72*LOG10(Kow)+0.49)
545    WRITE(*,547)
547    FORMAT('Enter foc    ',$)
       READ(*,*)foc
       Kp=Koc*foc
550    continue
       ce=(co(1)+solid*so)/(solid*Kp+one)
        WRITE(10,560)Kp
560     FORMAT('Kp=',1PE12.4)
       GOTO 25
C       ------------------------------------------------------------------
C          subroutine to determine Deff from Dm, porosity, and dry density
C        ------------------------------------------------------------------
585    continue
       WRITE(*,587)
587    FORMAT('Do you know the value of Deff?    ',$)
       READ(*,*)knoDeff
       IF (knoDeff .EQ. 'N' .OR. knoDeff .EQ. 'n')THEN
       GOTO 615
       END IF
       WRITE(*,610)
610    FORMAT('Enter Deff (cm^2/s)    ',$)
       READ(*,*)DinSecond
       d=DinSecond*60
       GOTO 170
C      Estimate Deff from other parameters.
615    CONTINUE
       WRITE(*,617)
617    FORMAT('Enter the intraparticle porosity    ',$)
       READ(*,*)poro
       WRITE(*,618)
618    FORMAT('Enter the solid dry density    ',$)
       READ(*,*)ps
       WRITE(*,619)
619    FORMAT('Enter the molecular diffusivity (cm^2/sec)    ',$)
       READ(*,*)Dm
        d=Dm*poro**2/Kp/(1-poro)/ps*60
        WRITE(10,625)poro
625     FORMAT('intraparticle porosity=',1PE12.4)
        WRITE(10,627)Ks
627     FORMAT('half-saturation coefficient (mole/ml)=',1PE15.4)
        WRITE(10,630)tk
630     FORMAT('rate constant (mole/ml-min)=',1PE15.4)
        WRITE(10,635)ps
635     FORMAT('solid dry density=',1PE12.4)
        WRITE(10,636)Dm
636     FORMAT('molecular diffusivity=',1PE15.4)
        WRITE(10,637)
637     FORMAT(' ')
        WRITE(10,638)
638     FORMAT('The following columns are time, aqu conc., sorbed conc.')
```

```
      WRITE(10,642)
642   FORMAT('aqu conc. in units of moles/ml and sorbed in moles/gram')
      WRITE(10,639)
639   FORMAT(' ')
      GOTO 170
640   CONTINUE
C     ------------------------------------------------------------------
C         subroutine to set grid numbers and maximum time step
C     ------------------------------------------------------------------
      tmin=TimeStep
      DO 692 n=1, ng
        ngrid(n)=1.0 +INT((rad(n)/gridsize(n)/2))*2
c        ngrid(n)=1.0 +INT((rad(n)/gridsize(n)/2))**2
        tmint=(rad(n)**2/d/(ngrid(n)-1)**2)/2
       IF (tmin .GT. tmint) THEN
       tmin=tmint
       END IF
        dx(n)=one/(ngrid(n)-1)
        h(n)=fs(n)*solid*dx(n)**2/(ps-ps*poro)
692   CONTINUE
      GOTO 175
C-----------------------------------------------------------------------
C                  set time step sizes and coefficients
C     ------------------------------------------------------------------
720   continue
      DO 735 n=1, ng
730       g(n)=d*tmin/(rad(n)*dx(n))**2
735   CONTINUE
      GOTO 185
C     ------------------------------------------------------------------
C             iteration and output of simulation
C     ------------------------------------------------------------------
C      This part of the program is the actual finite difference program.
760   continue
      DO 965 nc=1, ncycle
        c=co(nc)
        num(ncycle)=INT((te(nc)-te(nc-1))/TimeStep)
        DO 960 nk=1, num(ncycle)
C        This begins the iteration loop.
785   continue
         aa=zero
         bb=zero
         DO 835 ni=1, ng
          sumj=zero
             DO 823 nj=2, ngrid(ni)-1
          ut(ni,nj)=u(ni,nj)+g(ni)*(u(ni,nj+1)-two*u(ni,nj)+u(ni,nj-1))
          sumj=sumj+(3+(-1)**nj)*(nj-1)*(ut(ni,nj)-u(ni,nj))
823          CONTINUE
          aa=aa+h(ni)*(sumj-(ngrid(ni)-1)*u(ni,ngrid(ni)))
          bb=bb+h(ni)*(ngrid(ni)-1)*Kp*ps*(1-poro)
835      CONTINUE
C        ct is the updated aqueous concentration. Equation 3.18 in Wu.
C        the units of ct are moles per cm3 liquid
         ct=(c-aa)/(one+bb)
         ts=ts+tmin
         c=ct
         DO 880 n1=1, ng
```

```
            DO 870 nm=1, ngrid(n1)-1
                u(n1,nm)=ut(n1,nm)
870         CONTINUE
            u(n1,ngrid(n1))=Kp*ps*(1-poro)*c
880       CONTINUE
          IF (ts .LT. te(nc-1)+TimeStep*nk) THEN
          GOTO 785
          END IF
          ss=zero
          DO 925 ni=1, ng
              sumk=zero
                 DO 915 nj=2, ngrid(ni)-1
                    sumk=sumk+(3+(-1)**nj)*(nj-1)*ut(ni,nj)
915              CONTINUE
              ss=ss+fs(ni)*dx(ni)**2*(sumk+(ngrid(ni)-1)*u(ni,ngrid(ni)))
925       CONTINUE
C         The units of ca are moles/cm3 liquid and ssp are moles/cm3 total
C
C         Incorporation of  Monod kinetics into the sorption model
C         in finite difference form. If only first-order kinetics
C         are desired the following equation would be changed.
C         ********************************************************************
926       ct=c - (tk*c/(Ks+c))*Timestep
C         ********************************************************************
          c=ct
          ca=c
C         The next line sets the sorbed phase at zero if no solids
C         were added to the system.
          IF (solid .EQ. 0)THEN
          ss=0
          END IF
C         ssp is in units of moles per gram of soil since ps is units of
C         gram per cm3 solid and 1-n is cm3 solid per cm3 total
          ssp=ss/(ps-ps*poro)
          t1=ts
           WRITE(*,955)t1,ca,ssp
955        FORMAT(1PE11.5,'              ',1PE11.5,'              '1PE11.5)
           WRITE(10,958)t1,ca,ssp
958        FORMAT(1PE11.5,'   '1PE11.5,'   '1PE11.5)
960     CONTINUE
965   CONTINUE
      END
```

Appendix D

Naphthalene and Nitrate Concentration Data

The following appendix includes the experimental data plotted in Figures 6-2 to 6-8 of this report. Concentration and standard deviation where possible, are presented as a function of time. Nitrate concentration is reported as mg/liter NO_3^-, sulfate concentration as mg/liter SO_4^{2-}, and ND refers to nondetectable level of < 0.01 mg/liter. Nitrite was not detectable in any samples.

Time (days)	Naphthalene conc. mg/l	Nitrate conc. mg/l	Sulfate conc. mg/l
Blanks			
0	3.6 (0)	37.1 (0)	0
22	3.8 (0)	23.8	0
Samples			
1	3.1	35.2	4.0
5	1.7 (0.21)		
13	0.14 (0.036)	25.7 (8.9)	3.2 (0.35)
15	0.089	15.8	3.0
18	ND	20.7 (7.3)	3.2 (1.5)
22	ND	17.6 (5.4)	2.6 (0.21)

Data corresponds to Figure 6-2, Experiment no. 3.

Time (days)	Naphthalene conc. mg/l	Nitrate conc. mg/l
Blanks		
1	2.4 (0.92)	134 (0)
26	1.9 (0.25)	114 (0)
Samples		
1	2.0	134
3	2.0	131
8	1.6	123.6
11	0.22	95.6
14	0.31	-
18	0.052	146.7
22	ND	106.7

Data corresponds to Figure 6-3, Experiment no. 1.

Time (days)	Naphthalene conc. mg/l	Nitrate conc. mg/l
Blanks		
1	2.4 (0.92)	134 (0)
26	1.9 (0.25)	114 (0)
Samples		
1	2.0	135.3
3	1.7	92.6
8	0.87	84.1
11	0.40	37.8
14	0.038	79.1
18	ND	42.0
22	ND	36.2
26	ND	

Data corresponds to Figure 6-4, Experiment no. 2.

Time (days)	Naphthalene conc. mg/l	Nitrate conc. mg/l	Sulfate conc mg/l
Blanks			
1	7.2 (0.42)	37.4	1.0 (0.13)
29	7.8 (3.0)	36.5 (2.1)	
Controls			
29	4.8 (1.1)	37.7 (3.2)	5.0 (0.0)
Samples			
1	5.3	37.4	1.1
4	5.6 (0.78)	24.2 (8.2)	1.5 (0.42)
12	3.5 (1.5)	48.4 (2.3)	1.4 (0)
16	0.78 (0.056)	38.7 (10.3)	1.4 (0)
23	ND	24.8 (6.8)	1.4 (0)
28	ND	16.2	1.7

Data corresponds to Figure 6-5, Experiment no. 4.

Time (days)	Naphthalene conc. mg/l	Nitrate conc. mg/l	Sulfate conc. mg/l
Blanks			
1	7.0 (0.21)	35.7 (0)	0.58 (0)
29	3.0 (0.85)	12.6 (2.3)	0
Controls			
29	3.5 (0.56)	37.4 (0)	6.2 (3.5)
Samples			
1	3.6	50.1	1.2
4	4.0 (1.1)	40.4 (0.64)	1.2 (0)
12	1.1 (0.14)	14.6 (0.49)	1.4 (0)
16	1.3	11.2	
23	ND	10.4 (0.49)	1.4 (0)
28	ND	11.2 (0.52)	1.7 (0)
29	ND	11.4	1.2

Data corresponds to Figure 6-6, Experiment no. 5.

Time (days)	Naphthalene conc. mg/l	Nitrate conc. mg/l
Blanks		
1	7.3	52.9
22	5.3 (0.21)	46.5 (0.71)
Controls		
1	1.9	74
22	2.0	53 (3.4)
Samples		
1	3.6 (0.30)	37 (0.21)
3	2.8	14.8
5	2.9 (1.6)	12.0 (2.0)
8	1.3	1.4
11	0.50	1.7
15	0.050	0
19	ND	0
22	ND	0

Data corresponds to Figure 6-7, Experiment no. 6.

Appendix E

Sorption and Desorption Isotherm Experimental Data

One day sorption equilibrium. Data in Figure 5-4.

Sorption		Desorption	
Equilibrium Concentration mg/l	Sorption Capacity mg/g	Equilibrium Concentration mg/l	Sorption Capacity mg/g
5.8	0.064	2.7	0.038
4.6	0.068	2.7	0.042
5.0	0.064	2.6	0.038
5.2	0.060	2.7	0.034
1.9	0.043	2.1	0.026
1.9	0.044	2.2	0.034
2.5	0.041	2.0	0.032
2.1	0.027	1.9	0.021
1.1	0.031	1.4	0.027
1.7	0.028	1.4	0.024
1.8	0.028	1.3	0.024
1.2	0.021	0.94	0.019
1.0	0.019	0.50	0.018
0.77	0.022	0.46	0.022
1.0	0.021	0.57	0.20

Three day sorption equilibrium. Data in Figure 5-5.

Sorption		Desorption	
Equilibrium Concentration mg/l	Sorption Capacity mg/g	Equilibrium Concentration mg/l	Sorption Capacity mg/g
3.0	0.038	1.3	0.028
3.1	0.038	1.6	0.022
3.2	0.036	1.7	0.020
3.4	0.034	1.1	0.019
2.1	0.023	0.84	0.015
1.8	0.024	0.91	0.014
2.0	0.023	0.94	0.014
1.9	0.023	0.65	0.011
1.1	0.017	0.72	0.011
1.3	0.016	0.69	0.012
1.4	0.016	0.48	0.012
1.2	0.016		
0.82	0.013		
0.98	0.012		
0.78	0.013		
0.83	0.013		

Thirty-six day sorption equilibrium. Data in Figure 5-6.

Sorption		Desorption	
Equilibrium Concentration mg/l	Sorption Capacity mg/g	Equilibrium Concentration mg/l	Sorption Capacity mg/g
8.1	0.10	4.3	0.062
3.9	0.067	3.7	0.052
4.1	0.067	3.8	0.051
4.0	0.062	3.9	0.046
4.1	0.066	4.0	0.051
3.1	0.045	3.2	0.037
3.2	0.045	3.2	0.038
3.0	0.046	3.3	0.038
2.9	0.045	2.4	0.039
2.0	0.034	2.2	0.031
1.9	0.034	2.2	0.030
2.1	0.034	2.1	0.034
2.7	0.034	2.3	0.030

Adsorption Data for Barnes-Hamerly Soil with Naphthol. Data in Figure 5-1.

Values in parentheses are the standard deviations of samples averaged.

Amount of soil grams	Equilibrium Concentration mg/l	Sorption Capacity mg/g
3.0000	19.4 (0.23)	0.173 (0.0069)
6.0000	13.5 (0.21)	0.135 (0.0012)
9.0000	11.0 (0.21)	0.103 (0.0010)
12.0000	8.80 (0.26)	0.0832 (0.0022)
15.0000	7.10 (0.28)	0.0704 (0.0013)
20.0000	2.40 (0.058)	0.0600 (0.0017)
25.0000	0.73 (0.12)	0.0480 (0.0019)

Adsorption Data for Barnes-Hamerly Soil with Acenaphthene. Data in Figure 5-3.

Values in parentheses are the standard deviations of samples averaged.

Amount of soil grams	Equilibrium Concentration mg/l	Sorption Capacity mg/g
1.5000	2.0 (0.25)	0.094 (0.0080)
3.0000	0.96 (0.12)	0.0604 (0.0018)
5.0000	0.46 (0.040)	0.0406 (0.0014)
10.0000	0.26 (0.062)	0.0207 (0.00017)

Appendix F

Sample Characterization of Bacterial Strains

A few soil samples were tested to examine the type of bacteria present in the soil. Before analysis, samples were prepared as follows.

10 ml of a phosphate buffer of neutral pH and approximately 2 ml of 4 percent glutaraldehyde were added to the centrifuged solid phase of a sample which had been reserved from an experiment in which naphthalene had reached nondetectable levels. The sample was then resuspended and mailed overnight in a refrigerated container. Analyses and data interpretation were performed by the laboratory of Dr. William C. Ghiorse, Department of Microbiology, Cornell University, Ithaca, New York. Detailed explanation of the following characterization methods can be found in Balkwill, D.L., and W.C. Ghiorse, "Characterization of Subsurface Bacteria Associated with Two Shallow Aquifers in Oklahoma," *Applied and Environmental Microbiology,* Vol. 50, p. 580-588, 1985.

The total population of bacteria was 3.0 (+/- 0.6) x 10^7 cells/ml as estimated by an acridine orange direct count procedure. Also observed were approximately 7 x 10^5 fungal spores/ml and occasional fungal and actinomycete-like filaments. The laboratory isolated nine different colony types of bacteria from aerobically incubated low-nutrient agar plates but did not enrich for denitrifying naphthalene degraders.

Table F-1 shows the characterization of the slurry samples. The primary colonies were restreaked to isolate uniform colonies, and cells were examined in wet mounts by phase contrast microscopy by employing a 100X objective lens of a Zeiss Standard 18 microscope. The KOH test for gram-reaction was done according to the references listed. This test correlates with actual staining results for approximately 90 percent of natural isolates (Moaledj, 1986).

From this work, most of the isolates were Gram-positive. Some of spores were *Bacillus*-like judging by spore formation, by this was not confirmed. Other spores may have been coryneform- or actinomycete-like, but this group is very difficult taxonomically (see Bergey's Manual, eight edition). It was concluded that the isolate appeared to be an assortment of soil bacteria which most likely can grow anaerobically as well as aerobically though this was not tested for.

Table F-1: Characterization of bacteria from sample where naphthalene was degraded under denitrification conditions.

Isolate	Grown on dilute 5% PTYG, 2% agar plates: Original colony description	Transferred colony description	Wet mount description	KOH [a] test	Probable Gram Reaction [b]
Pit B	tiny, light pink	tiny, light pink	small, very dense coccoid rods, in chains, some look like spores (PHB-bodies?) [coryneform?][c]	-	+
Pit C	tiny, yellow, smooth edge	tiny, light pink	pleomorphic, as above, but also longer, irregular shaped rods, seem to divide into into chains of coccoid rods [coryneform?]	-	+
Pit D	translucent, medium wrinkled surface, possible spreader(?)	small, irregular edge	short, motile rods and coccoid rods [pseudomonad?]	+	-
Pit E	irregular, jagged edge dense opaque center with translucent edge, medium —> large size	medium size, irregular edge	spores or very dense coccoid rods [coryneform?]	-	+
Pit F	large, bubbly, irregular edge	large spreader, irregular bubbly edge	*Bacillus* with endospores, many cells in chains [*Bacillus*]	-	+
Pit G	large, opaque, slight irregular edge	medium size, slight scalloped, irregular edge	*Bacillus* with endospores [*Bacillus*]	-	+
Pit H	medium size, smooth edge	medium size, smooth edge, opaque	small rods [coryneform?]	-	+
Pit I	small, actinomycete like colony	medium size, white raised, actinomycete-like	bacterial filaments [actinomycete]	colonies too difficult to scrape off plate	+

[a]See Gregersen, T. European J. Appl. Microbiol. Biotechnol. 5:123-127 (1978).
Ryu, E. Japan J. Vet. Sci. 1:209-210 (1939).

[b]See Moaledj, K. J. Microbiol. Methods. 5:303-310 (1986).

[c]brackets indicate best guess to guide further testing.